

AD A 11 7 743

(12)

155800-1-F₁

Final Technical Report

RADIANCE CALCULATIONS FOR OPTIMIZATION OF SENSORS DESIGNED FOR REMOTE BATHYMETRY

Volume 1

FRED J. TANIS
Applications Division

JULY 1982

Naval Research Laboratory
Washington, D.C. 20375

Contract No.: N00014-81-C-2350

DTIC
SEARCHED
SERIALIZED
AUG 2 1982

DTIC FILE COPY

ENVIRONMENTAL
RESEARCH INSTITUTE OF MICHIGAN
BOX 8618 • ANN ARBOR • MICHIGAN 48107

DISTRIBUTION STATEMENT A
Approved for public release;
Distribution Unlimited

82 07 14 008

TECHNICAL REPORT STANDARD TITLE PAGE

1. Report No. 155800-1-F ₁		2. Government Accession No. AD-A117 743		3. Recipient's Catalog No.	
4. Title and Subtitle RADIANCE CALCULATIONS FOR OPTIMIZATION OF SENSORS DESIGNED FOR REMOTE BATHYMETRY				5. Report Date JULY 1982	
				6. Performing Organization Code	
7. Author(s) FRED J. TANIS				8. Performing Organization Report No. 155800-1-F ₁	
9. Performing Organization Name and Address Environmental Research Institute of Michigan P.O. Box 8618, Applications Division Ann Arbor, MI 48107				10. Work Unit No.	
				11. Contract or Grant No. N00014-81-C-2350	
12. Sponsoring Agency Name and Address Naval Research Laboratory Washington, DC 20375				13. Type of Report and Period Covered Final Technical Report	
				14. Sponsoring Agency Code	
15. Supplementary Notes					
16. Abstract An extensive set of radiance calculations have been generated for each of twelve representative bottom types using an existing water radiance and atmospheric radiative transfer model. Total radiance values were calculated under two separate (Elterman) atmospheric states for a sensor platform altitude of 50 km. Calculations were also made for a sensor placed just below the sea surface. The model parameters were iterated over representative water depths and water types. A preliminary visual band optimization analysis was made over the input parameters. The suitability of Landsat-D Thematic mapper (TM) bands is also addressed.					
17. Key Words Model Calculations Bottom Reflectance Spectra Thematic Mapper Scanner Optimal Band Placement				18. Distribution Statement DISTRIBUTION STATEMENT A Approved for public release; Distribution is unlimited.	
19. Security Classif. (of this report) Unclassified		20. Security Classif. (of this page) Unclassified		21. No. of Pages iv+23+A-112	22. Price

PAGES _____
ARE
MISSING
IN
ORIGINAL
DOCUMENT

PREFACE

This report is submitted by the Environmental Research Institute of Michigan in fulfillment of requirements for contract N00014-81-C-2350 under sponsorship of the Naval Research Laboratory. The technical representative for the contracting officer was Dr. Peter Mitchell of NRL. The principal investigator was Mr. Fabian Polcyn with important contributions to the technical program made by Mr. Fred J. Tanis. This research was conducted by the Applications Division under the direction of Mr. Donald S. Lowe. This study was initiated by Mr. James Hammack/DMA and has benefitted from his comments and directives. The author wishes to acknowledge the assistance of Mr. Fred J. Thomson, manager of the Resources and Technology Department and Ms. Nancy J. Ballard for her secretarial services and assistance in the preparation of Volume 2.

TABLE OF CONTENTS

Volume I

1.0 Summary	1
2.0 Introduction	3
3.0 Radiance Calculation Procedure	7
3.1 Water Radiance Model	7
3.2 Selection of Model Parameters	8
3.3 Computational Results	11
4.0 Preliminary Band Analysis And Interpretation	19
REFERENCES	23
Appendix A: Total Radiance Spectra for Selected Bottom Types	A-1

Volume II

Appendix B: Tables of Total Radiance Values for Selected Bottom Types



Accession For
NTIS GRAS1
DTIC TAB
Unannounced
Justification: *Per*
the original
By _____
Distribution/_____
Availability Codes
Avail and/or
Dist _____
A

LIST OF FIGURES

<u>FIGURE</u>	<u>TITLE</u>	<u>PAGE</u>
1	Portion of the Bahamas Photobathymetric Calibration Survey Areas	5
2	Irradiance Extinction Coefficient for Five Water Types: Clear Oceanic Types I(1), II(2), III(3), and Coastal Types 1(4) and 3(5)	10
3	Bottom Reflectance Spectra for Pure Coraline Sand and Turtle Grass	12
4	Bottom Reflectance Spectra for Algal Mat Mixture and Fire Coral	13
5	Bottom Reflectance Spectra for Flat Carbonate Rock and Manatee Grass	14
6	Bottom Reflectance Spectra for Sand Sample Collected on 7/22/80 and Sand Sample Collected on 7/26/80	15
7	Bottom Reflectance Spectra for Large Star Coral and Gorgonian Sea Fan	16
8	Bottom Reflectance Spectra for Green Algae and Encrusting Coral	17

1.0 SUMMARY

In this study the approach has been to use an existing water radiance model (WATRAD) to generate an extensive set of radiance calculations for each of twelve selected bottom types. Total radiance values were calculated at the sensor platform under two Elterman atmospheric states and for a sensor looking downward and positioned just below the sea surface. These model parameters were in turn iterated over five representative Jerlov water types. Calculations were made for nine water depths from 1 to 40 meters. All of the resulting calculations have been plotted as a series of total radiance spectra in Appendix A and compiled as tables in Appendix B. Preliminary examination of these radiance values suggest that Thematic Mapper (TM) band 2 (520-600nm) which is positioned in the spectral region of greatest light penetration will have subsequently the greatest sensitivity to water depth changes. The spectral range from 500 to 600nm is the optimum region for placement of bands for bathymetry applications. The precise location of the center wavelength and bandwidth depends both on the water clarity type and on the bottom materials. At very shallow depths the total radiance spectral regions consistent with TM1 and TM2 are dominated by the bottom reflectance spectral characteristics and especially in cases where the bottom type consist of highly reflective sands or corals. TM3 (630-690nm) appears to be for the most part insensitive to bottom type in the 0 to 3 meter range. At moderate to maximum depths (10-40m) the spectral characteristics are controlled by the atmospheric transmittance and path radiance components.

Based upon available bottom spectra from the 1980 Bahamas Photobathymetric Calibration Survey it appears that many vegetative and coral types will have similar bottom reflectance properties and that the density of bottom vegetation on a sand or highly reflective coral bottom may be the more important parameter. In summary the calculations made in the present study suggest that a bathymetry algorithm using TM data

should be partitioned into a water depth range and separate subalgorithms be applied within each region. For example, the algorithm used to calculate moderate to deep water depths should attempt to minimize errors caused by atmospheric variations.

2.0 INTRODUCTION

Algorithm development for satellite remote bathymetry has been supported by the Defense Mapping Agency (DMA) and the Office of Naval Research (ONR) in several projects [1,2,3]. Emphasis has centered on development of algorithms which utilize the Landsat green band (MSS-4) and red band (MSS-5) to map the more extensive areas of the world which receive satellite coverage. Substantial efforts have also been made to develop algorithms for airborne systems utilizing active passive scanners [4]. The launch of Landsat-D in July 1982 will offer still another opportunity to develop new and improve algorithms to chart the shallow waters using the thematic mapper (TM) bands. The availability of three (TM) bands, one of which is optimally located for shallow water penetration, plus greater radiometric sensitivity should result in greater water depth mapping accuracy. With the prospect for continued development of new spaceborne sensors it becomes important that the optimum bands be determined for remote bathymetry.

In a previous study emphasis was placed on analysis for optimum spectral bandwidth and band location for use in satellite bathymetry [5,6]. In these studies the ERIM water radiance model WATRAD was used to examine spectral bandwidth and band location for operating in three Jerlov water types and under three atmospheric states. These calculations assumed a single bottom reflectance spectrum for a sand type bottom. Experience has indicated that processing techniques must be developed which account for varying bottom reflectivity. It has been suggested that we need sensors to operate with spectral bandwidths and locations relative to different bottom communities so that depth accuracy is enhanced. Previous use of band ratio techniques have been limited because of the high attenuation of the red wavelengths in Landsat band MSS-5. In the previous study it has been suggested that spectral bands could be placed so that the effects due to different bottom vegetation communities will be minimized or can be removed by processing.

In this regard, it may be possible to spectrally discriminate bottom communities using techniques developed for terrestrial vegetation. One approach is to provide separate depth calculations be made for each community or vegetation class. In the present study we investigated and analyzed the catalog of spectral measurements collected under the 1980 calibration survey and examined the opportunities to operate with a methodology which will reduce the need to separate bottom communities.

The 1980 Grand Bahama Bank Photo-Bathymetric calibration Survey has provided detailed bottom reflectance measurements for representative bottom communities. Survey areas are shown in Figure 1. These spectra have been assembled into a catalog of reflectance spectra to aid technique development [7]. One of the primary objectives of this study is to analyze this catalog of spectra and make sufficient calculations from which one can determine the feasibility of an approach which reduces the need to separate bottom communities. In addition the spatial effects of different percentages of two or more types within a sensor resolution element must be examined since the combined spectra would contain different spectral features. The objective is to determine which pair of bands would eliminate or effectively reduce the expected depth error due to varying bottom reflectivity. The approach taken in this study was to first make a large number of parametric radiance calculations based upon representative bottom sample spectra. These calculations were then in turn analyzed and interpreted on a preliminary basis for optimum band selection.

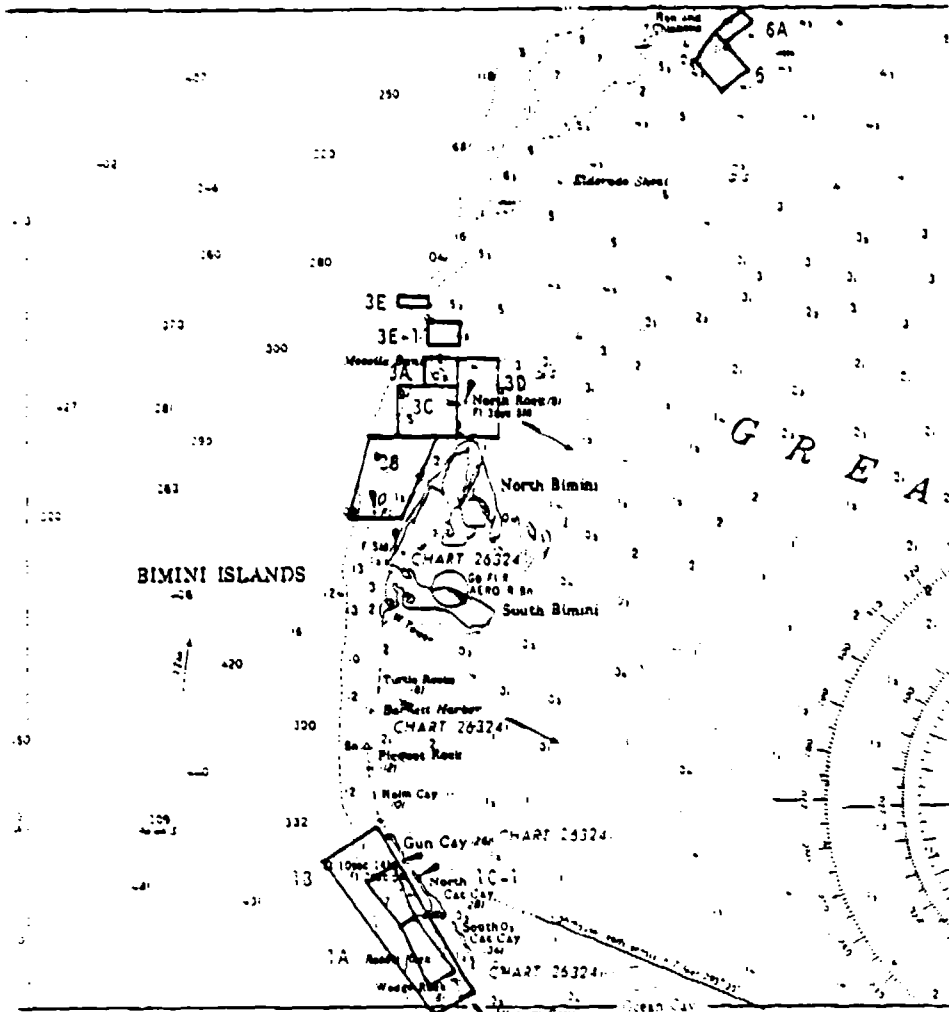


Figure 1. Portion of the Bahamas Photobathymetric Calibration Survey Areas

3.0 RADIANCE CALCULATION PROCEDURE

A previously developed water radiance model WATRAD was utilized to radiometrically simulate the atmospheric state, air/water interface, scattering and absorption losses in the water, and reflection from a shallow bottom surface. Knowing the spectral radiance at the detector the problem is then seen to be one of adjusting the parameters of the detector system in order to produce an output signal suitable to the bathymetry application. Consideration was not given to the detector spectral or spatial apertures. The theoretical water radiance model is described in section 3.1. The selection of model parameters is discussed in section 3.2 and the computational results are described in section 3.3.

3.1 WATER RADIANCE MODEL

The interaction of light with shallow water bodies is described by physical optics and the radiative transfer equation. Basically, the process involves reflection and refraction at the water surface, volume scattering and absorption in the water column, and reflection from the bottom substrate. The water radiance model used to calculate total radiance values for selected bottom types is a modification of the quasi-single scattering approximation. This model includes effects from bottom reflection, from the air-water interface, from scattering by particles, Rayleigh scattering, and absorption. This approximation has computational speed over numerical integration or Monte Carlo solutions of the exact radiative transfer equation and yield results within in the range of measurement accuracy. In the WATRAD program an atmospheric model is combined with the water radiance model to estimate the radiance, L_2 , for an airborne or satellite platform. In this model the total radiance received by the sensor is given by the following equation.

$$L_z = [n^2 T_s L_w + r_s L_s] T_a + L_p$$

where n = index of refraction
 T_s = transmittance of the air-water interface
 L_w = upwelling underwater radiance
 r_s = reflectance of the air-water interface
 L_s = sky radiance
 T_a = atmospheric transmittance
 L_p = path radiance.

Previous evaluation of this model has shown it to closely approximate field photometer and airborne scanner measurements [2]. The version of WATRAD used in the present program provides a means of simulating the entire radiometric path from extraterrestrial solar radiation through the atmosphere, through the air/water interface, through the water column, reflection from the bottom material, back to the aperture of the airborne sensor. Calculations were made in the present study using noise free parameters. Versions of WATRAD have been constructed to allow calculation of the distribution of radiance values when the detector system, atmospheric haze, or bottom reflectance is considered noisy.

3.2 SELECTION OF MODEL PARAMETERS

There are two sets of parameters for the WATRAD model. The atmospheric parameters include horizontal visibility (related to optical thickness), sensor platform altitude, aerosol type, solar zenith angle, and view angle. The water parameters include irradiance attenuation coefficient, volume scattering function, and bottom reflectance. In order to test the sensitivity of band selection on atmospheric state calculations were made for two modified Elterman atmospheres with horizontal visibilities of 23 and 10 km representing a clear and slightly hazy condition. Aerosol particle size distributions were assumed to be

represented by Diermendjian values for marine haze [8]. The optical differences in model atmospheres is due principally to concentration of haze forming aerosol particles which are large compared to visible wavelengths. As a result optimum band selection is somewhat independent of atmospheric state and also sensor altitude [5]. Calculations were also made for the case of a sensor positioned just below the sea surface. Nine water depths were selected between 1 and 40 meters at a spacing defined by equal amounts of light attenuation. The primary parameters driving these radiance calculations were bottom reflectance and water type. As discussed above the goal is to develop remote bathymetry methods which minimize the effects of varying bottom reflectance. Selection of water types refers specifically to the irradiance attenuation coefficient (K) which was used to scale the values of the absorption and scattering coefficients within the water radiance model. Values of K selected were those for five Jerlov water types: Clear Oceanic I, II, III, and Coastal 1,3 [9]. K -values provided by Jerlov were interpolated and extrapolated using cubic spline techniques to values at sixty one wavelengths needed for these radiance calculations. Resulting K -spectra are shown in Figure 2. Corresponding scattering functions were obtained from Kullenberg's measurements in the Sargasso sea and from Petzold's measurements [10,11]. The scattering function was approximated by first decomposing the total volume scattering function into a Rayleigh and a particulate component. The Rayleigh portion was taken as 0.002m^{-1} at 0.53 microns with functional form of λ^{-4} . The particle volume scattering function was assumed to be independent of the wavelength and scaled by the value of K . The water types selected describe conditions over a broad range from those of the clearest oceanic waters (Jerlov Type I) to those of many coastal waters (Jerlov Coastal Type 3). This latter water clarity probably represents typically best conditions for many coastal waters. Generally typical conditions for most coastal waters are worse than water type 3. As part of the 1980 calibration survey extensive reflectance measurements were

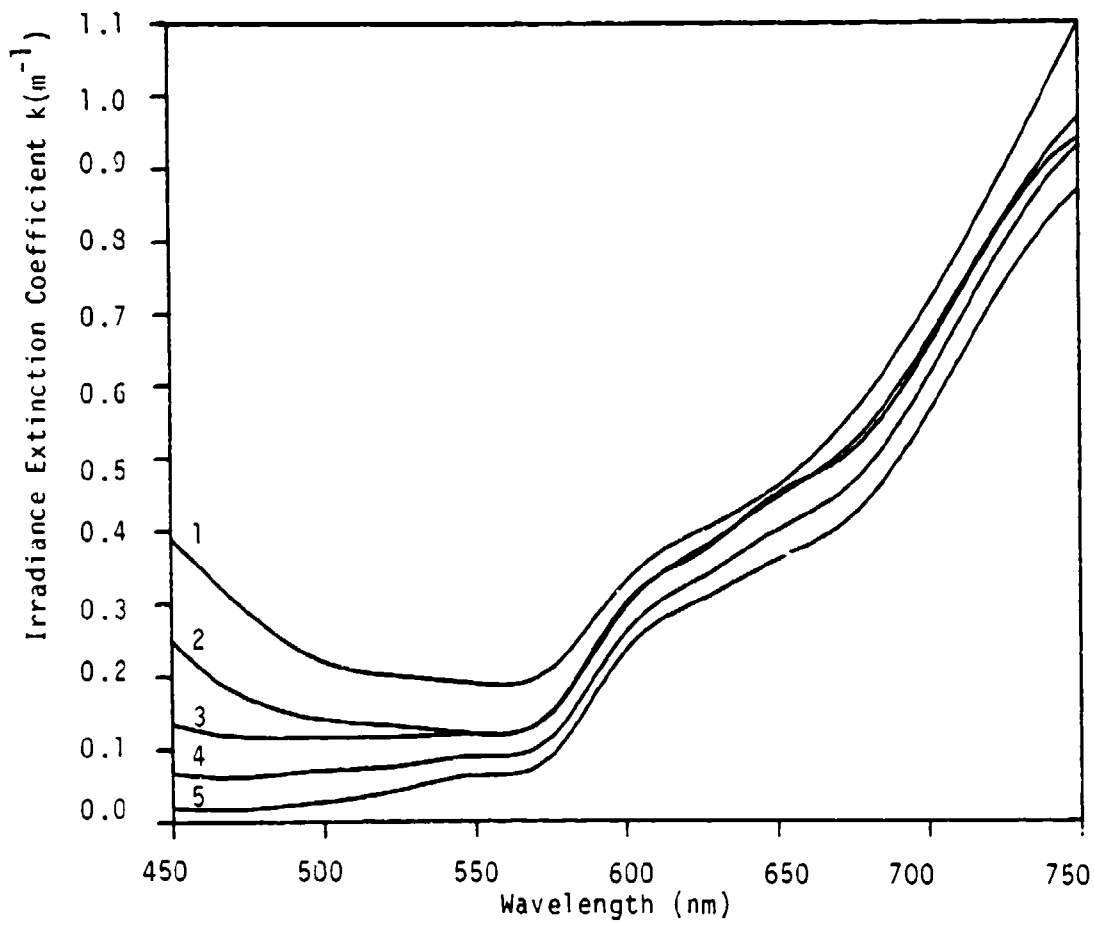


Figure 2. Irradiance Extinction Coefficient for Five Water Types: Clear Oceanic Types I(1), II(2), III(3), and Coastal Types 1(4) and 3(5).

made for bottom samples collected near Bimini Island. The measurements were subsequently assembled into a catalog of bottom reflectance spectra [7]. From these spectra we selected the following twelve representative samples which were used in these model calculations.

1. Algal Mat Mixture
2. Fire Coral
3. Gorgonian Sea Fan
4. Large Star Coral
5. Green Algae
6. Encrusting Coral
7. Coraline Sand
8. Bottom Sand 7/22/80
9. Bottom Sand 7/19/80
10. Flat Carbonate Rock
11. Manatee Grass
12. Turtle Grass

Individual spectra for each of these bottom samples is shown in Figures 3 through 8. Each plot is a spline approximation to the sixty one separate wavelengths at 5 nm intervals from 450 to 750nm. These bottom sample types were considered representative of the dominant communities found in the vicinity of Bimini Island and elsewhere on the Great Bahama Bank [12].

3.3 COMPUTATIONAL RESULTS

The combination of possible parameters as discussed above resulted in generating 180 separate data sets each consisting total radiance values at sixty-one wavelengths and nine water depths. Thus nearly 100,000 model calculations were made in the present effort. This large volume of results has been organized and presented as total radiance spectra in appendix A and as tabular values in Appendix B. Indexes to both appendices describe the individual configuration of parameter values used in the to generate the radiance values.

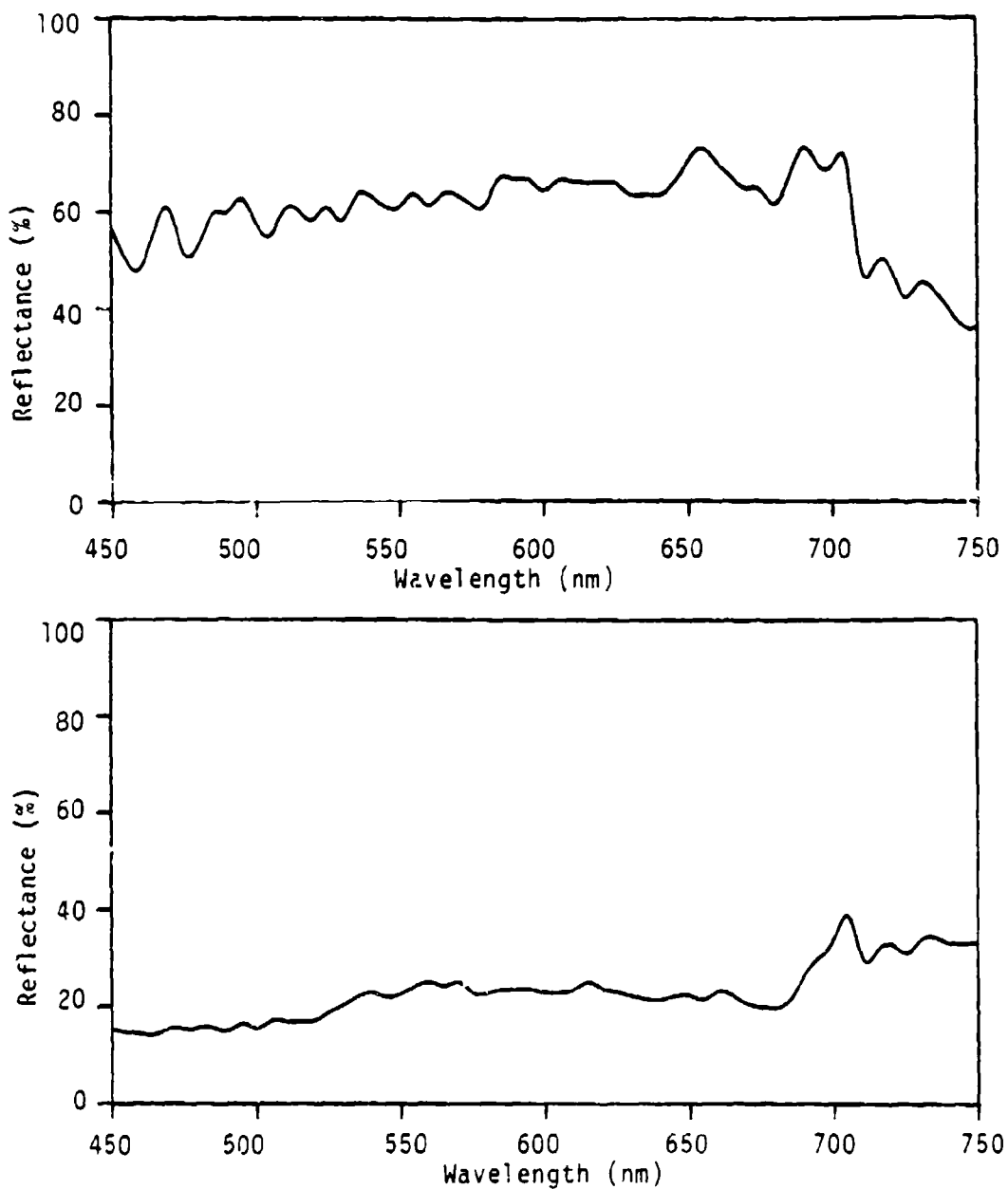


Figure 3. Bottom Reflectance Spectra for Pure Coraline Sand (Upper Panel) and Turtle Grass (Lower Panel).

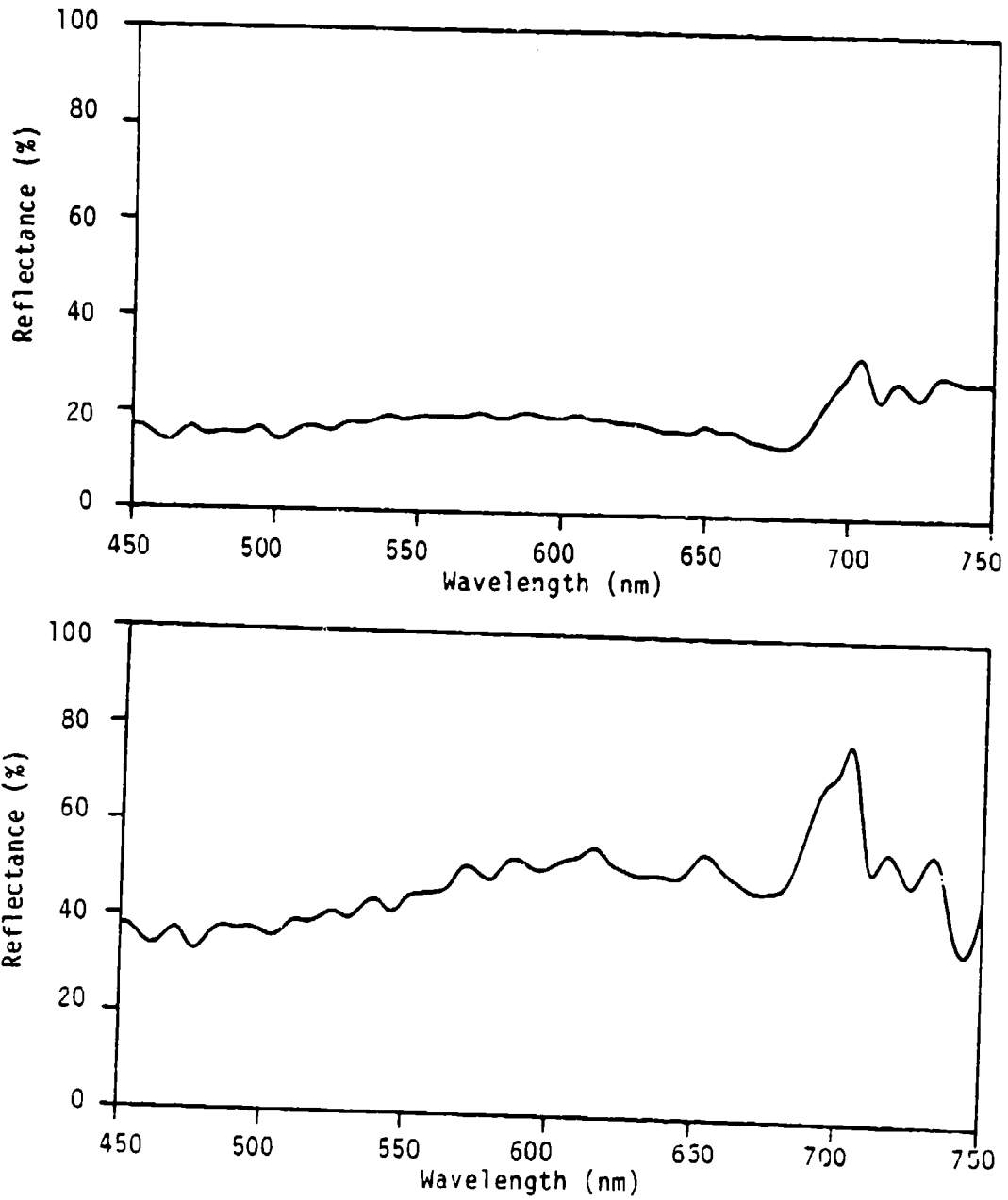


Figure 4. Bottom Reflectance Spectra for Algal Mat Mixture (Upper Panel) and Fire Coral (Lower Panel).

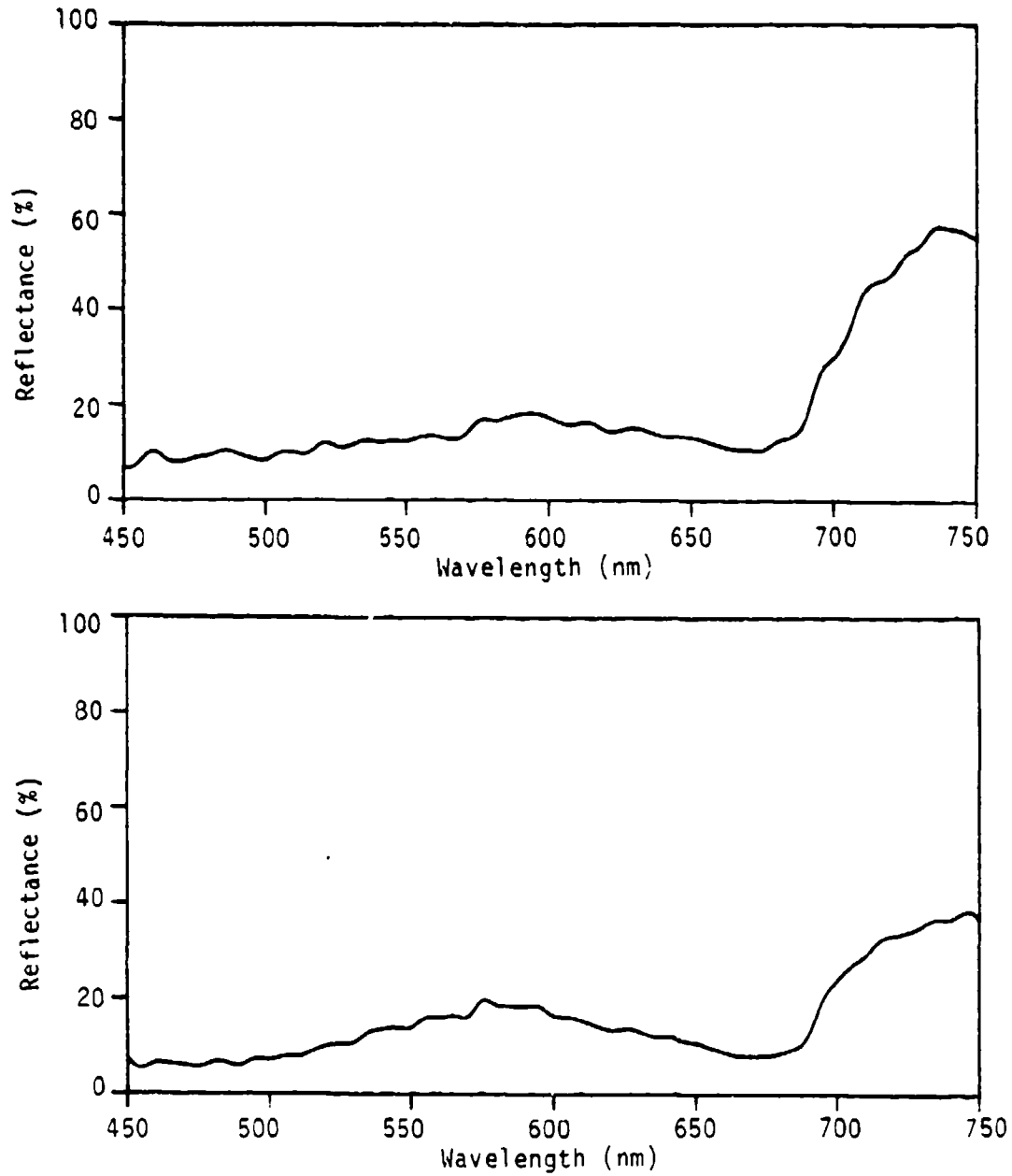


Figure 5. Bottom Reflectance Spectra for Flat Carbonate Rock (Upper Panel) and Manatee Grass (Lower Panel).

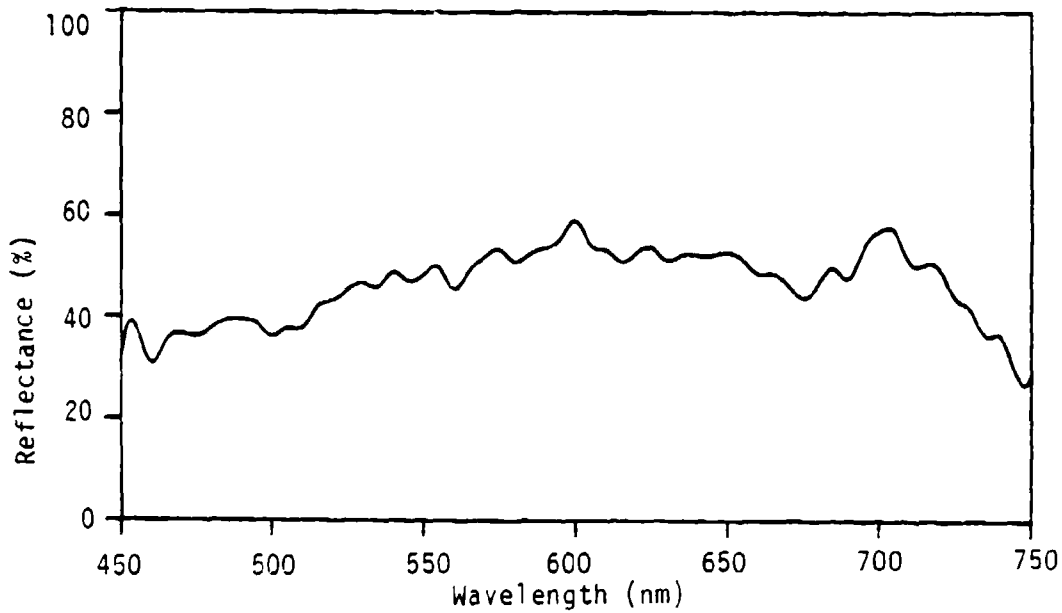
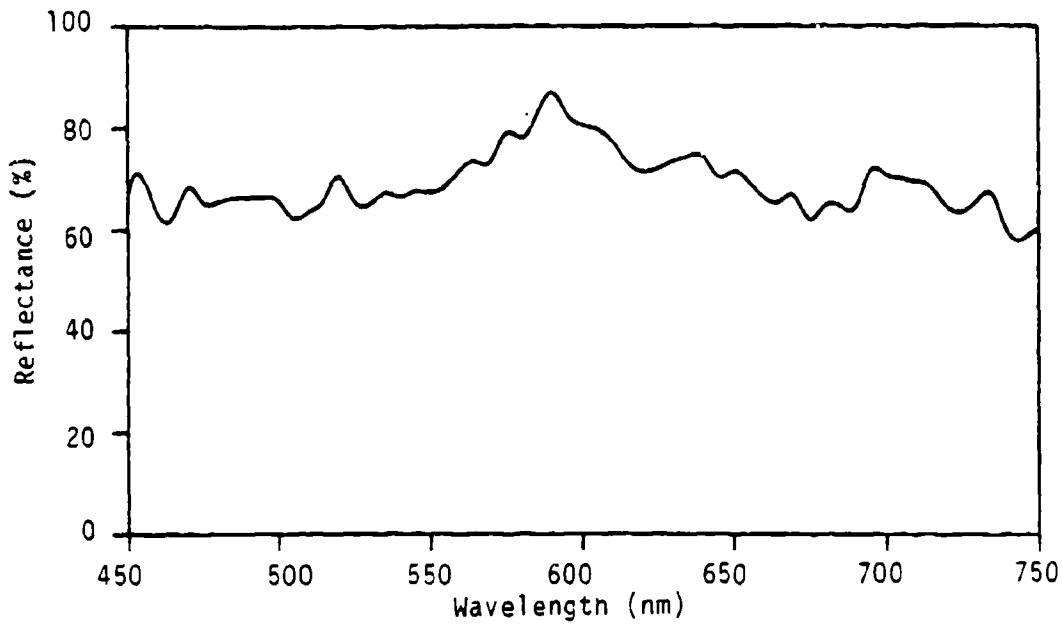


Figure 6. Bottom Reflectance Spectra for Sand Sample Collected on 7/22/80 (Upper Panel) and Sand Sample Collected on 7/26/80 (Lower Panel).

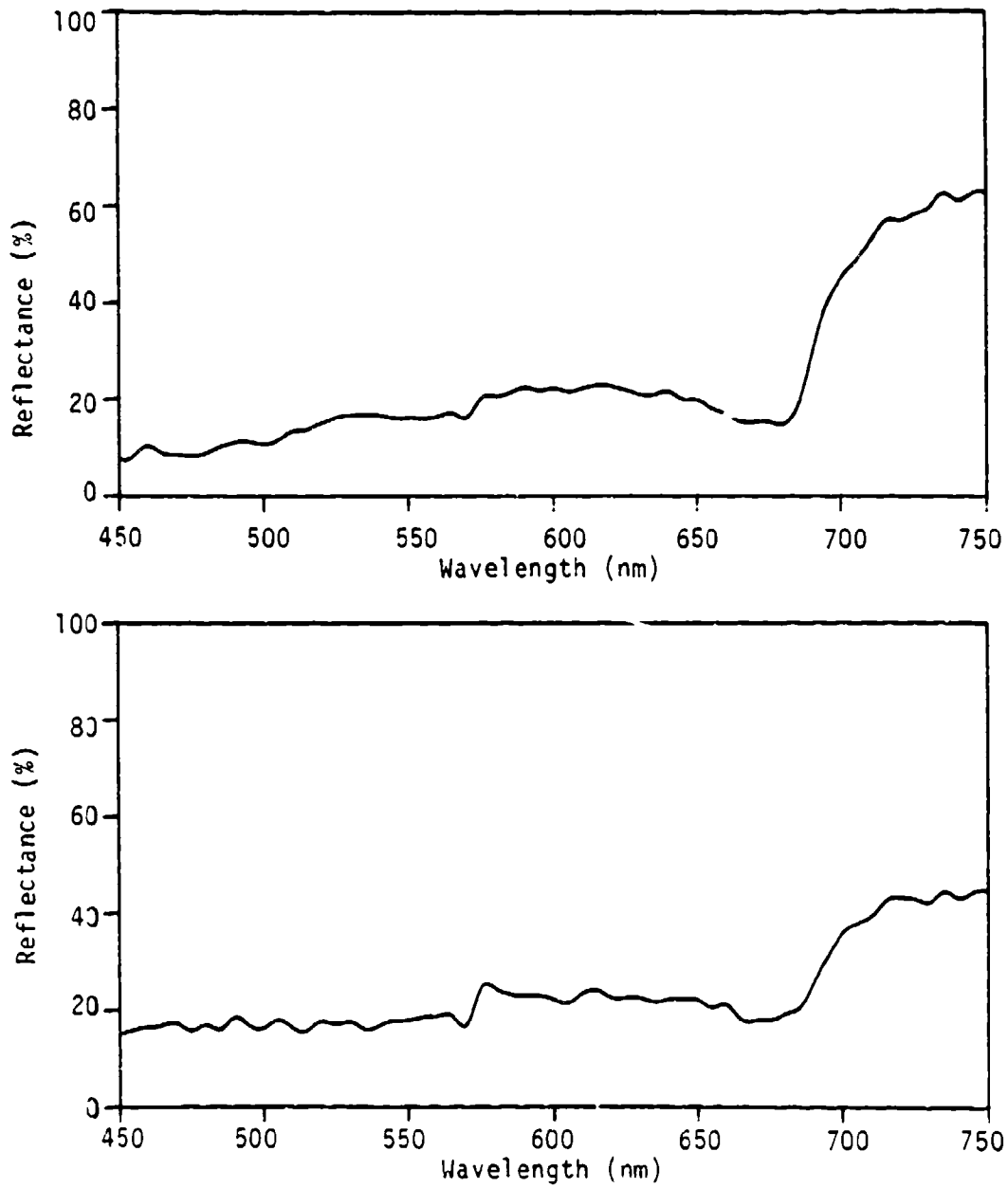


Figure 7. Bottom Reflectance Spectra for Large Star Coral (Upper Panel) and Gorgonian Sea Fan (Lower Panel).

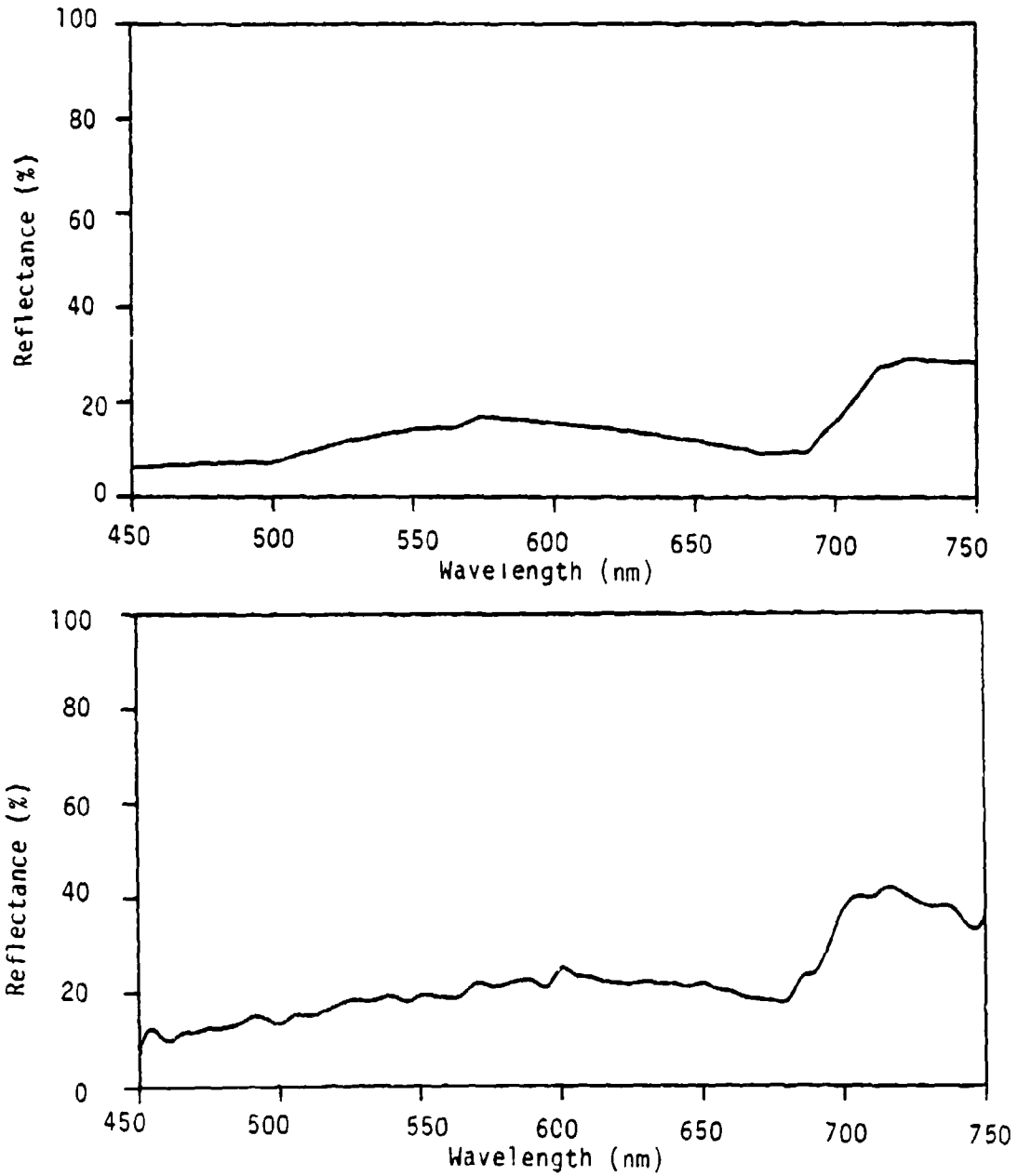


Figure 8. Bottom Reflectance Spectra for Green Algae (Upper Panel) and Encrusting Coral (Lower Panel).

4.0 PRELIMINARY BAND ANALYSIS AND INTERPRETATION

The radiance spectra and corresponding numerical values of appendices A and B show the input sensitivity of a spaceborne detector to water depth for all wavelengths between 450 and 750 nm. Furthermore this sensitivity is demonstrated for several bottom types, water types, and atmospheric states. One can make a visual examination of the figures in appendix A in order to gain insight as to what spectral bands look most promising for the bathymetry application. In studying these results we first noted, as expected, that the sand bottom radiances were substantially more sensitive to water depth than calculations made with any vegetative type. The greatest sensitivity is shown in those cases where the remote sensor is placed below the surface. The introduction of an atmosphere (visibility equals 23 and 10 km) into the calculations greatly reduces radiometric differences in signal due to water depth. In our model this loss is entirely due to the transmittance of the atmosphere. Comparing the below the surface cases to those with 50 km of atmosphere the latter curves are elevated by the path radiance term. A statistical analysis of all total radiance values given in appendix B as generated by the WATRAD model is beyond the scope of the present effort. It was agreed by DMA that a sufficient analysis would be one that is preliminary and made largely by visual interpretation. We have examined the spectral curves in Appendix A and on that basis make the following comments with attention to TM bands since TM is the next sensor of opportunity for satellite bathymetry. There are three TM bands which are appropriate to bathymetry calculations: TM1(450-520nm), TM2(520-600nm), and TM3(630-690nm). In the depth range of 10 to 40 meters the shape of the radiance spectra is controlled by the atmospheric path radiance contribution and that due to specular reflectance of skylight. In general the greatest sensitivity to water depth occurs in TM2. TM3 will be sensitive to depths less than 5 meters (600-750nm). Higher irradiance attenuation associated with a decrease in water

clarity results in an increased sensitivity at the shallower depths and a corresponding decrease at greater depths. The expected condition can be seen dramatically by comparing spectral curves for Jerlov water types I and II for a sensor position just below the sea surface. In the former there can be observed for several bottom types including large star coral the absence of any sensitivity to depth for wavelengths smaller than 475nm. The displacement of the curves which essentially superimpose each other is due to the backscatter of light from the water column. In the case of Jerlov II for the same model parameters there exist radiance differences across the same depth range. Shallow water spectra reflect detailed characteristics of the bottom reflectance curve used in making the model calculations. In this regard the small undulation observed in many of the spectral curves at 575nm is also present in the bottom reflectance curves and are probably due to measurement instrumentation rather than actual bottom reflectance spectral characteristics. In general there is a decreasing sensitivity of total radiance to depth for greater depths across the entire spectral region of study (450-750nm). In going from a clear (visibility=23km) atmosphere to one with noticeable haze (visibility = 10km) there is an increase in the spectral radiance due to increase in the path radiance component and a slight decrease in the sensitivity of total radiance to water depth. There does not appear to be two or more bands in the region of maximum penetration which could be used to discriminate bottom type. TM3 appears to be capable of discriminating very shallow water depths (0-3m) with minimum sensitivity to bottom type. For depths greater than three meters radiance in TM3 is largely absorbed and this band becomes ineffective for direct discrimination of water depths.

A brief investigation was made into the significance of bottom type mixtures. A single band regression algorithm was applied to radiance values contained in Appendix B. First a mixture of two very distinct bottom types was considered, pure sand (sample from 7/26/80) and algal mat mixture. Radiance table values in the TM2 band were average and

then regressed against the water depth parameter. Separate regressions were made for weighted mixtures of 0, 20, 40, 60, 80, and 100 percent sand bottom type and the balance as algal mat mixture. Individual regression equations had the following form.

$$z = C_1 L_N(\Delta L) + C_2$$

where ΔL is the total radiance difference between deep water and at depth z . The regression coefficient C_1 was found to be nearly independent of mixture with an approximate value of -7.0 . Values of C_2 were determined to be 7.5, 9.7, 11.4, 12.8, 14.2, and 14.6, respectively for each of the above weighted mixtures. Thus, plotted as depth z versus $L_N(\Delta L)$ these mixture single band depth equations are represented as a series of parallel lines.

As a second effort the same analysis was performed for two spectrally similar bottom types, flat carbonate rock and manatee grass. The resulting regression equations were for practical purposes indistinguishable. These results suggest that small changes in mixture of two very distinct bottom types may be more important to the bathymetry problem than consideration of separate vegetative and coral types. Further it may be impossible to distinguish without highly detailed spectral measurement a mixture of sand and vegetation from some other vegetation or coral type. In this regard a ratio of $TM2/TM3$ may be useful to discriminate bottom type with large differences in reflective properties. However, a more complete analysis of the tabulated radiance values is needed to understand the importance of individual vegetative types.

REFERENCES

1. E. Doak, J. Livisay, D. Lyzenga, J. Ott, and F. Polcyn, Evaluation of water depth extraction techniques using Landsat and aircraft data, ERIM Report No. 135900-2-F, January 1980.
2. D.R. Lyzenga, Coastal remote sensing investigations, Volume 1: Marine Environment, ERIM Report No. 134400-11-F, April 1980.
3. D. Lyzenga and J. Livisay, Documentation of computer software for multispectral bathymetry analysis, ERIM Report No. 148900-1-F, April 1980.
4. D.R. Lyzenga, J.S. Ott, J.P. Livisay, and F.C. Polcyn, Remote bathymetry with a multispectral active/passive airborne system, ERIM Report No. 149600-1-F, February 1982.
5. D.R. Lyzenga and F.C. Polcyn, Analysis of optimum spectral resolution and band location for satellite bathymetry, ERIM Report No. 128200-1-F, January 1978.
6. D.R. Lyzenga, C.T. Wezernak, and F.C. Polcyn, Spectral band positioning for purposes of bathymetry and mapping bottom features from satellite altitudes, ERIM Report No. 115300-5-T, 1976.
7. F.C. Polcyn, F.J. Tanis, and J.P. Livisay, Photo-bathymetric calibration project Great Bahama Bank, 7 July - 2 August 1980, ERIM Report 154100-9-F, May 1982.
8. D. Deirmendjian, Electromagnetic scattering on spherical polydispersions, Elsevier, New York, 1969.
9. N.G. Jerlov, Optical Oceanography, Elsevier Pub. Co., Amsterdam, 1968.
10. G. Kullenberg, Scattering of light by Sargosso Sea Water, Deep-Sea Research 15, 423, 1968.
11. T.J. Petzold, Volume scattering functions for selected ocean waters, Vis. Lab. Tech. Rep. 72-78, Scripps Institution of Oceanography, 1972.
12. L.L. Stewart, University of Connecticut, Marine Sciences Institute, March 1982, Personal communication.

APPENDIX A

TOTAL RADIANCE SPECTRA FOR SELECTED BOTTOM TYPES

This appendix contains spectral plots of radiance values ($\text{mW} \cdot \text{micron}^{-1} \cdot \text{cm}^{-2} \cdot \text{sr}^{-1}$) for twelve representative bottom types. These values were generated using the Environment Research Institute of Michigan's (ERIM) water radiance and atmospheric radiation transfer model (WATRAD).¹ These plots describe spectral variations in total radiance as a function of bottom type flora, atmospheric state and water type. Each figure panel contains nine separate spectra corresponding to nine water depths (1.0, 2.0, 3.0, 5.0, 7.0, 10.0, 15.0, 25.0, 40.0 meters). The uppermost spectral curve in each figure has a water depth value of 1.0 meters. The lowest spectra corresponds to 40.0 meters, etc. Total radiance values were calculated under two separate (Elterman) atmospheric states for a sensor platform altitude of 50 km. Calculations were also made for a sensor placed just below the water surface. Each of these atmospheric states was combined with five water types. The five water types are Jerlov² oceanic types I, II, III and coastal types 1 and 3 which are respectively labelled in each figure as types 1, 2, 3, 4, 5. All radiance values were calculated with a 30° solar zenith angle and a nadir view angle. A list of total radiance spectra is given in Table A1.

¹D. Lyzenga and F. Thomson. Basic remote sensing investigation for beach reconnaissance. Final technical report #1089u0-11-F, prepared for the Office of Naval Research, July 1978.

²N.G. Jerlov. Marine Optics, Elsevier Publishing Company, New York, 1976.

TABLE A1. LIST OF FIGURES
TOTAL RADIANCE SPECTRA FOR SELECTED BOTTOM TYPES

<u>FIGURE NUMBER</u>	<u>BOTTOM TYPE</u>	<u>VISIBILITY</u>	<u>WATER TYPES</u>	<u>PAGE</u>
A-1	Coraline Sand	23 KM	1,2	A-5
A-2	Coraline Sand	23 KM	3,4	A-6
A-3	Coraline Sand	23 KM	5	A-7
A-4	Coraline Sand	10 KM	1,2	A-8
A-5	Coraline Sand	10 KM	3,4	A-9
A-6	Coraline Sand	10 KM	5	A-10
A-7	Coraline Sand	N/A	1,2	A-11
A-8	Coraline Sand	N/A	3,4	A-12
A-9	Coraline Sand	N/A	5	A-13
A-10	Turtle Grass	23 KM	1,2	A-14
A-11	Turtle Grass	23 KM	3,4	A-15
A-12	Turtle Grass	23 KM	5	A-16
A-13	Turtle Grass	10 KM	1,2	A-17
A-14	Turtle Grass	10 KM	3,4	A-18
A-15	Turtle Grass	10 KM	5	A-19
A-16	Turtle Grass	N/A	1,2	A-20
A-17	Turtle Grass	N/A	3,4	A-21
A-18	Turtle Grass	N/A	5	A-22
A-19	Algal Mat Mixture	23 KM	1,2	A-23
A-20	Algal Mat Mixture	23 KM	3,4	A-24
A-21	Algal Mat Mixture	23 KM	5	A-25
A-22	Algal Mat Mixture	10 KM	1,2	A-26
A-23	Algal Mat Mixture	10 KM	3,4	A-27
A-24	Algal Mat Mixture	10 KM	5	A-28
A-25	Algal Mat Mixture	N/A	1,2	A-29
A-26	Algal Mat Mixture	N/A	3,4	A-30
A-27	Algal Mat Mixture	N/A	5	A-31
A-28	Sand 7/26/80	23 KM	1,2	A-32
A-29	Sand 7/26/80	23 KM	3,4	A-33
A-30	Sand 7/26/80	23 KM	5	A-34
A-31	Sand 7/26/80	10 KM	1,2	A-35
A-32	Sand 7/26/80	10 KM	3,4	A-36
A-33	Sand 7/26/80	10 KM	5	A-37
A-34	Sand 7/26/80	N/A	1,2	A-38
A-35	Sand 7/26/80	N/A	3,4	A-39
A-36	Sand 7/26/80	N/A	5	A-40

TABLE A1. (Continued)

<u>FIGURE NUMBER</u>	<u>BOTTOM TYPE</u>	<u>VISIBILITY</u>	<u>WATER TYPES</u>	<u>PAGE</u>
A-37	Flat Carbonate Rock	23 KM	1,2	A-41
A-38	Flat Carbonate Rock	23 KM	3,4	A-42
A-39	Flat Carbonate Rock	23 KM	5	A-43
A-40	Flat Carbonate Rock	10 KM	1,2	A-44
A-41	Flat Carbonate Rock	10 KM	3,4	A-45
A-42	Flat Carbonate Rock	10 KM	5	A-46
A-43	Flat Carbonate Rock	N/A	1,2	A-47
A-44	Flat Carbonate Rock	N/A	3,4	A-48
A-45	Flat Carbonate Rock	N/A	5	A-49
A-46	Manatee Grass	23 KM	1,2	A-50
A-47	Manatee Grass	23 KM	3,4	A-51
A-48	Manatee Grass	23 KM	5	A-52
A-49	Manatee Grass	10 KM	1,2	A-53
A-50	Manatee Grass	10 KM	3,4	A-54
A-51	Manatee Grass	10 KM	5	A-55
A-52	Manatee Grass	N/A	1,2	A-56
A-53	Manatee Grass	N/A	3,4	A-57
A-54	Manatee Grass	N/A	5	A-58
A-55	Sand 7/22/80	23 KM	1,2	A-59
A-56	Sand 7/22/80	23 KM	3,4	A-60
A-57	Sand 7/22/80	23 KM	5	A-61
A-58	Sand 7/22/80	10 KM	1,2	A-62
A-59	Sand 7/22/80	10 KM	3,4	A-63
A-60	Sand 7/22/80	10 KM	5	A-64
A-61	Sand 7/22/80	N/A	1,2	A-65
A-62	Sand 7/22/80	N/A	3,4	A-66
A-63	Sand 7/22/80	N/A	5	A-67
A-64	Large Star Coral	23 KM	1,2	A-68
A-65	Large Star Coral	23 KM	3,4	A-69
A-66	Large Star Coral	23 KM	5	A-70
A-67	Large Star Coral	10 KM	1,2	A-71
A-68	Large Star Coral	10 KM	3,4	A-72
A-69	Large Star Coral	10 KM	5	A-73
A-70	Large Star Coral	N/A	1,2	A-74
A-71	Large Star Coral	N/A	3,4	A-75
A-72	Large Star Coral	N/A	5	A-76
A-73	Gorgonian Sea Fan	23 KM	1,2	A-77
A-74	Gorgonian Sea Fan	23 KM	3,4	A-78
A-75	Gorgonian Sea Fan	23 KM	5	A-79
A-76	Gorgonian Sea Fan	10 KM	1,2	A-80
A-77	Gorgonian Sea Fan	10 KM	3,4	A-81
A-78	Gorgonian Sea Fan	10 KM	5	A-82

TABLE A1. (Continued)

<u>FIGURE NUMBER</u>	<u>BOTTOM TYPE</u>	<u>VISIBILITY</u>	<u>WATER TYPES</u>	<u>PAGE</u>
A-79	Gorgonian Sea Fan	N/A	1,2	A-83
A-80	Gorgonian Sea Fan	N/A	3,4	A-84
A-81	Gorgonian Sea Fan	N/A	5	A-85
A-82	Green Algae	23 KM	1,2	A-86
A-83	Green Algae	23 KM	3,4	A-87
A-84	Green Algae	23 KM	5	A-88
A-85	Green Algae	10 KM	1,2	A-89
A-86	Green Algae	10 KM	3,4	A-90
A-87	Green Algae	10 KM	5	A-91
A-88	Green Algae	N/A	1,2	A-92
A-89	Green Algae	N/A	3,4	A-93
A-90	Green Algae	N/A	5	A-94
A-91	Fire Coral	23 KM	1,2	A-95
A-92	Fire Coral	23 KM	3,4	A-96
A-93	Fire Coral	23 KM	5	A-97
A-94	Fire Coral	10 KM	1,2	A-98
A-95	Fire Coral	10 KM	3,4	A-99
A-96	Fire Coral	10 KM	5	A-100
A-97	Fire Coral	N/A	1,2	A-101
A-98	Fire Coral	N/A	3,4	A-102
A-99	Fire Coral	N/A	5	A-103
A-100	Encrusting Coral	23 KM	1,2	A-104
A-101	Encrusting Coral	23 KM	3,4	A-105
A-102	Encrusting Coral	23 KM	5	A-106
A-103	Encrusting Coral	10 KM	1,2	A-107
A-104	Encrusting Coral	10 KM	3,4	A-108
A-105	Encrusting Coral	10 KM	5	A-109
A-106	Encrusting Coral	N/A	1,2	A-110
A-107	Encrusting Coral	N/A	3,4	A-111
A-108	Encrusting Coral	N/A	5	A-112

Total Radiance Values (mw/(micron*cm*cm*sr))

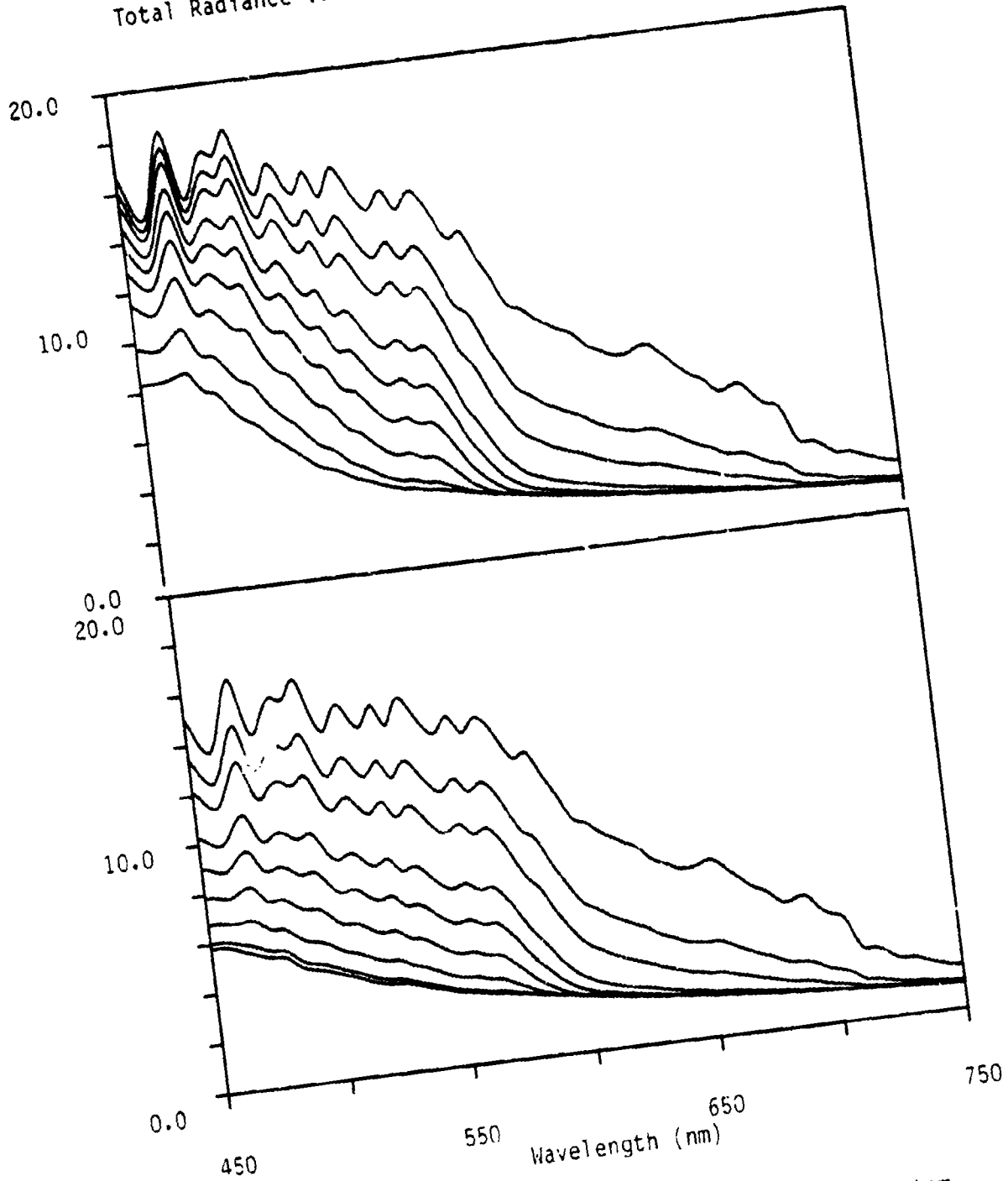


Figure A-1. Total radiance spectra for a Coraline Sand bottom type at selected water depths (1,2,3,5,7,10,15,25, and 40 m). Curves in the upper panel were generated for a visibility of 23 km and with water type 1 and in the lower panel for water type 2.

Total Radiance Values (mw/(micron*cm*cm*sr))

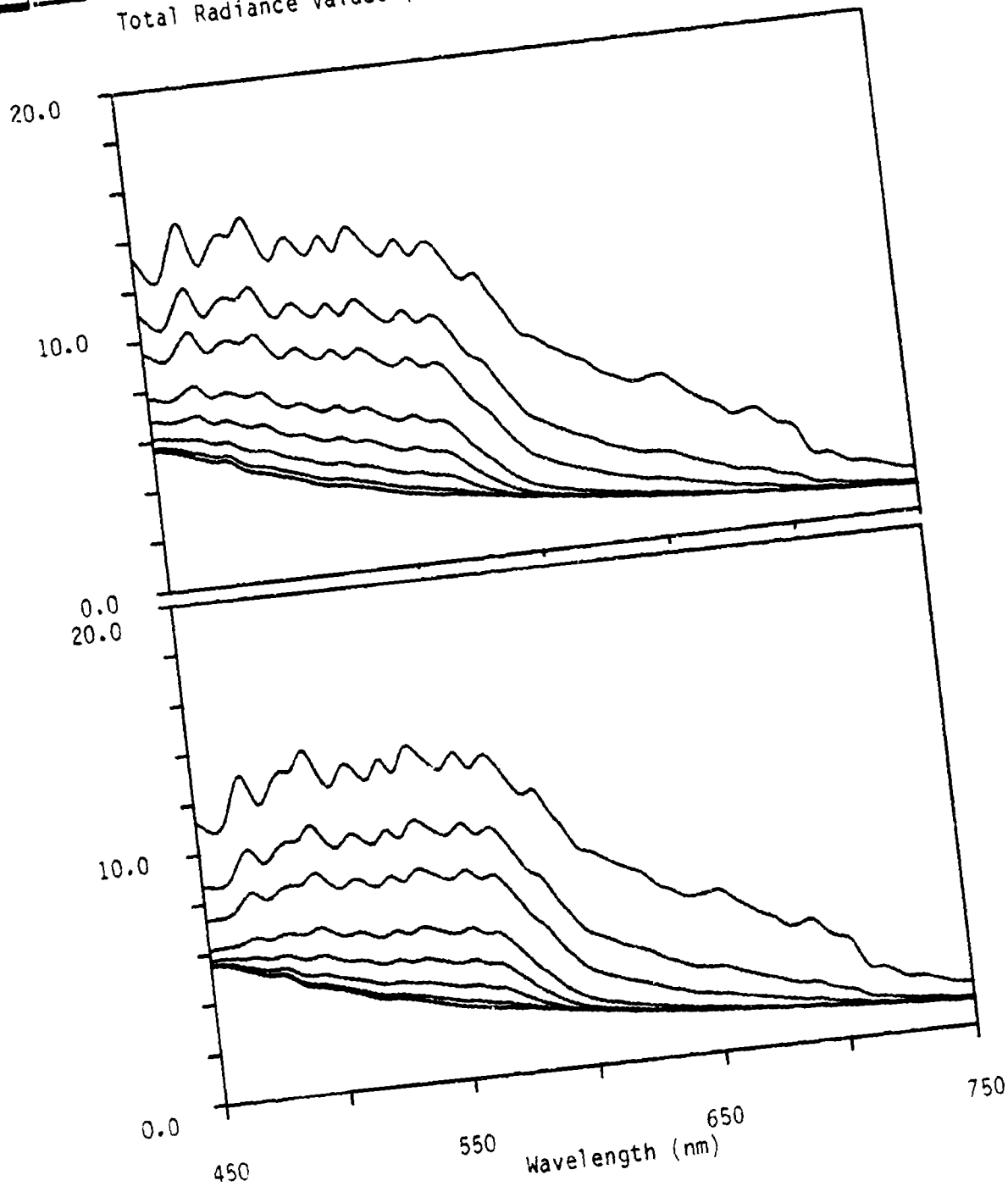


Figure A-2. Total radiance spectra for a Coraline Sand bottom type at selected water depths (1,2,3,5,7,10,15,25, and 40 m). Curves in the upper panel were generated for a visibility of 23 km and with water type 3 and in the lower panel for water type 4.

Total Radiance Values (mw/(micron*cm*cm*sr))

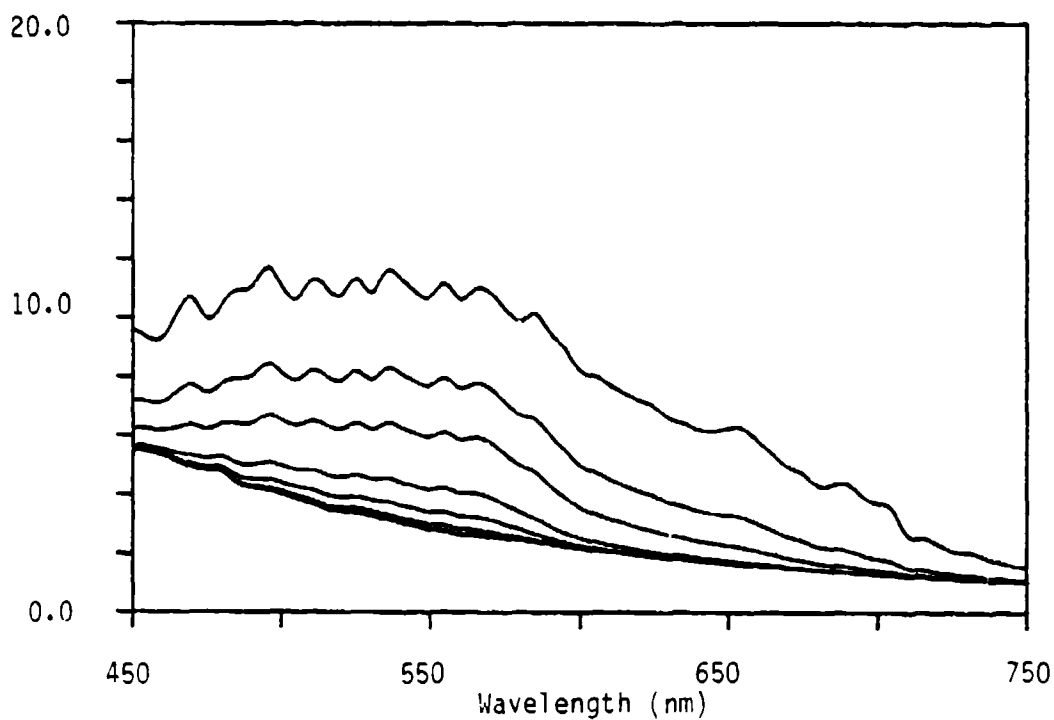


Figure A-3. Total radiance spectra for a Coraline Sand bottom type at selected water depths (1,2,3,5,7,10,15,25, and 40 m). Curves in the above panel were generated for a visibility of 23 km and with water type 5.

Total Radiance Values (mw/(micron*cm*cm*sr))

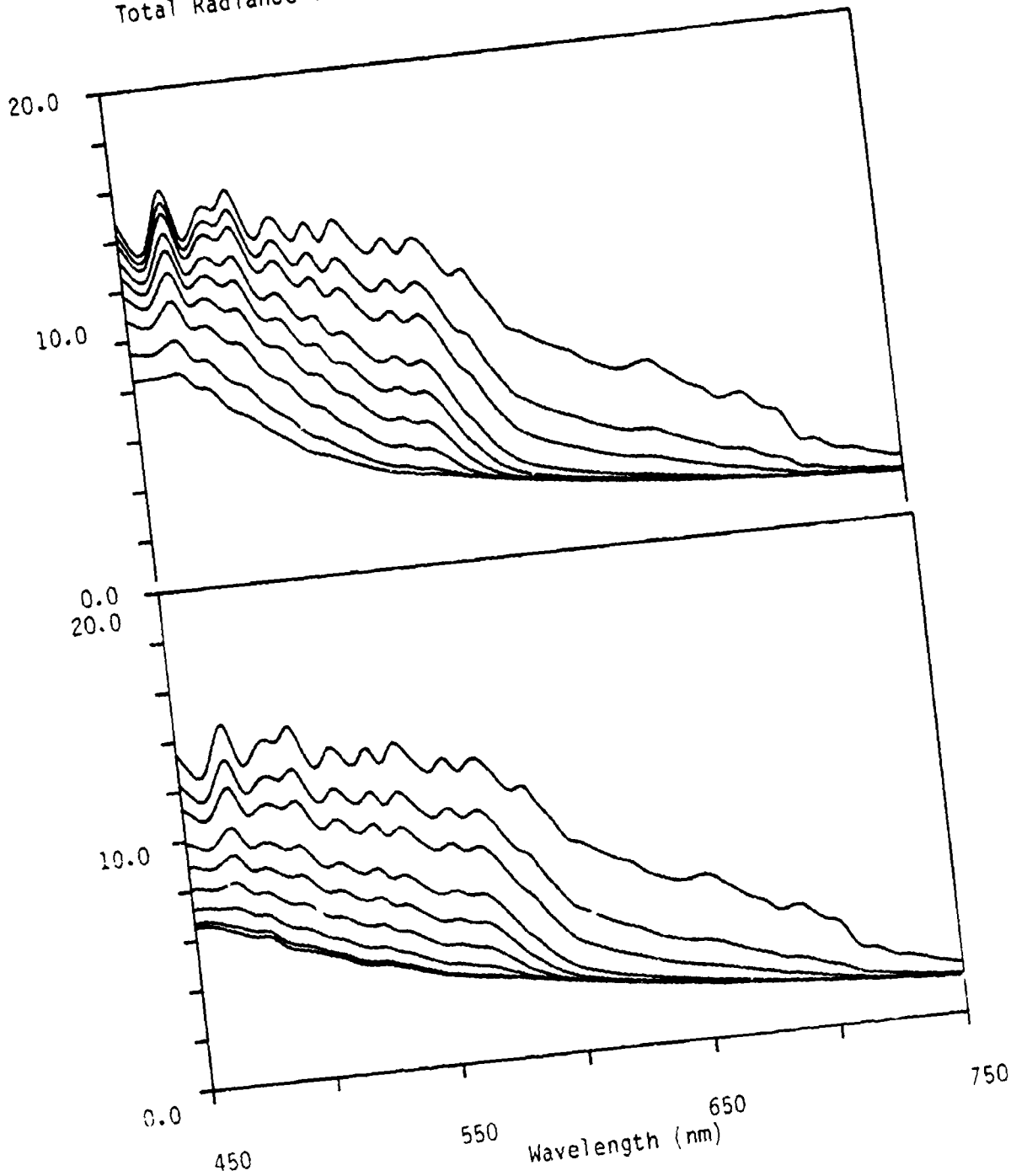


Figure A-4. Total radiance spectra for a Coraline Sand bottom type at selected water depths (1,2,3,5,7,10,15,25, and 40 m). Curves in the upper panel were generated for a visibility of 10 km and with water type 1 and in the lower panel for water type 2.

Total Radiance Values (mw/(micron*cm*cm*sr))

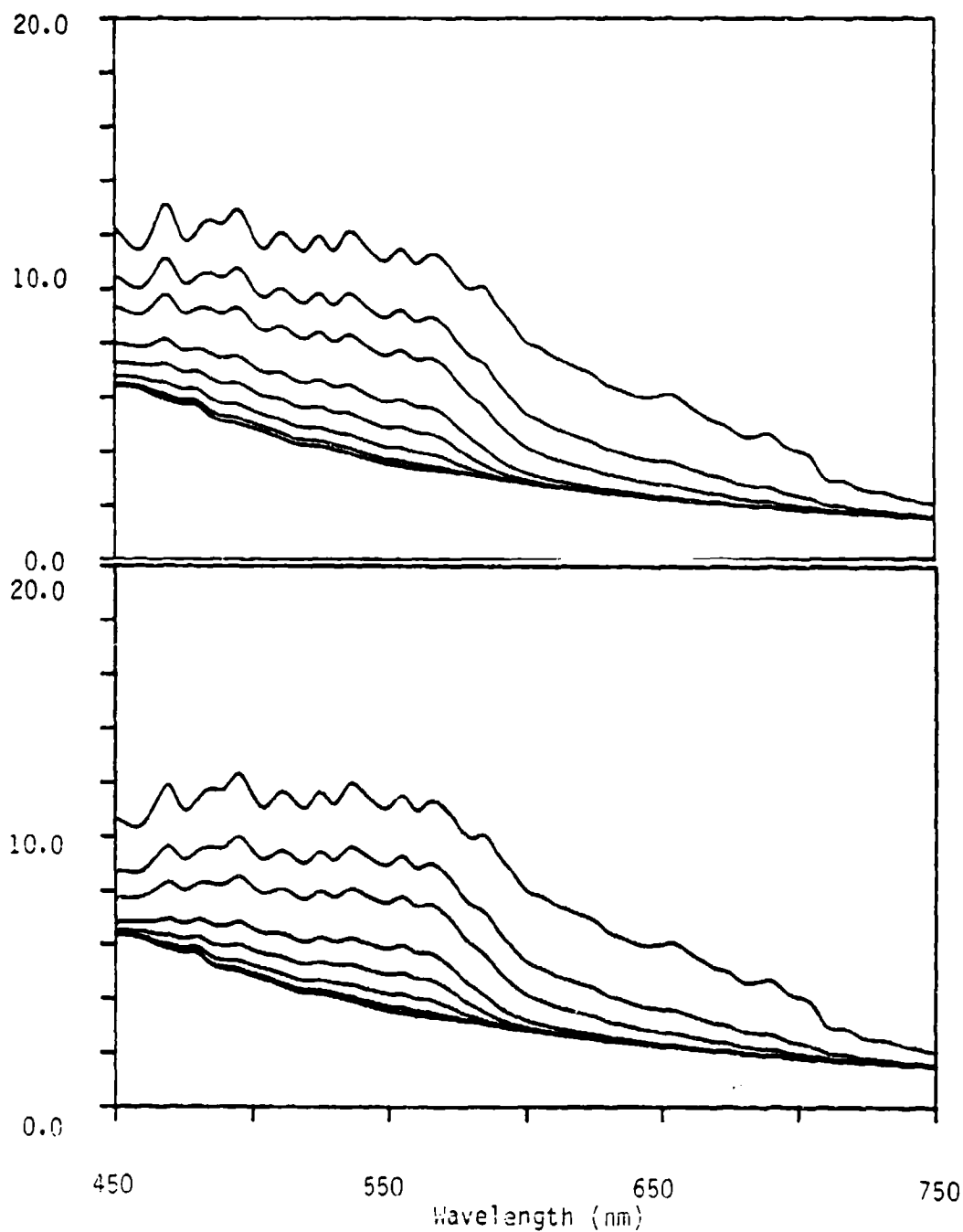


Figure A-5. Total radiance spectra for a Coraline Sand bottom type at selected water depths (1,2,3,5,7,10,15,25, and 40 m). Curves in the upper panel were generated for a visibility of 10 km and with water type 3 and in the lower panel for water type 4.

Total Radiance Values (mw/(micron*cm*cm*sr))

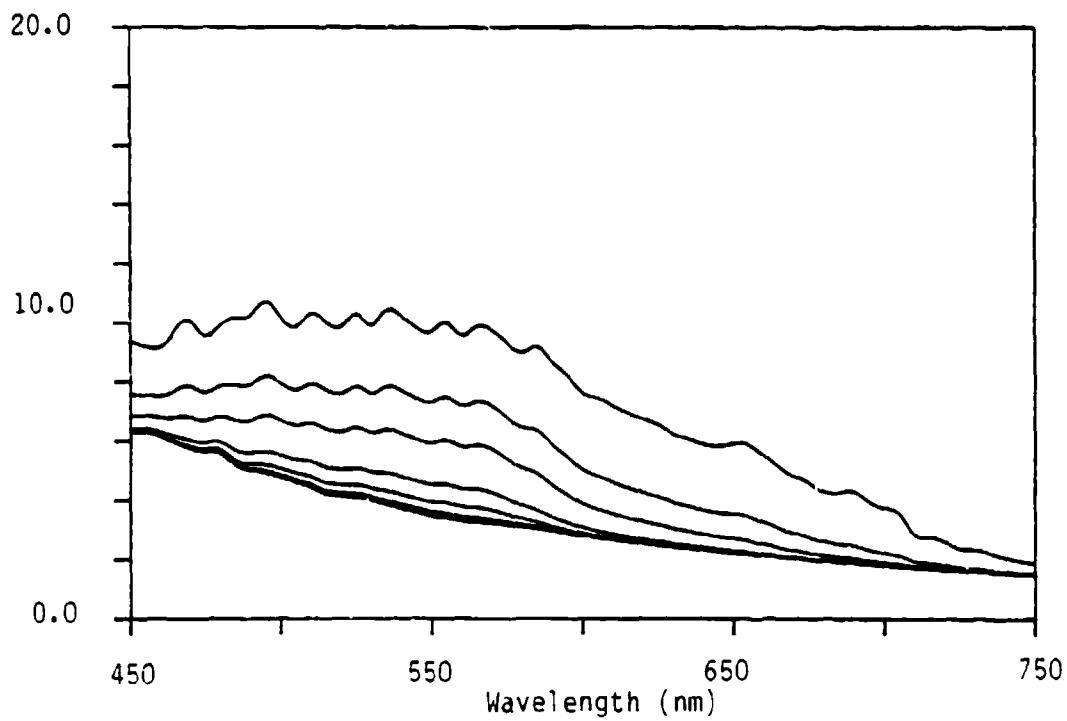


Figure A-6. Total radiance spectra for a Coraline Sand bottom type at selected water depths (1,2,3,5,7,10,15,25, and 40 m). Curves in the above panel were generated for a visibility of 10 km and with water type 5.

Total Radiance Values (mw/(micron*cm*cm*sr))

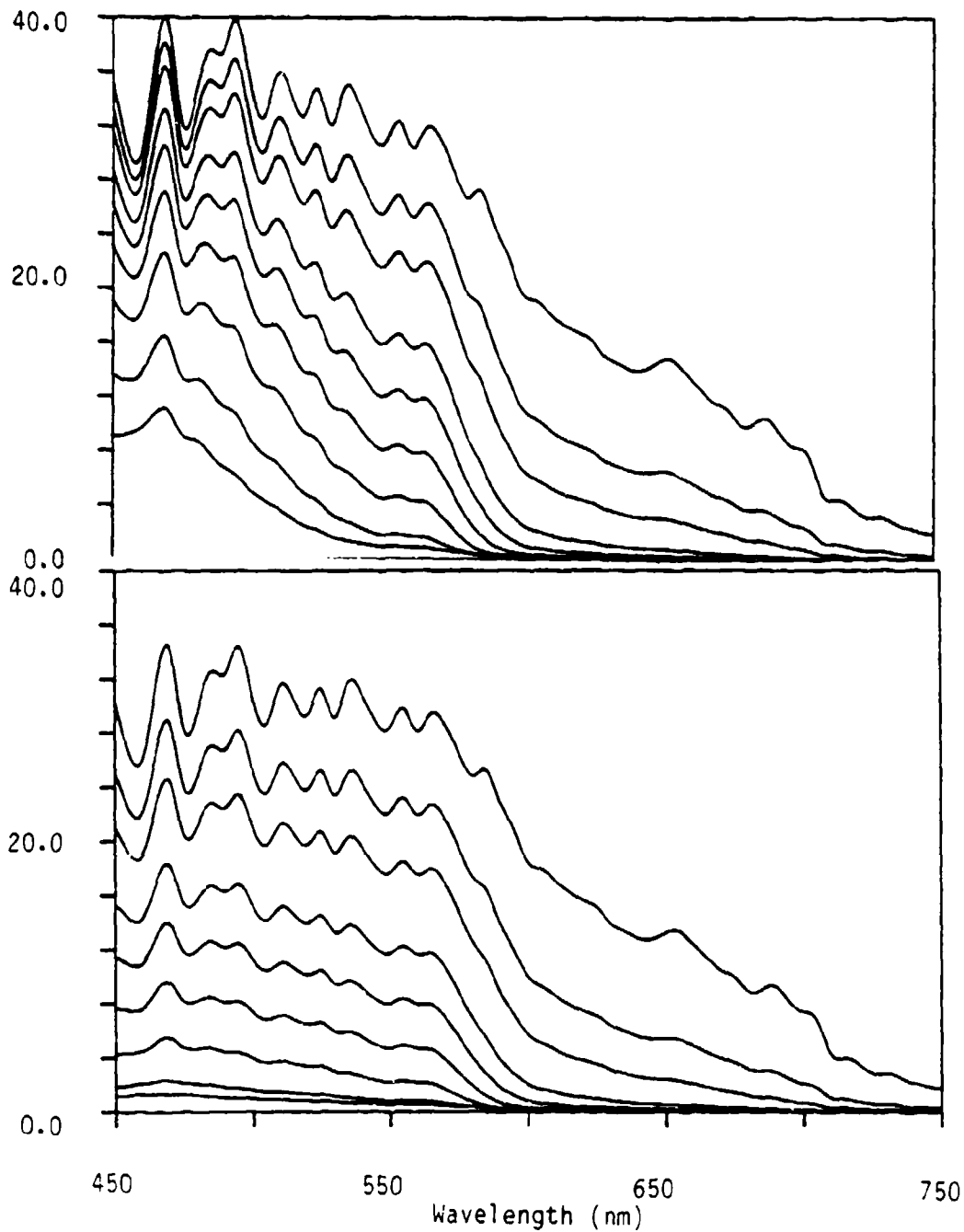


Figure A-7. Total radiance spectra for a Coraline Sand bottom type at selected water depths (1, 2, 3, 5, 7, 10, 15, 25, and 40 m). Curves in the upper panel were generated with water type 1 and in the lower panel for water type 2. Spectra were calculated for a sensor position just below the sea surface.

Total Radiance Values (mw/(micron*cm*cm*sr))

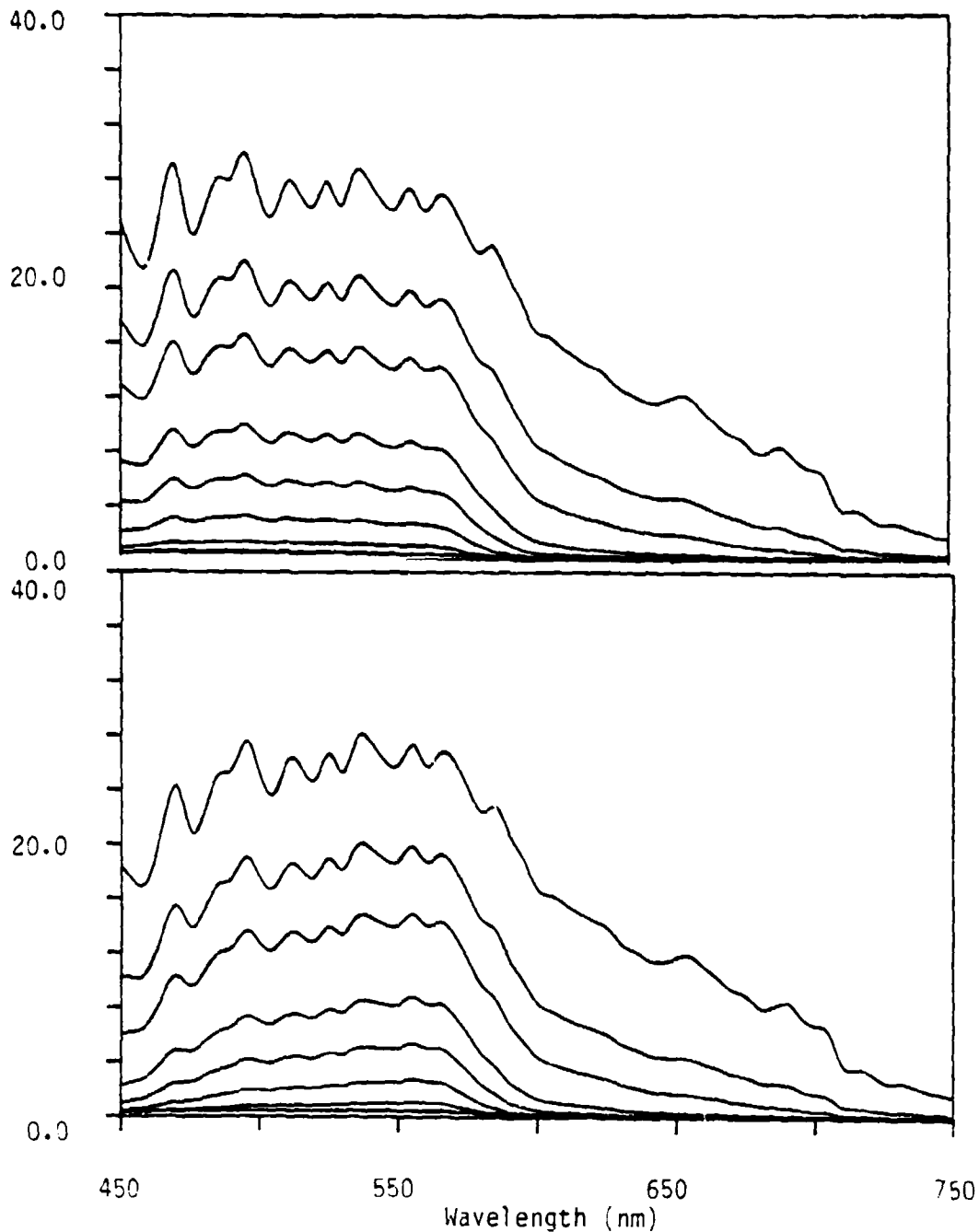


Figure A-8. Total radiance spectra for a Coraline Sand bottom type at selected water depths (1,2,3,5,7,10,15,25, and 40 m). Curves in the upper panel were generated with water type 3 and in the lower panel for water type 4. Spectra were calculated for a sensor position just below the sea surface.

Total Radiance Values (mw/(micron*cm*cm*sr))

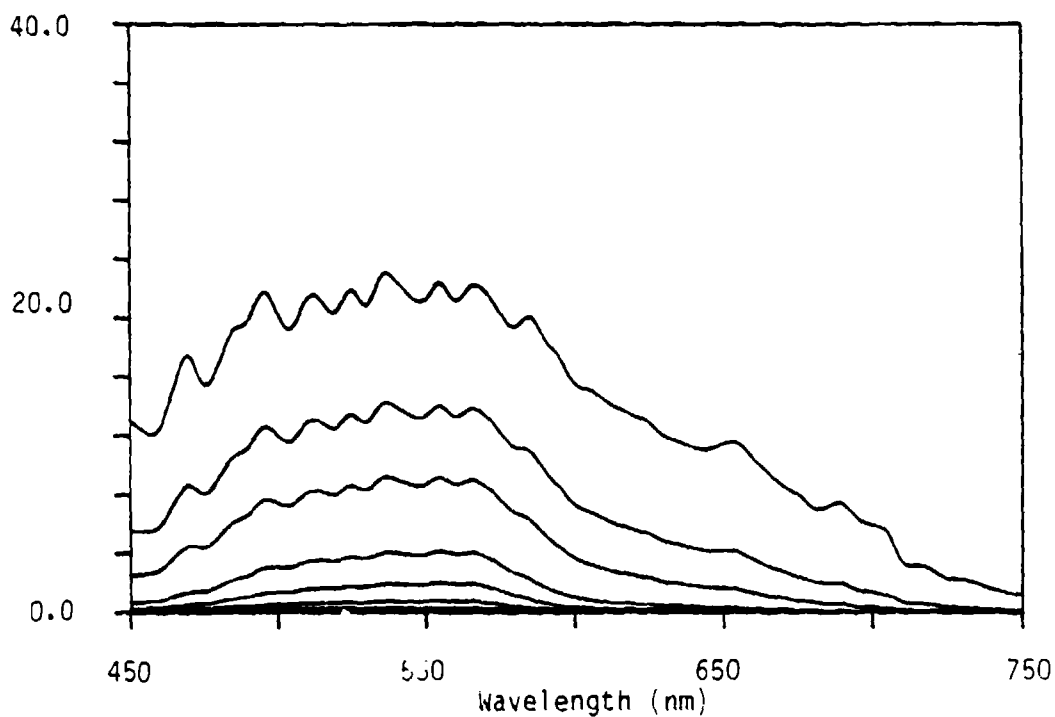


Figure A-9. Total radiance spectra for a Coraline Sand bottom type at selected water depths (1,2,3,5,7,10,15,25, and 40 m). Curves in the above panel were generated with water type 5. Spectra were calculated for a sensor position just below the sea surface.

Total Radiance Values (mw/(micron*cm*cm*sr))

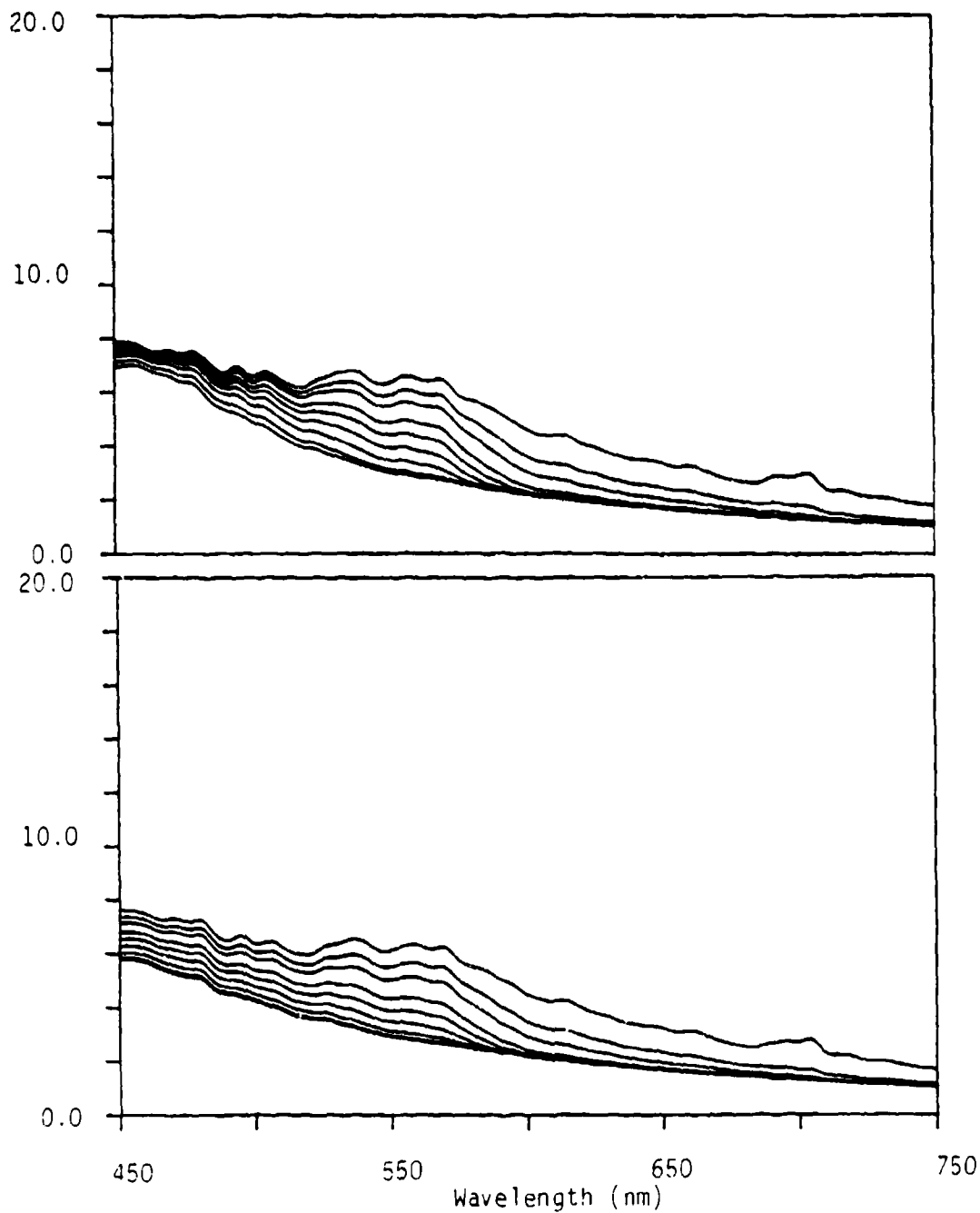


Figure A-10. Total radiance spectra for a Turtle Grass bottom type at selected water depths (1,2,3,5,7,10,15,25, and 40 m). Curves in the upper panel were generated for a visibility of 23 km and with water type 1 and in the lower panel for water type 2.

Total Radiance Values (mw/(micron*cm*cm*sr))

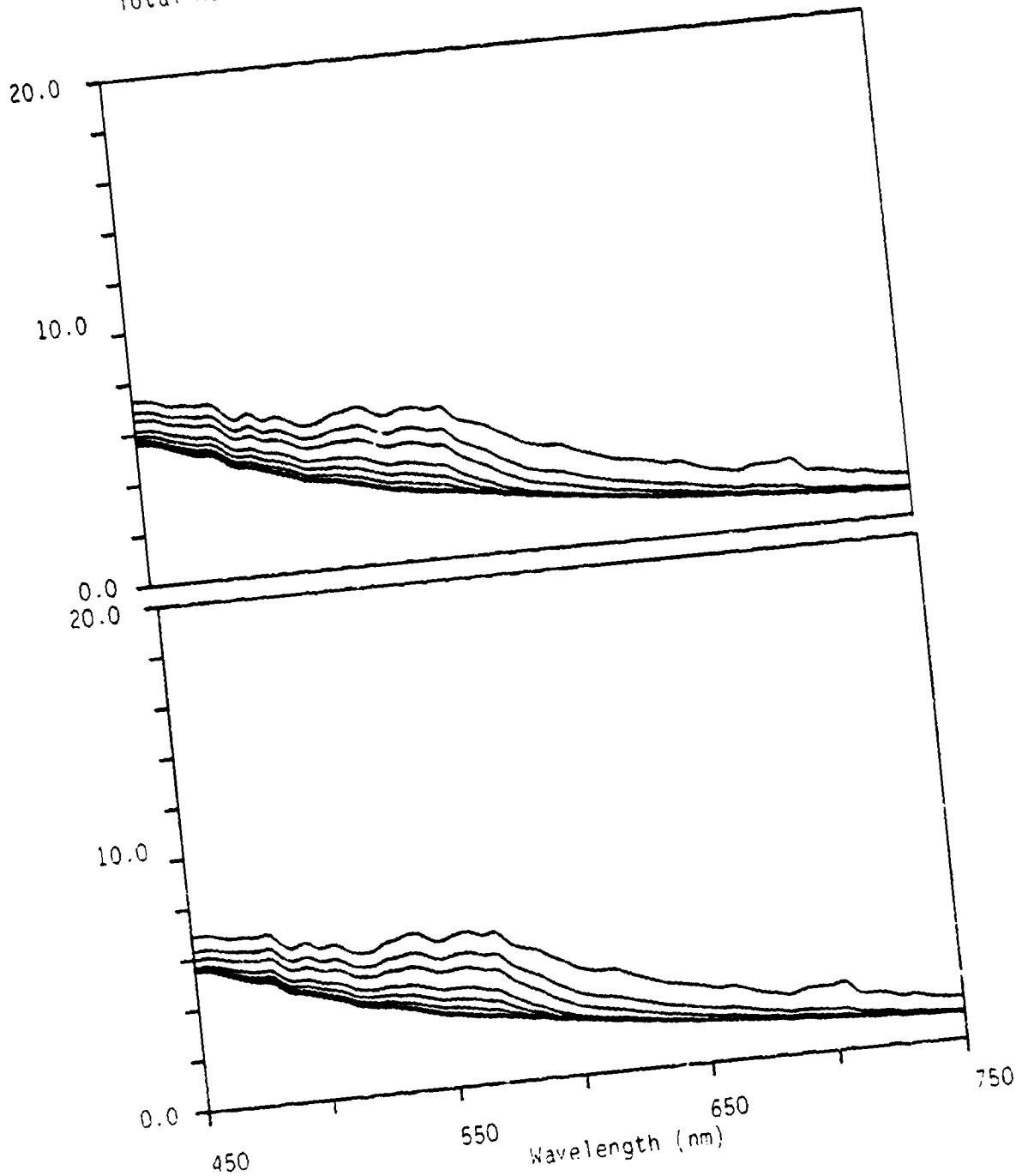


Figure A-11. Total radiance spectra for a Turtle Grass bottom type at selected water depths (1, 2, 3, 5, 7, 10, 15, 25, and 40 m). Curves in the upper panel were generated for a visibility of 23 km and with water type 3 and in the lower panel for water type 1.

Total Radiance Values (mw/(micron*cm*cm*sr))

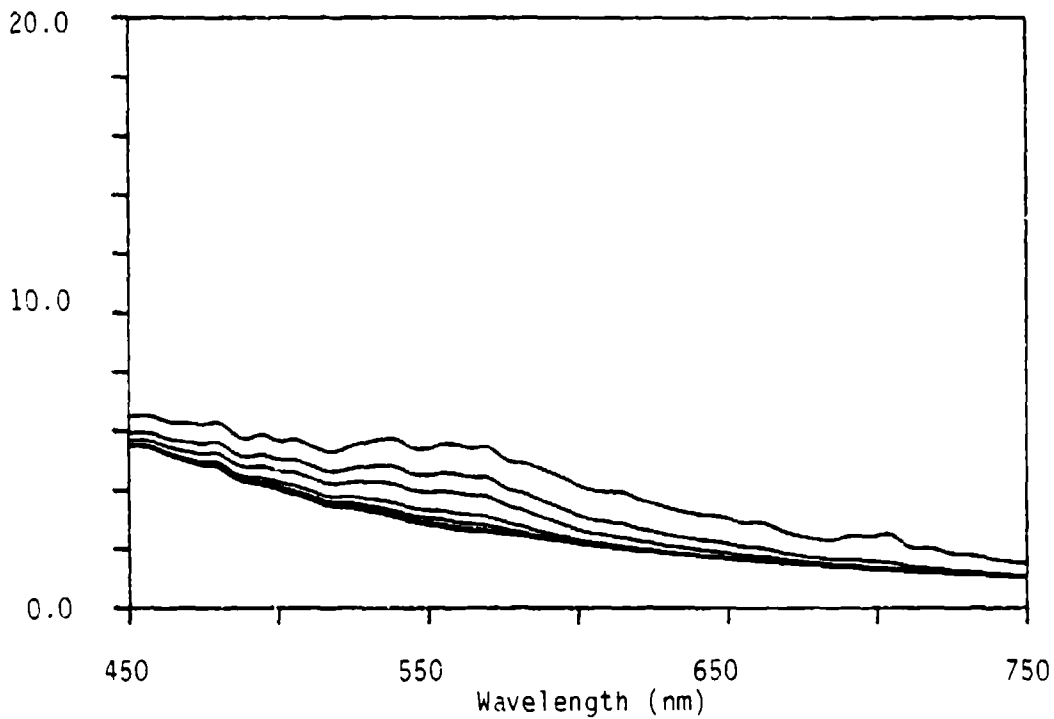


Figure A-12. Total radiance spectra for a Turtle Grass bottom type at selected water depths (1,2,3,5,7,10,15,25, and 40 m). Curves in the above panel were generated for a visibility of 23 km and with water type 5.

Σ ERIM

Total Radiance Values (mw/(micron*cm*cm*sr))

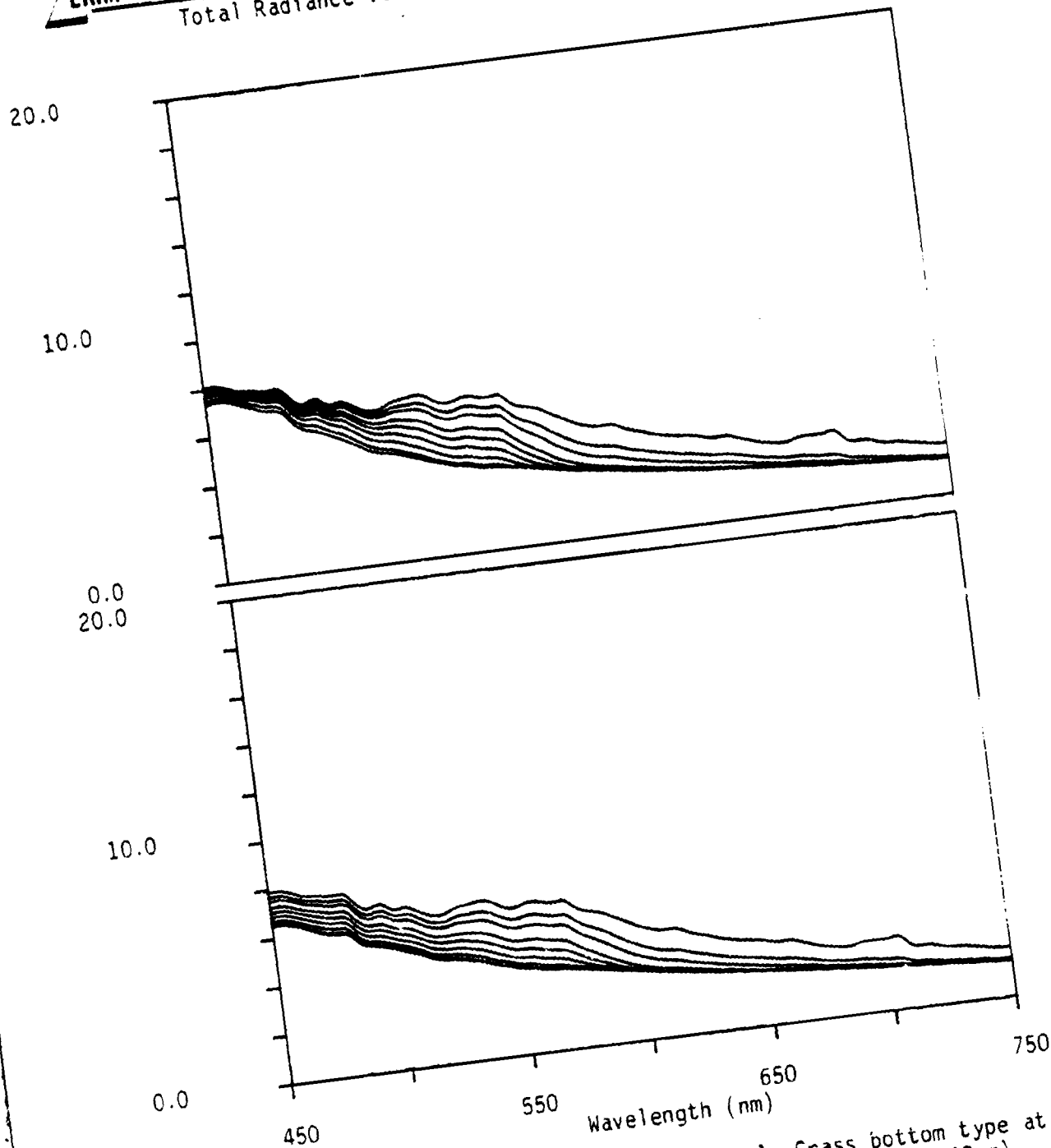


Figure A-13. Total radiance spectra for a Turtle Grass bottom type at selected water depths (1,2,3,5,7,10, 15,25, and 40 m). Curves in the upper panel were generated for a visibility of 10 km and with water type 1 and in the lower panel for water type 2.

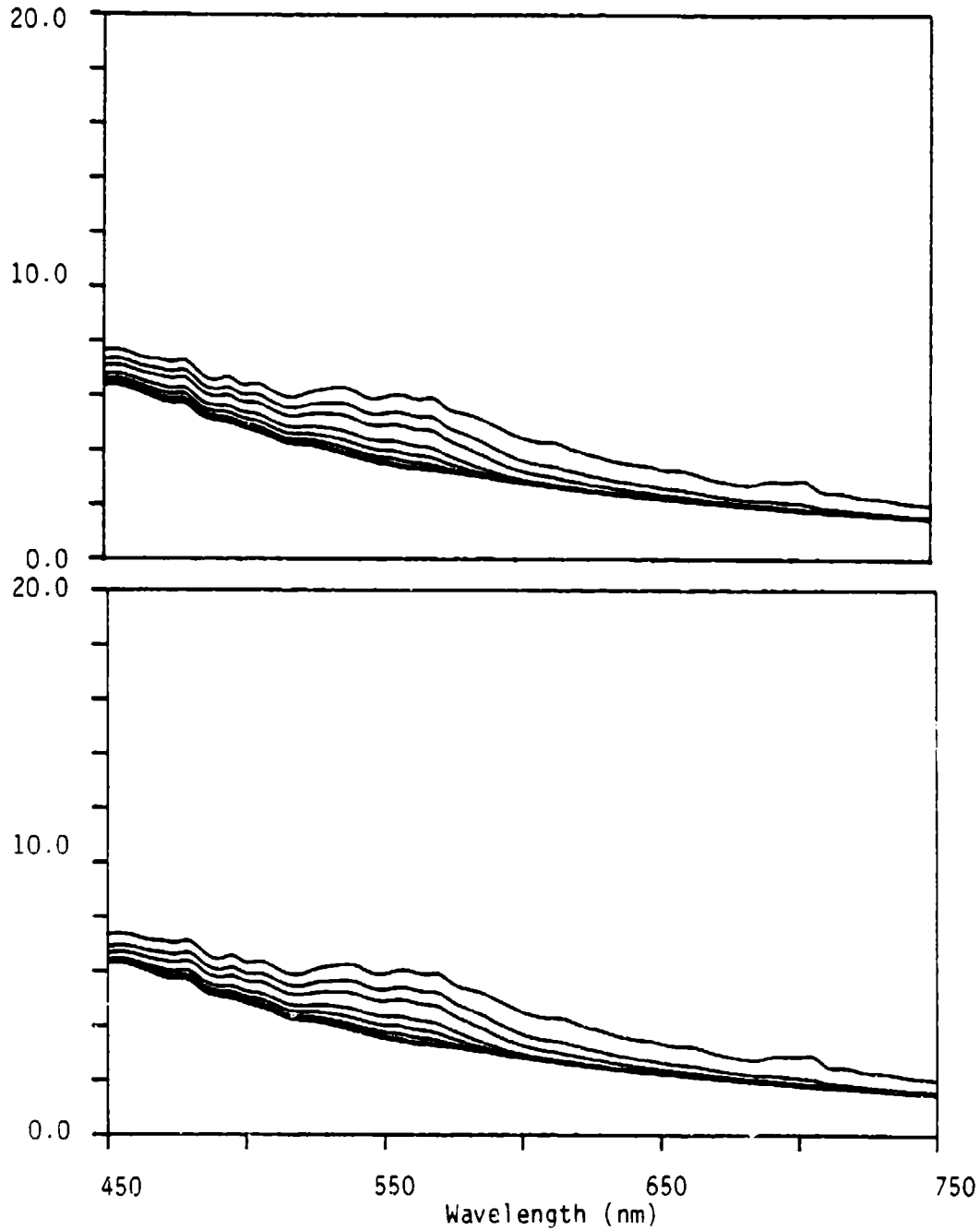


Figure A-14. Total radiance spectra for a Turtle Grass bottom type at selected water depths (1,2,3,5,7,10, 15,25, and 40 m). Curves in the upper panel were generated for a visibility of 10 km and with water type 3 and in the lower panel for water type 4.

Total Radiance Values (mw/(micron*cm*cm*sr))

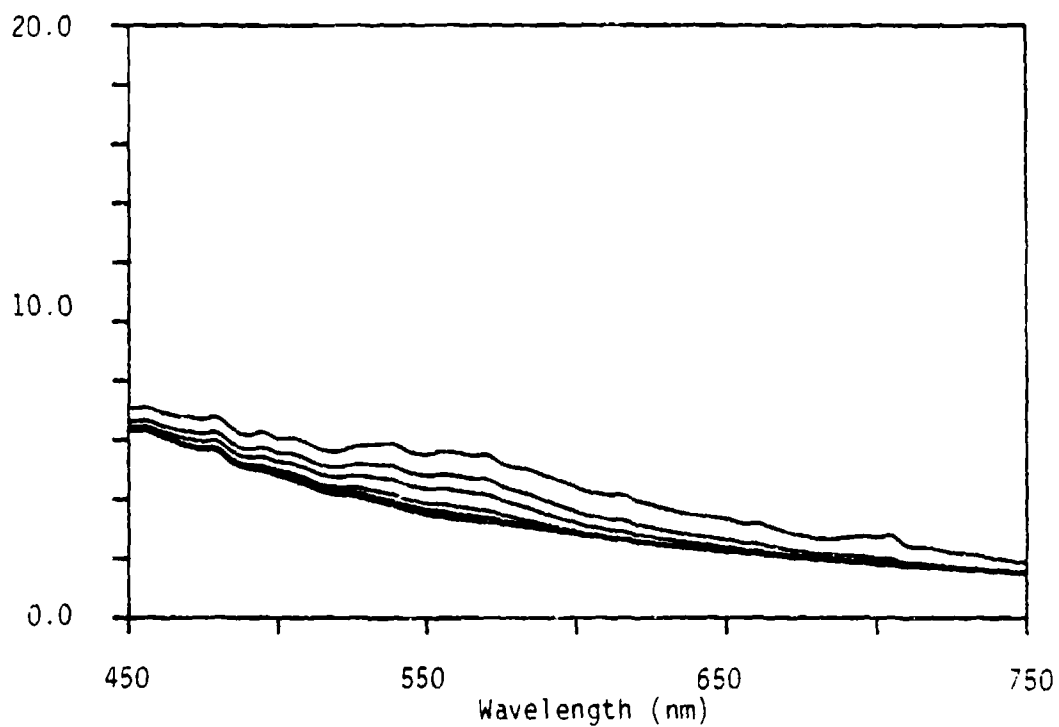


Figure A-15. Total radiance spectra for a Turtle Grass bottom type at selected water depths (1,2,3,5,7,10,15,25, and 40 m). Curves in the above panel were generated for a visibility of 10 km and with water type 5.

Total Radiance Values (mw/(micron*cm*cm*sr))

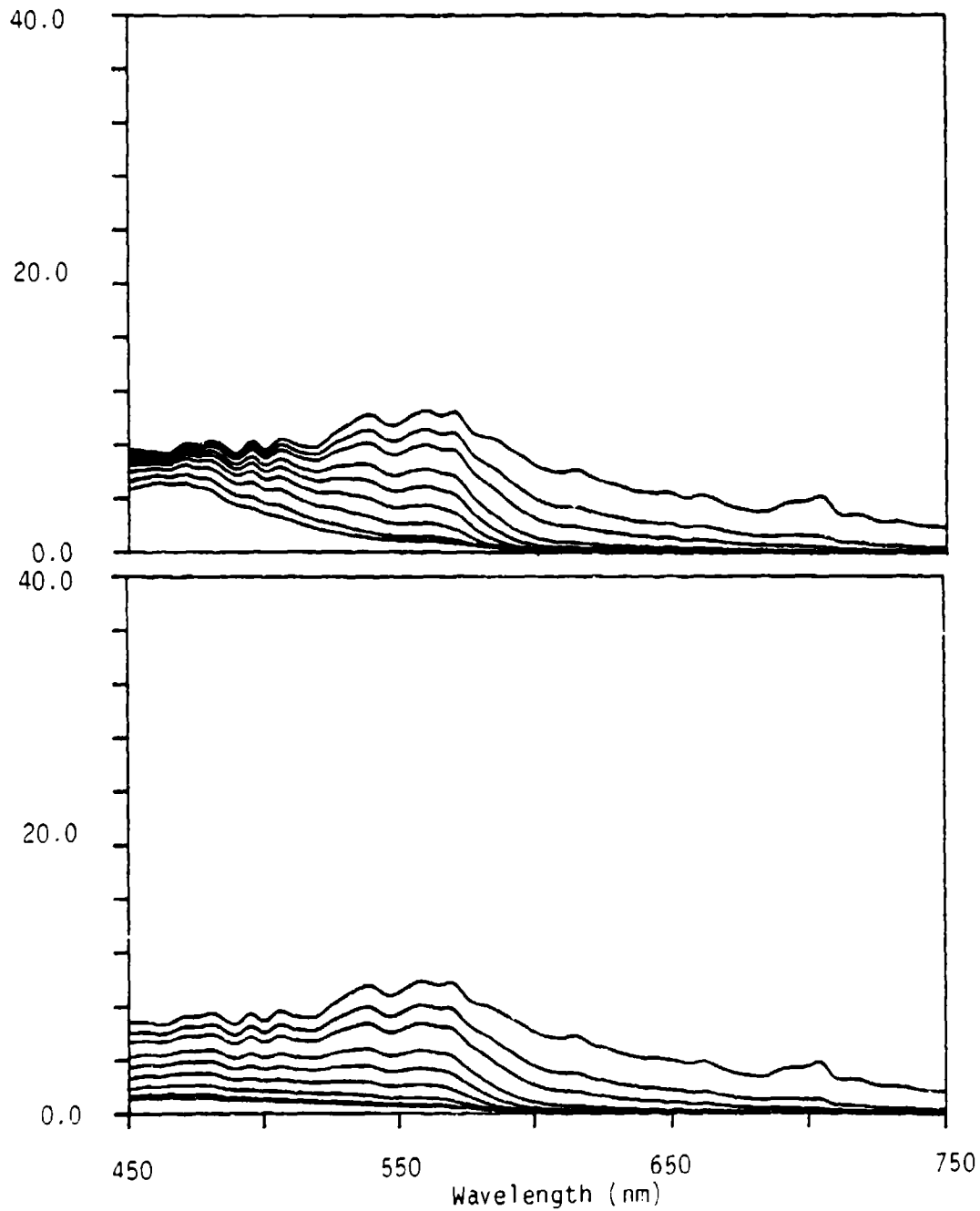


Figure A-16. Total radiance spectra for a Turtle Grass bottom type at selected water depths (1,2,3,5,7,10,15,25, and 40 m). Curves in the upper panel were generated with water type 1 and in the lower panel for water type 2. Spectra were calculated for a sensor position just below the sea surface.

Total Radiance Values (mw/(micron*cm*cm*sr))

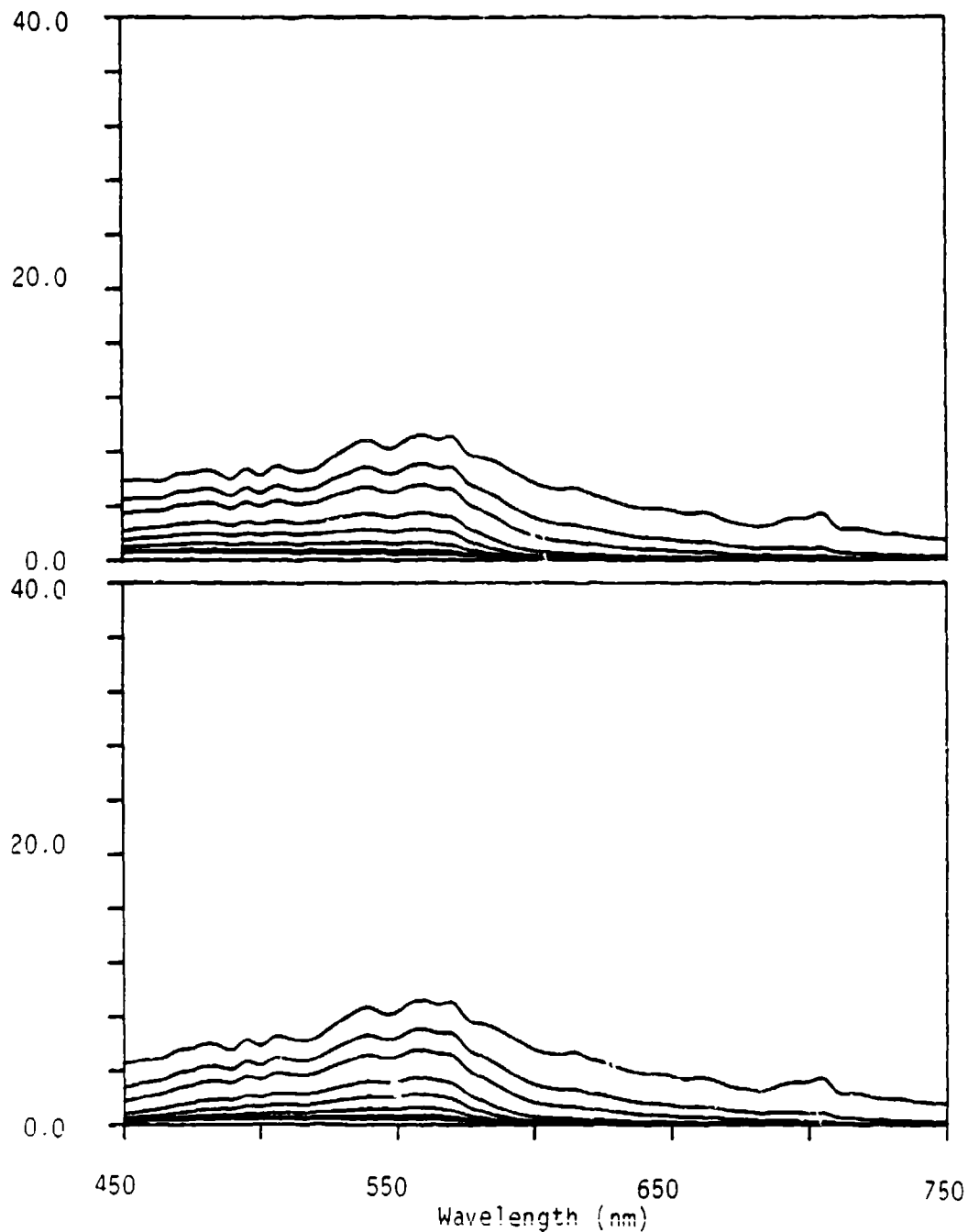


Figure A-17. Total radiance spectra for a Turtle Grass bottom type at selected water depths (1,2,3,5,7,10,15,25, and 40 m). Curves in the upper panel were generated with water type 3 and in the lower panel for water type 4. Spectra were calculated for a sensor position just below the sea surface.

Total Radiance Values (mw/(micron*cm*cm*sr))

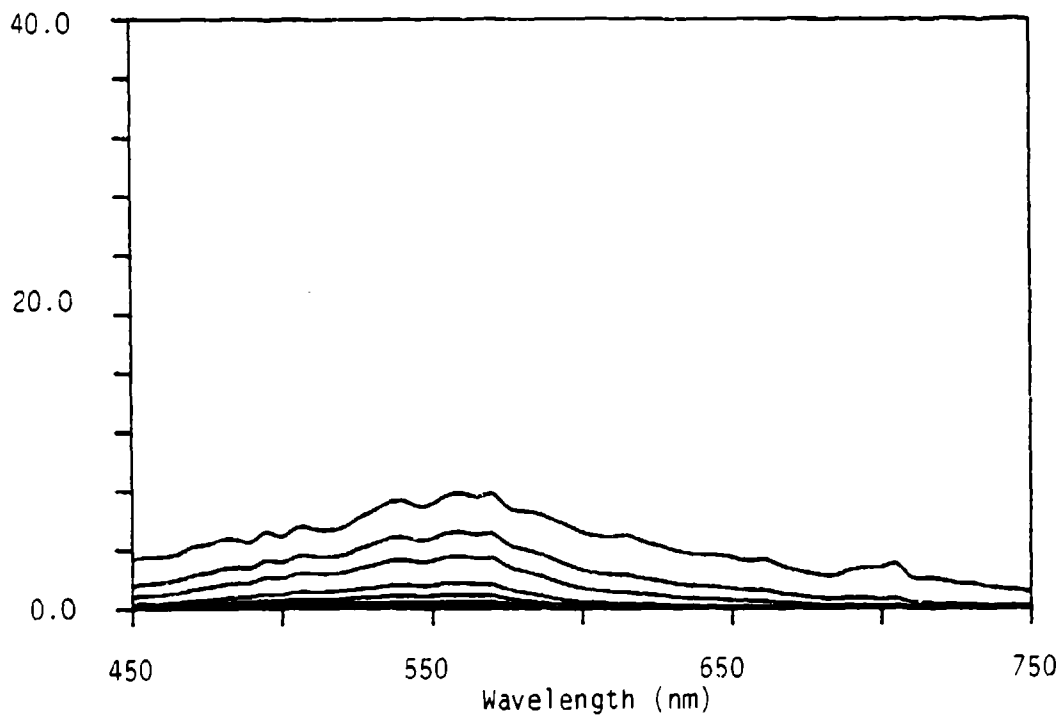


Figure A-18. Total radiance spectra for a Turtle Grass bottom type at selected water depths (1,2,3,5,7,10,15,25, and 40 m). Curves in the above panel were generated with water type 5. Spectra were calculated for a sensor position just below the sea surface.

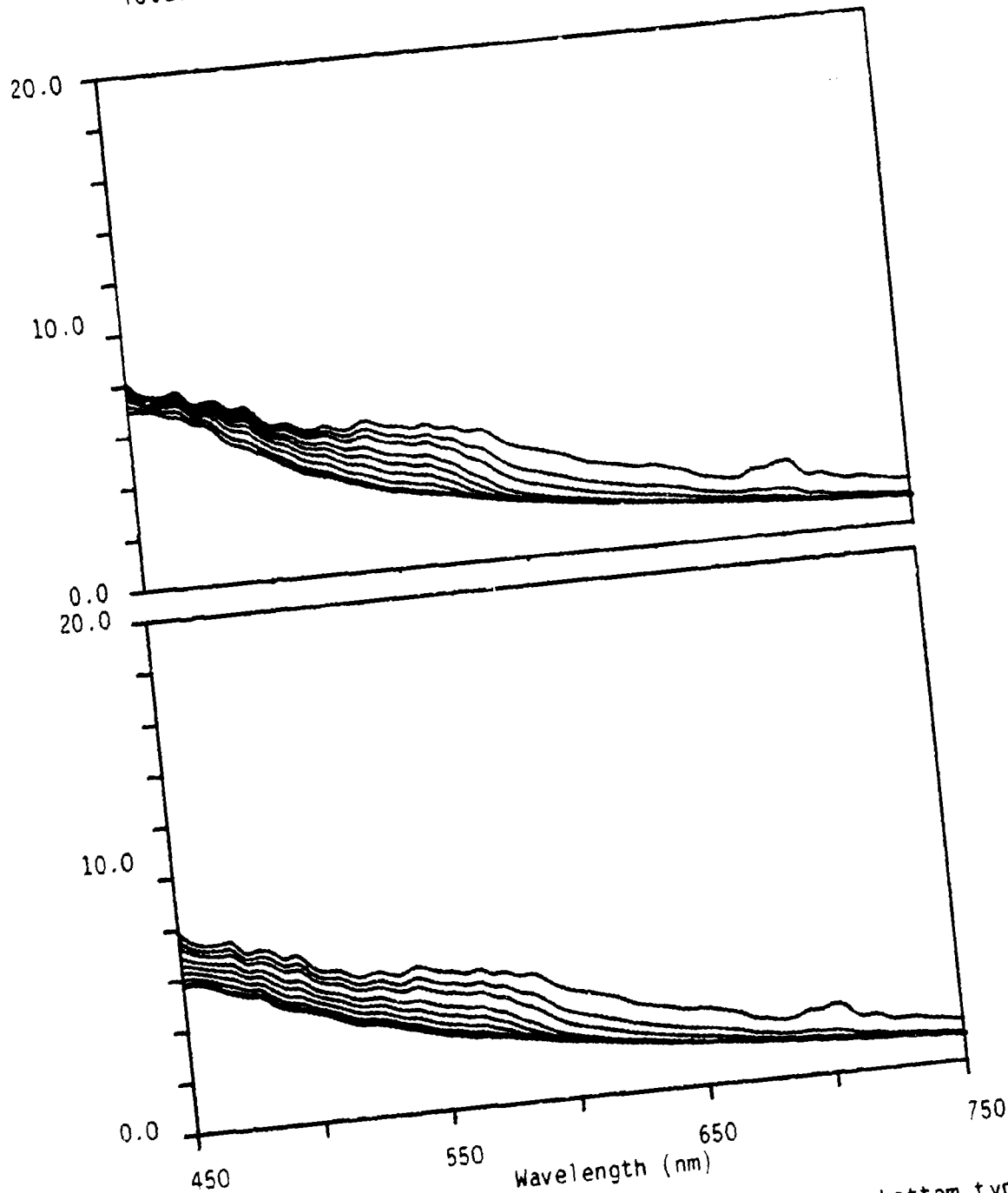


Figure A-19. Total radiance spectra for a Algal Mat Mixture bottom type at selected water depths (1,2,3,5,7,10, 15,25, and 40 m). Curves in the upper panel were generated for a visibility of 23 km and with water type 1 and in the lower panel for water type 2.

Total Radiance Values (mw/(micron*cm*cm*sr))

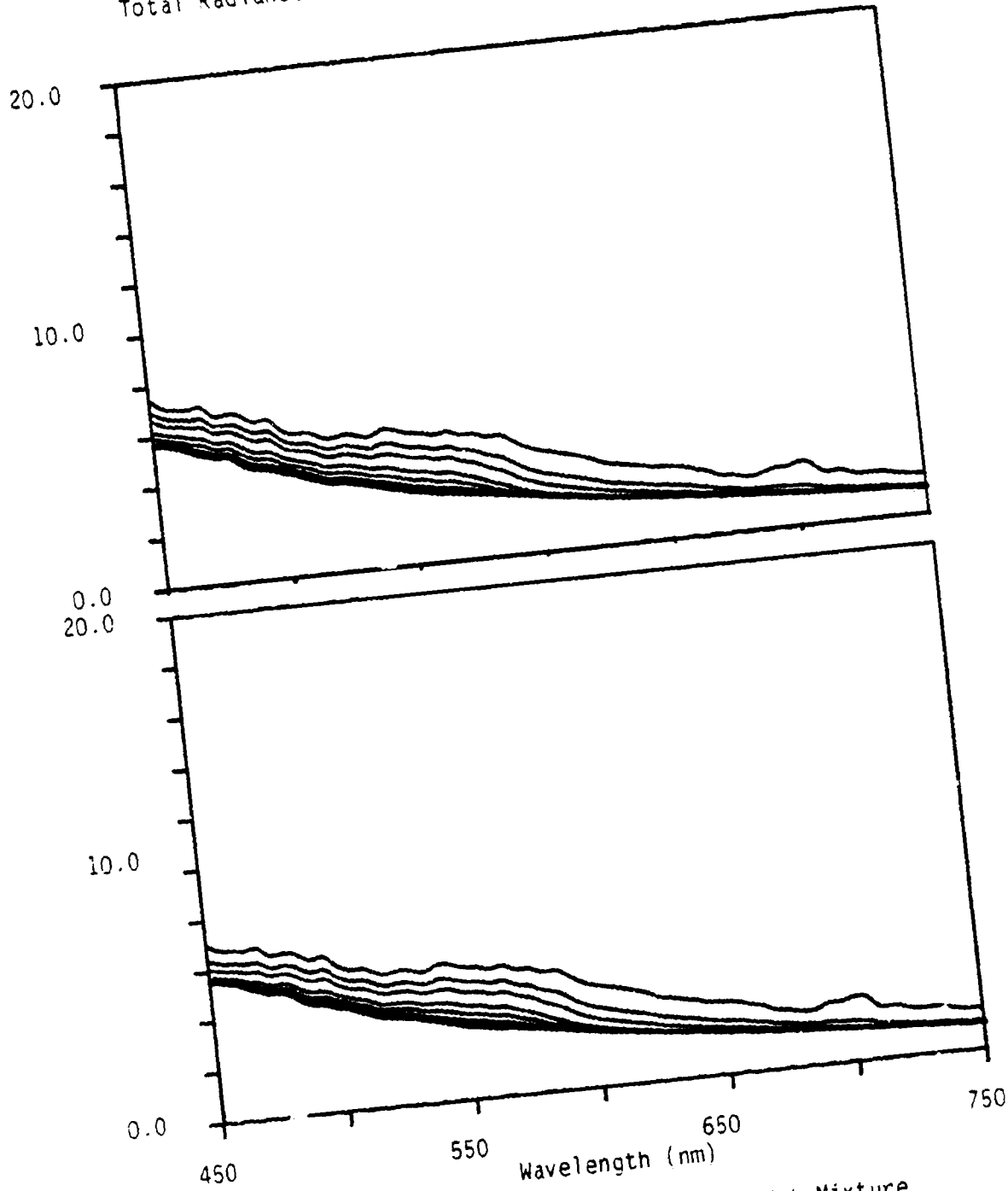


Figure A-20. Total radiance spectra for a Algal Mat Mixture bottom type at selected water depths (1,2,3,5,7,10,15,25, and 40 m). Curves in the upper panel were generated for a visibility of 23 km and with water type 3 and in the lower panel for water type 4.

Total Radiance Values (mw/(micron*cm*cm*sr))

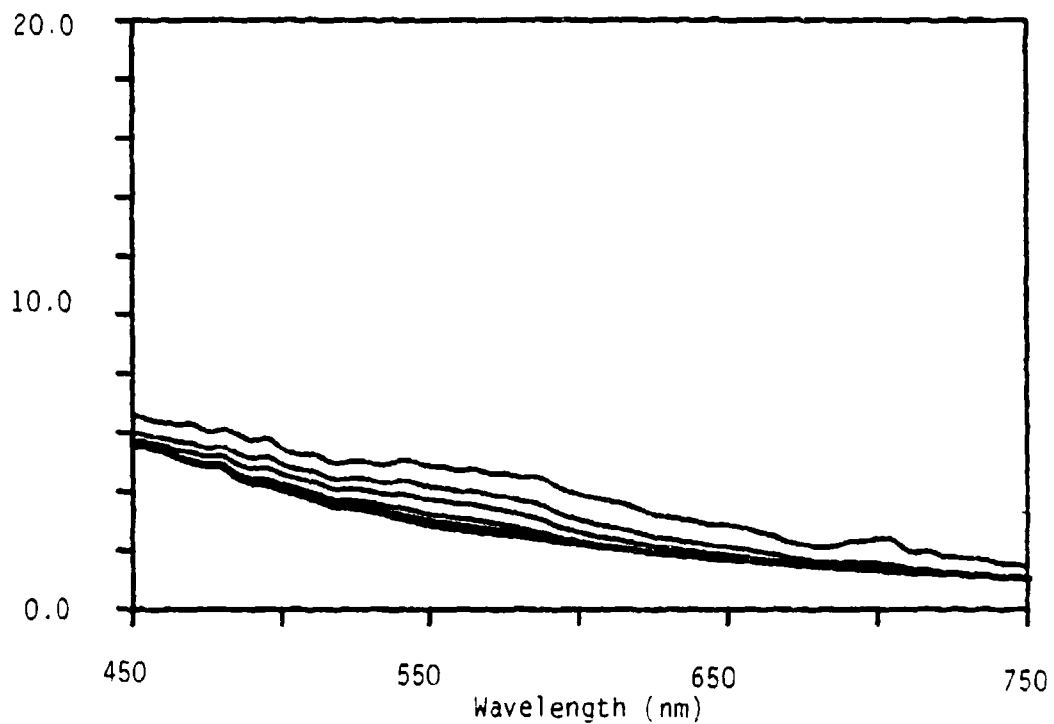


Figure A-21. Total radiance spectra for a Algal Mat Mixture bottom type at selected water depths (1,2,3,5,7,10,15,25, and 40 m). Curves in the above panel were generated for a visibility of 23 km and with water type 5.

Total Radiance Values (mw/(micron*cm*cm*sr))

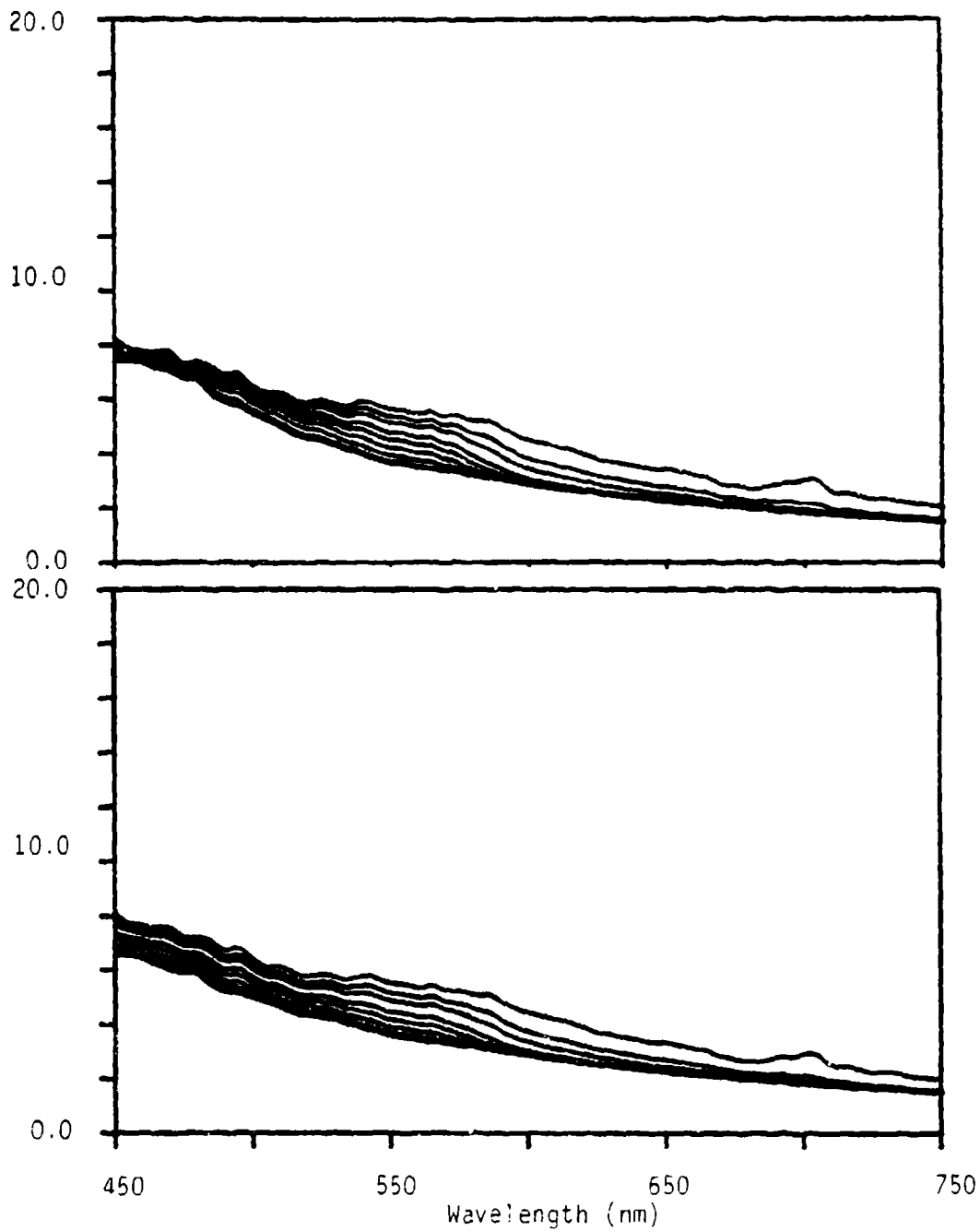


Figure A-22. Total radiance spectra for a Algal Mat Mixture bottom type at selected water depths (1,2,3,5,7,10,15,25, and 40 m). Curves in the upper panel were generated for a visibility of 10 km and with water type 1 and in the lower panel for water type 2.

Total Radiance Values (mw/(micron*cm*cm*sr))

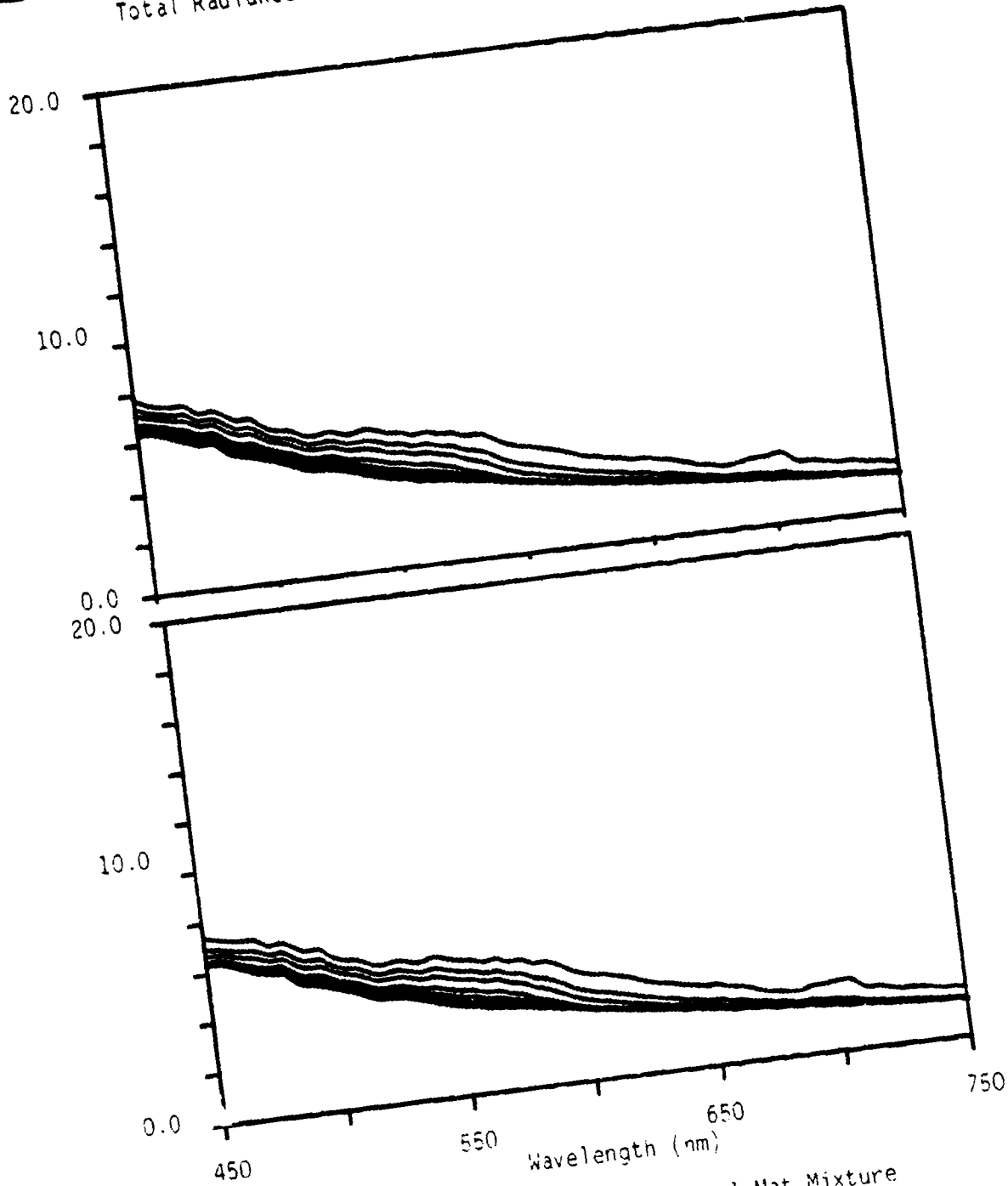


Figure A-23. Total radiance spectra for a Algal Mat Mixture bottom type at selected water depths (1,2,3,5,7,10,15,25, and 40 m). Curves in the upper panel were generated for a visibility of 10 km and with water type 3 and in the lower panel for water type 4.

Total Radiance Values (mw/(micron*cm*cm*sr))

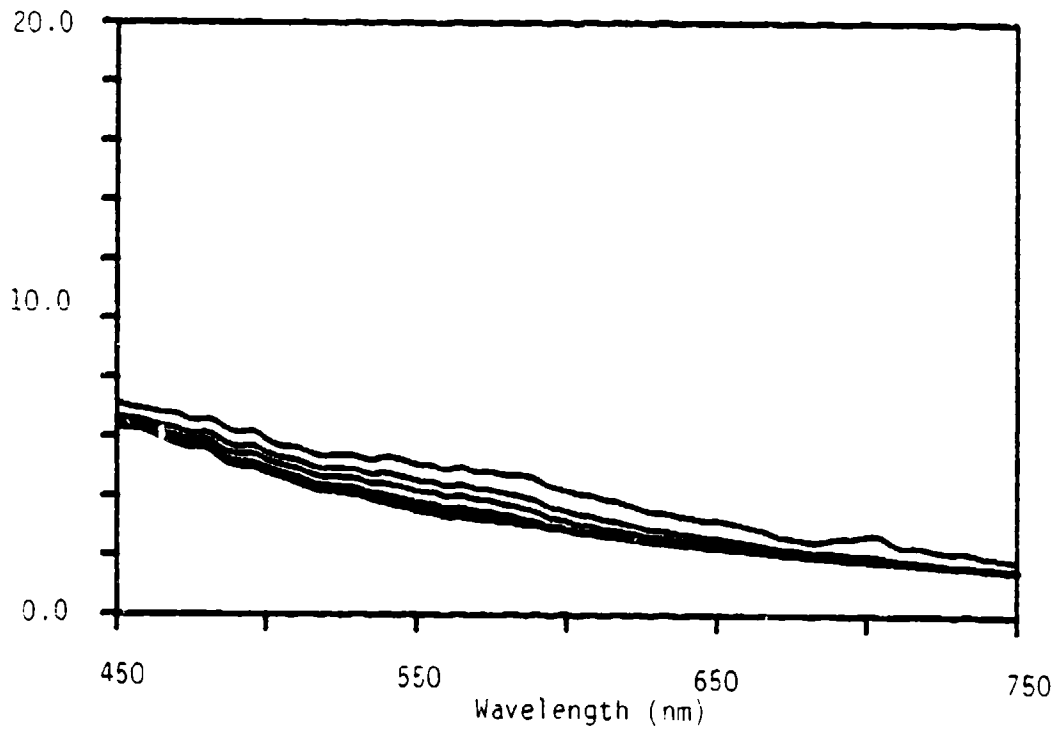


Figure A-24. Total radiance spectra for a Algal Mat Mixture bottom type at selected water depths (1,2,3,5,7,10,15,25, and 40 m). Curves in the above panel were generated for a visibility of 10 km and with water type 5.

Total Radiance Values (mw/(micron*cm*cm*sr))

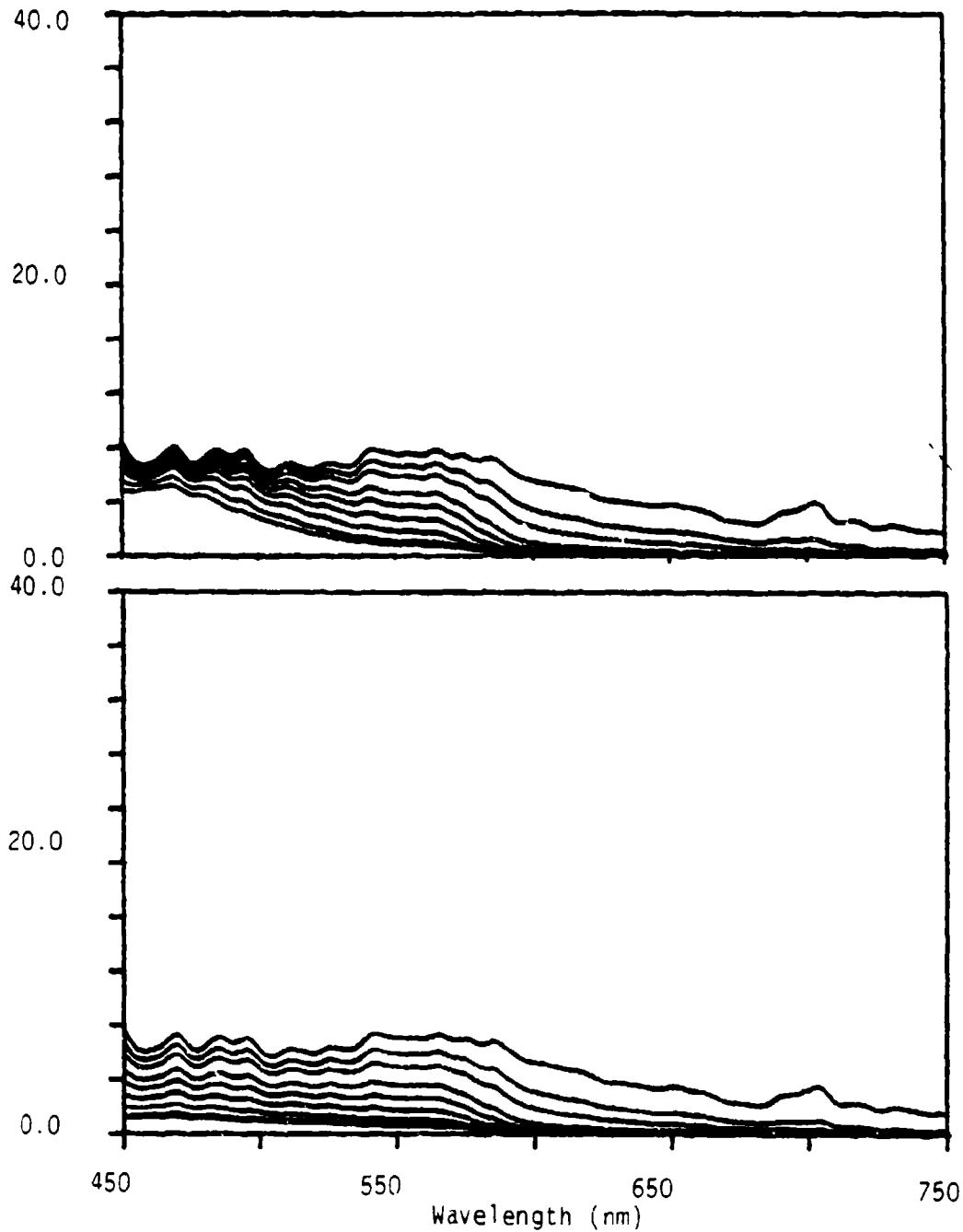


Figure A-25. Total radiance spectra for a Algal Mat Mixture bottom type at selected water depths (1,2,3,5,7,10,15,25, and 40 m). Curves in the upper panel were generated with water type 1 and in the lower panel for water type 2. Spectra were calculated for a sensor position just below the sea surface.

Total Radiance Values (mw/(micron*cm*cm*sr))

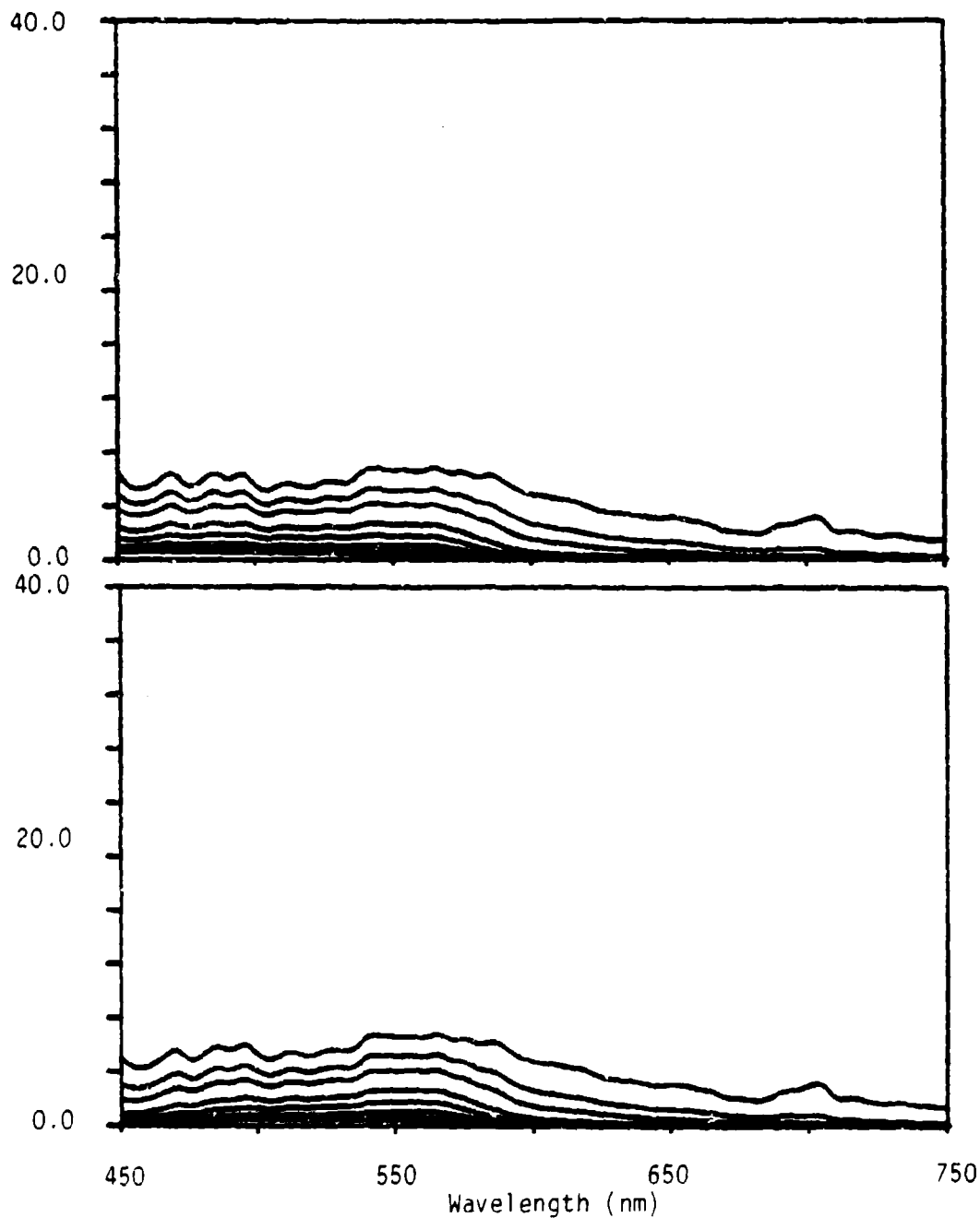


Figure A-26. Total radiance spectra for a Algal Mat Mixture bottom type at selected water depths (1,2,3,5,7,10, 15,25, and 40 m). Curves in the upper panel were generated with water type 3 and in the lower panel for water type 4. Spectra were calculated for a sensor position just below the sea surface.

Total Radiance Values (mw/(micron*cm*cm*sr))

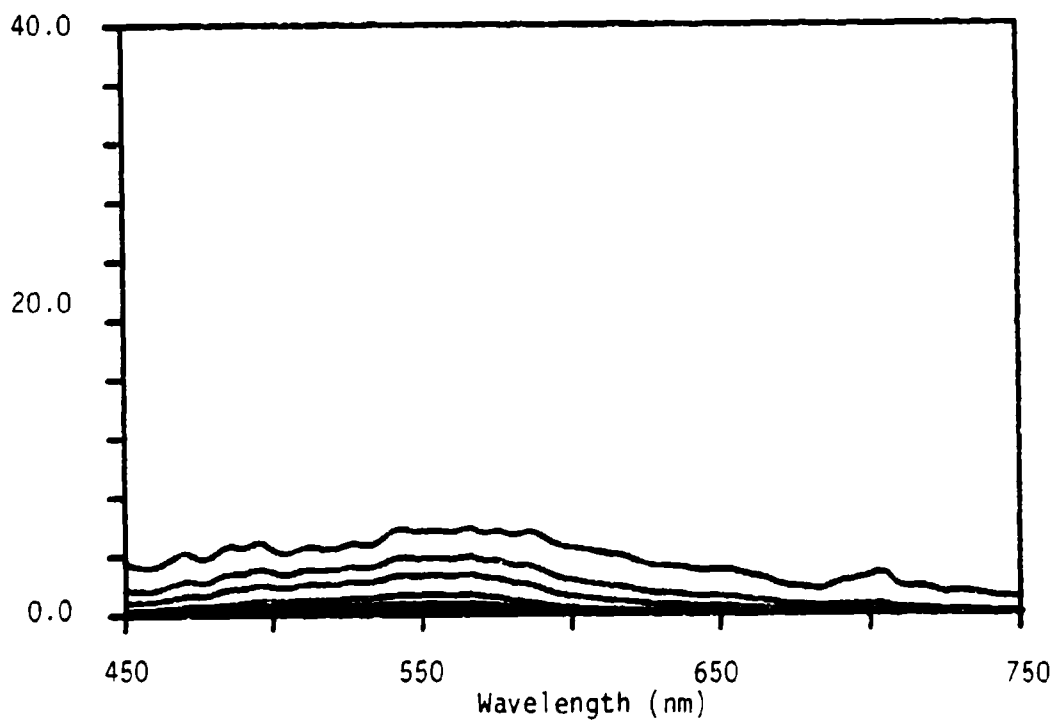


Figure A-27. Total radiance spectra for a Algal Mat Mixture bottom type at selected water depths (1,2,3,5,7,10,-15,25, and 40 m). Curves in the above panel were generated with water type 5. Spectra were calculated for a sensor position just below the sea surface.

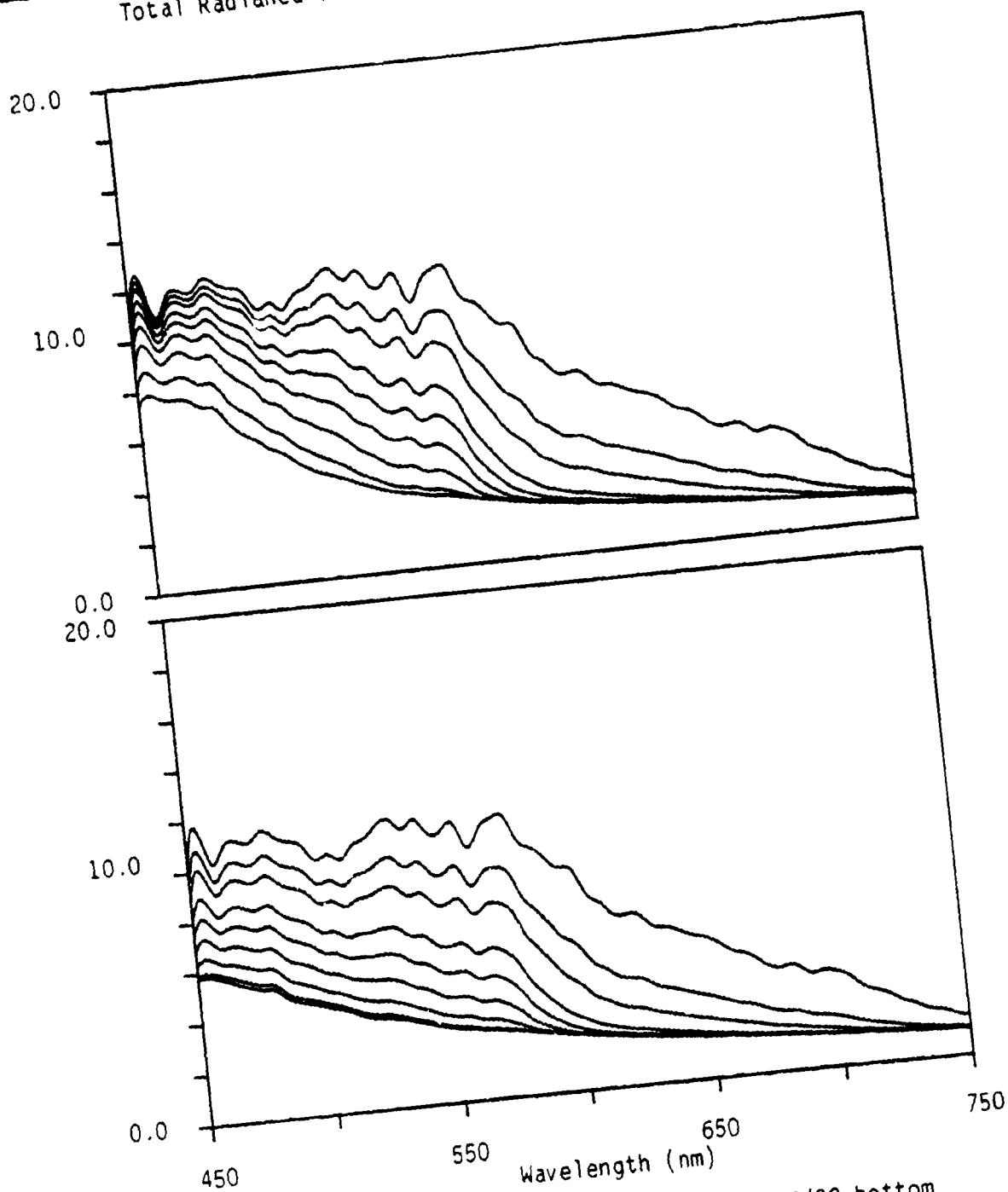


Figure A-28. Total radiance spectra for a Sand 7/26/80 bottom type at selected water depths (1, 2, 3, 5, 7, 10, 15, 25, and 40 m). Curves in the upper panel were generated for a visibility of 23 km and with water type 1 and in the lower panel for water type 2.

Total Radiance Values (mw/(micron*cm*cm*sr))

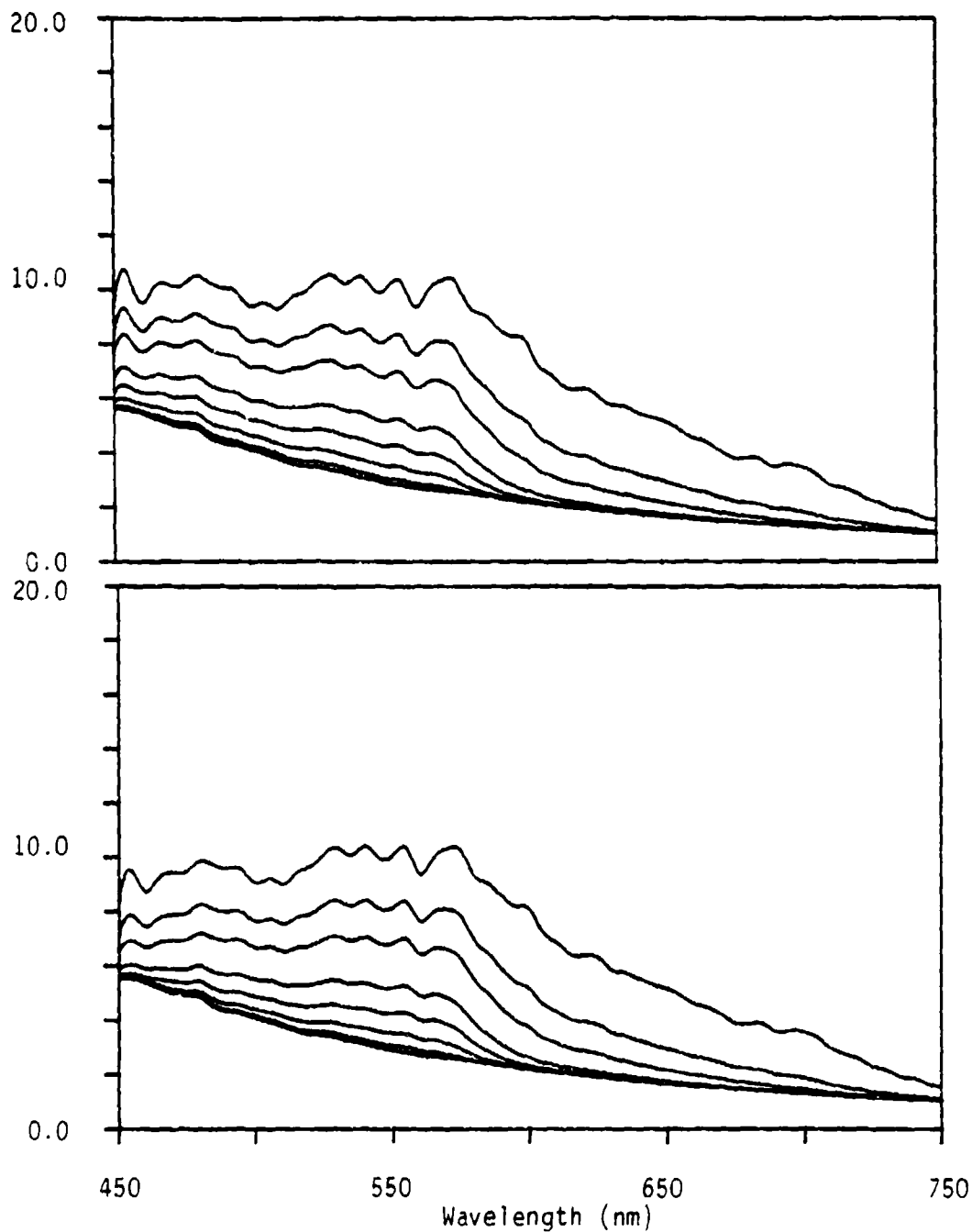


Figure A-29. Total radiance spectra for a Sand 7/26/80 bottom type at selected water depths (1,2,3,5,7,10,15,25, and 40 m). Curves in the upper panel were generated for a visibility of 23 km and with water type 3 and in the lower panel for water type 4.

Total Radiance Values (mw/(micron*cm*cm*sr))

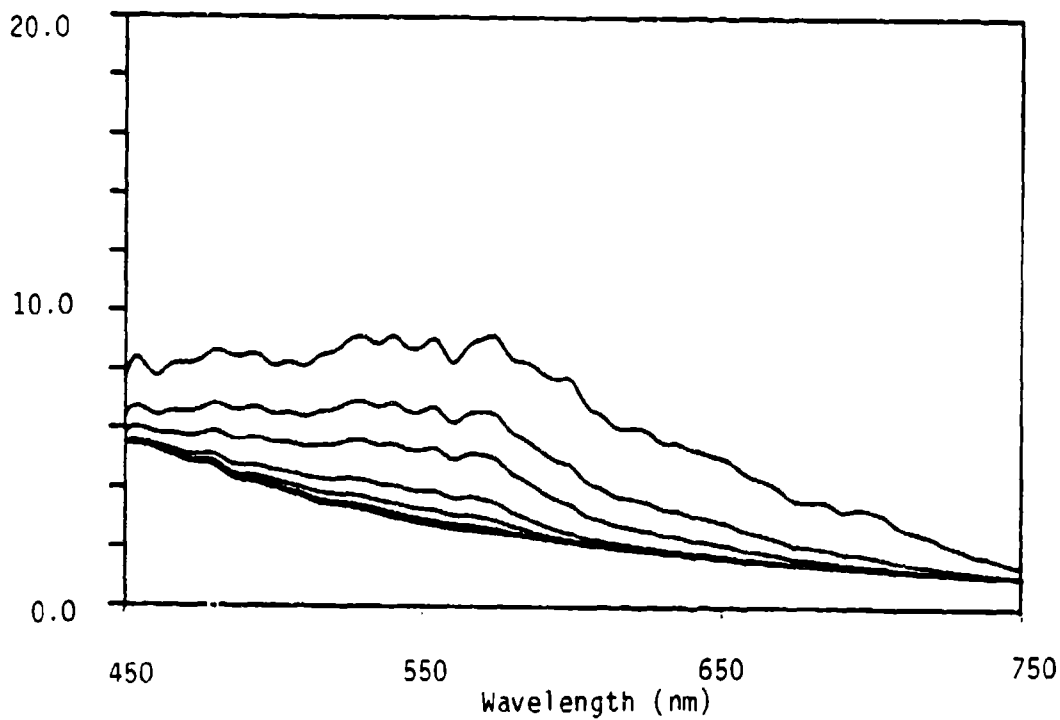


Figure A-30. Total radiance spectra for a Sand 7/26/80 bottom type at selected water depths (1,2,3,5,7,10,15,25, and 40 m). Curves in the above panel were generated for a visibility of 23 km and with water type 5.

Total Radiance Values (mw/(micron*cm*cm*sr))

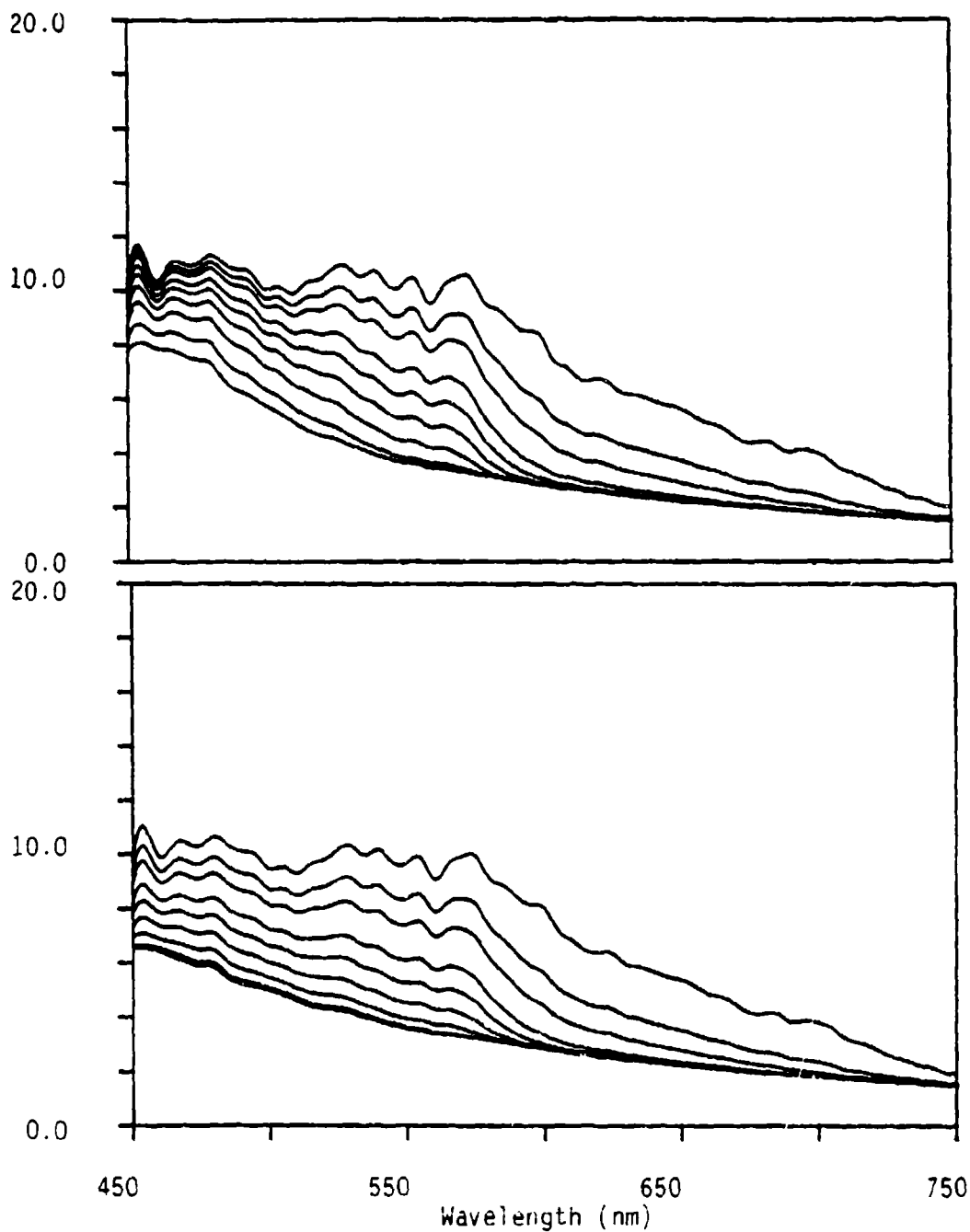


Figure A-31. Total radiance spectra for a Sand 7/26/80 bottom type at selected water depths (1,2,3,5,7,10,15,25, and 40 m). Curves in the upper panel were generated for a visibility of 10 km and with water type 1 and in the lower panel for water type 2.

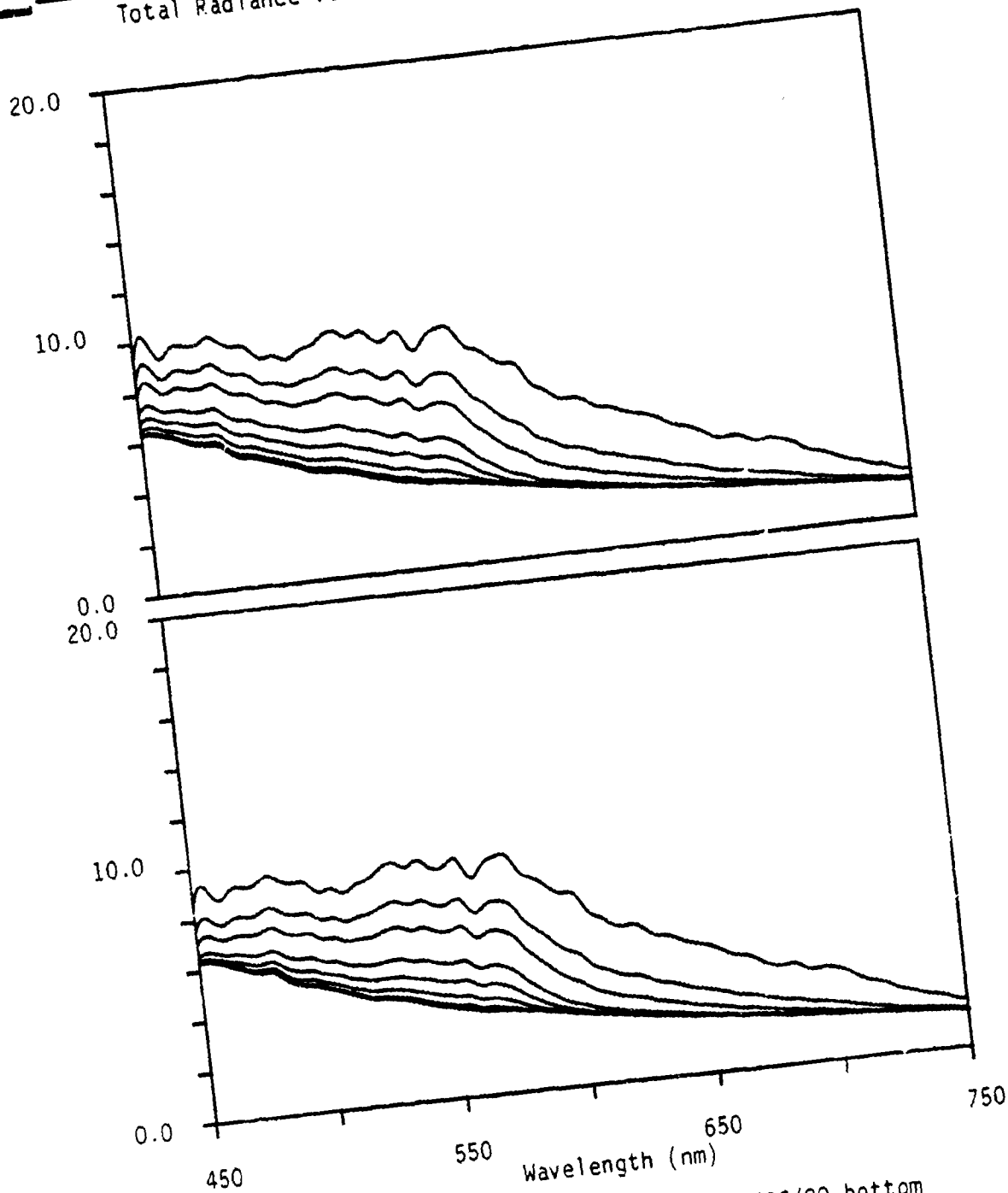


Figure A-32. Total radiance spectra for a Sand 7/26/80 bottom type at selected water depths (1, 2, 3, 5, 7, 10, 15, 25, and 40 m). Curves in the upper panel were generated for a visibility of 10 km and with water type 3 and in the lower panel for water type 4.

Total Radiance Values (mw/(micron*cm*cm*sr))

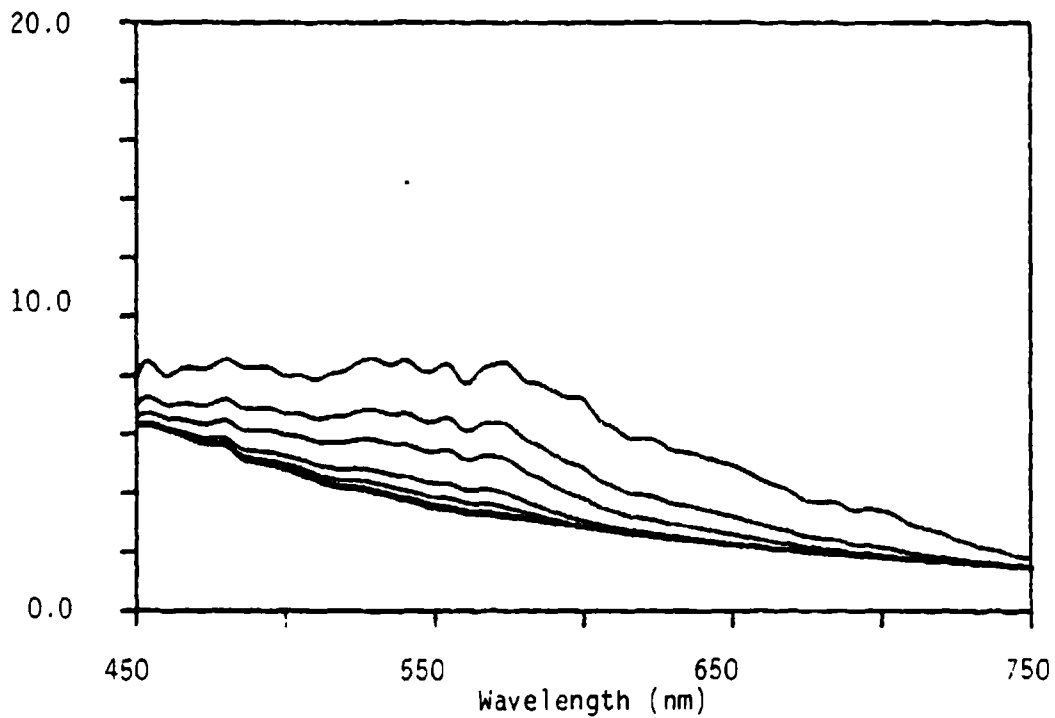


Figure A-33. Total radiance spectra for a Sand 7/26/80 bottom type at selected water depths (1,2,3,5,7,10,15,25, and 40 m). Curves in the above panel were generated for a visibility of 10 km and with water type 5.

Total Radiance Values (mw/(micron*cm*cm*sr))

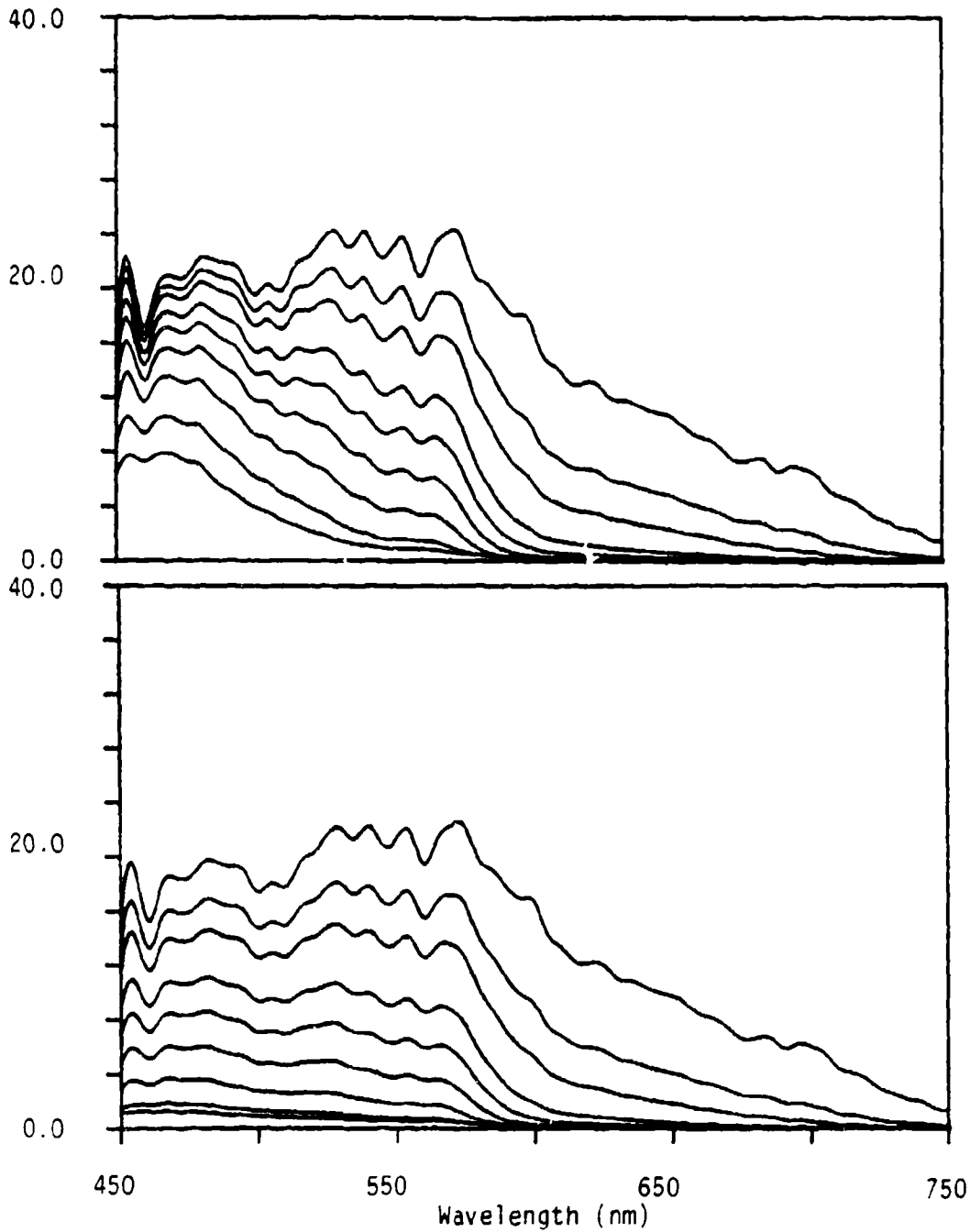


Figure A-34. Total radiance spectra for a Sand 7/26/80 bottom type at selected water depths (1,2,3,5,7,10,15,25, and 40 m). Curves in the upper panel were generated with water type 1 and in the lower panel for water type 2. Spectra were calculated for a sensor position just below the sea surface.

Total Radiance Values (mw/(micron*cm*cm*sr))

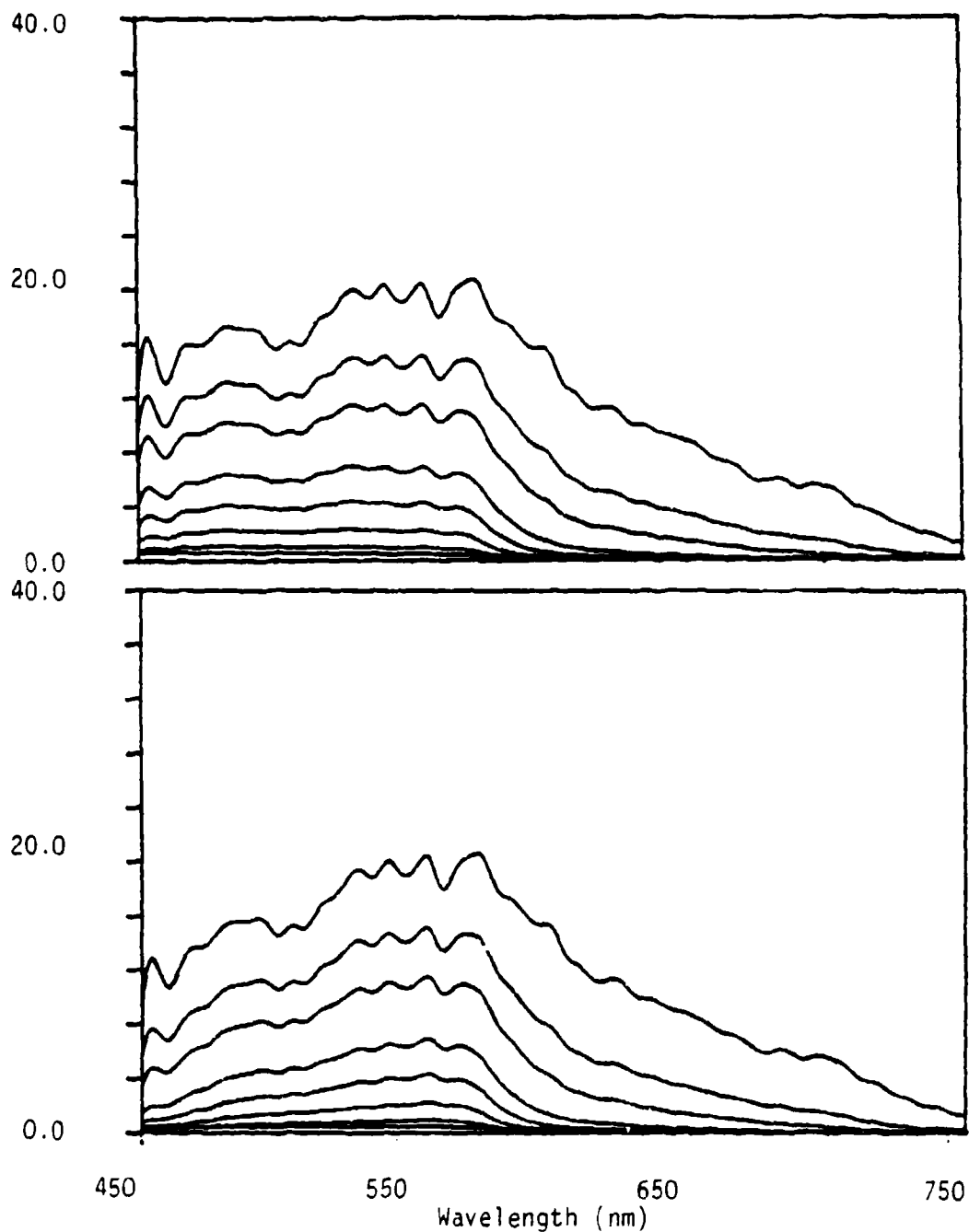


Figure A-35. Total radiance spectra for a Sand 7/26/80 bottom type at selected water depths (1,2,3,5,7,10, 15,25, and 40 m). Curves in the upper panel were generated with water type 3 and in the lower panel for water type 4. Spectra were calculated for a sensor position just below the sea surface.

Total Radiance Values (mw/(micron*cm*cm*sr))

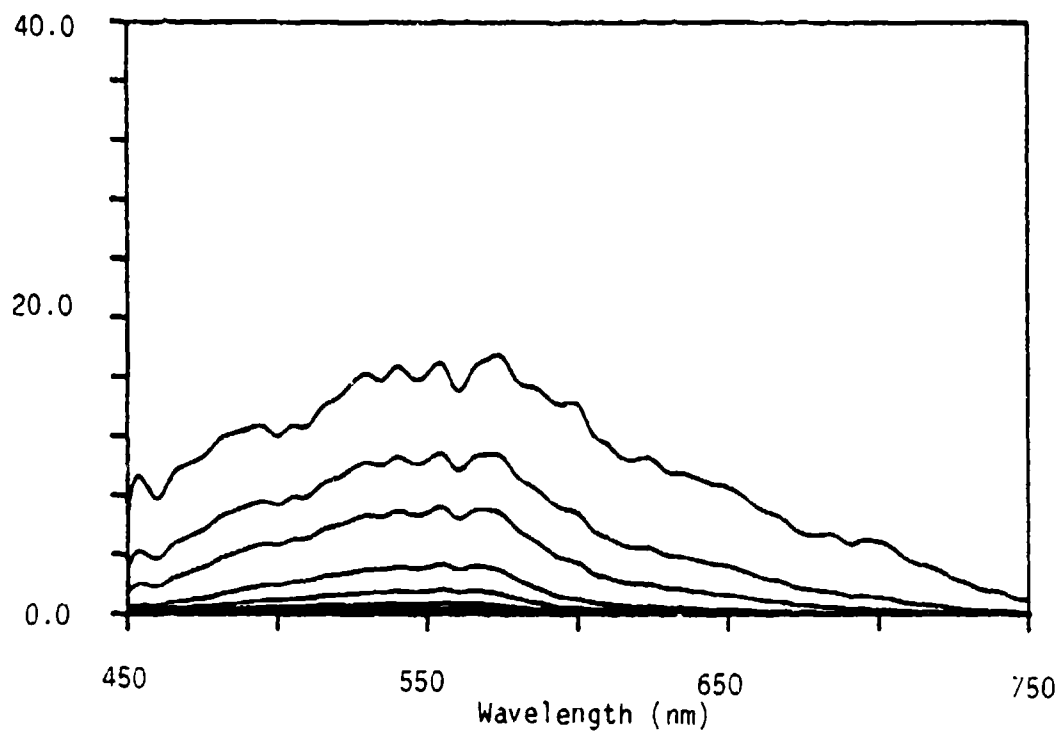


Figure A-36. Total radiance spectra for a Sand 7/26/80 bottom type at selected water depths (1,2,3,5,7,10,15,25, and 40 m). Curves in the above panel were generated with water type 5. Spectra were calculated for a sensor position just below the sea surface.

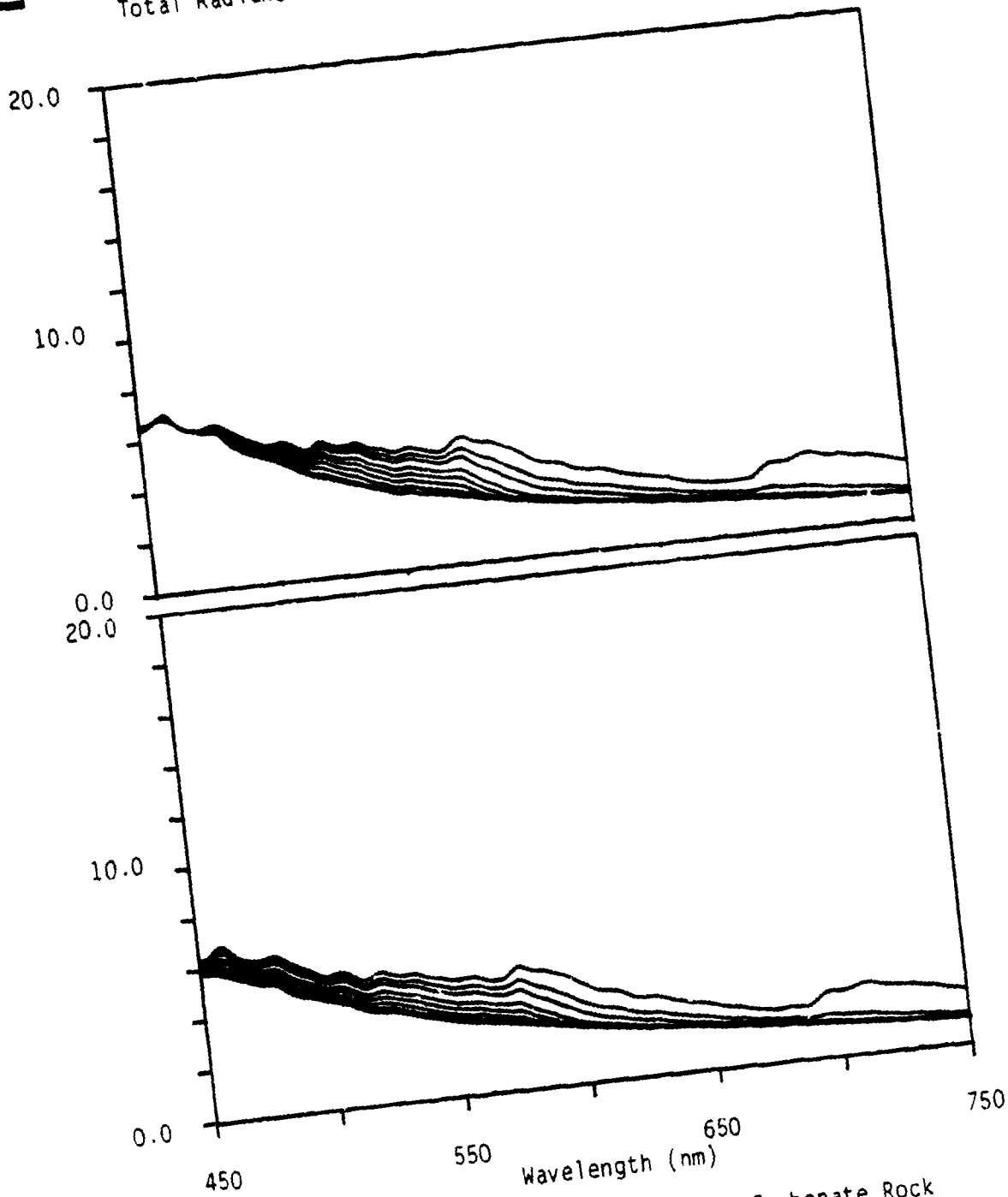


Figure A-37. Total radiance spectra for a Flat Carbonate Rock bottom type at selected water depths (1,2,3,5,7,10, 15,25, and 40 m). Curves in the upper panel were generated for a visibility of 23 km and with water type 1 and in the lower panel for water type 2.

Total Radiance Values (mw/(micron*cm*cm*sr))

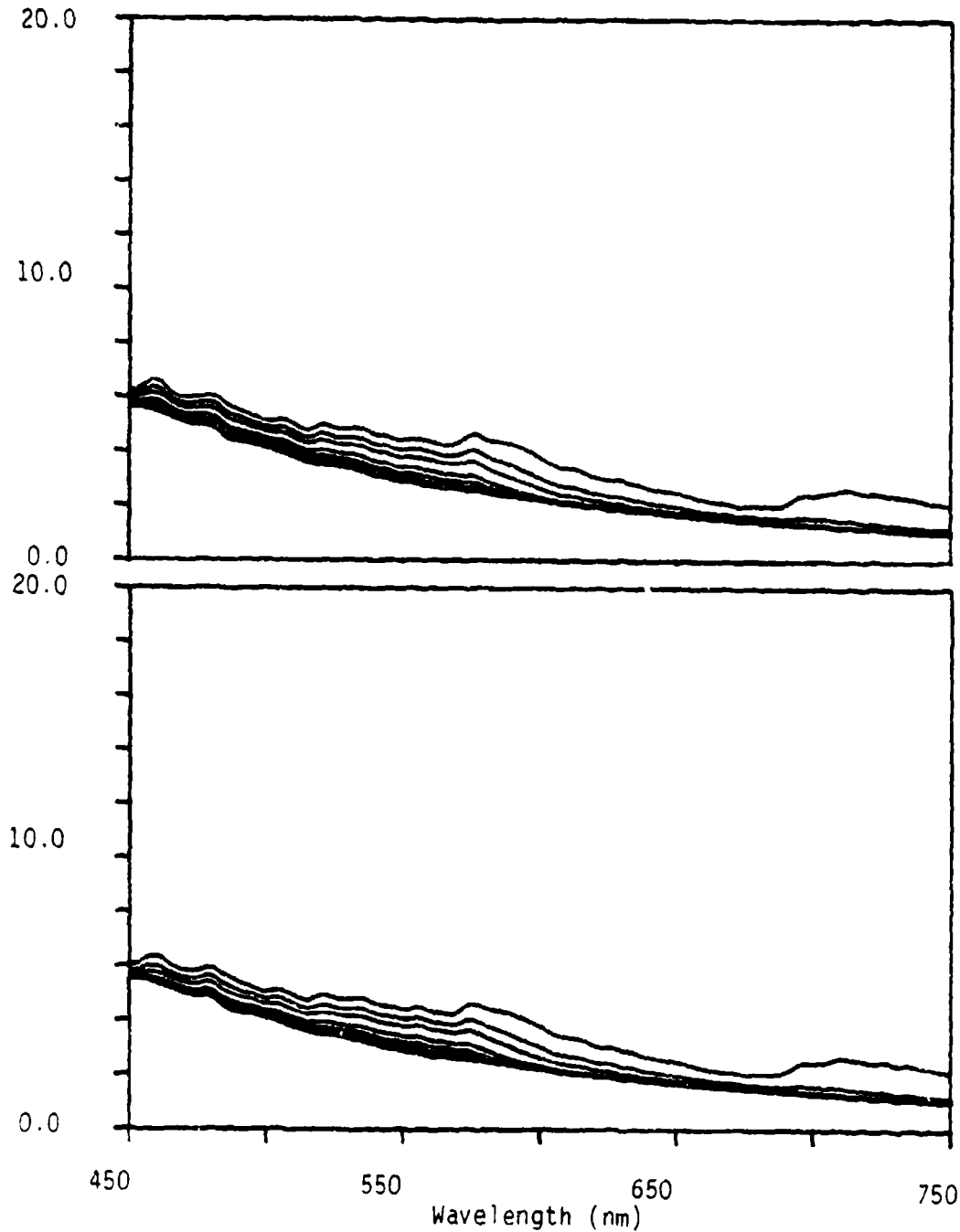


Figure A-38. Total radiance spectra for a Flat Carbonate Rock bottom type at selected water depths (1,2,3,5,7,10, 15,25, and 40 m). Curves in the upper panel were generated for a visibility of 23 km and with water type 3 and in the lower panel for water type 4.

Total Radiance Values (mw/(micron*cm*cm*sr))

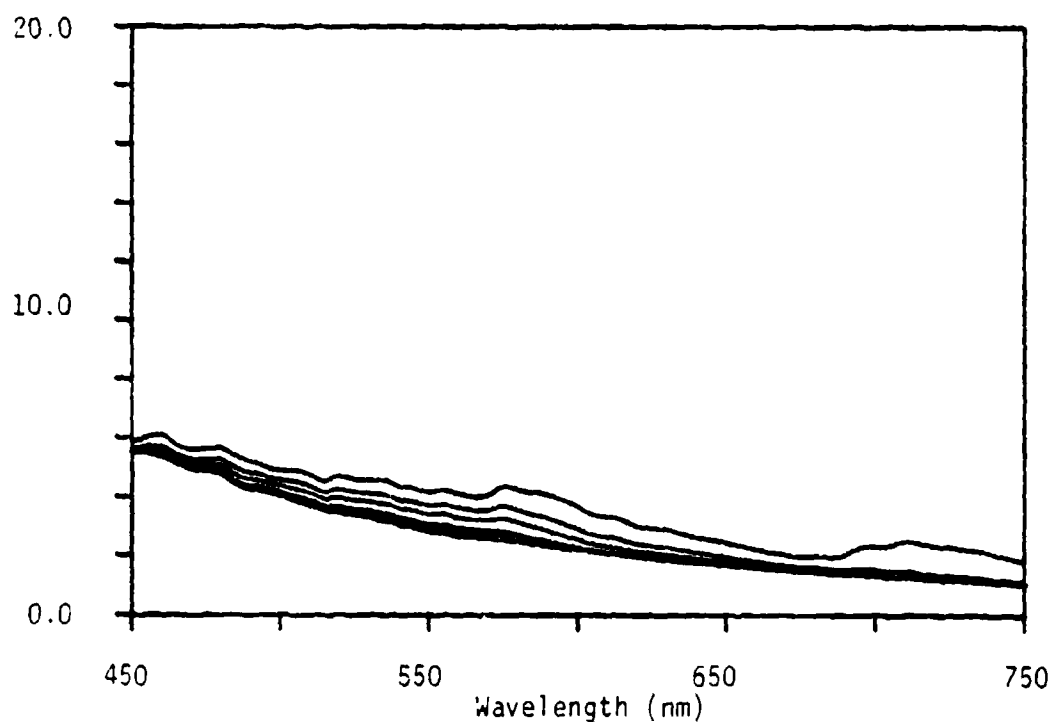


Figure A-39. Total radiance spectra for a Flat Carbonate Rock bottom type at selected water depths (1,2,3,5,7,10, 15,25, and 40 m). Curves in the above panel were generated for a visibility of 23 km and with water type 5.

ERIM

Total Radiance Values (mw/(micron*cm*cm*sr))

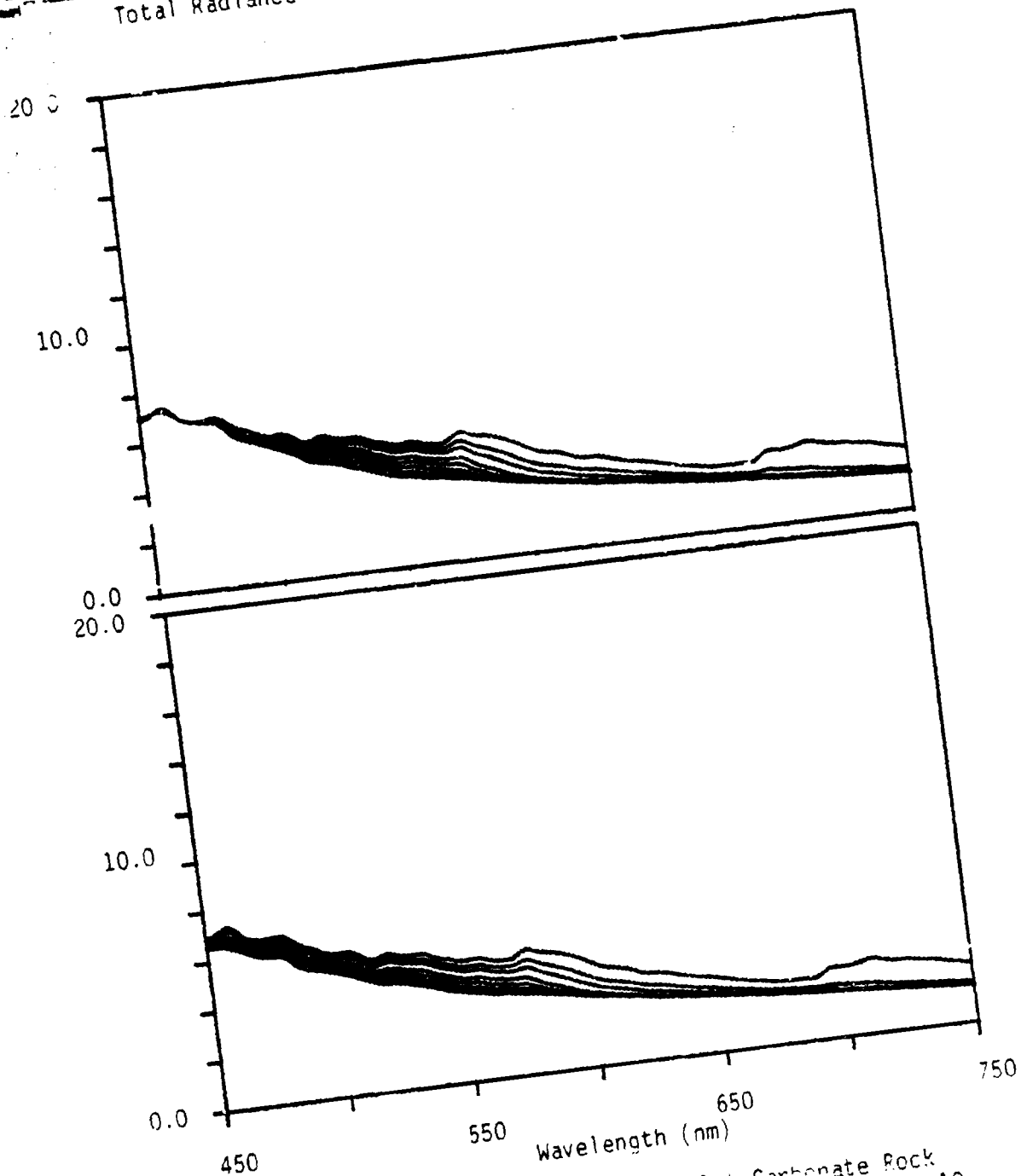


Figure A-40. Total radiance spectra for a Flat Carbonate Rock bottom type at selected water depths (1, 2, 3, 5, 7, 10, 15, 25, and 40 m). Curves in the upper panel were generated for a visibility of 10 km and with water type 1 and in the lower panel for water type 2.

Σ ERIM

Total Radiance Values (mw/(micron*cm*cm*sr))

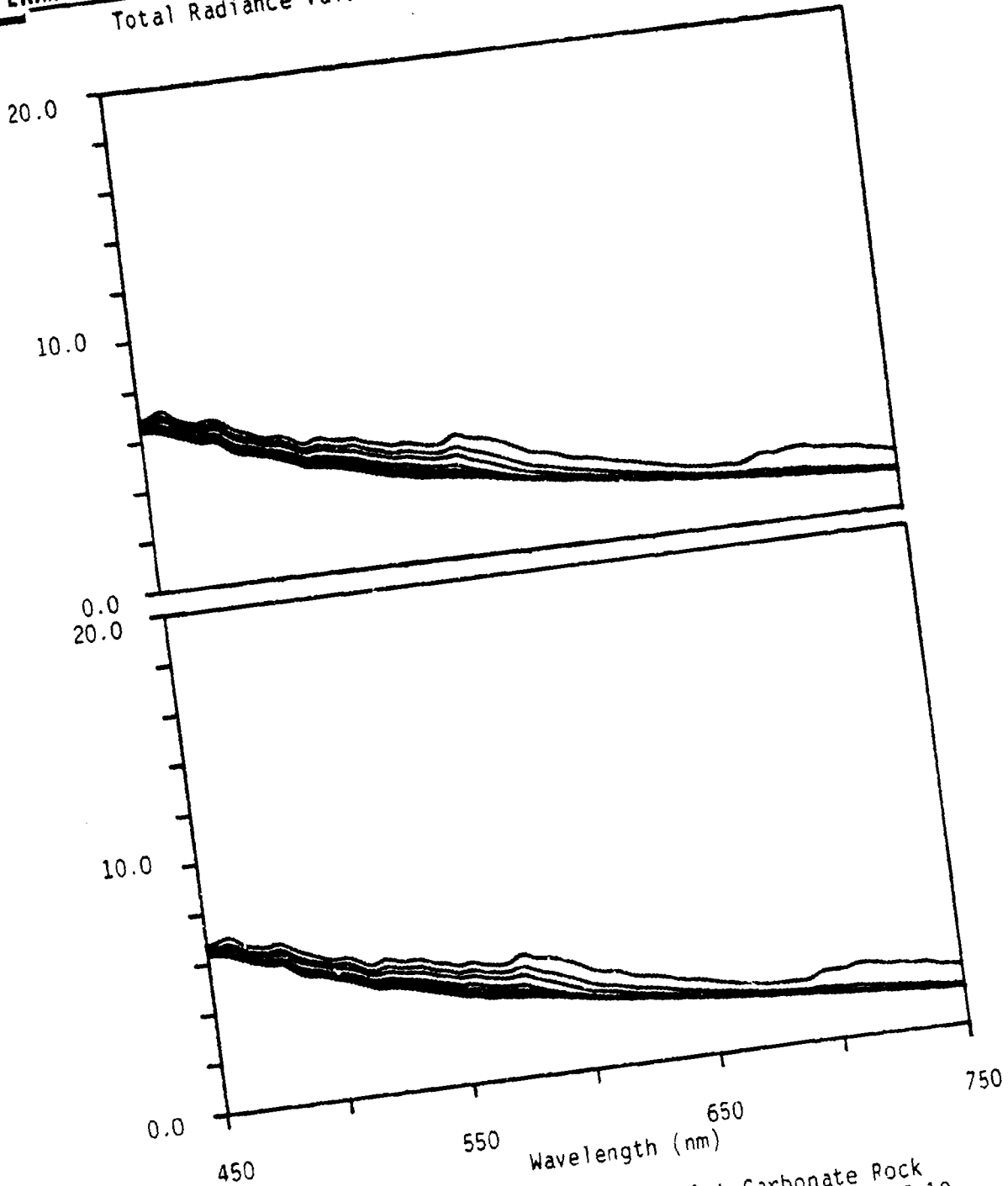


Figure A-41. Total radiance spectra for a Flat Carbonate Rock bottom type at selected water depths (1,2,3,5,7,10, 15,25, and 40 m). Curves in the upper panel were generated for a visibility of 10 km and with water type 3 and in the lower panel for water type 4.

Total Radiance Values (mw/(micron*cm*cm*sr))

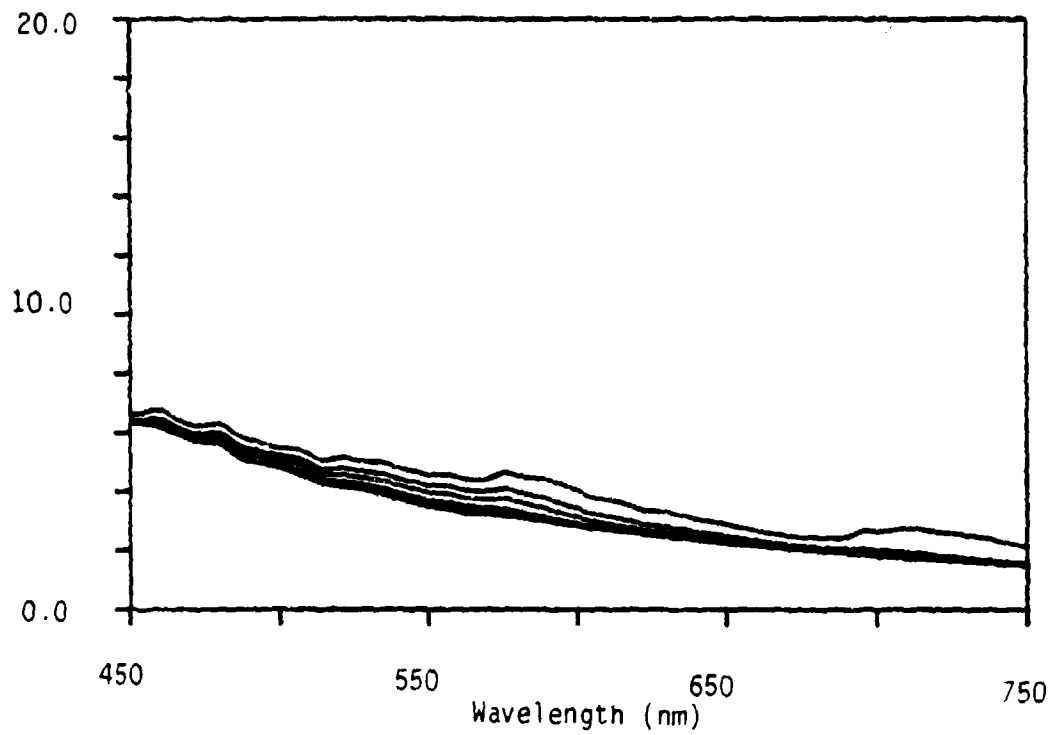


Figure A-42. Total radiance spectra for a Flat Carbonate Rock bottom type at selected water depths (1,2,3,5,7,10, 15,25, and 40 m). Curves in the above panel were generated for a visibility of 10 km and with water type 5.

Total Radiance Values (mw/(micron*cm*cm*sr))

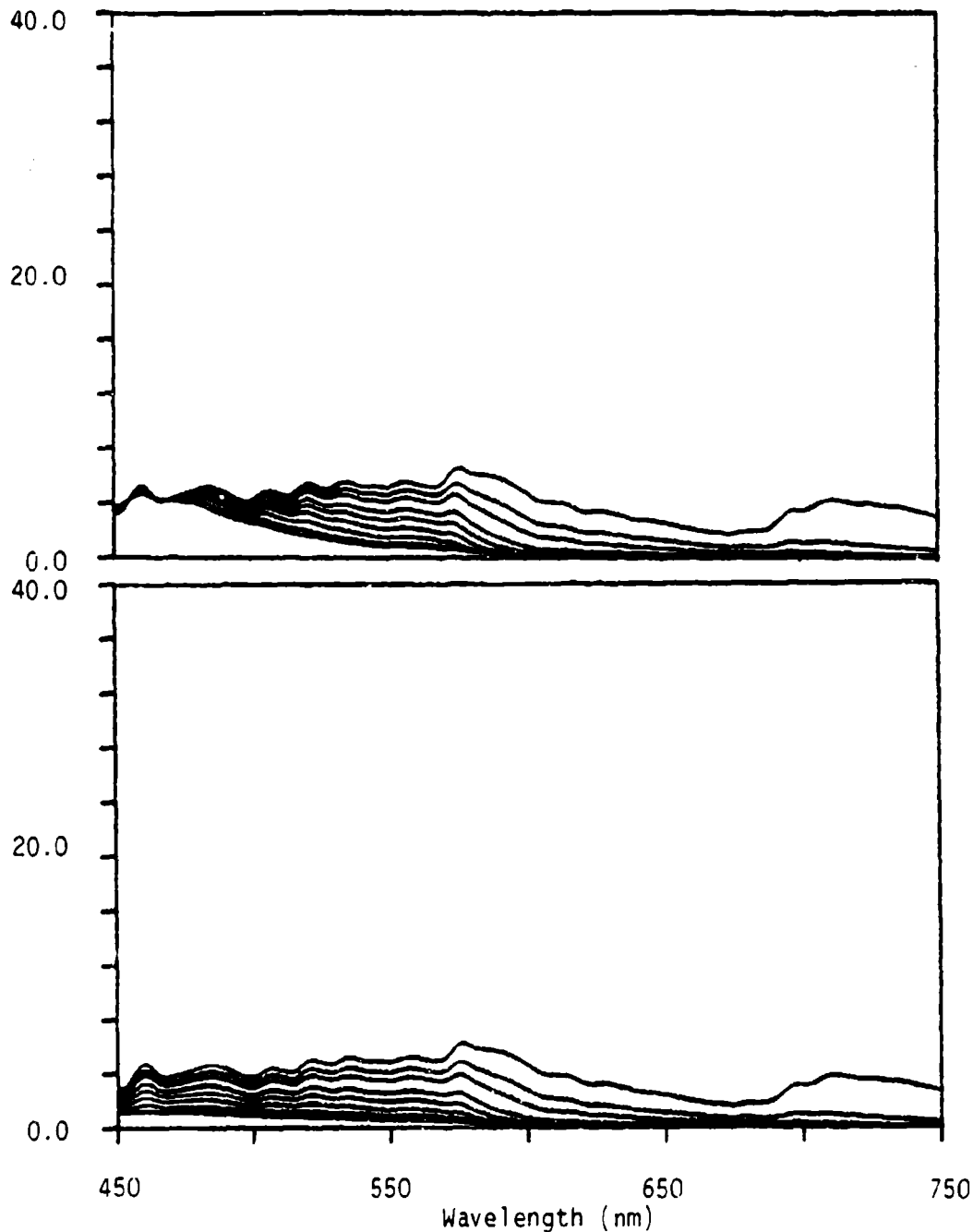


Figure A-43. Total radiance spectra for a Flat Carbonate Rock bottom type at selected water depths (1,2,3,5,7,10, 15,25, and 40 m). Curves in the upper panel were generated with water type 1 and in the lower panel for water type 2. Spectra were calculated for a sensor position just below the sea surface.

Total Radiance Values (mw/(micron*cm*cm*sr))

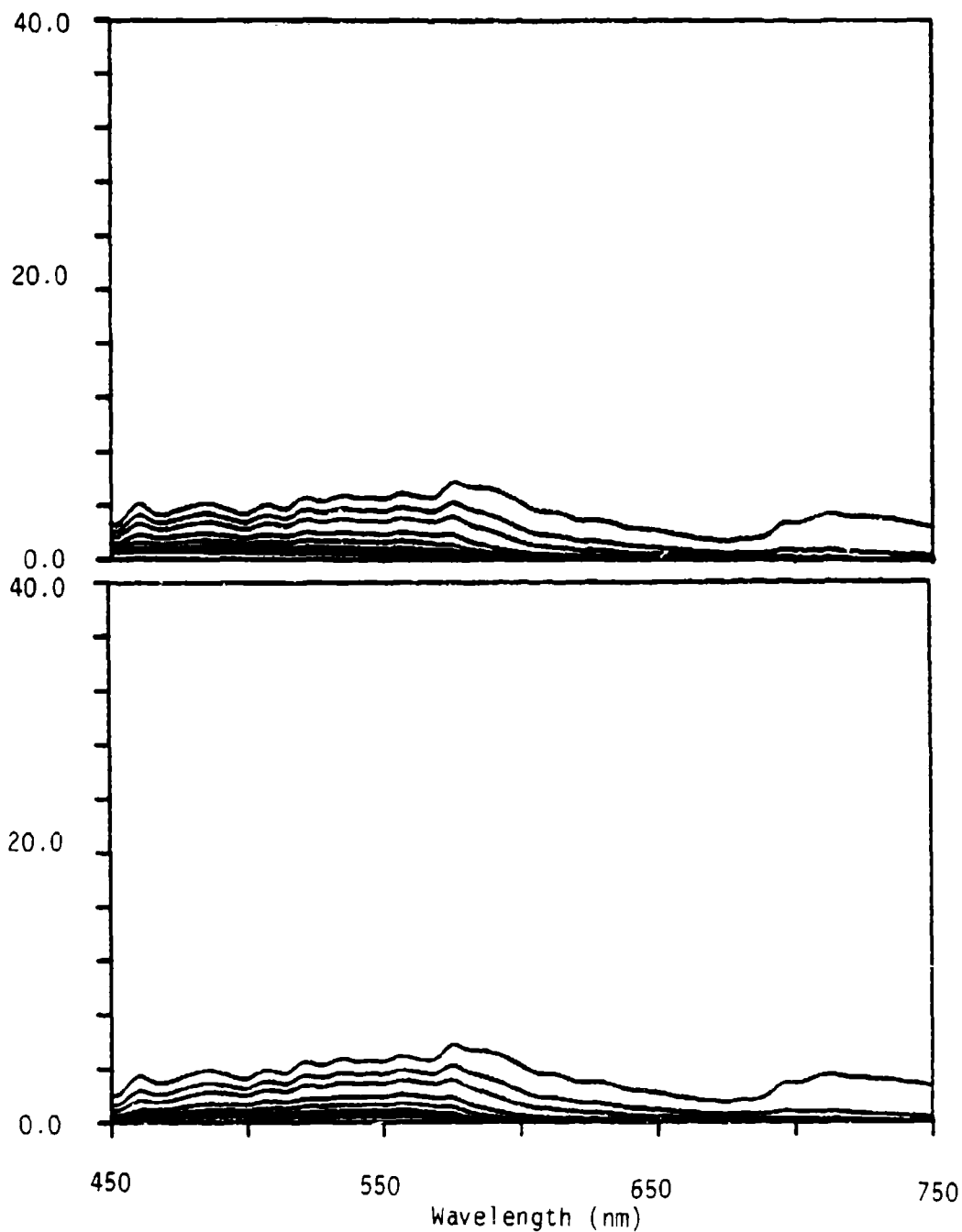


Figure A-44. Total radiance spectra for a Flat Carbonate Rock bottom type at selected water depths (1,2,3,5,7,10, 15,25, and 40 m). Curves in the upper panel were generated with water type 3 and in the lower panel for water type 4. Spectra were calculated for a sensor position just below the sea surface.

Total Radiance Values ($\text{mw}/(\text{micron} \cdot \text{cm} \cdot \text{cm} \cdot \text{sr})$)

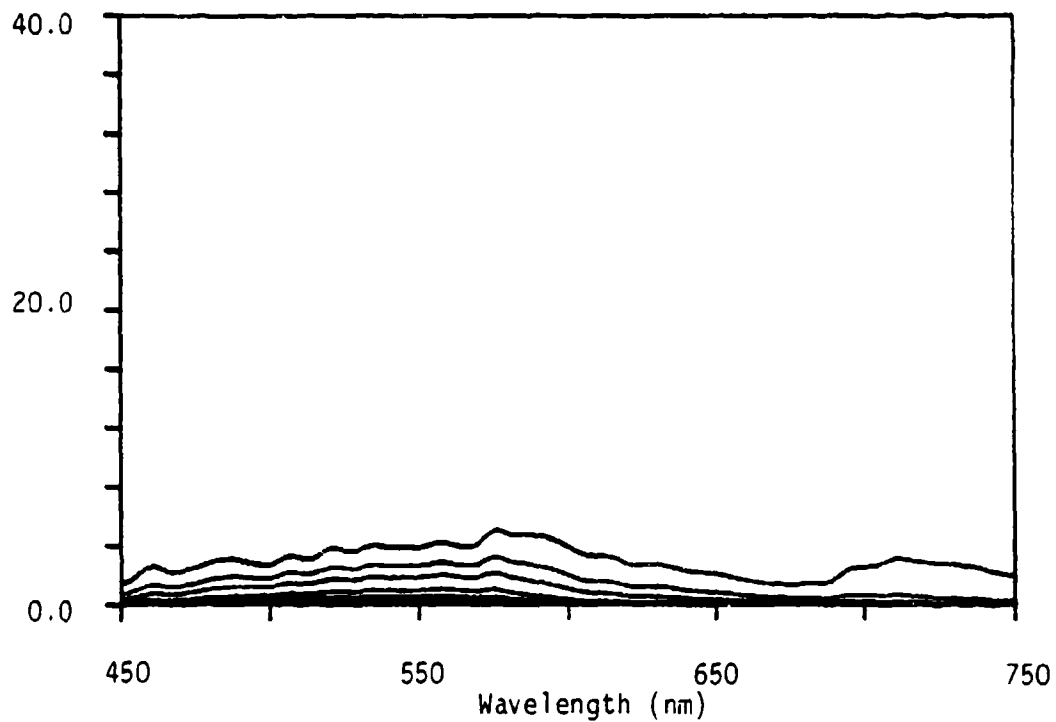


Figure A-45. Total radiance spectra for a Flat Carbonate Rock bottom type at selected water depths (1, 2, 3, 5, 7, 10, 15, 25, and 40 m). Curves in the above panel were generated with water type 5. Spectra were calculated for a sensor position just below the sea surface.

Total Radiance Values (mw/(micron*cm*cm*sr))

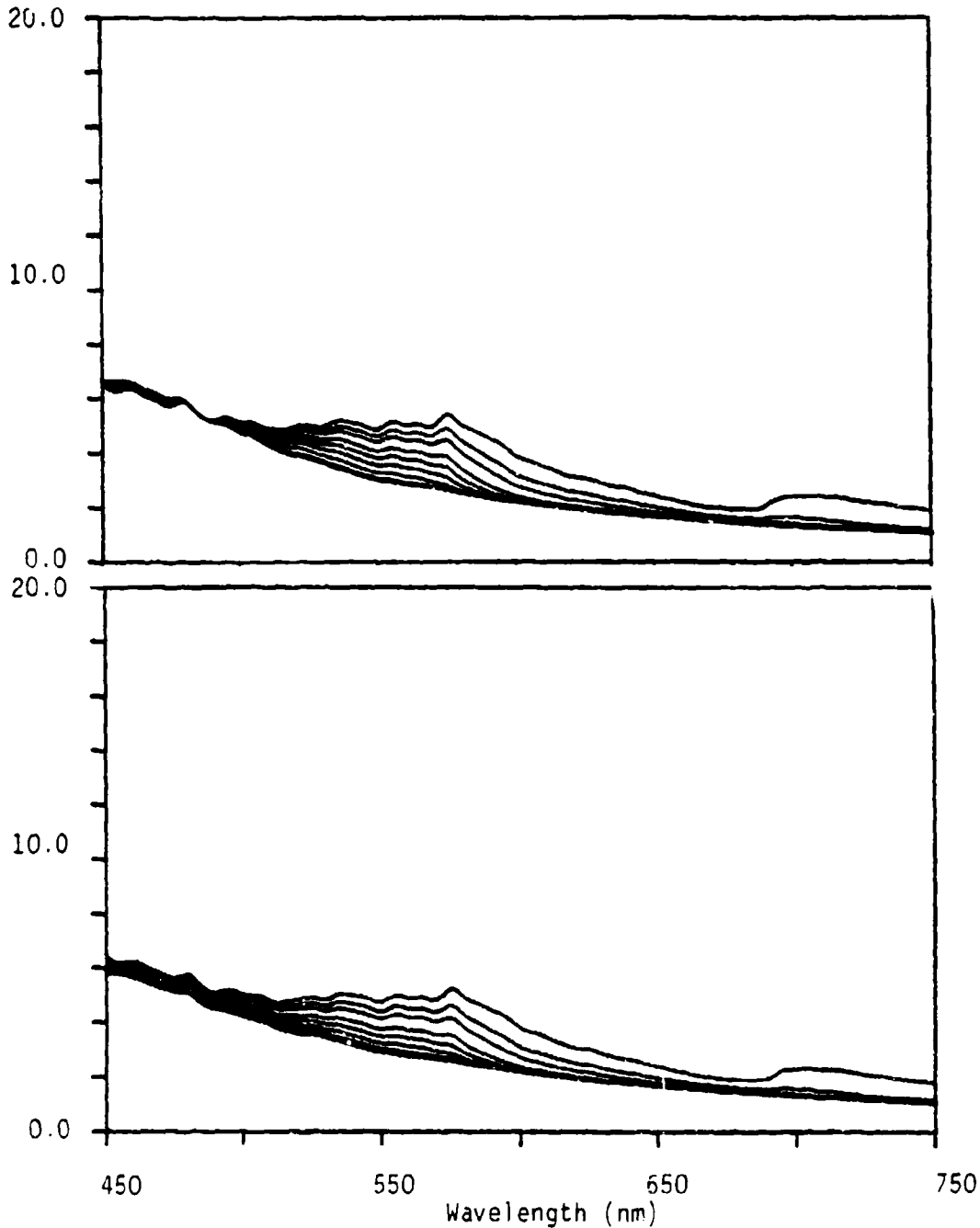


Figure A-46. Total radiance spectra for a Manatee Grass bottom type at selected water depths (1,2,3,5,7,10, 15,25, and 40 m). Curves in the upper panel were generated for a visibility of 23 km and with water type 1 and in the lower panel for water type 2.

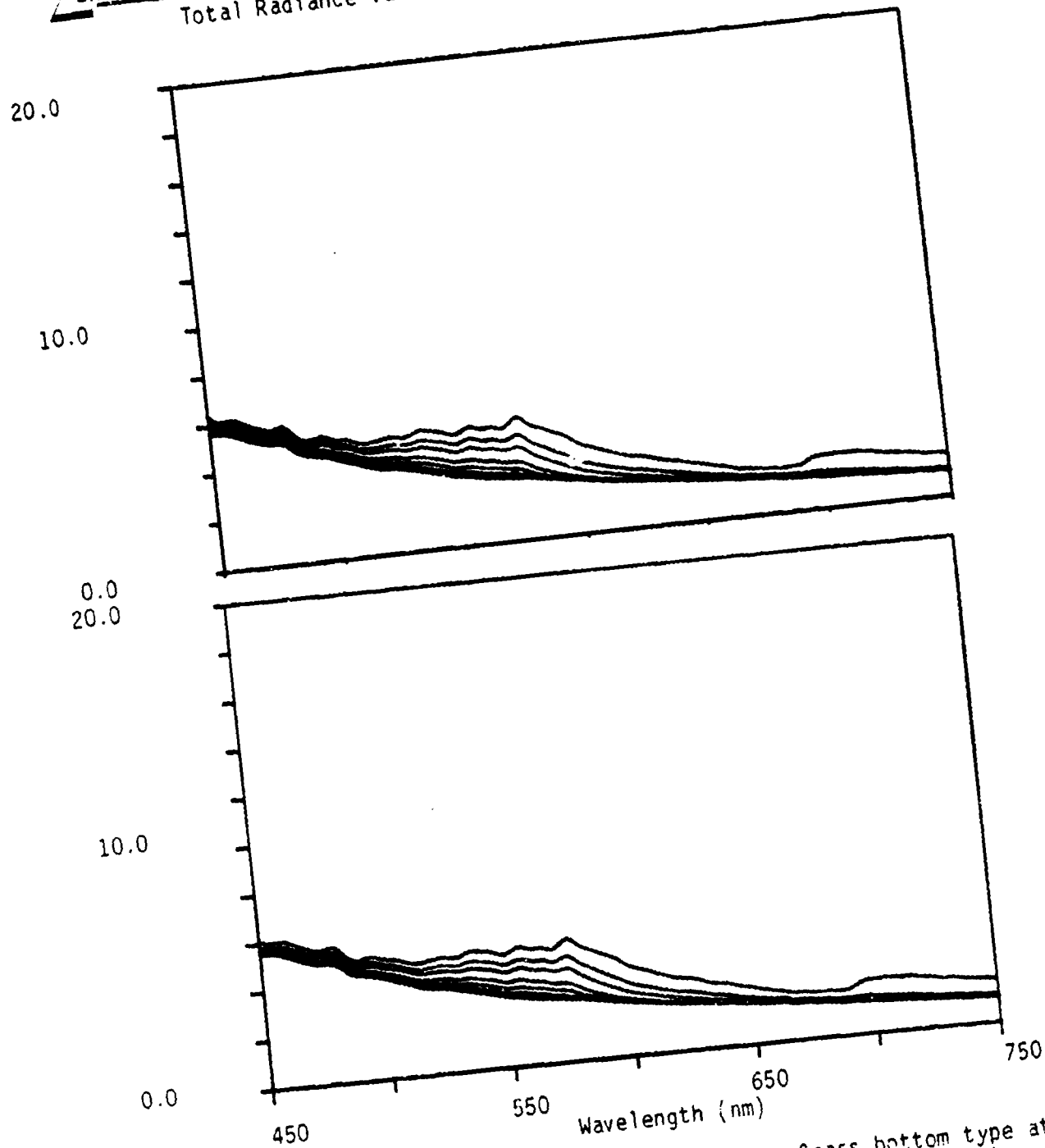


Figure A-47. Total radiance spectra for a Manatee Grass bottom type at selected water depths (1,2,3,5,7,10, 15,25, and 40 m). Curves in the upper panel were generated for a visibility of 23 km and with water type 3 and in the lower panel for water type 4.

Total Radiance Values (mw/(micron*cm*cm*sr))

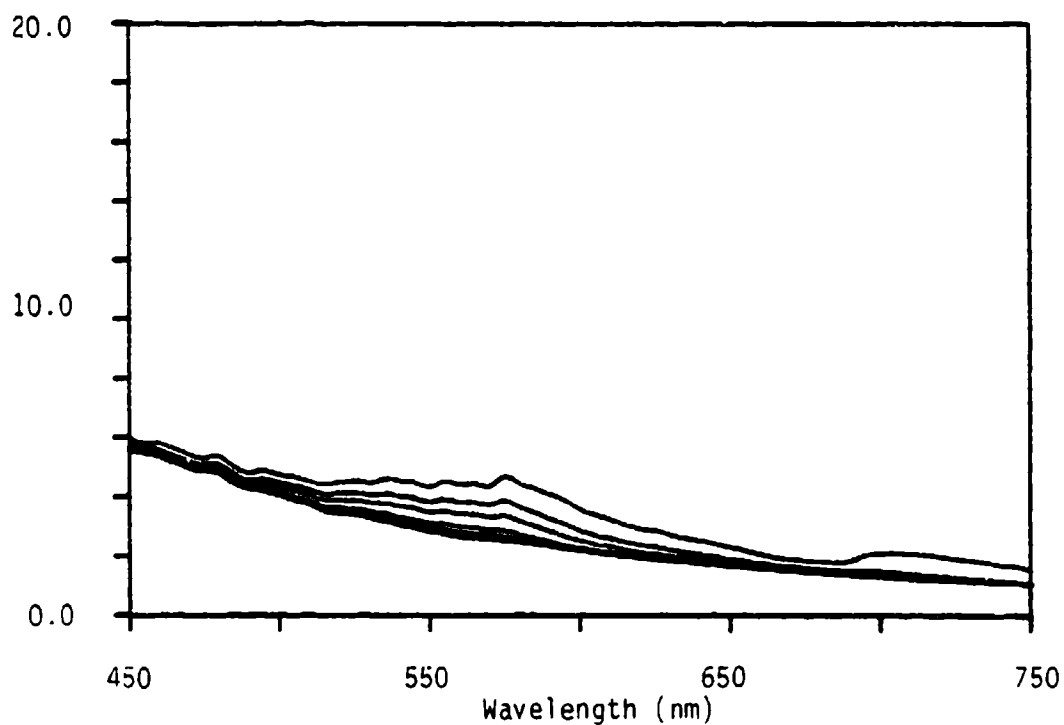


Figure A-48. Total radiance spectra for a Manatee Grass bottom type at selected water depths (1,2,3,5,7,10,15,25, and 40 m). Curves in the above panel were generated for a visibility of 23 km and with water type 5.

ERIM

Total Radiance Values (mw/(micron*cm*cm*sr))

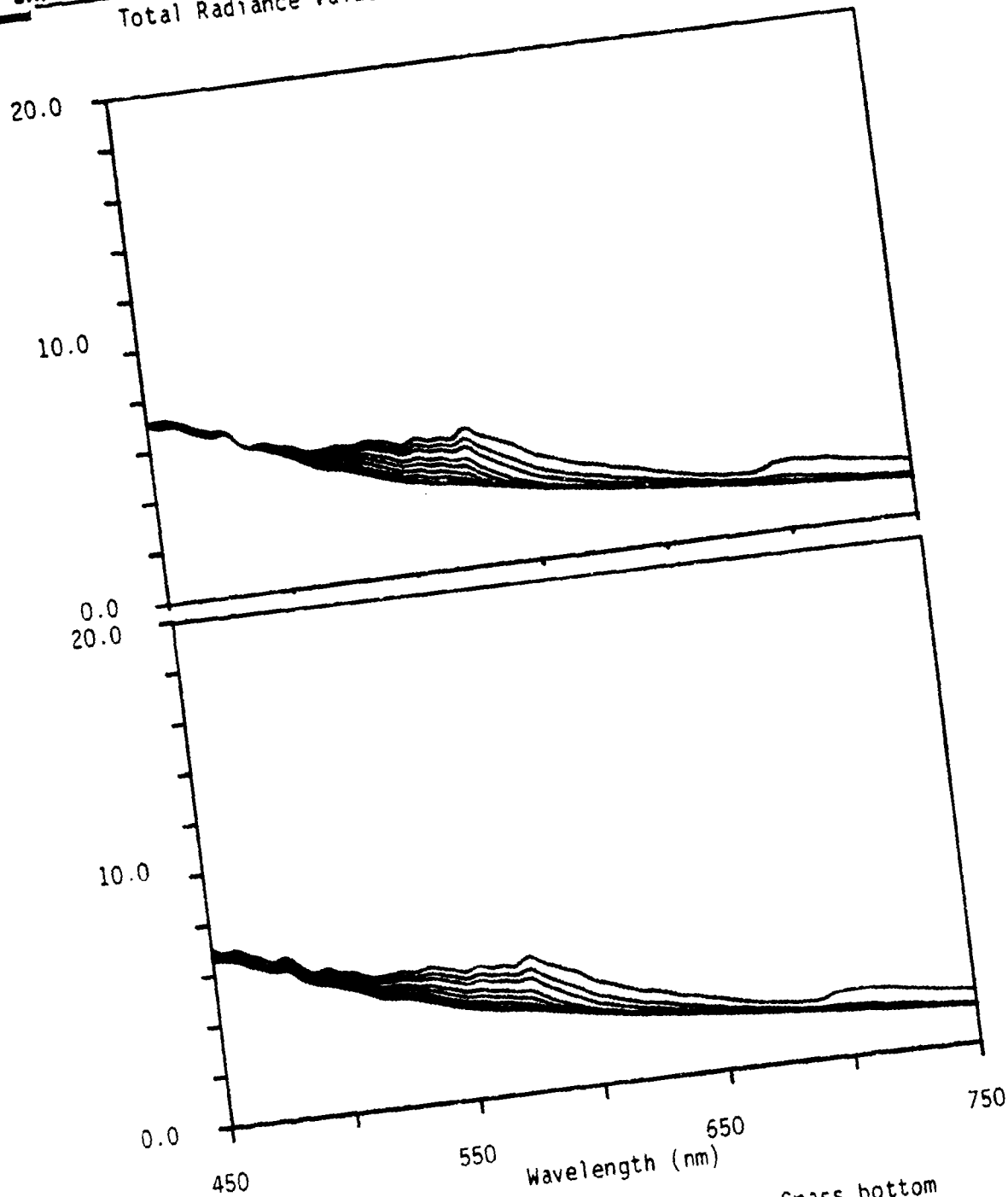


Figure A-49. Total radiance spectra for a Manatee Grass bottom type at selected water depths (1,2,3,5,7,10, 15,25, and 40 m). Curves in the upper panel were generated for a visibility of 10 km and with water type 1 and in the lower panel for water type 2.

Total Radiance Values (mw/(micron*cm*cm*sr))

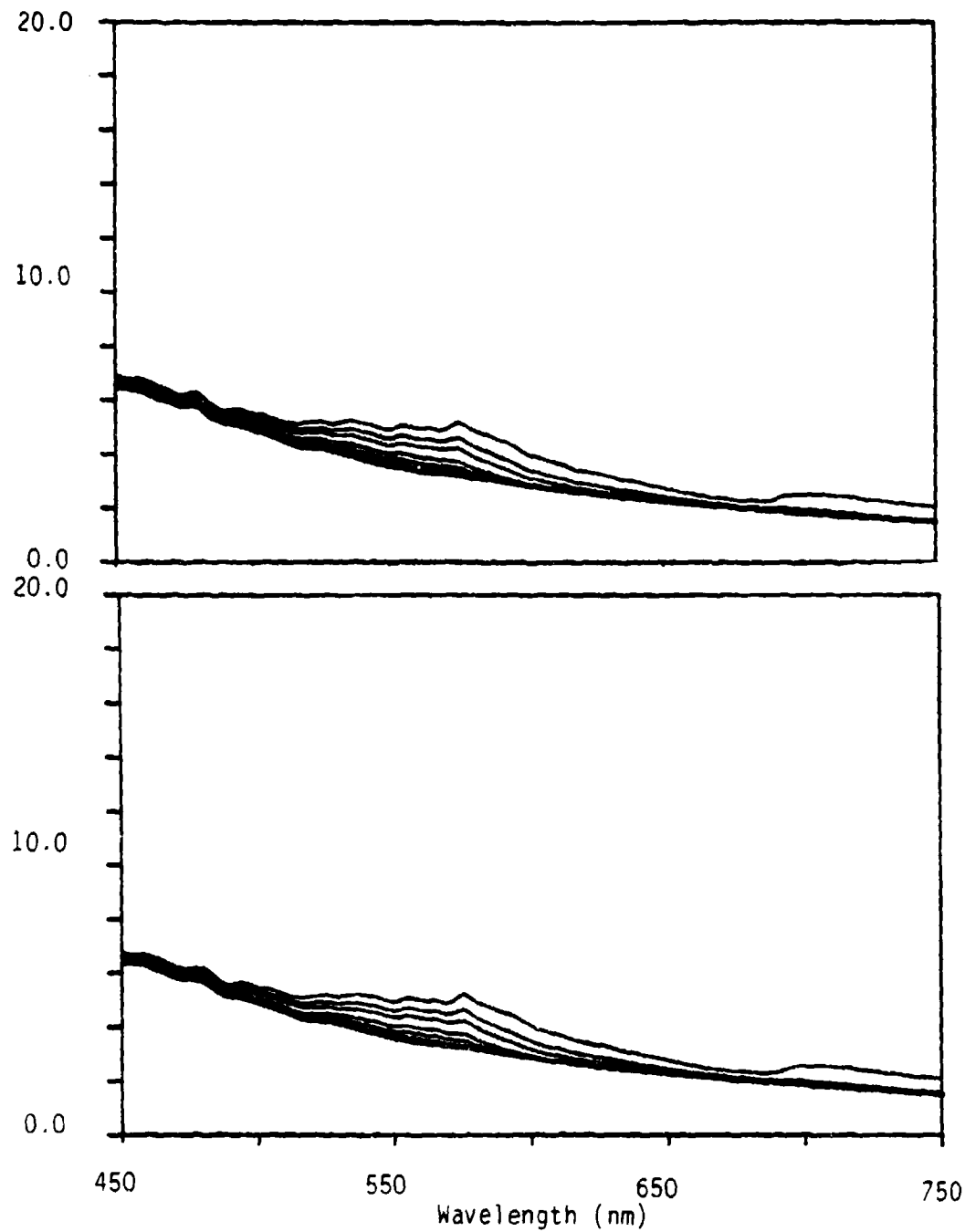


Figure A-50. Total radiance spectra for a Manatee Grass bottom type at selected water depths (1,2,3,5,7,10, 15,25, and 40 m). Curves in the upper panel were generated for a visibility of 10 km and with water type 3 and in the lower panel for water type 4.

Total Radiance Values (mw/(micron*cm*cm*sr))

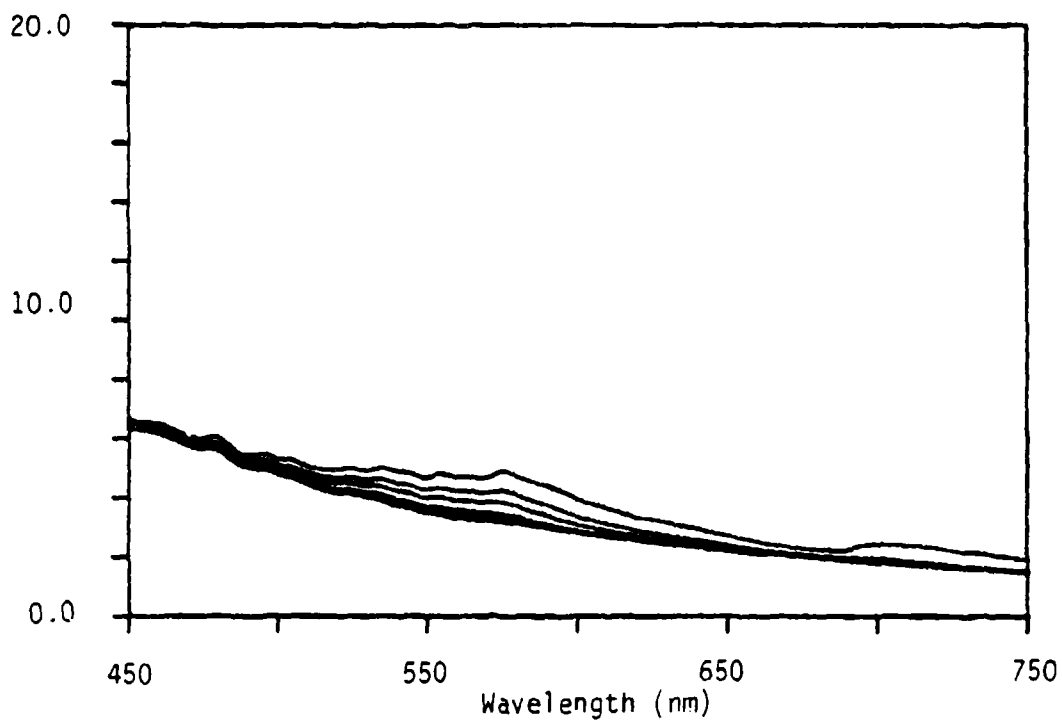


Figure A-51. Total radiance spectra for a Manatee Grass bottom type at selected water depths (1,2,3,5,7,10, 15,25, and 40 m). Curves in the above panel were generated for a visibility of 10 km and with water type 5.

Total Radiance Values (mw/(micron*cm*cm*sr))

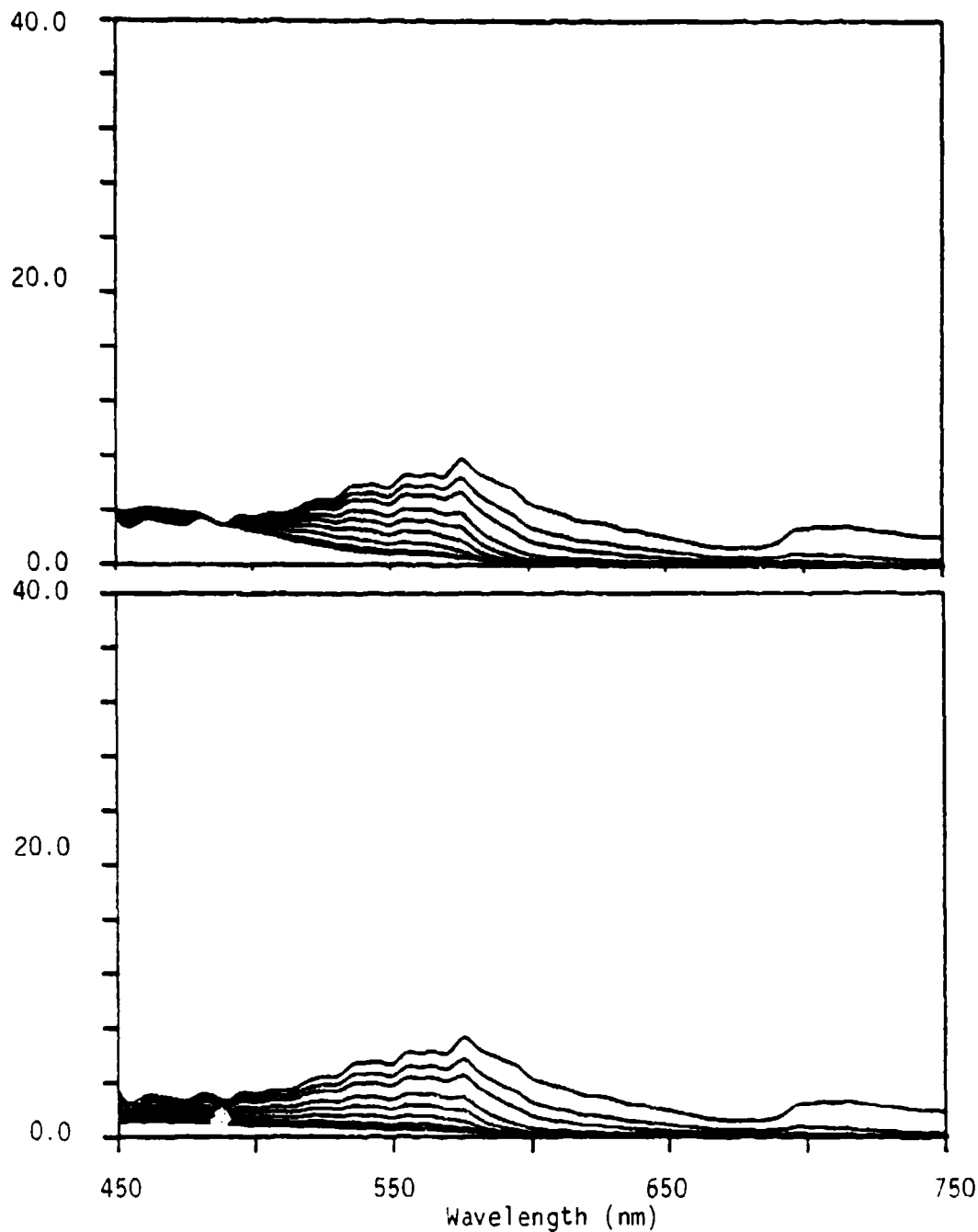


Figure A-52. Total radiance spectra for a Manatee Grass bottom type at selected water depths (1,2,3,5,7,10, 15,25, and 40 m). Curves in the upper panel were generated with water type 1 and in the lower panel for water type 2. Spectra were calculated for a sensor position just below the sea surface.

Total Radiance Values (mw/(micron*cm*cm*sr))

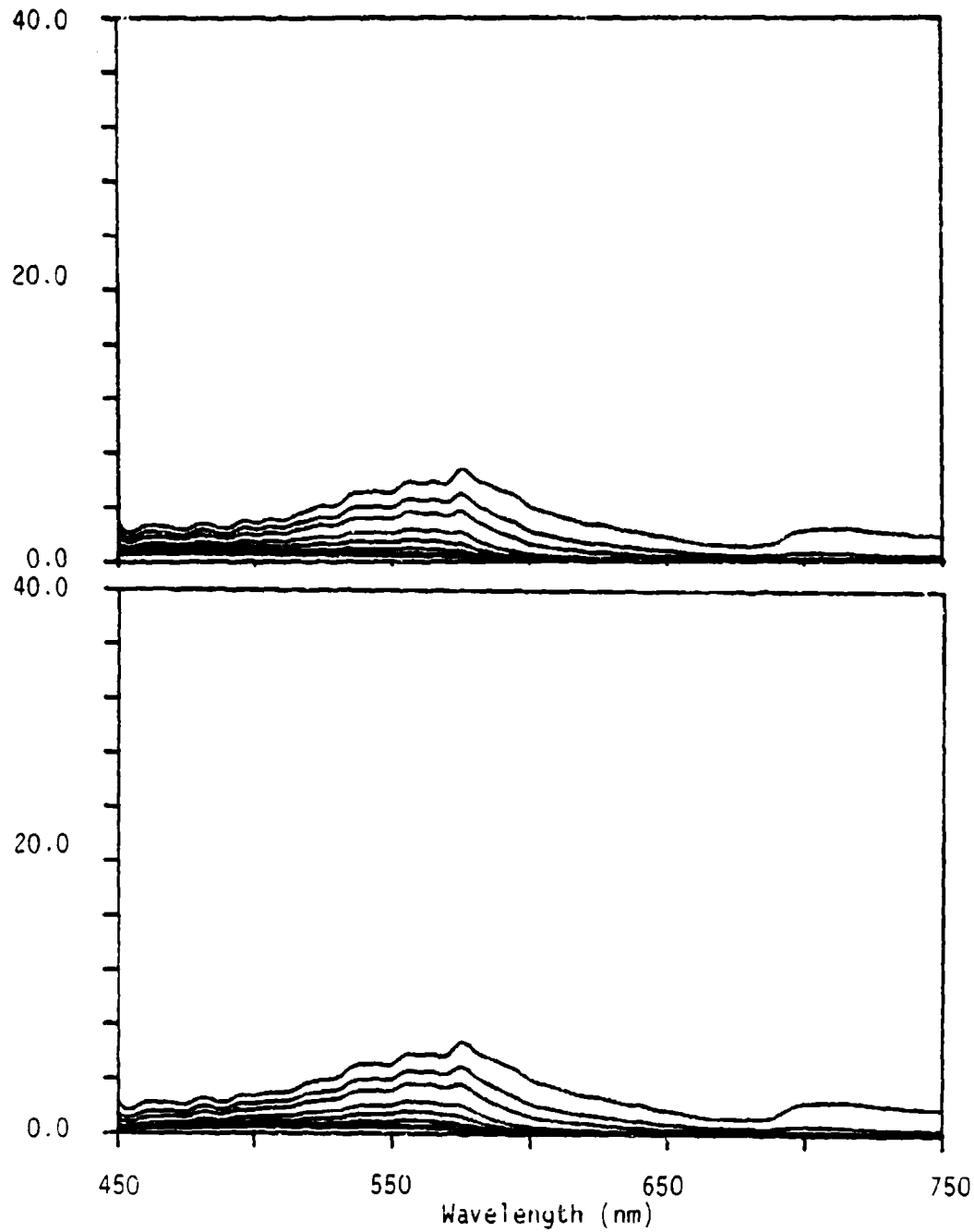


Figure A-53. Total radiance spectra for a Manatee Grass bottom type at selected water depths (1,2,3,5,7,10, 15,25, and 40 m). Curves in the upper panel were generated with water type 3 and in the lower panel for water type 4. Spectra were calculated for a sensor position just below the sea surface.

Total Radiance Values (mw/(micron*cm*cm*sr))

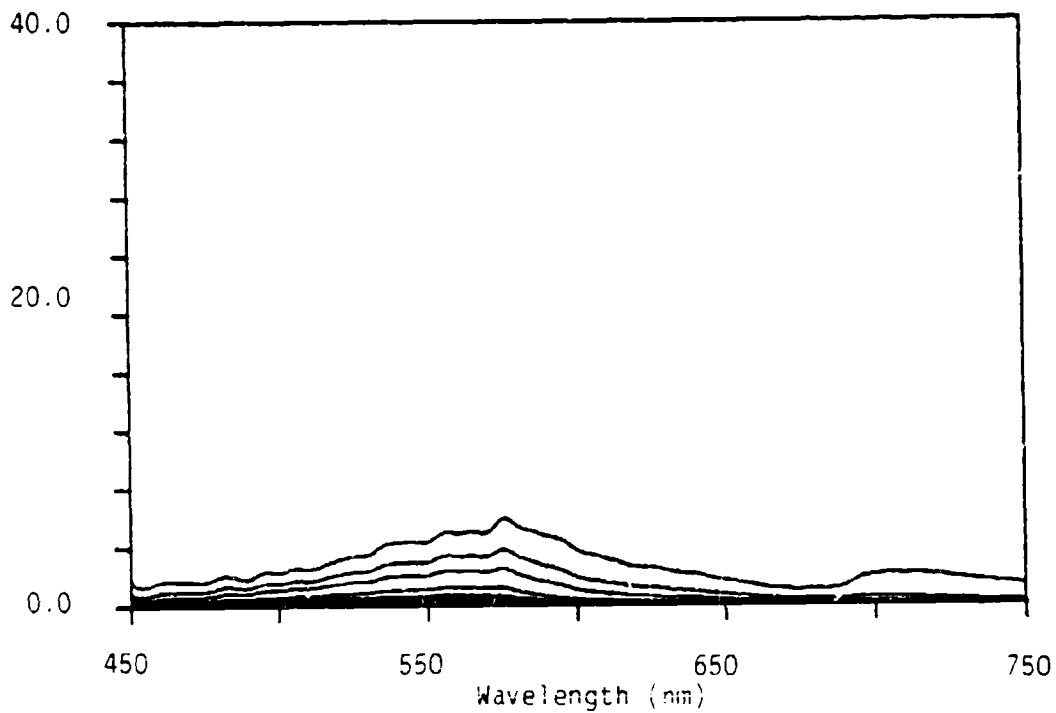


Figure A-54. Total radiance spectra for a Manatee Grass bottom type at selected water depths (1,2,3,5,7,10, 15,25, and 40 m). Curves in the above panel were generated with water type 8. Spectra were calculated for a sensor position just below the sea surface.

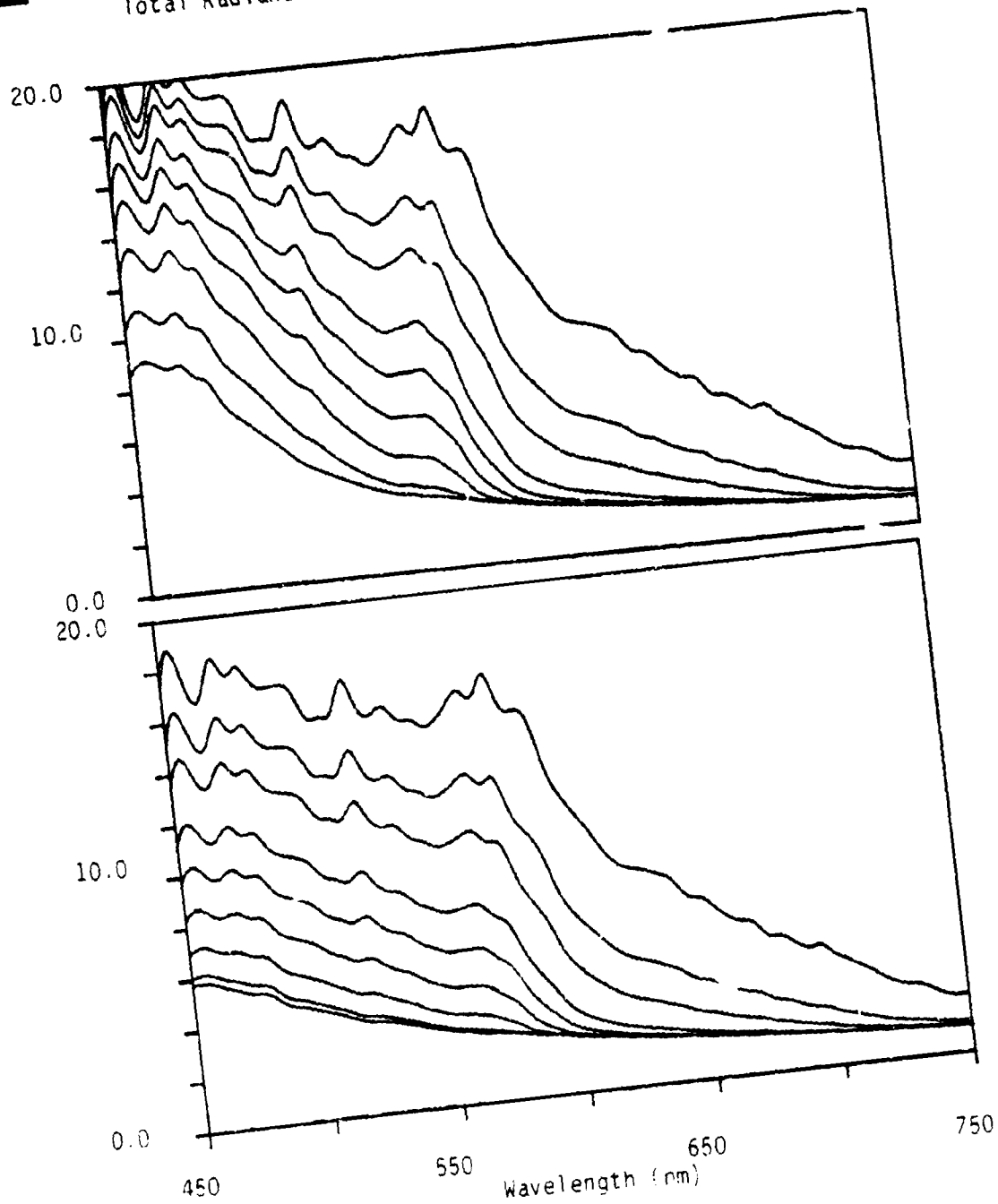


Figure A-55. Total radiance spectra for a Sand 7/22/80 bottom type at selected water depths (1, 2, 3, 5, 7, 10, 15, 25, and 40 m). Curves in the upper panel were generated for a visibility of 23 km and with water type 1 and in the lower panel for water type 2.

Total Radiance Values (mw/(micron*cm*cm*sr))

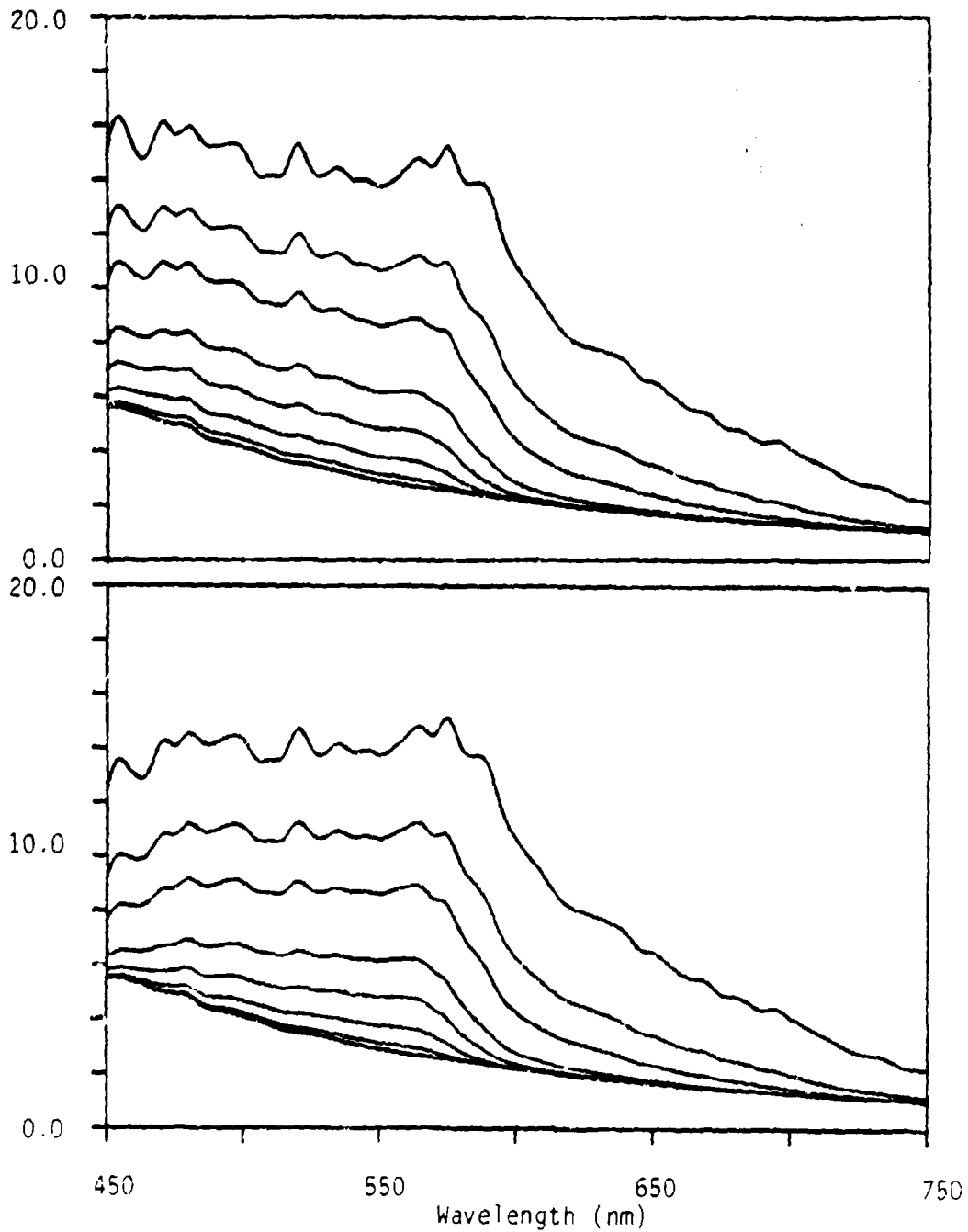


Figure A-56. Total radiance spectra for a Sand 7/22/80 bottom type at selected water depths (1,2,3,5,7,10, 15,25, and 40 m). Curves in the upper panel were generated for a visibility of 23 km and with water type 3 and in the lower panel for water type 4.

Total Radiance Values (mw/(micron*cm*cm*sr))

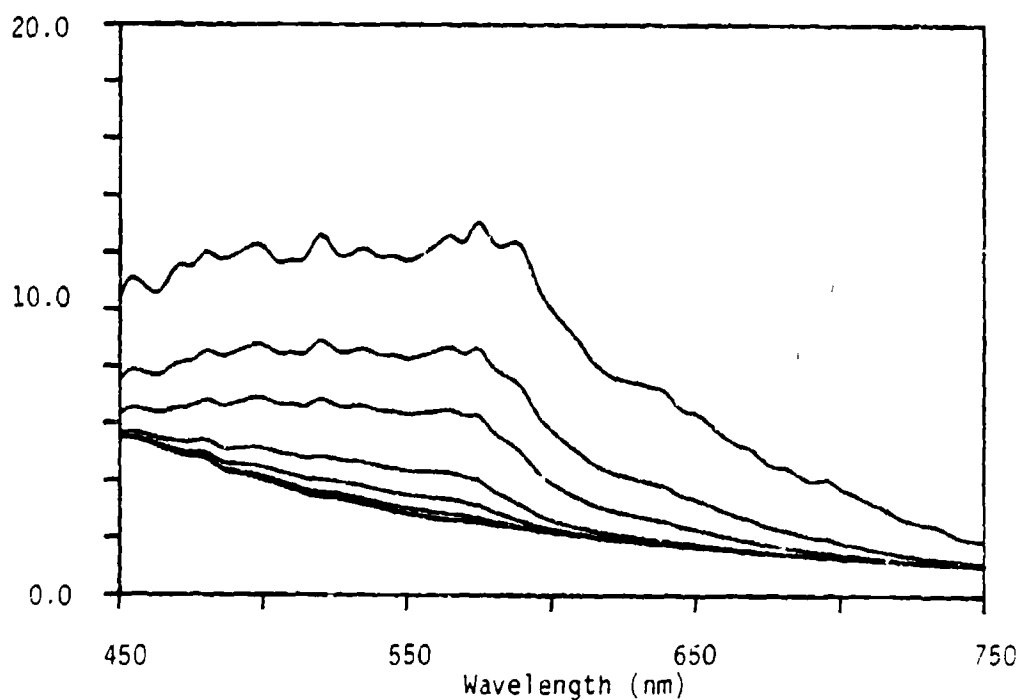


Figure A-57. Total radiance spectra for a Sand 7/22/80 bottom type at selected water depths (1,2,3,5,7,10,15,25, and 40 m). Curves in the above panel were generated for a visibility of 23 km and with water type 5.

ERIM

Total Radiance Values (mw/(micron*cm*cm*sr))

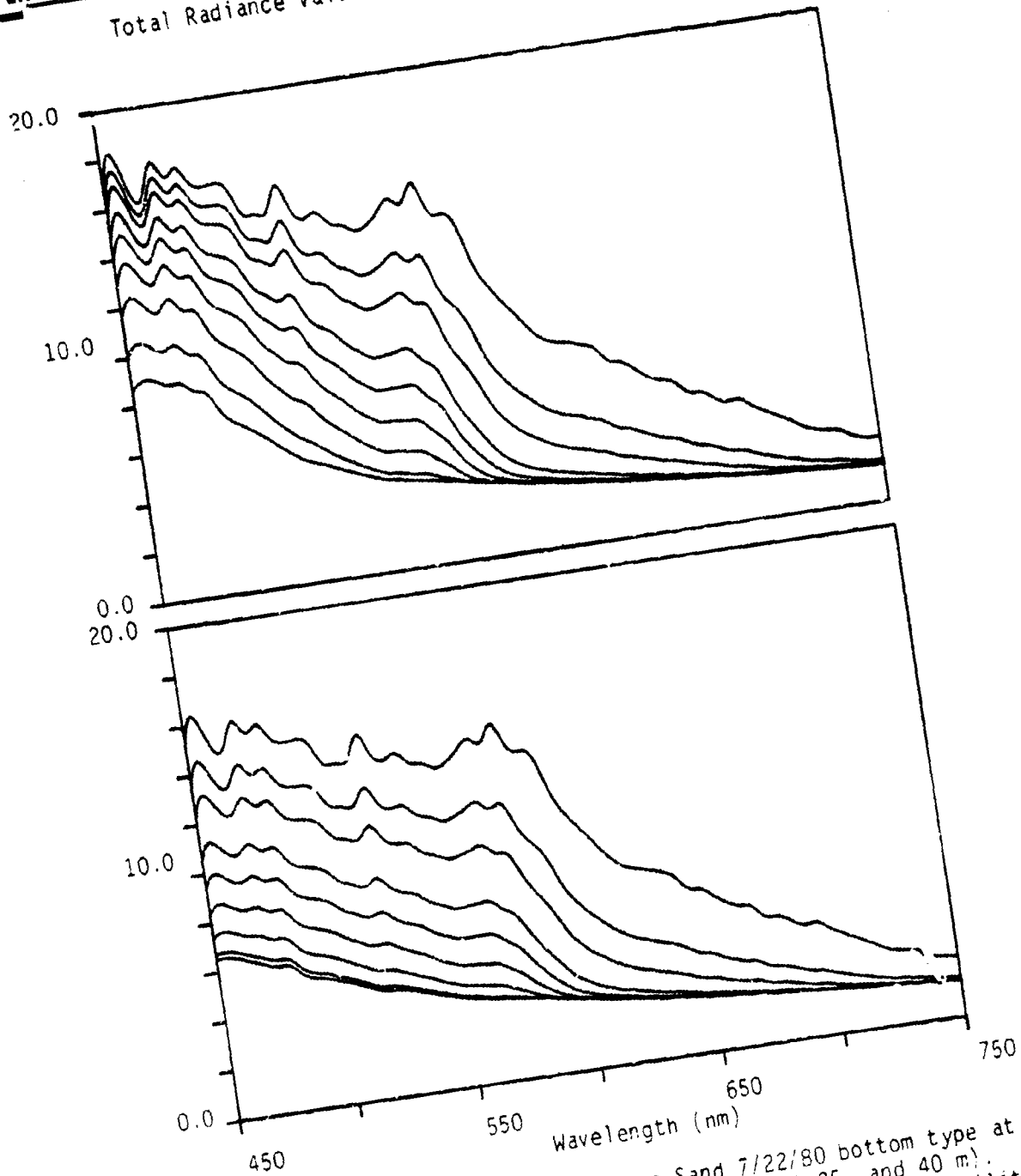


Figure A-58. Total radiance spectra for a Sand 7/22/80 bottom type at selected water depths (1, 2, 3, 5, 7, 10, 15, 25, and 40 m). Curves in the upper panel were generated for a visibility of 10 km and with water type 1 and in the lower panel for water type 2.

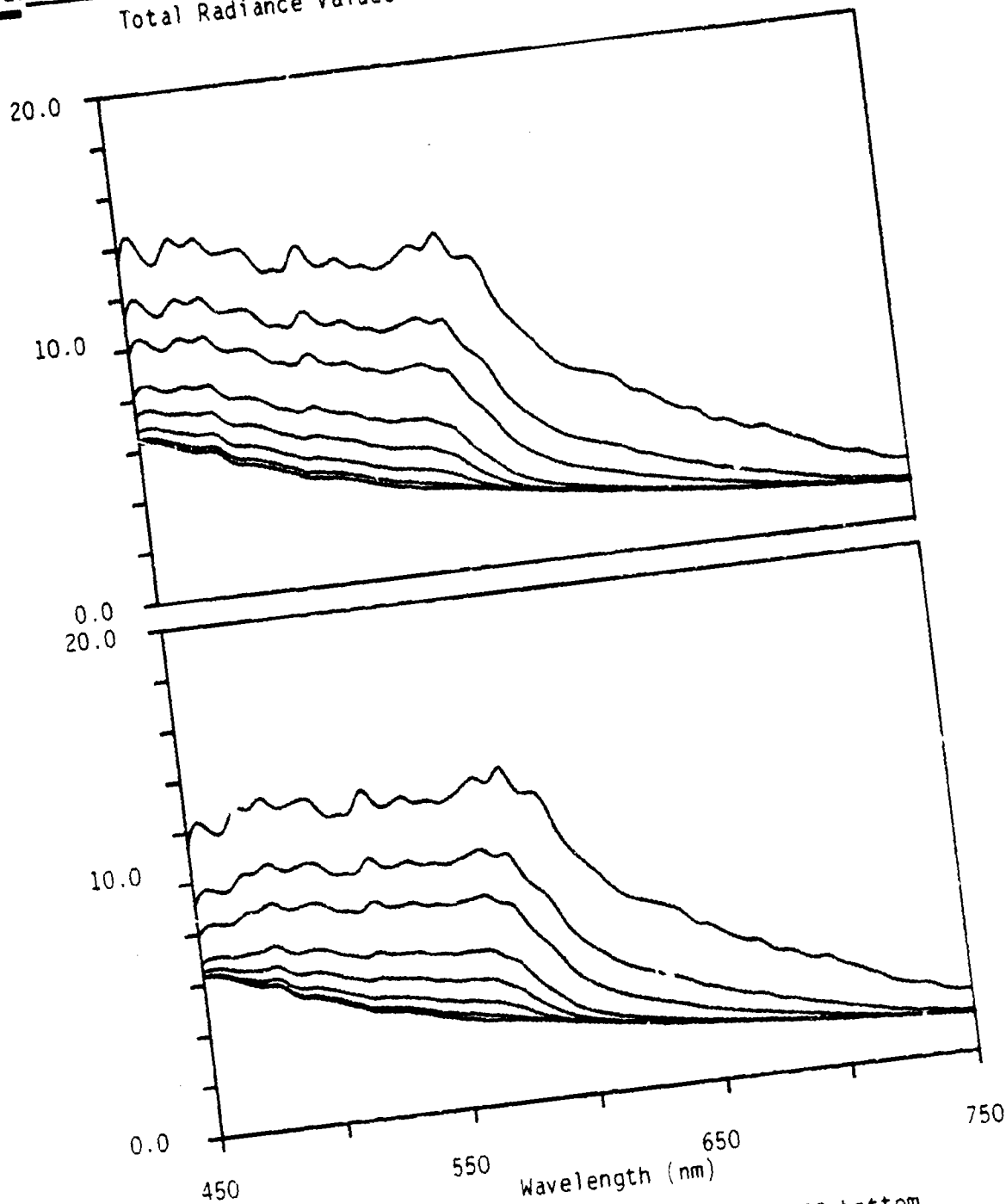


Figure A-59. Total radiance spectra for a Sand 7/22/80 bottom type at selected water depths (1,2,3,5,7,10, 15,25, and 40 m). Curves in the upper panel were generated for a visibility of 10 km and with water type 3 and in the lower panel for water type 4.

Total Radiance Values (mw/(micron*cm*cm*sr))

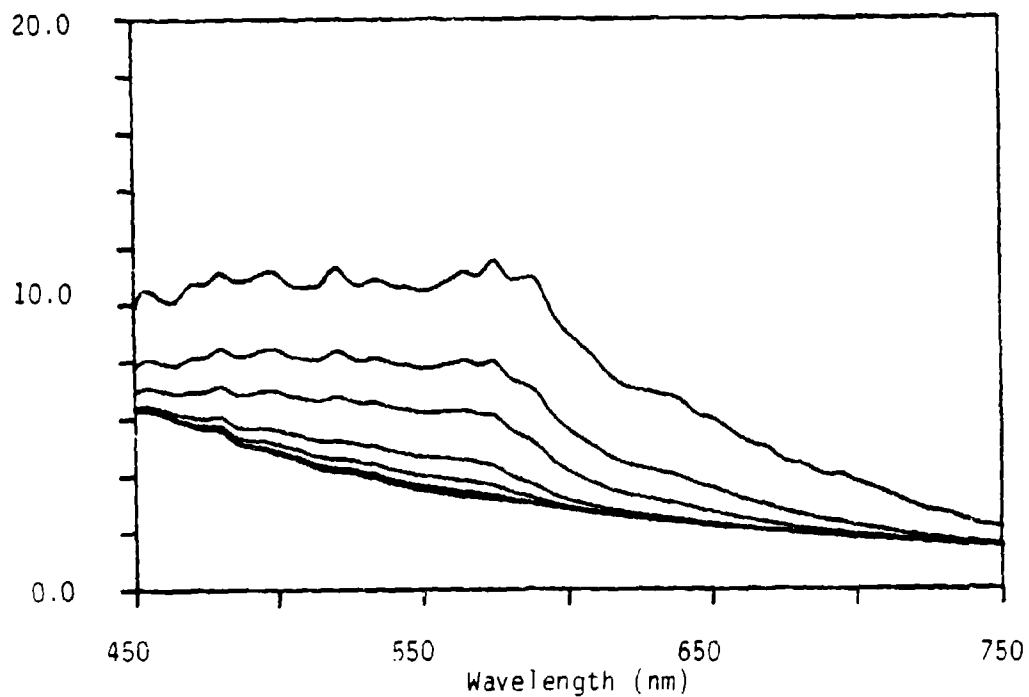


Figure A-60. Total radiance spectra for a Sand 7/22/80 bottom type at selected water depths (1,2,3,5,7,10, 15,25, and 40 m). Curves in the above panel were generated for a visibility of 10 km and with water type 5.

Total Radiance Values (mw/(micron*cm*cm*sr))

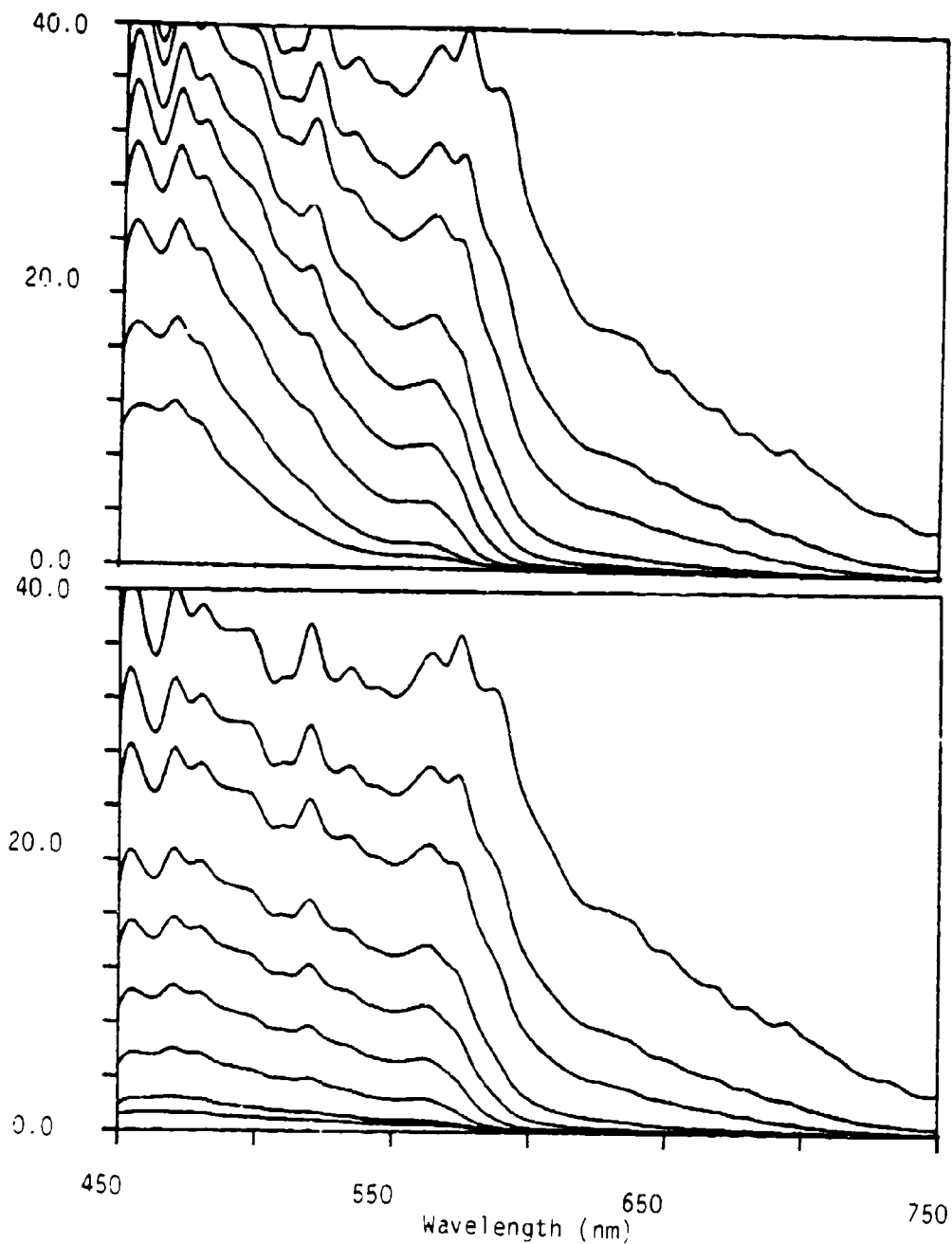


Figure A-61. Total radiance spectra for a Sand 7/22/80 bottom type at selected water depths (1,2,3,5,7,10, 15,25, and 40 m). Curves in the upper panel were generated with water type 1 and in the lower panel for water type 2. Spectra were calculated for a sensor position just below the sea surface.

Total Radiance Values (mw/(micron*cm*cm*sr))

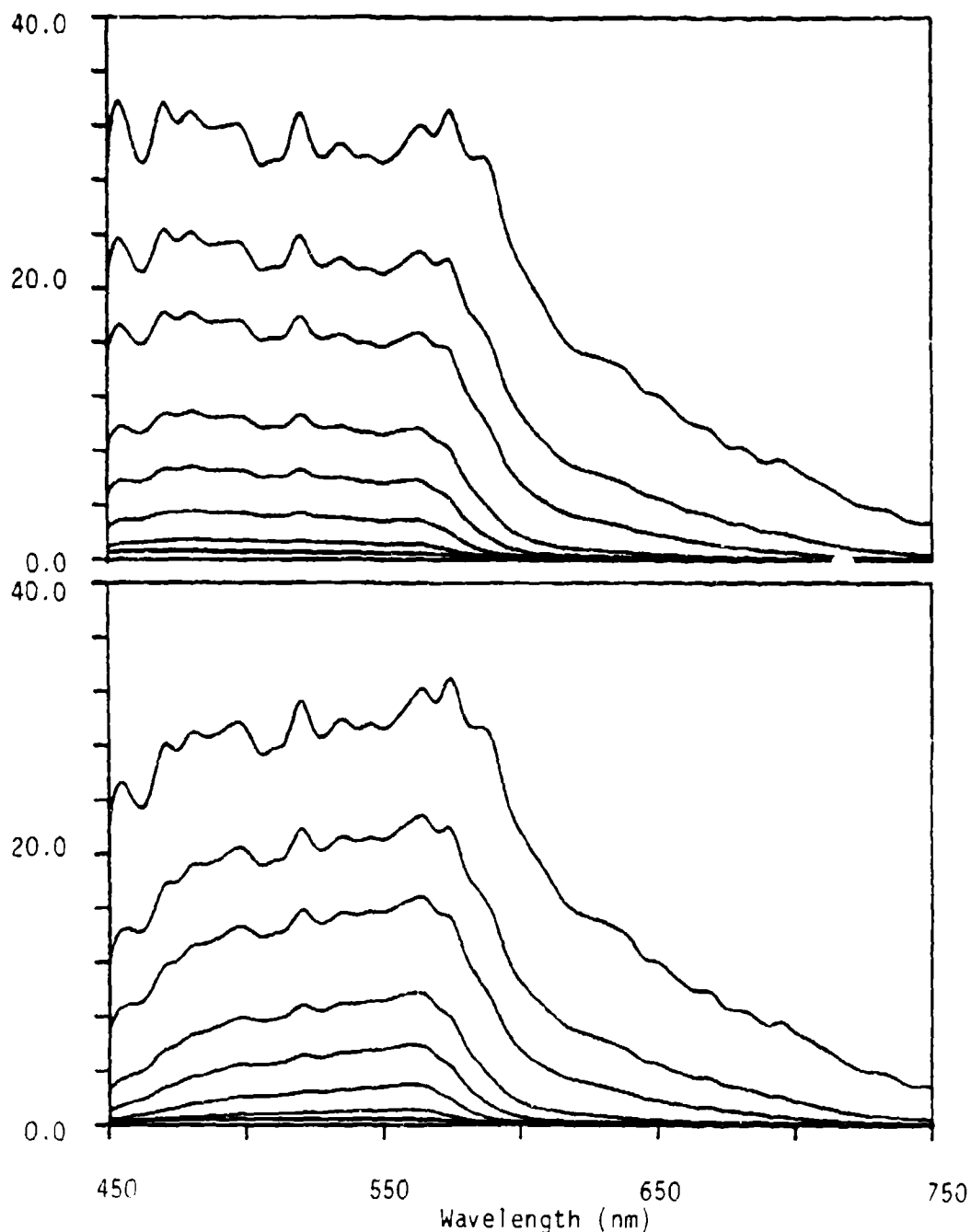


Figure A-62. Total radiance spectra for a Sand 7/22/80 bottom type at selected water depths (1,2,3,5,7,10, 15,25, and 40 m). Curves in the upper panel were generated with water type 3 and in the lower panel for water type 4. Spectra were calculated for a sensor position just below the sea surface.

Total Radiance Values (mw/(micron*cm*cm*sr))

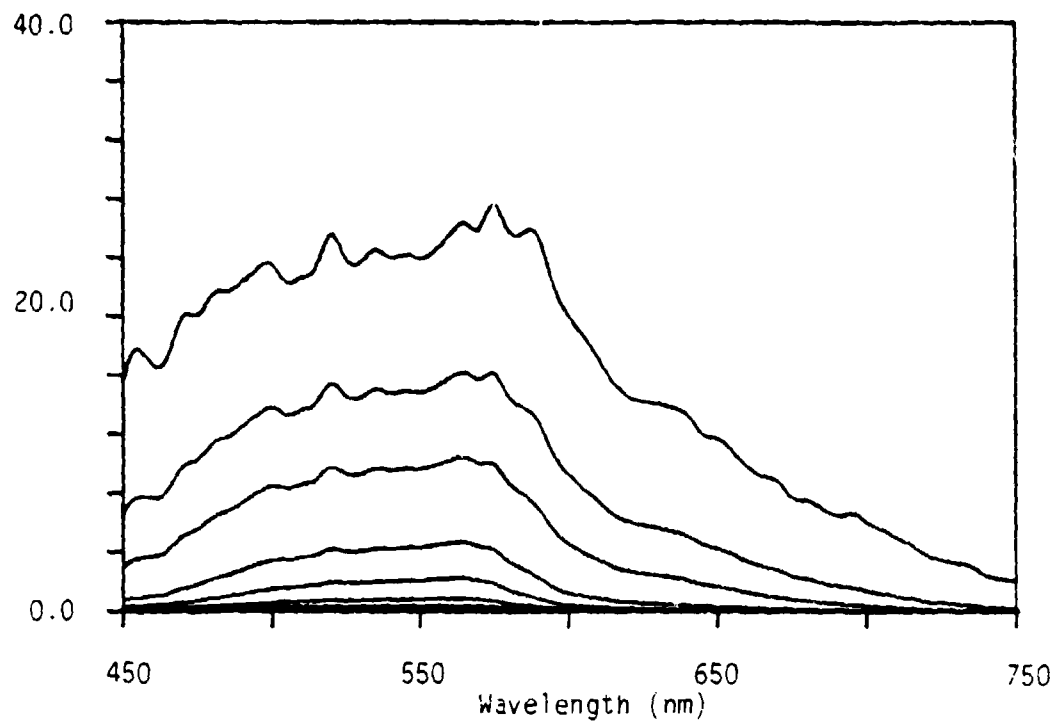


Figure A-63. Total radiance spectra for a Sand 7/22/80 bottom type at selected water depths (1,2,3,5,7,10, 15,25, and 40 m). Curves in the above panel were generated with water type 5. Spectra were calculated for a sensor position just below the sea surface.

Σ ERIM

Total Radiance Values (mw/(micron*cm*cm*sr))

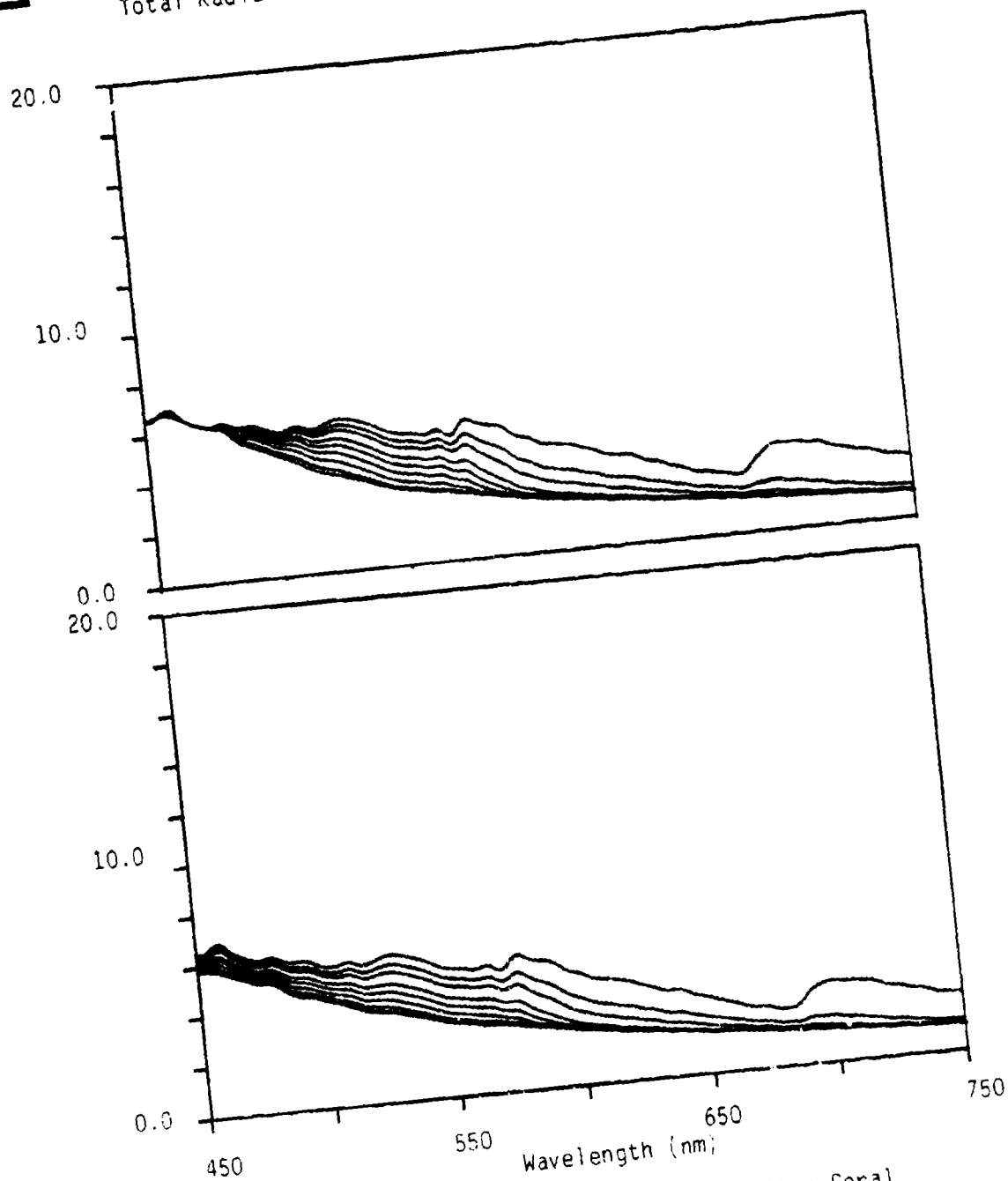


Figure A-64. Total radiance spectra for a Large Star Coral bottom type at selected water depths (1, 2, 3, 5, 7, 10, 15, 25, and 40 m). Curves in the upper panel were generated for a visibility of 23 km and with water type 1 and in the lower panel for water type 2.

Σ ERIM

Total Radiance Values (mw/(micron*cm*cm*sr))

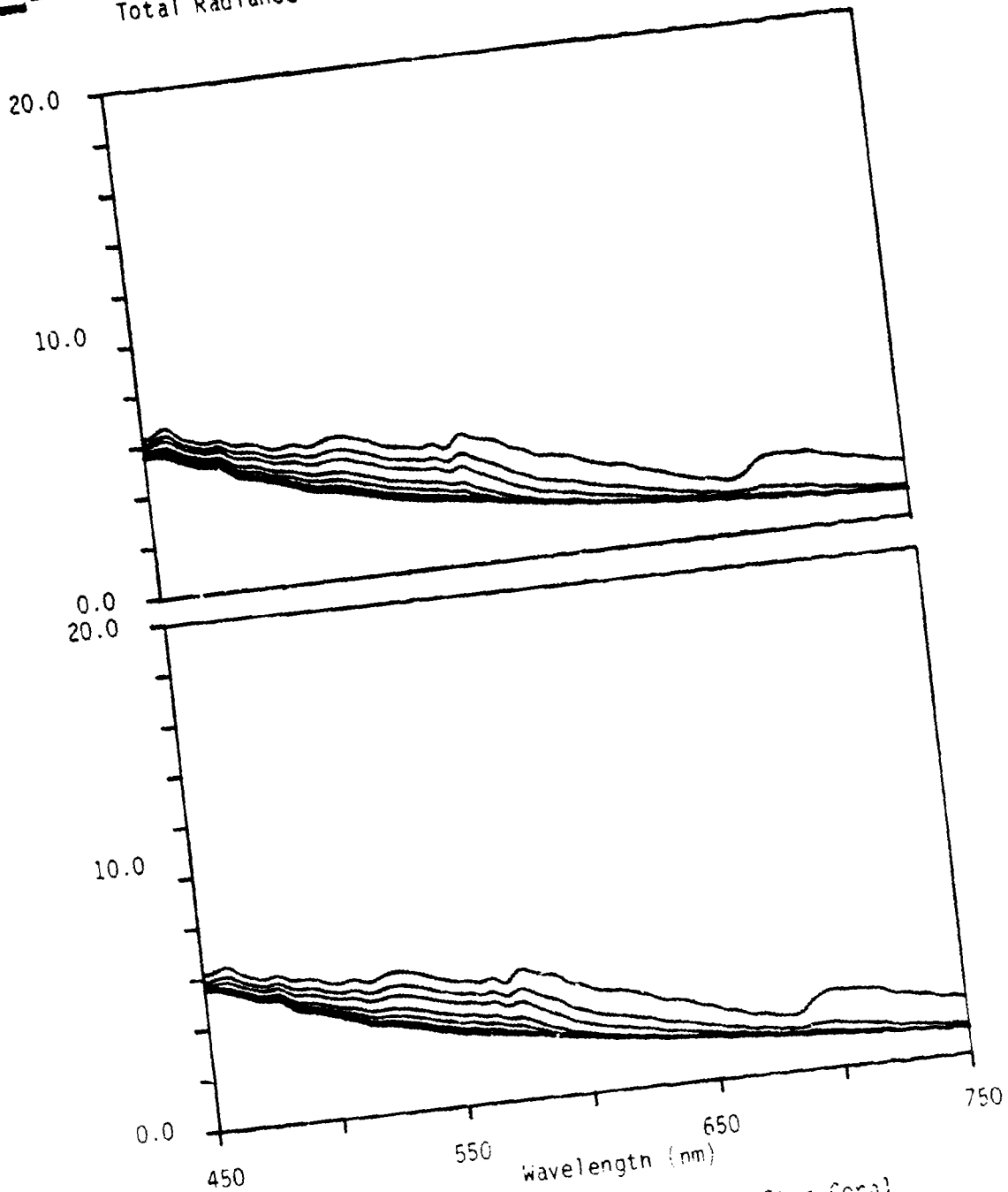


Figure A-65. Total radiance spectra for a large Star Coral bottom type at selected water depths (1, 2, 3, 5, 7, 10, 15, 25, and 40 m). Curves in the upper panel were generated for a visibility of 20 km and with water type 3 and in the lower panel for water type 4.

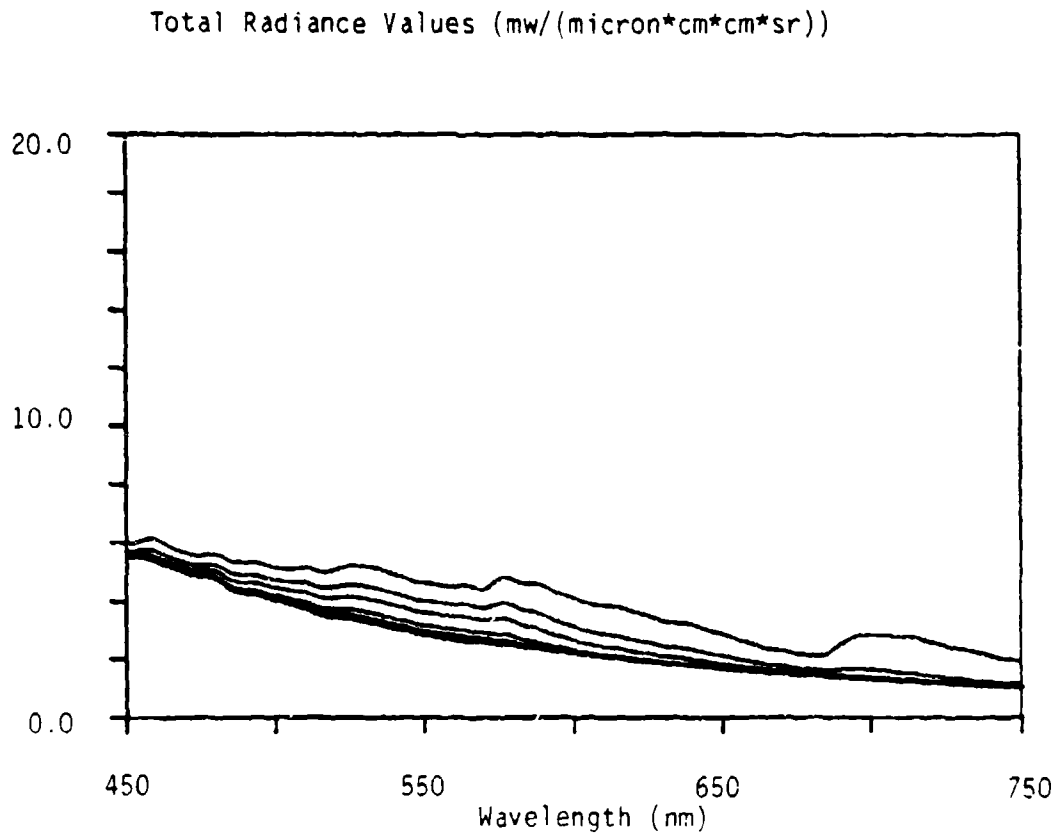


Figure A-66. Total radiance spectra for a Large Star Coral bottom type at selected water depths (1,2,3,5,7,10, 15,25, and 40 m). Curves in the above panel were generated for a visibility of 23 km and with water type 5.

Total Radiance Values (mw/(micron*cm*cm*sr))

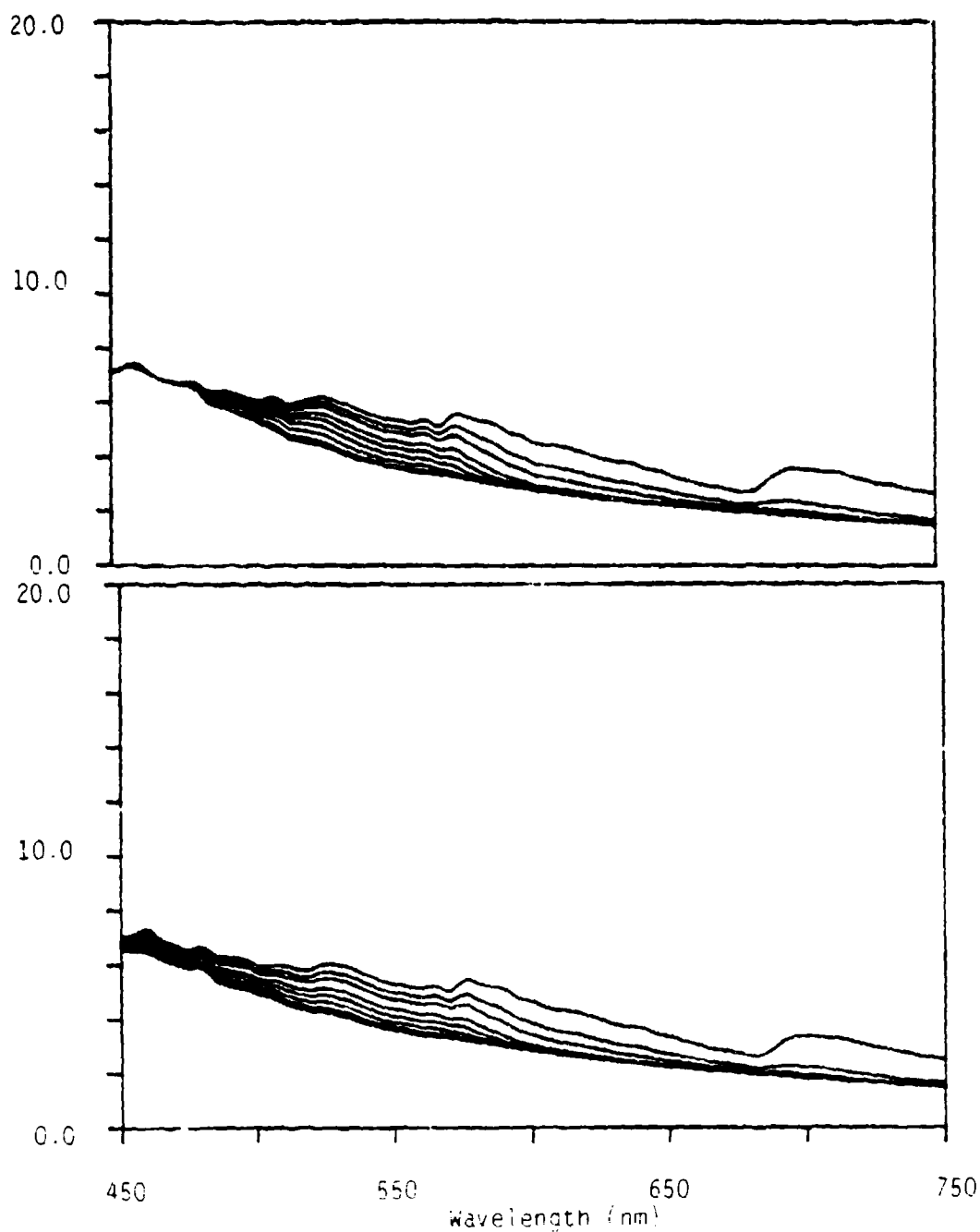


Figure A-67. Total radiance spectra for a Large Star Coral bottom type at selected water depths (1,2,3,5,7,10, 15,25, and 40 m). Curves in the upper panel were generated for a visibility of 10 km and with water type 1 and in the lower panel for water type 2.

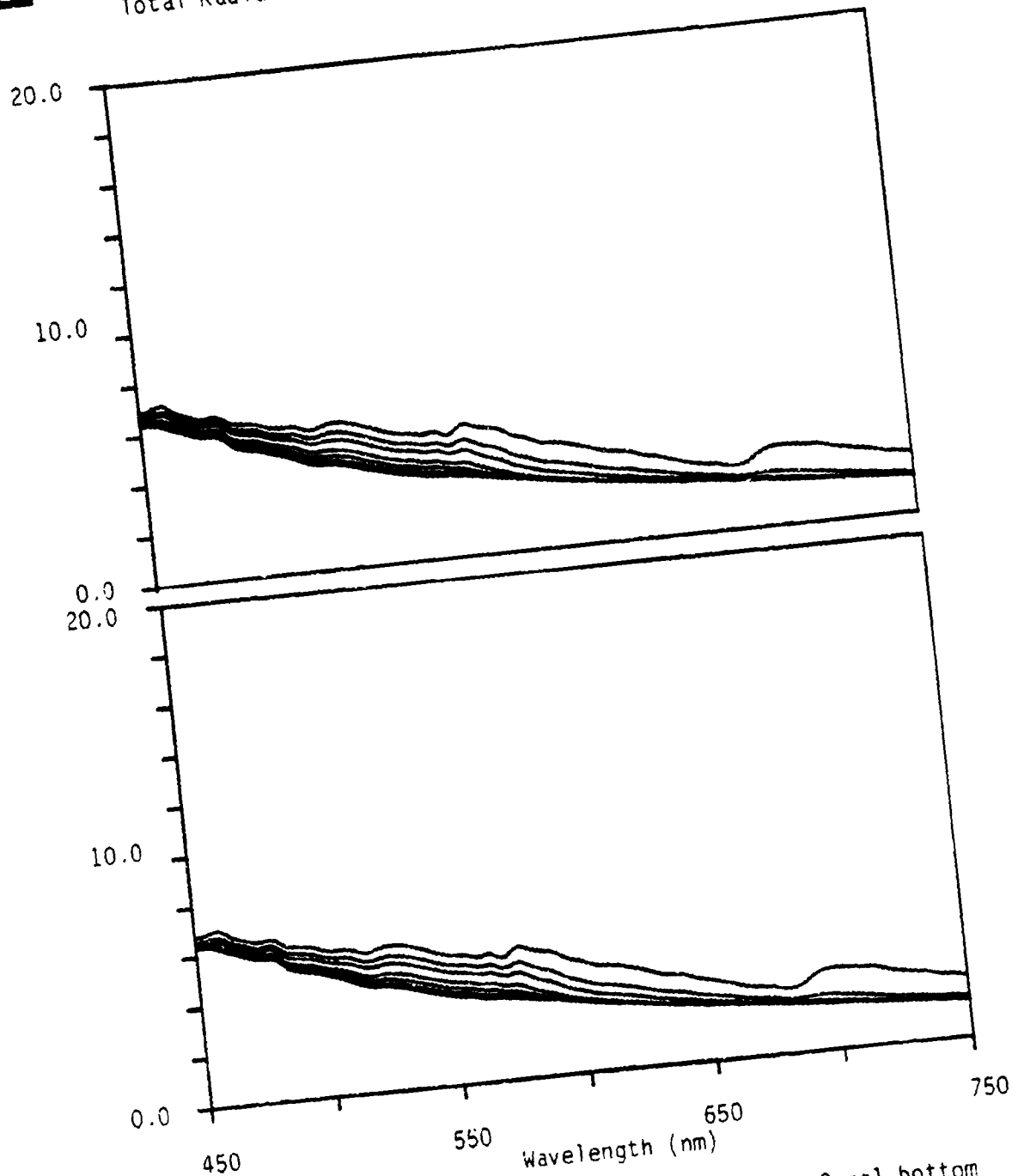


Figure A-68. Total radiance spectra for a Large Star Coral bottom type at selected water depths (1,2,3,5,7,10, 15,25, and 40 m). Curves in the upper panel were generated for a visibility of 10 km and with water type 3 and in the lower panel for water type 4.

Total Radiance Values (mw/(micron*cm*cm*sr))

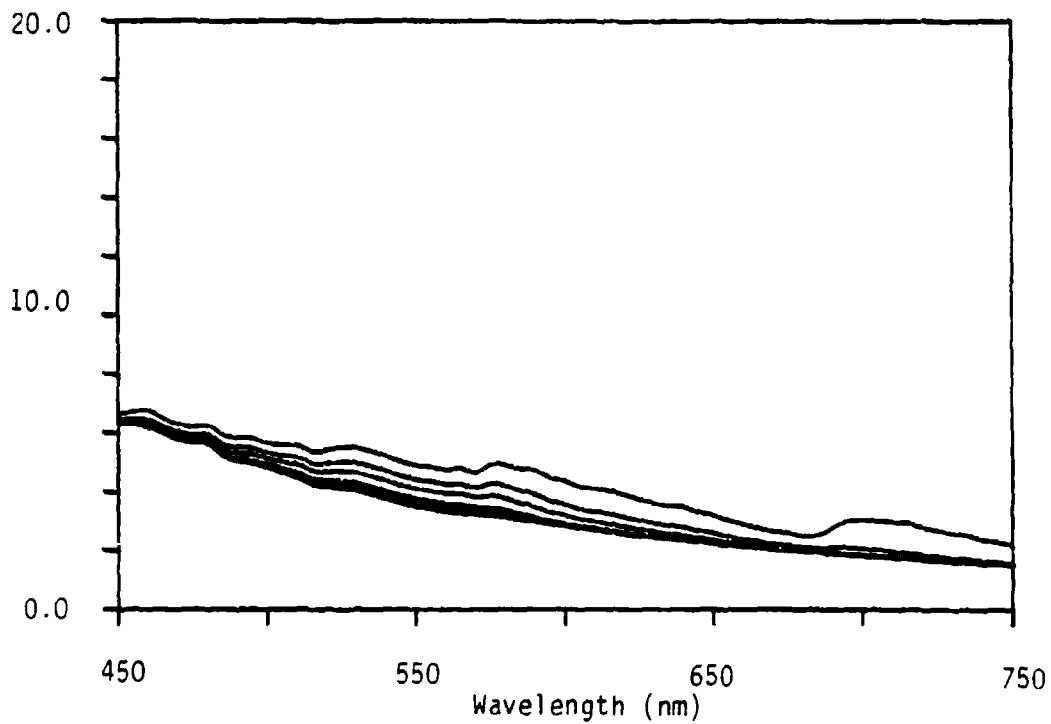


Figure A-69. Total radiance spectra for a Large Star Coral bottom type at selected water depths (1,2,3,5,7,10, 15,25, and 40 m). Curves in the above panel were generated for a visibility of 10 km and with water type 5.

Total Radiance Values (mw/(micron*cm*cm*sr))

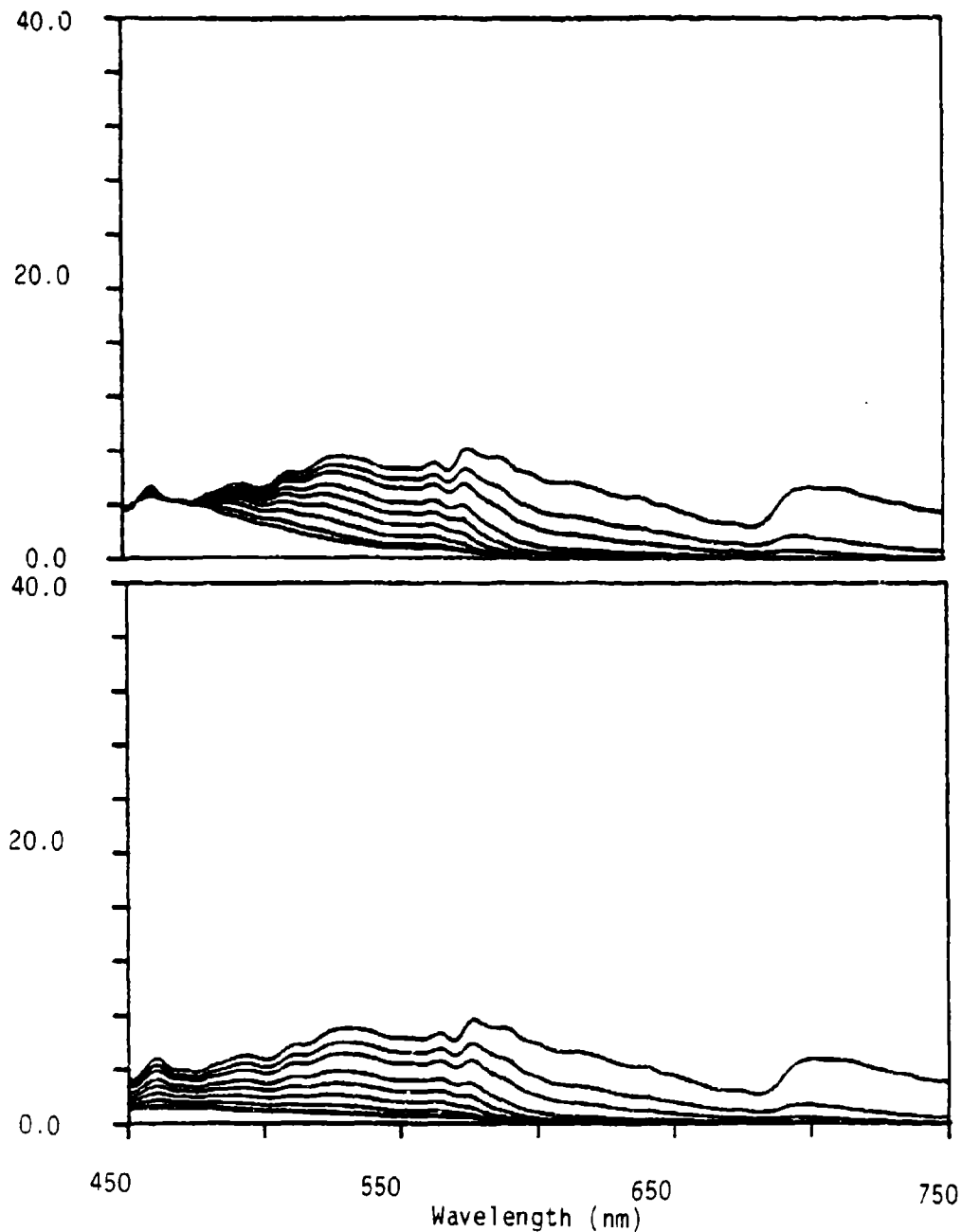


Figure A-70. Total radiance spectra for a Large Star Coral bottom type at selected water depths (1,2,3,5,7,10, 15,25, and 40 m). Curves in the upper panel were generated with water type 1 and in the lower panel for water type 2. Spectra were calculated for a sensor position just below the sea surface.

Total Radiance Values (mw/(micron*cm*cm*sr))

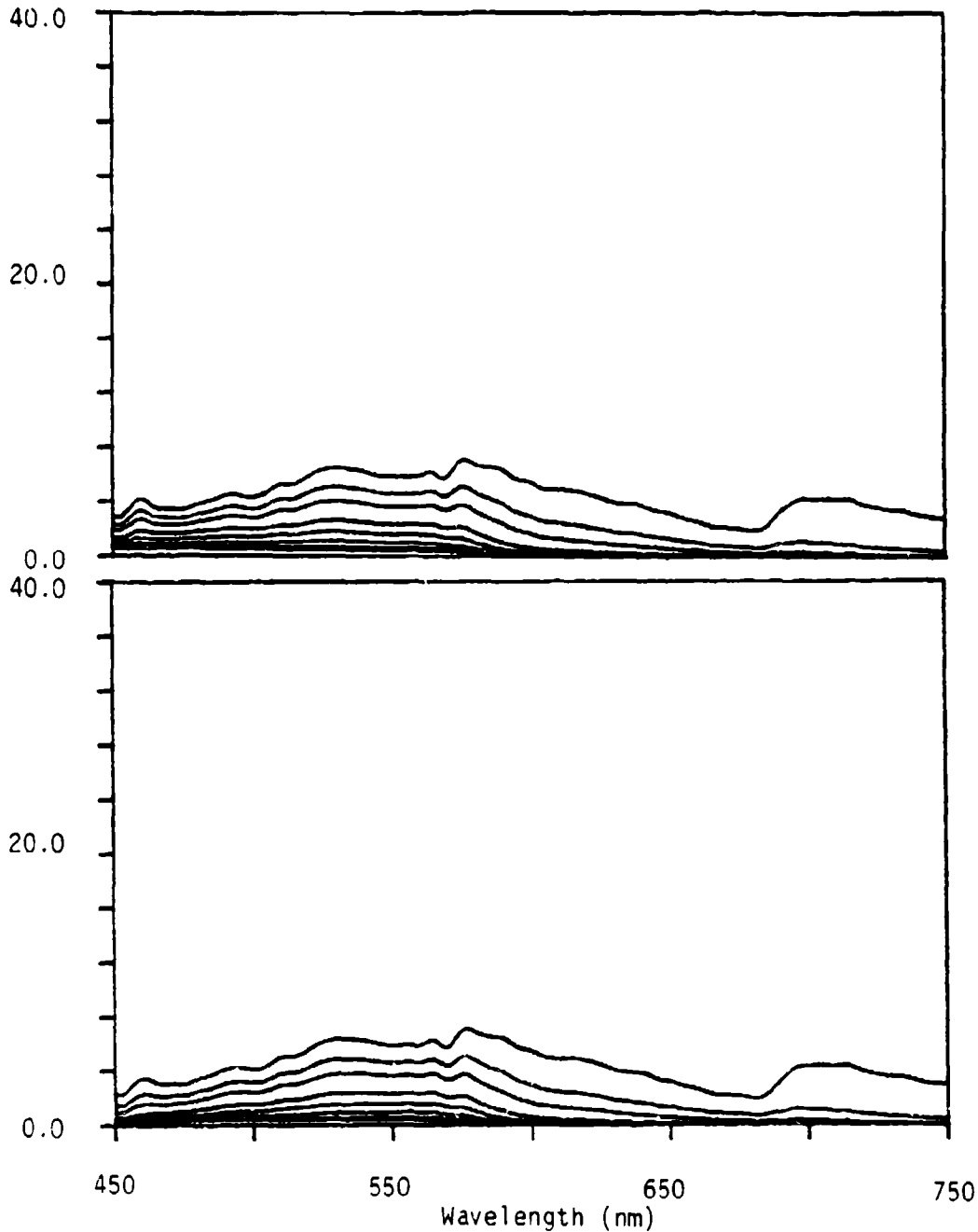


Figure A-71. Total radiance spectra for a Large Star Coral bottom type at selected water depths (1,2,3,5,7,10, 15,25, and 40 m). Curves in the upper panel were generated with water type 3 and in the lower panel for water type 4. Spectra were calculated for a sensor position just below the sea surface.

Total Radiance Values (mw/(micron*cm*cm*sr))

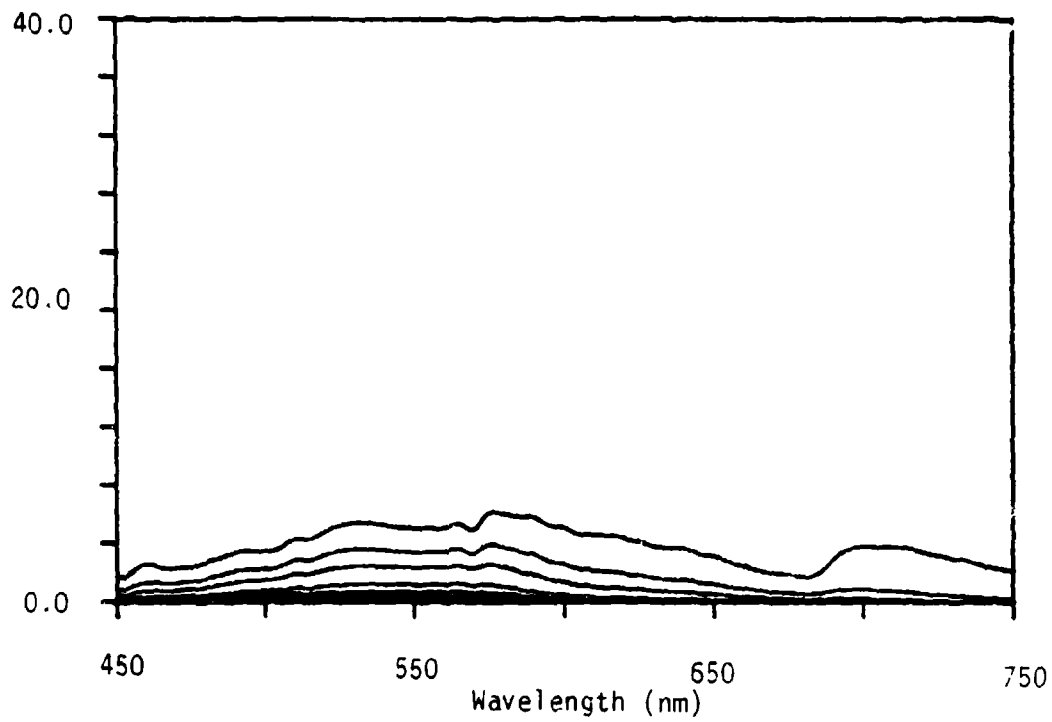


Figure A-72. Total radiance spectra for a Large Star Coral bottom type at selected water depths (1,2,3,5,7,10, 15,25, and 40 m). Curves in the above panel were generated with water type 5. Spectra were calculated for a sensor position just below the sea surface.

Total Radiance Values (mw/(micron*cm*cm*sr))

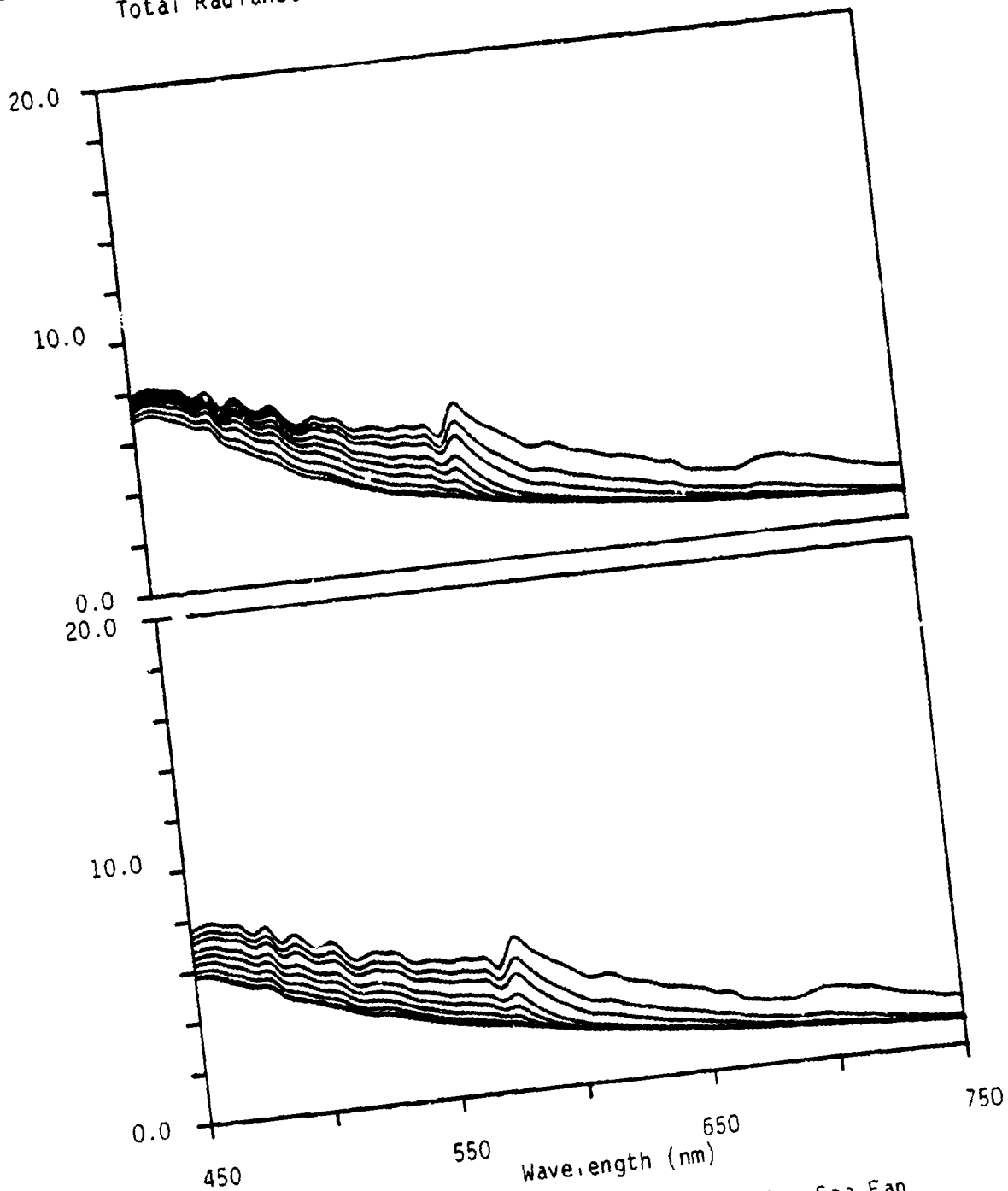


Figure A-73. Total radiance spectra for a Gorgonian Sea Fan bottom type at selected water depths (1, 2, 3, 5, 7, 10, 15, 25, and 40 m). Curves in the upper panel were generated for a visibility of 23 km and with water type 1 and in the lower panel for water type 2.

ERIM

Total Radiance Values (mw/(micron*cm*cm*sr))

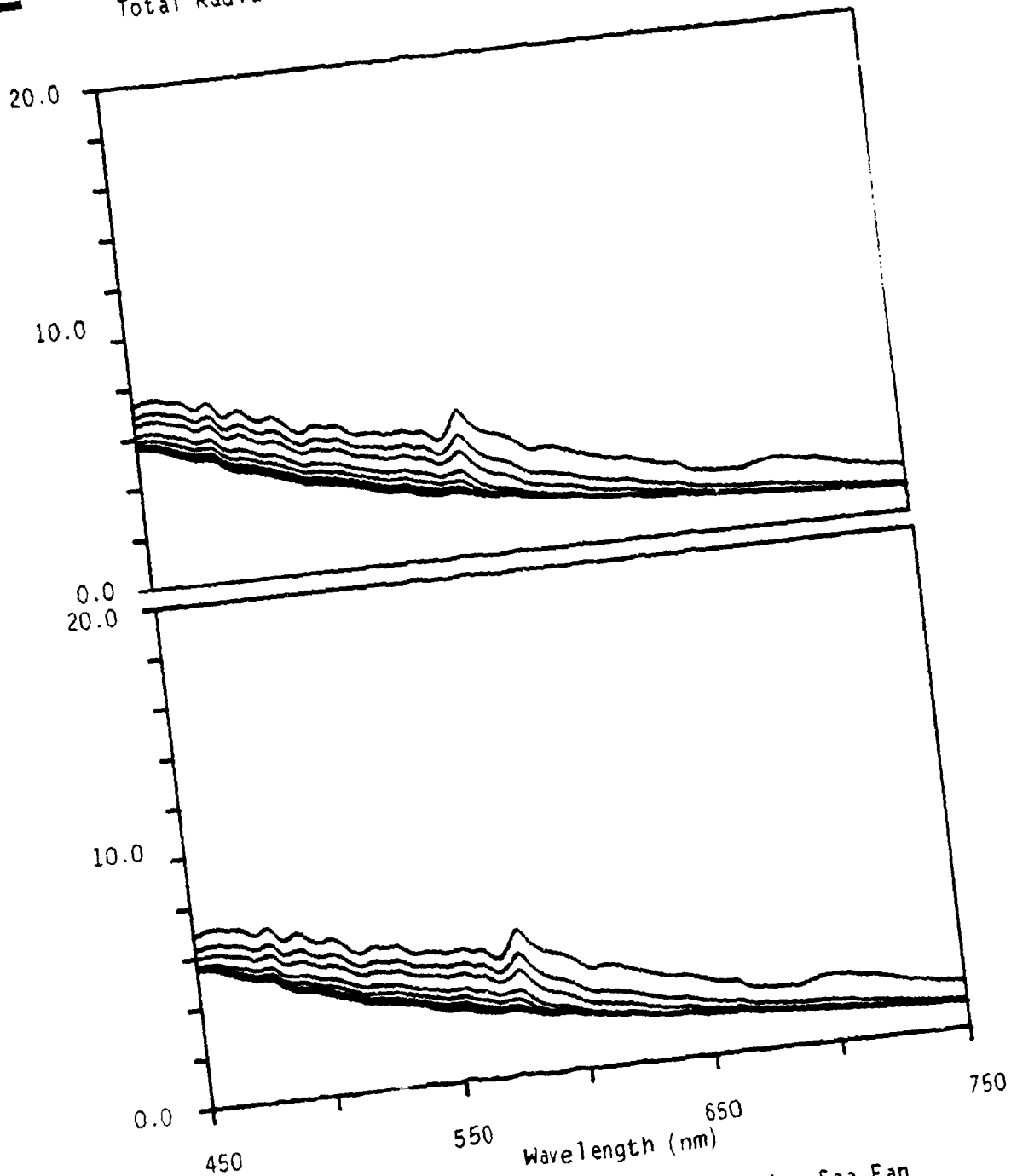


Figure A-74. Total radiance spectra for a Gorgonian Sea Fan bottom type at selected water depths (1,2,3,5,7,10, 15,25, and 40 m). Curves in the upper panel were generated for a visibility of 23 km and with water type 3 and in the lower panel for water type 4.

Total Radiance Values (mw/(micron*cm*cm*sr))

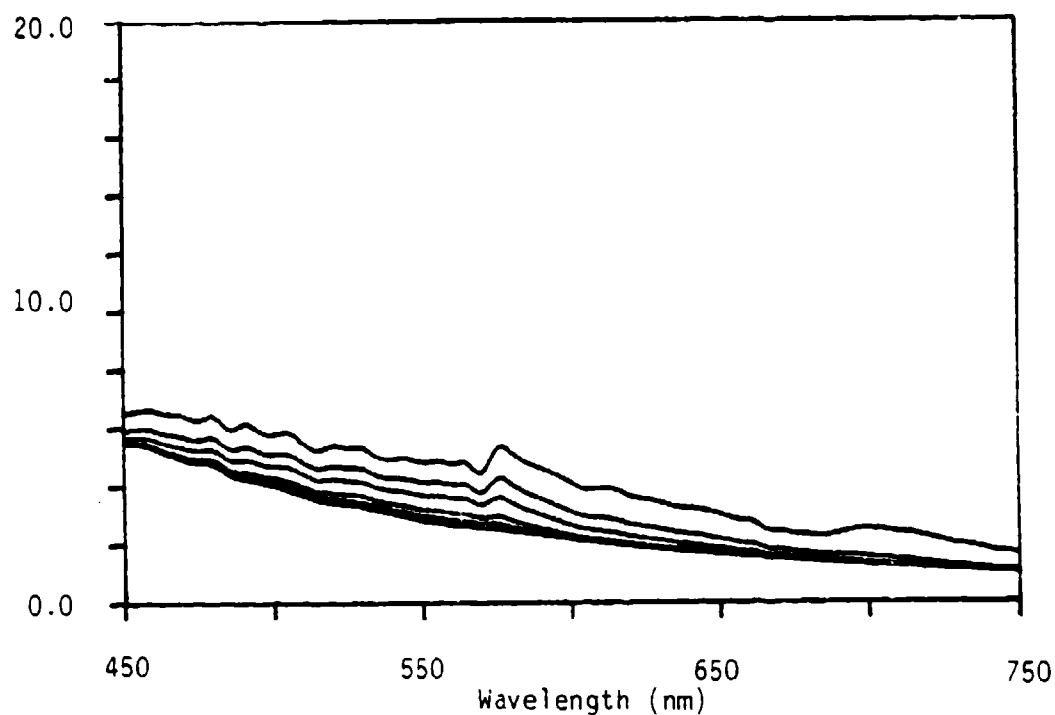


Figure A-75. Total radiance spectra for a Gorgonian Sea Fan bottom type at selected water depths (1,2,3,5,7,10, 15,25, and 40 m). Curves in the above panel were generated for a visibility of 23 km and with water type 5.

ERIM

Total Radiance Values (mw/(micron*cm*cm*sr))

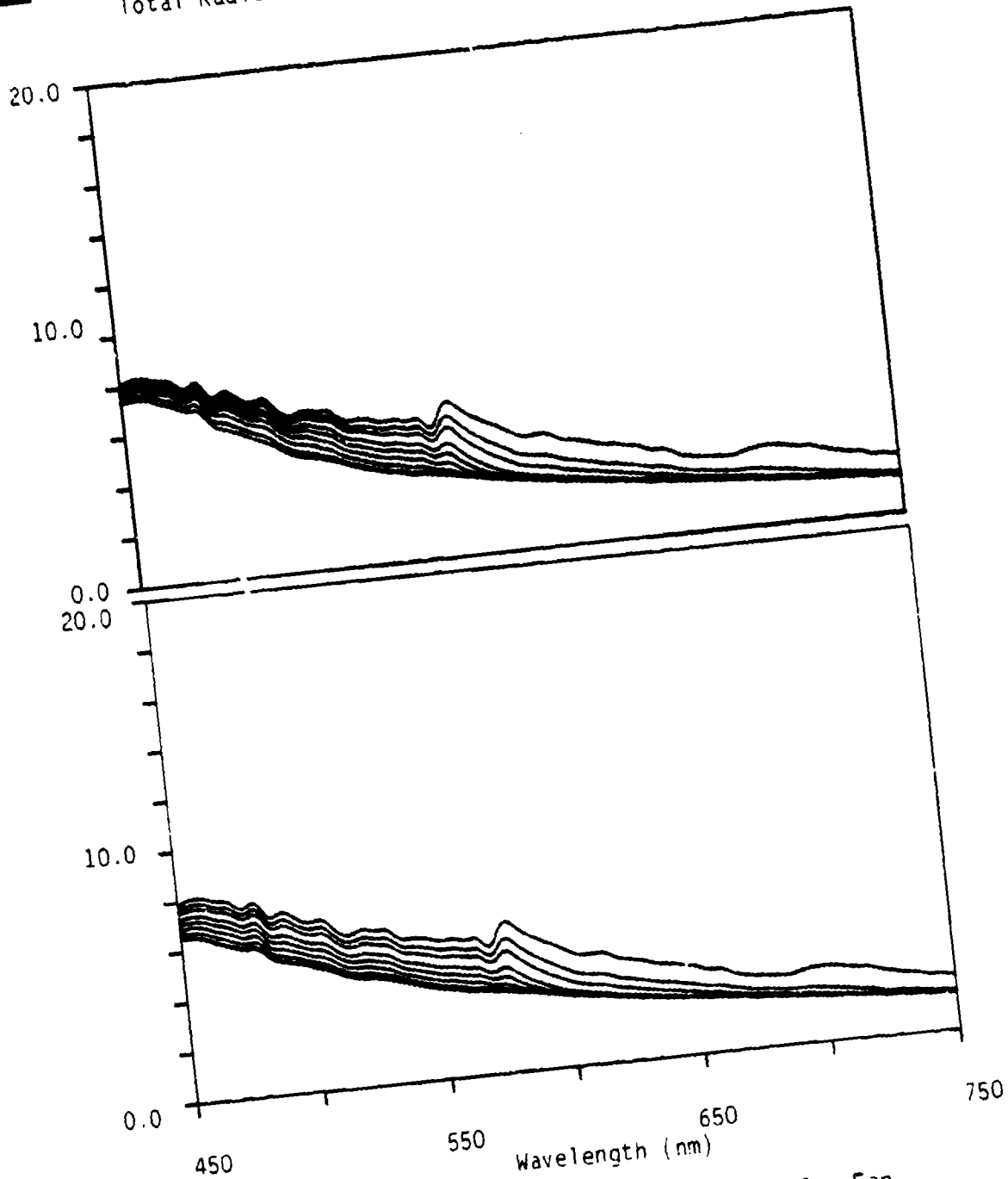


Figure A-76. Total radiance spectra for a Gorgonian Sea Fan bottom type at selected water depths (1,2,3,5,7,10, 15,25, and 40 m). Curves in the upper panel were generated for a visibility of 10 km and with water type 1 and in the lower panel for water type 2.

Total Radiance Values (mw/(micron*cm*cm*sr))

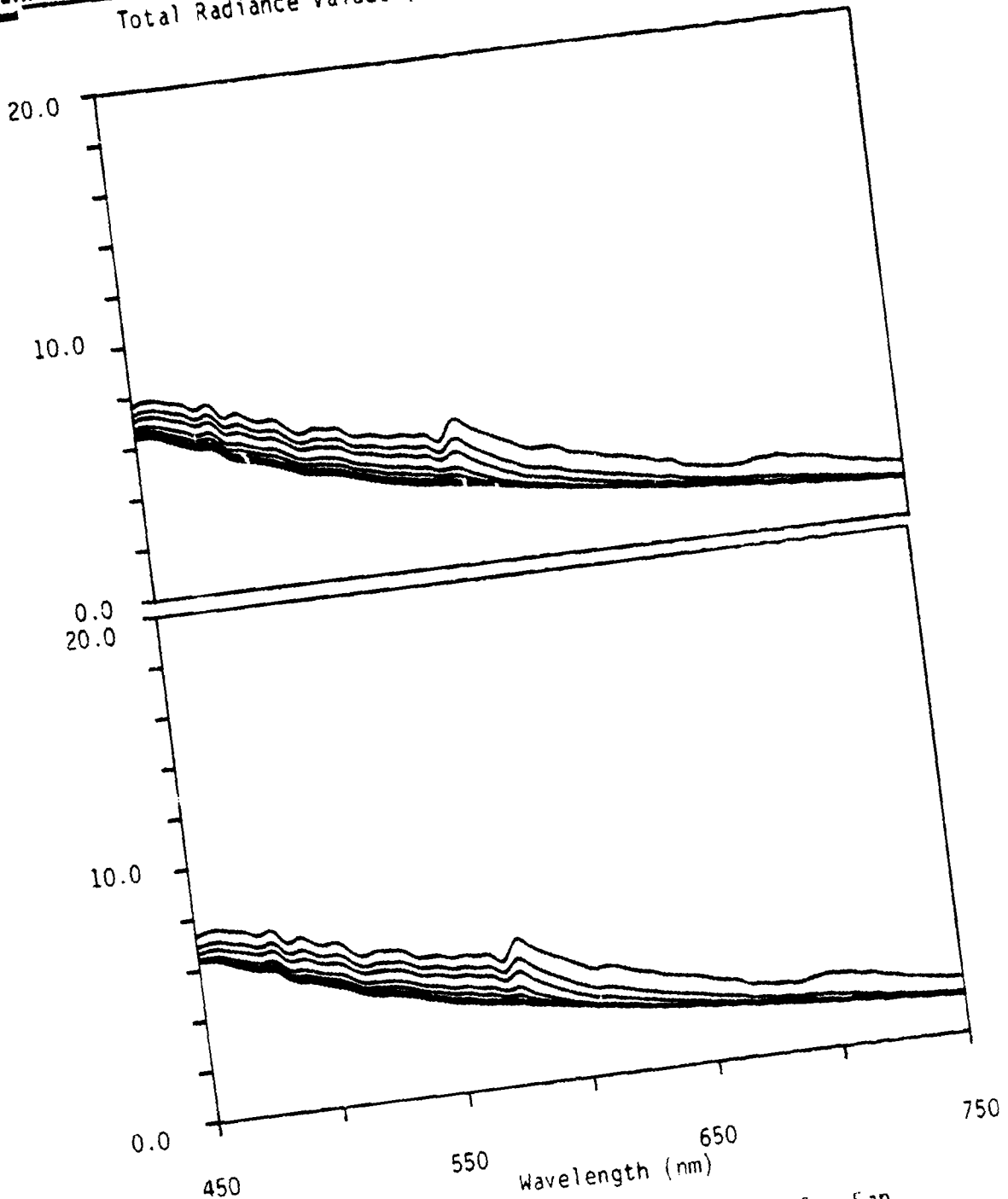


Figure A-77. Total radiance spectra for a Gorgonian Sea Fan bottom type at selected water depths (1,2,3,5,7,10, 15,25, and 40 m). Curves in the upper panel were generated for a visibility of 10 km and with water type 3 and in the lower panel for water type 4.

Total Radiance Values (mw/(micron*cm*cm*sr))

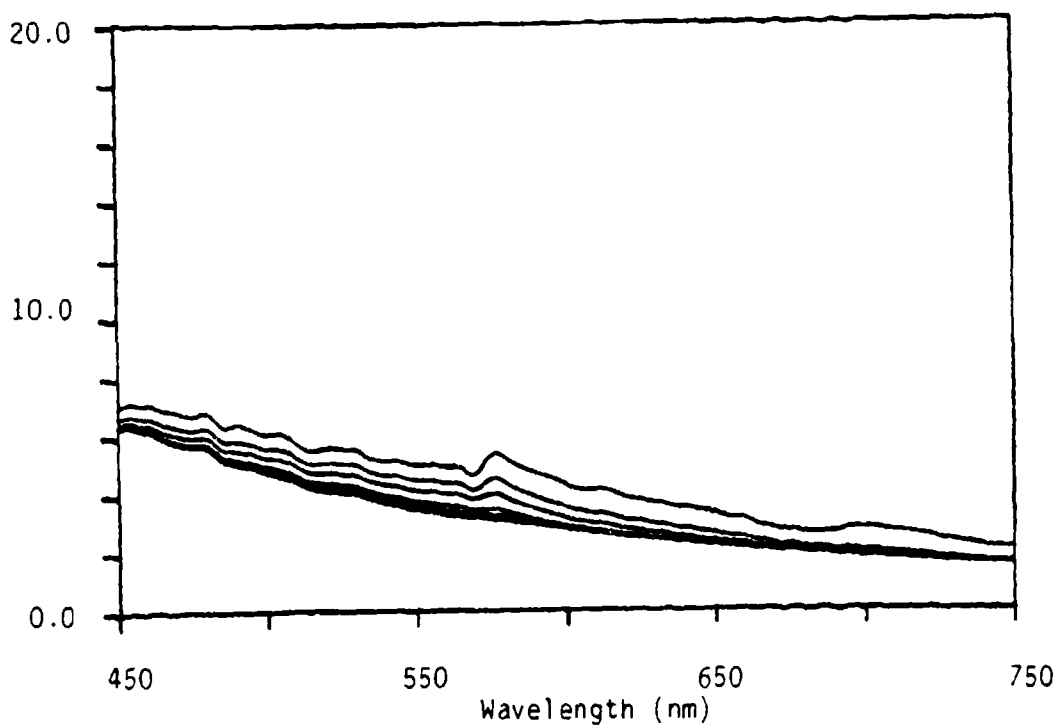


Figure A-78. Total radiance spectra for a Gorgonian Sea Fan bottom type at selected water depths (1,2,3,5,7,10, 15,25, and 40 m). Curves in the above panel were generated for a visibility of 10 km and with water type 5.

Total Radiance Values (mw/(micron*cm*cm*sr))

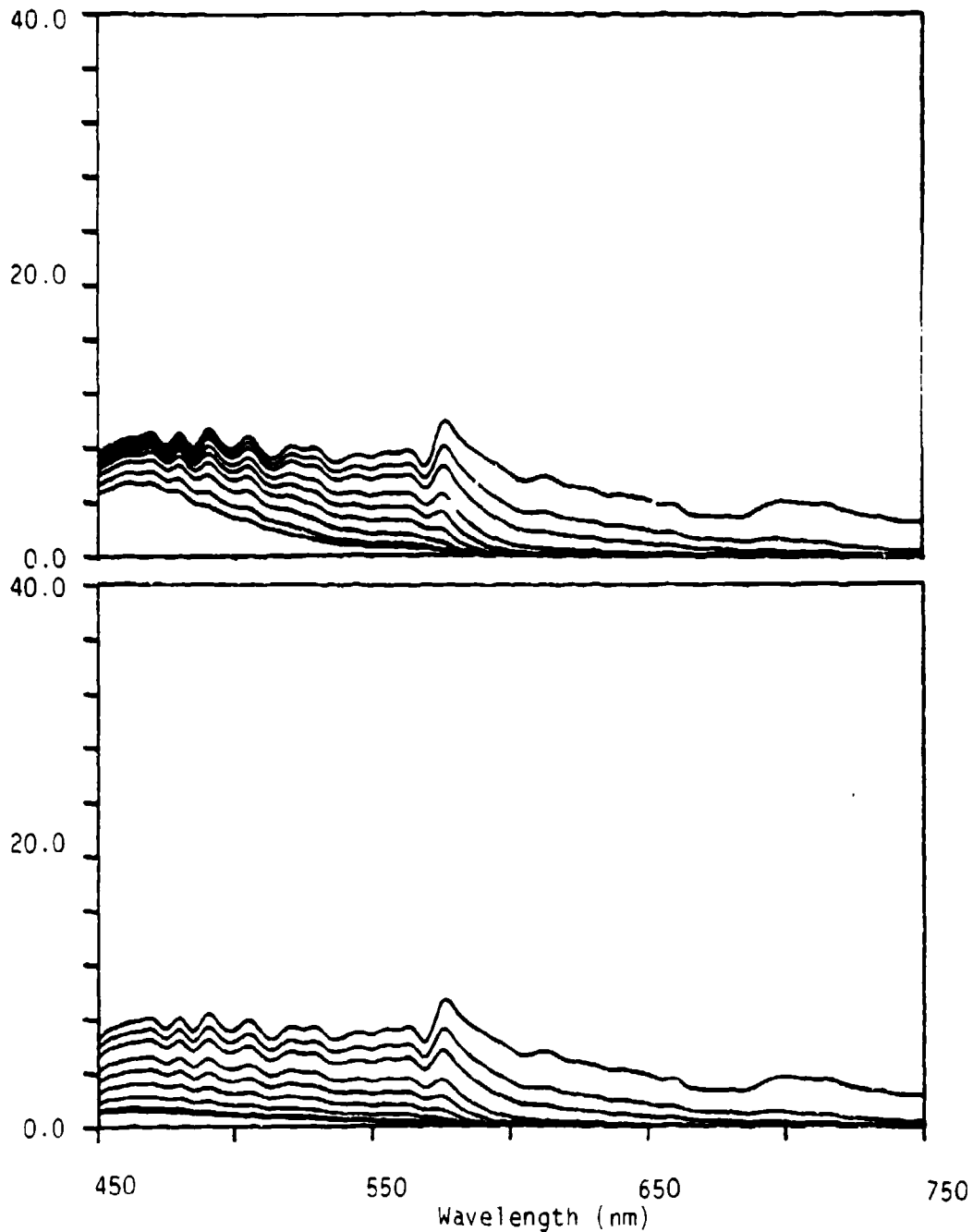


Figure A-79. Total radiance spectra for a Gorgonian Sea Fan bottom type at selected water depths (1,2,3,5,7,10, 15,25, and 40 m). Curves in the upper panel were generated with water type 1 and in the lower panel for water type 2. Spectra were calculated for a sensor position just below the sea surface.

Total Radiance Values (mw/(micron*cm*cm*sr))

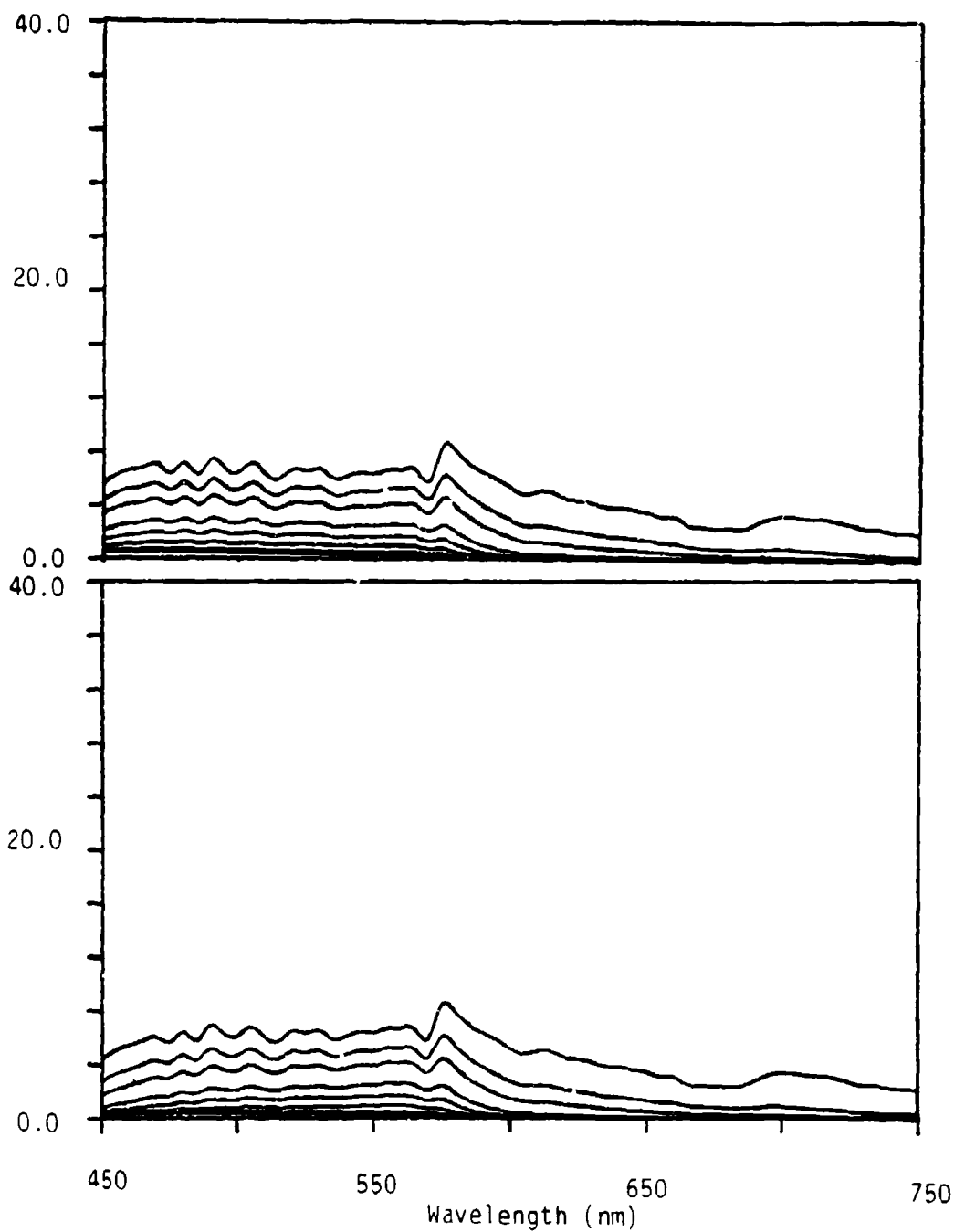


Figure A-80. Total radiance spectra for a Gorgonian Sea Fan bottom type at selected water depths (1,2,3,5,7,10, 15,25, and 40 m). Curves in the upper panel were generated with water type 3 and in the lower panel for water type 4. Spectra were recalculated for a sensor position just below the sea surface.

Total Radiance Values (mw/(micron*cm*cm*sr))

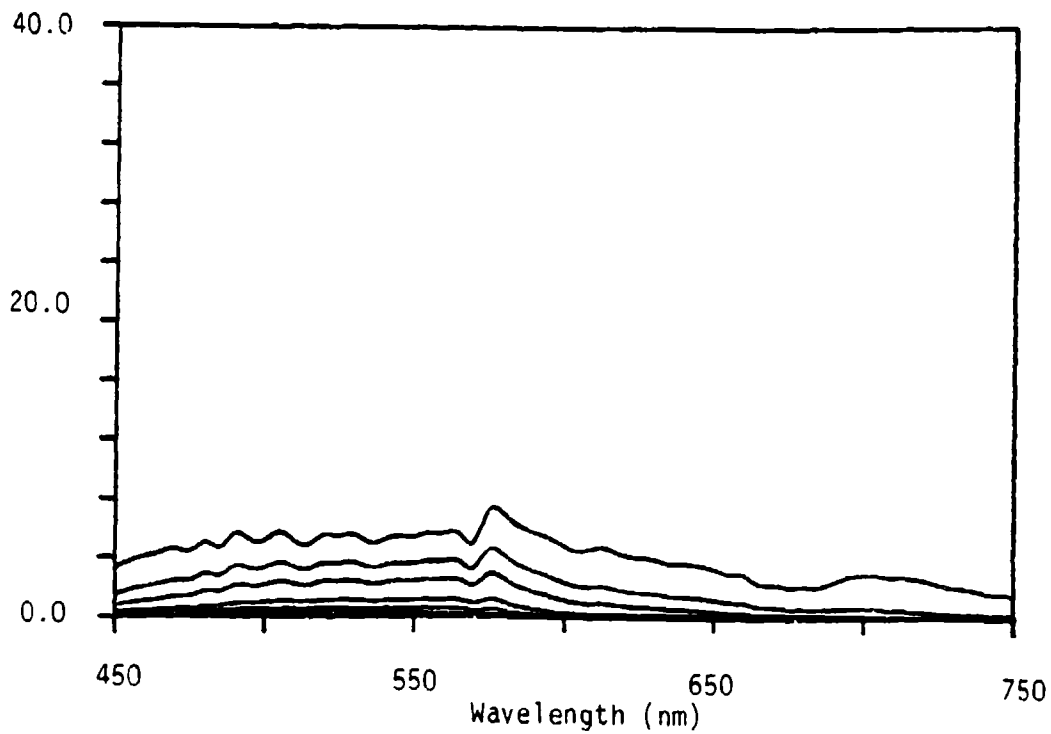


Figure A-81. Total radiance spectra for a Gorgonian Sea Fan bottom type at selected water depths (1,2,3,5,7,10, 15,25, and 40 m). Curves in the above panel were generated with water type 5. Spectra were calculated for a sensor position just below the sea surface.

ERIM

Total Radiance Values (mw/(micron*cm*cm*sr))

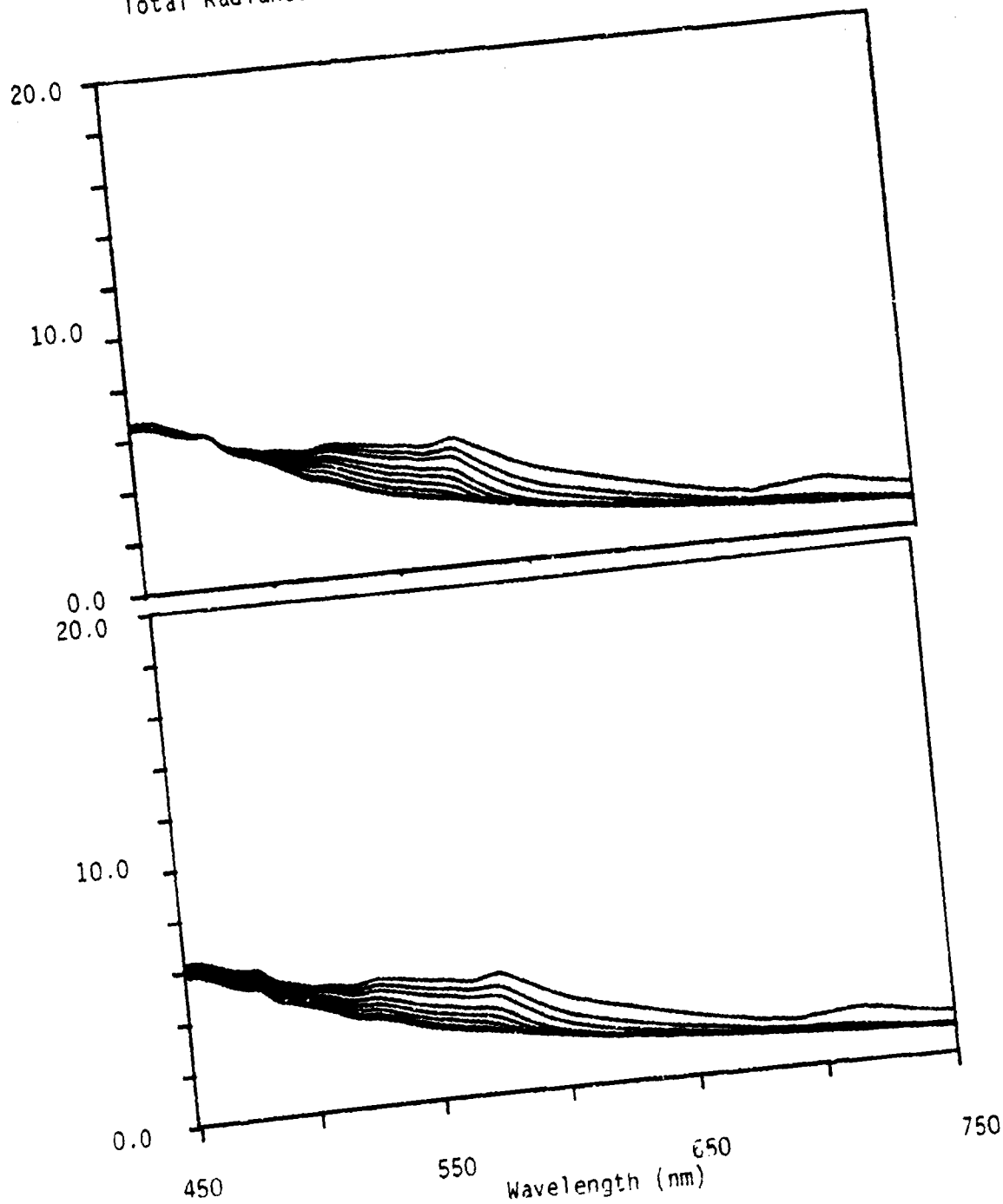


Figure A-82. Total radiance spectra for a Green Algae bottom type at selected water depths (1,2,3,5,7,10, 15,25, and 40 m). Curves in the upper panel were generated for a visibility of 23 km and with water type 1 and in the lower panel for water type 2.

A-86

Total Radiance Values (mw/(micron*cm*cm*sr))

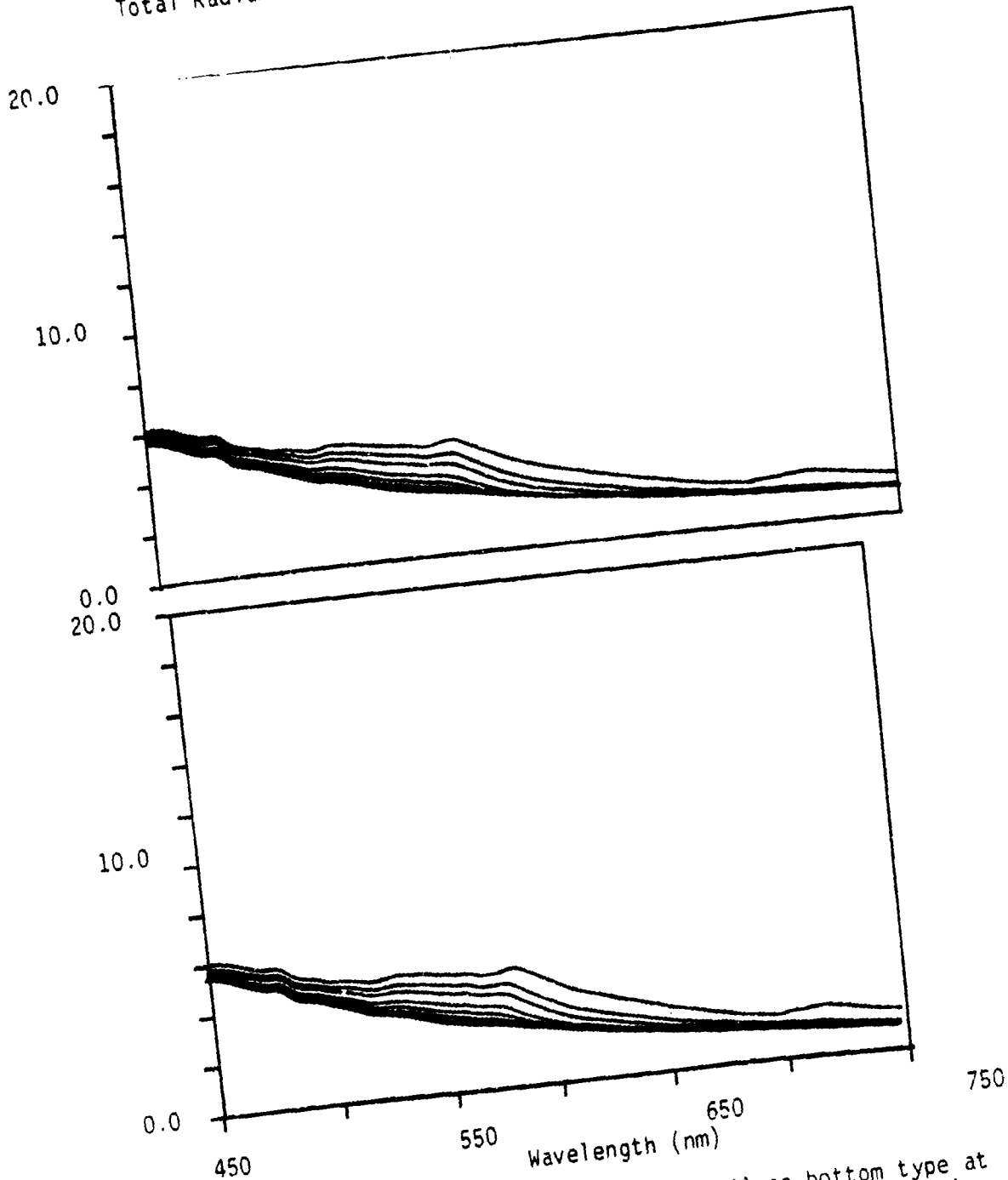


Figure A-83. Total radiance spectra for a Green Algae bottom type at selected water depths (1,2,3,5,7,10, 15,25, and 40 m). Curves in the upper panel were generated for a visibility of 23 km and with water type 3 and in the lower panel for water type 4.

Total Radiance Values (mw/(micron*cm*cm*sr))

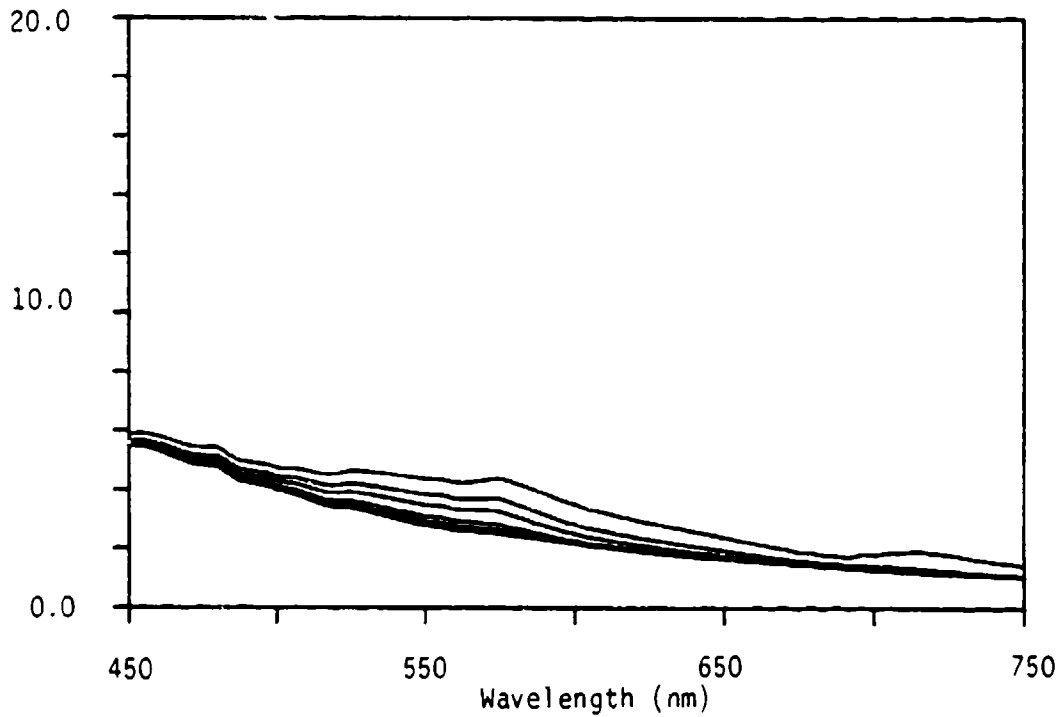


Figure A-84. Total radiance spectra for a Green Algae bottom type at selected water depths (1,2,3,5,7,10, 15,25, and 40 m). Curves in the above panel were generated for a visibility of 23 km and with water type 5.

Total Radiance Values (mw/(micron*cm*cm*sr))

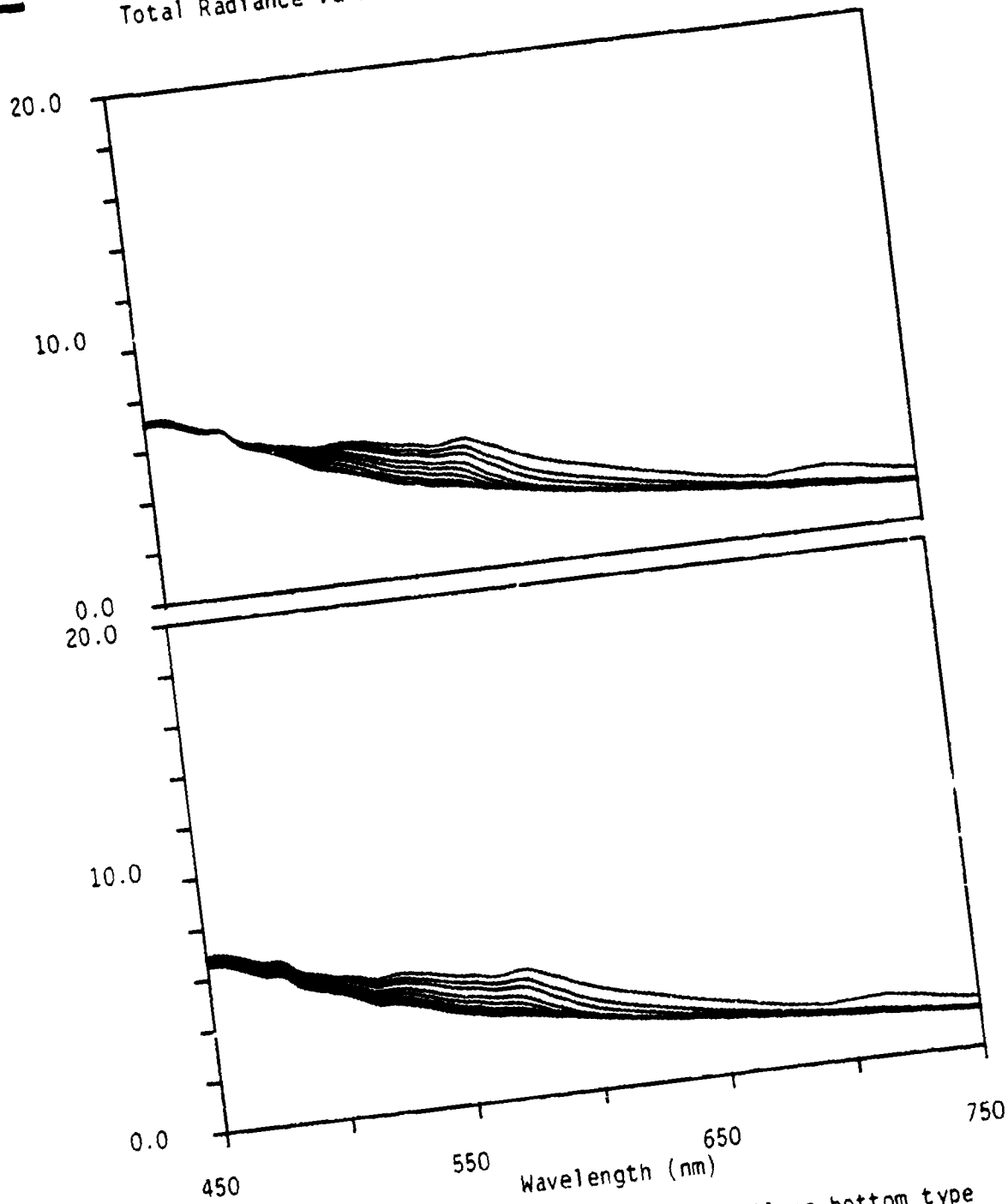


Figure A-85. Total radiance spectra for a Green Algae bottom type at selected water depths (1,2,3,5,7,10, 15,25, and 40 m). Curves in the upper panel were generated for a visibility of 10 km and with water type 1 and in the lower panel for water type 2.

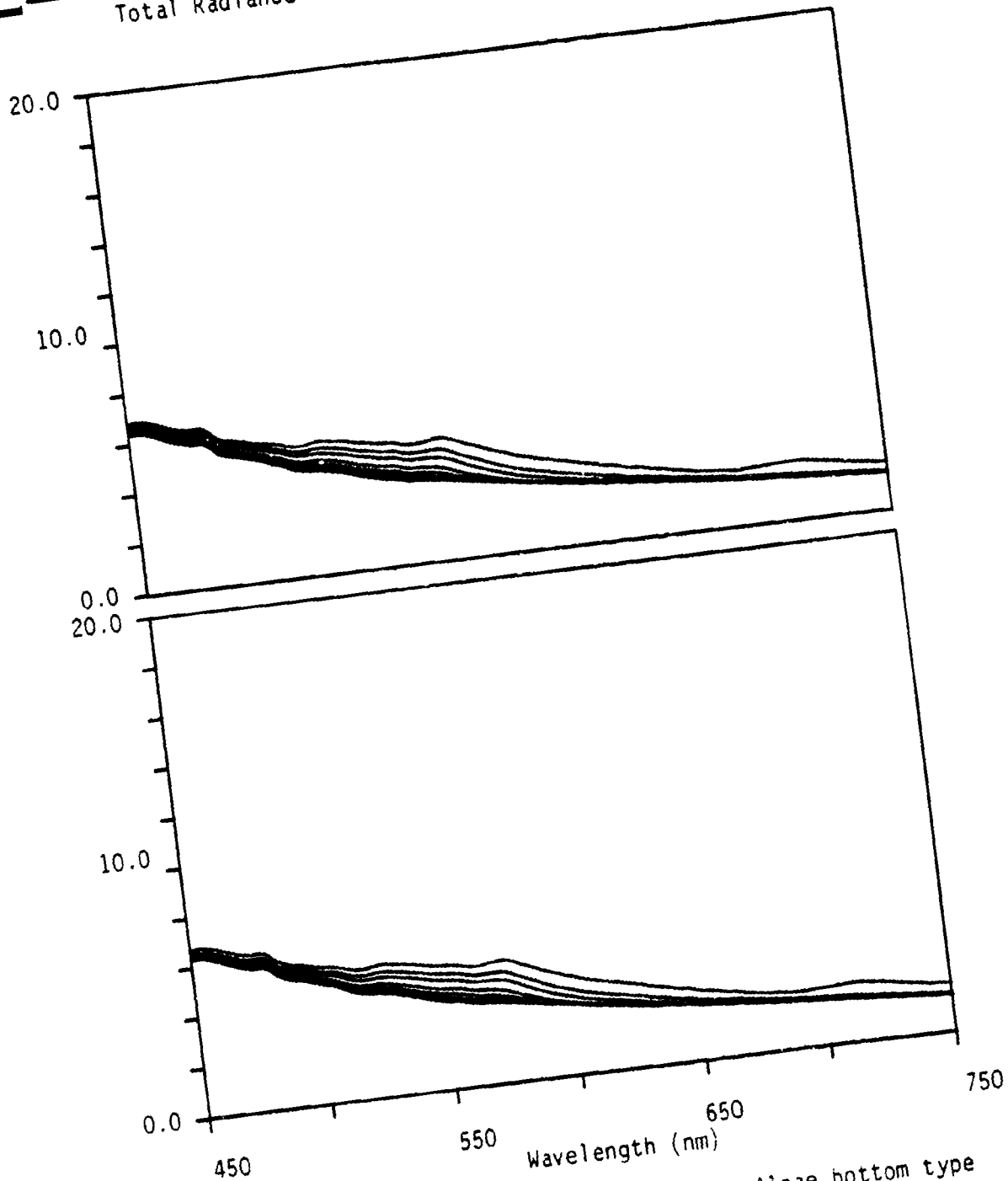


Figure A-86. Total radiance spectra for a Green Algae bottom type at selected water depths (1,2,3,5,7,10, 15,25, and 40 m). Curves in the upper panel were generated for a visibility of 10 km and with water type 3 and in the lower panel for water type 4.

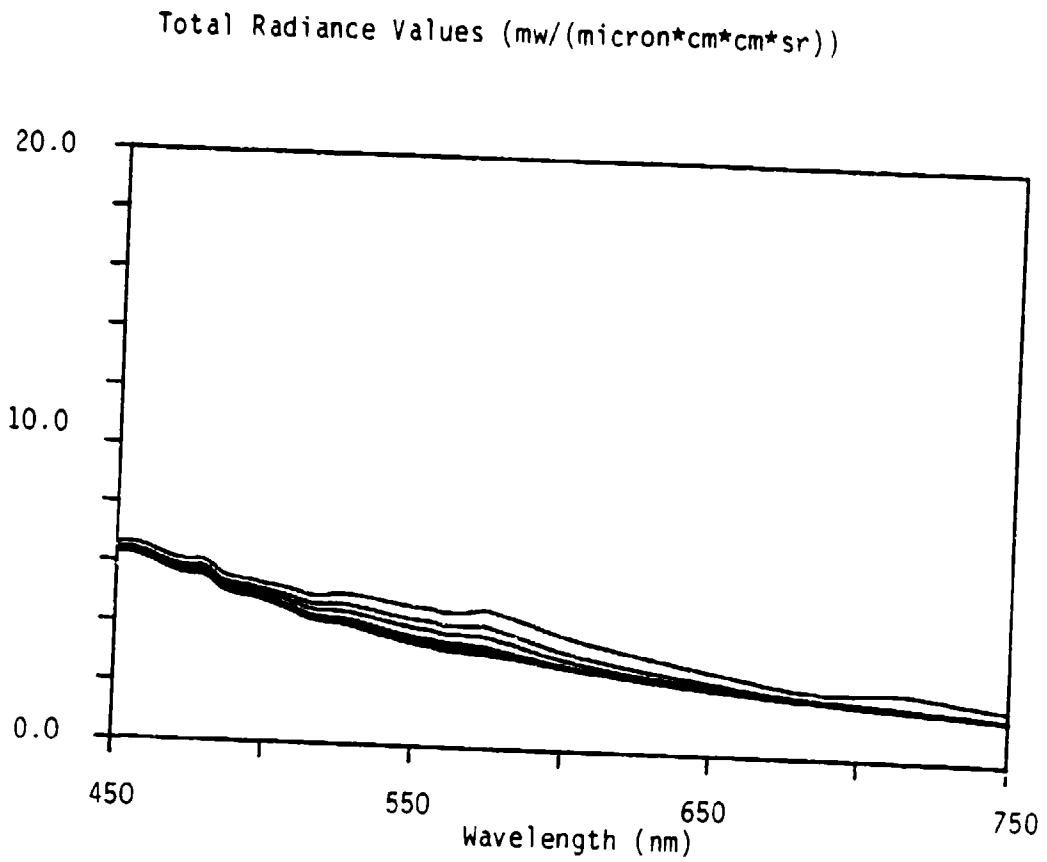


Figure A-87. Total radiance spectra for a Green Algae bottom type at selected water depths (1,2,3,5,7,10, 15,25, and 40 m). Curves in the above panel were generated for a visibility of 10 km and with water type 5.

Total Radiance Values (mw/(micron*cm*cm*sr))

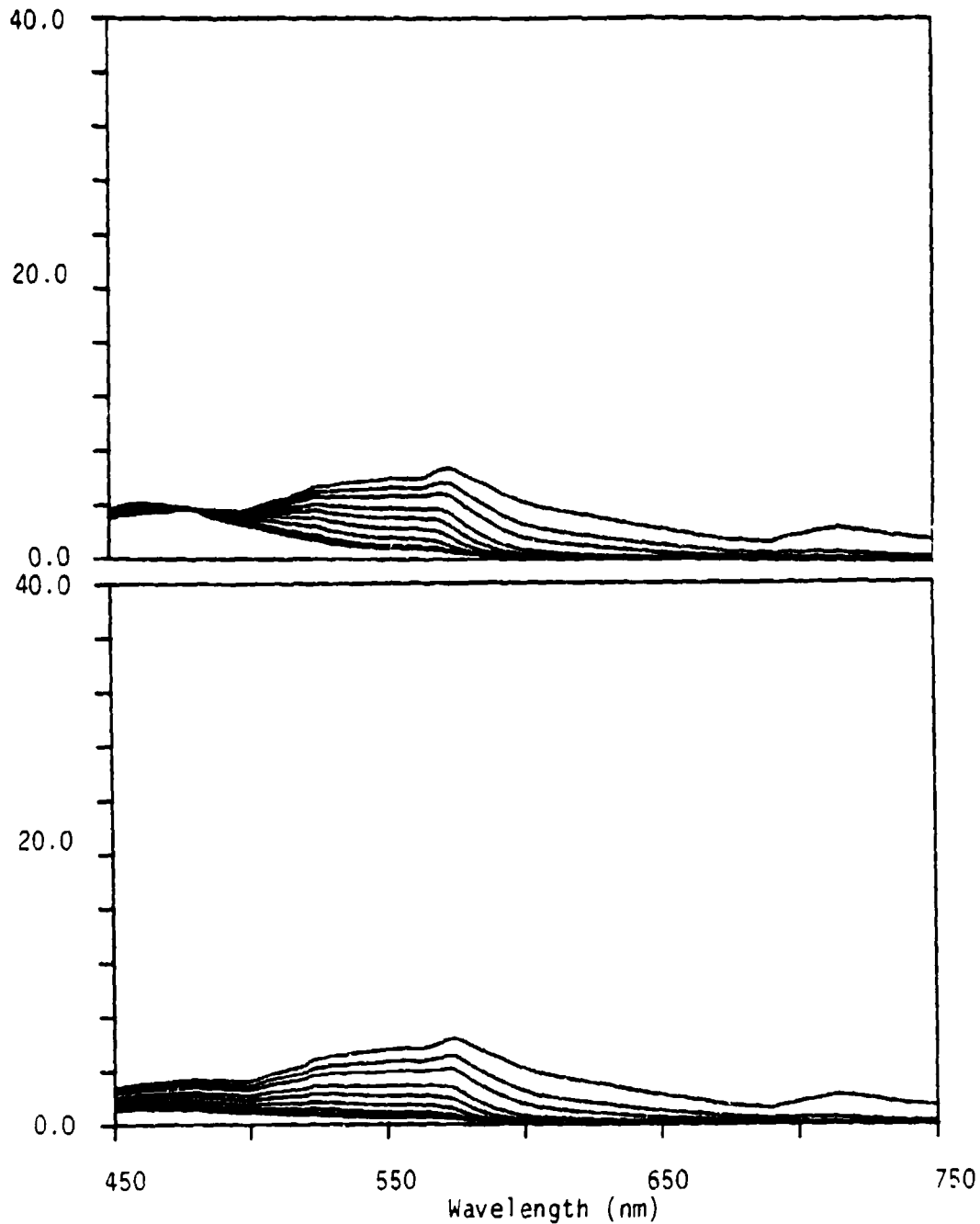


Figure A-88. Total radiance spectra for a Green Algae bottom type at selected water depths (1,2,3,5,7,10, 15,25, and 40 m). Curves in the upper panel were generated with water type 1 and in the lower panel for water type 2. Spectra were calculated for a sensor position just below the sea surface.

Total Radiance Values (mw/(micron*cm*cm*sr))

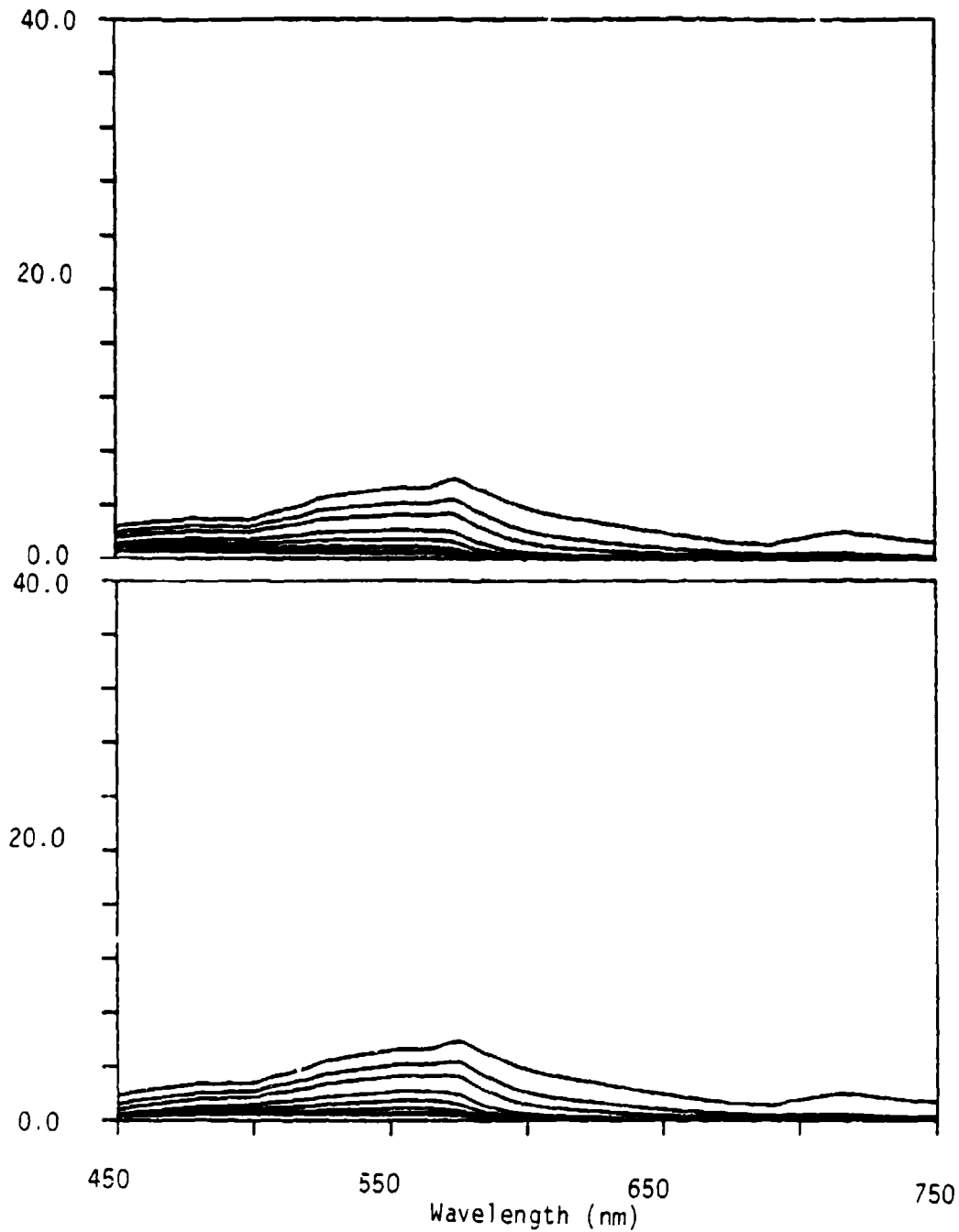


Figure A-89. Total radiance spectra for a Green Algae bottom type at selected water depths (1,2,3,5,7,10, 15,25, and 40 m). Curves in the upper panel were generated with water type 3 and in the lower panel for water type 4. Spectra were calculated for a sensor position just below the sea surface.

Total Radiance Values (mw/(micron*cm*cm*sr))

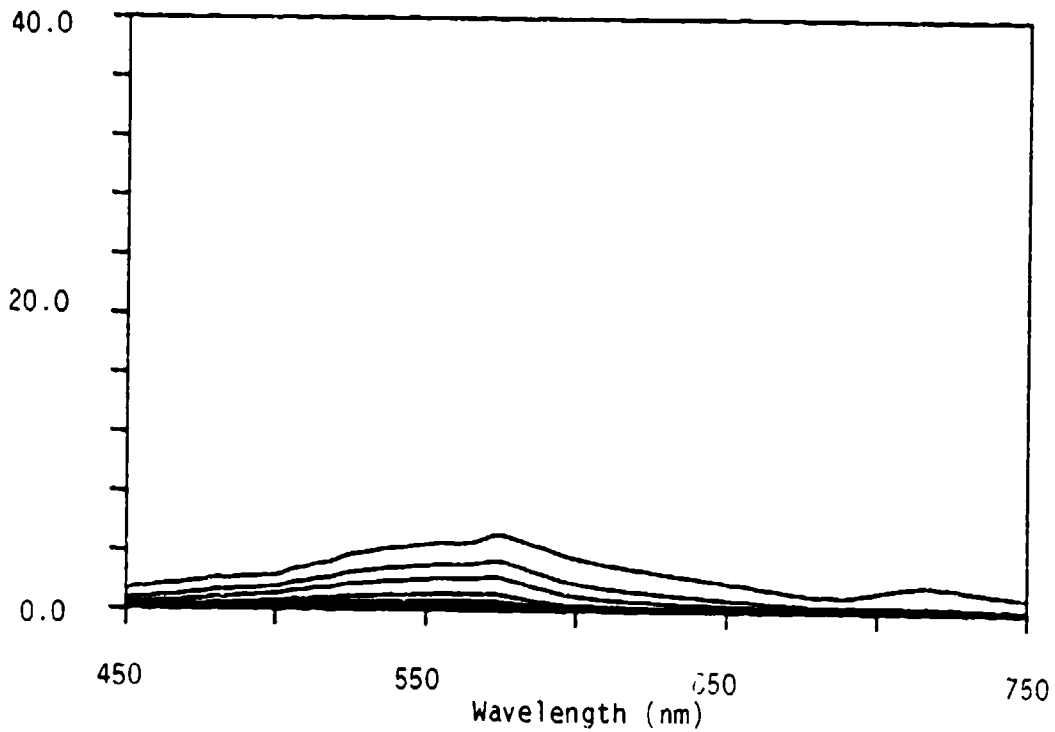


Figure A-90. Total radiance spectra for a Green Algae bottom type at selected water depths (1,2,3,5,7,10, 15,25, and 40 m). Curves in the above panel were generated with water type 5. Spectra were calculated for a sensor position just below the sea surface.

ERIM

Total Radiance Values (mw/(micron*cm*cm*sr))

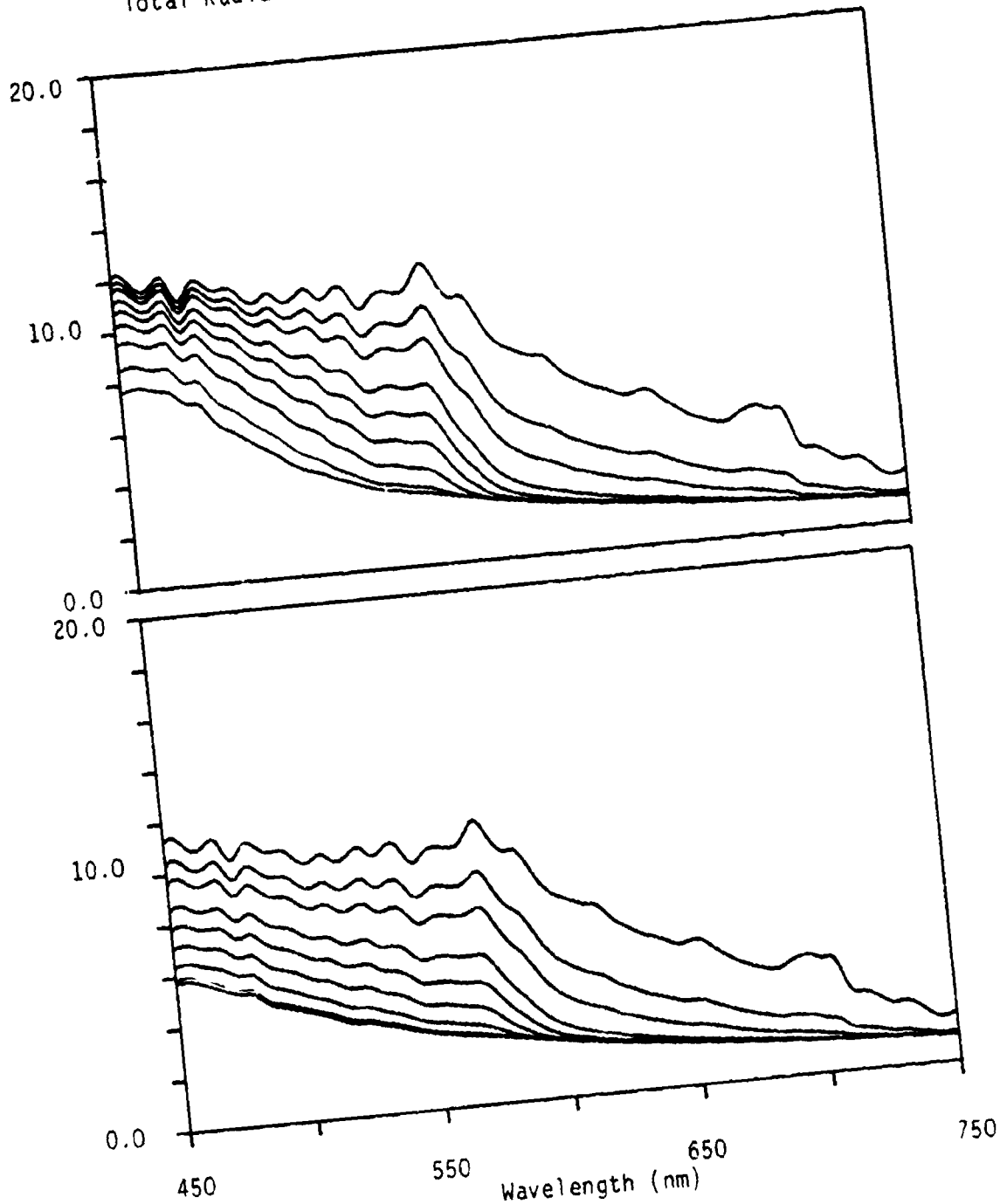


Figure A-91. Total radiance spectra for a Fire Coral bottom type at selected water depths (1, 2, 3, 5, 7, 10, 15, 25, and 40 m). Curves in the upper panel were generated for a visibility of 23 km and with water type 1 and in the lower panel for water type 2.

ERIM

Total Radiance Values (mw/(micron*cm*cm*sr))

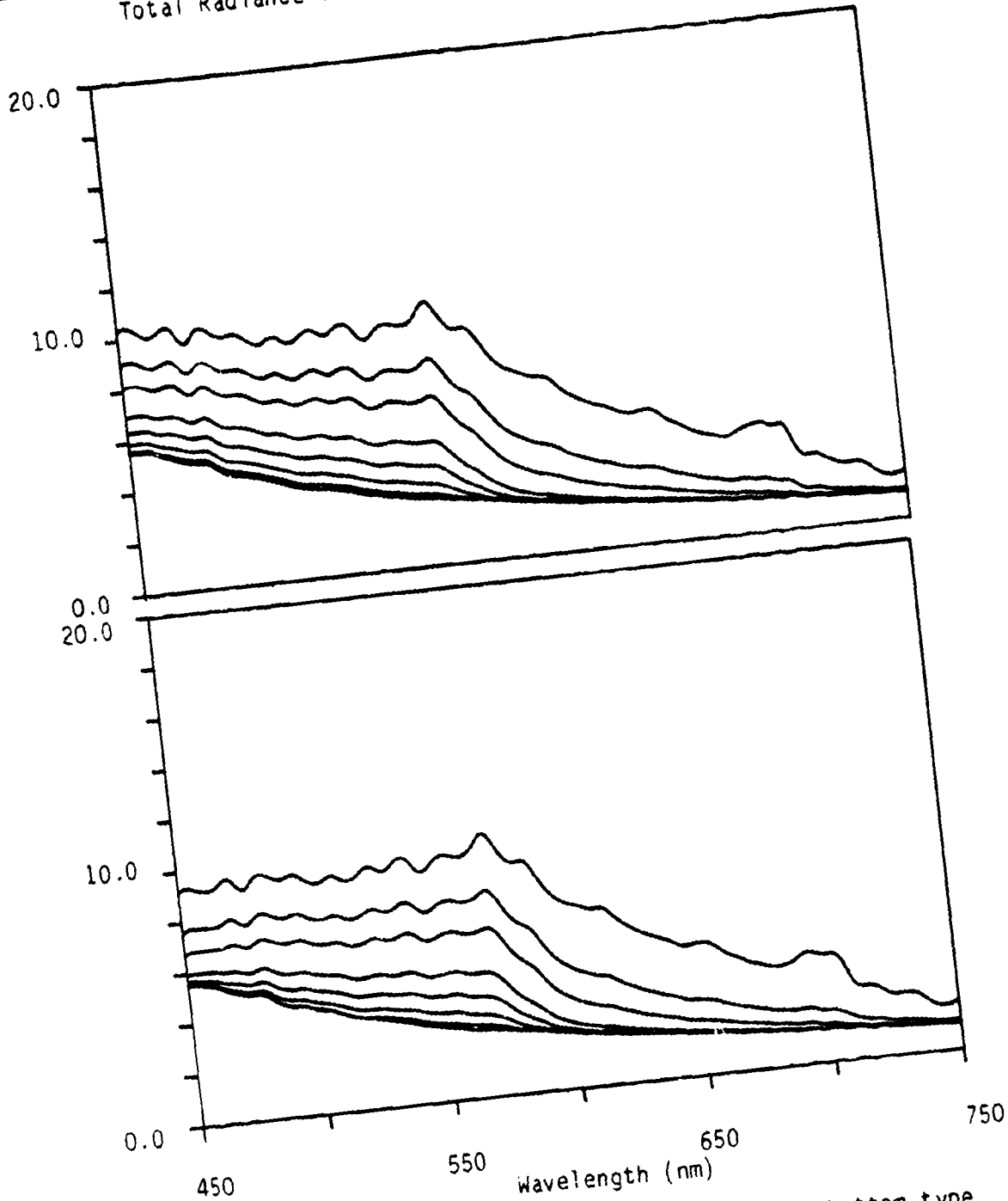


Figure A-92. Total radiance spectra for a Fire Coral bottom type at selected water depths (1,2,3,5,7,10, 15,25, and 40 m). Curves in the upper panel were generated for a visibility of 23 km and with water type 3 and in the lower panel for water type 4.

A-96

Total Radiance Values (mw/(micron*cm*cm*sr))

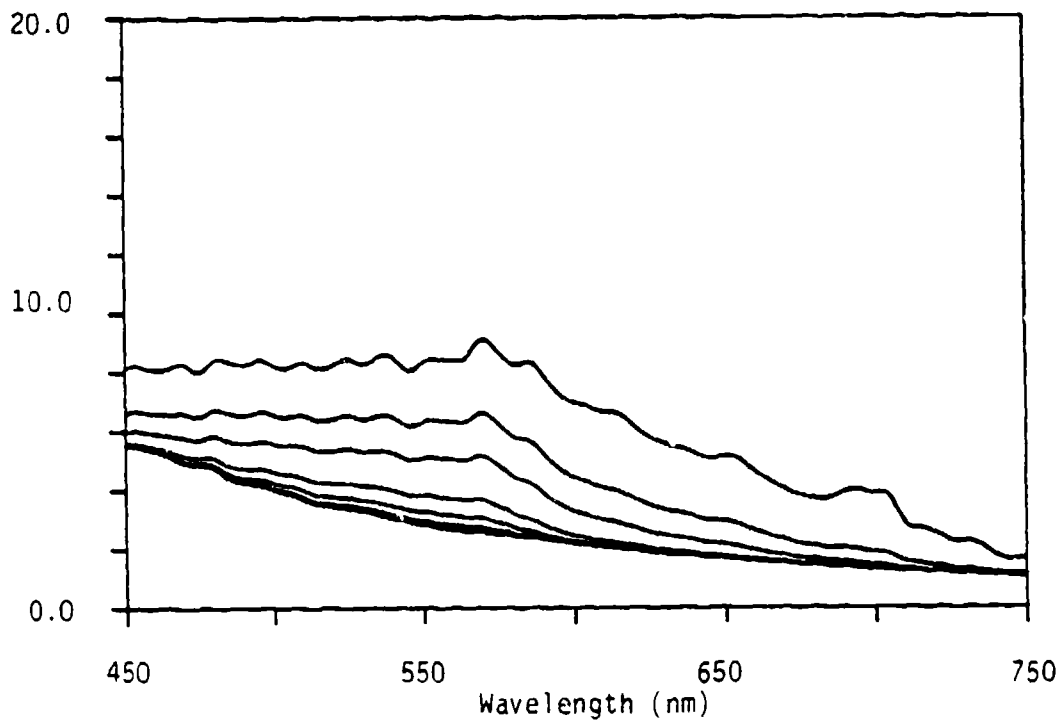


Figure A-93. Total radiance spectra for a Fire Coral bottom type at selected water depths (1,2,3,5,7,10, 15,25, and 40 m). Curves in the above panel were generated for a visibility of 23 km and with water type 5.

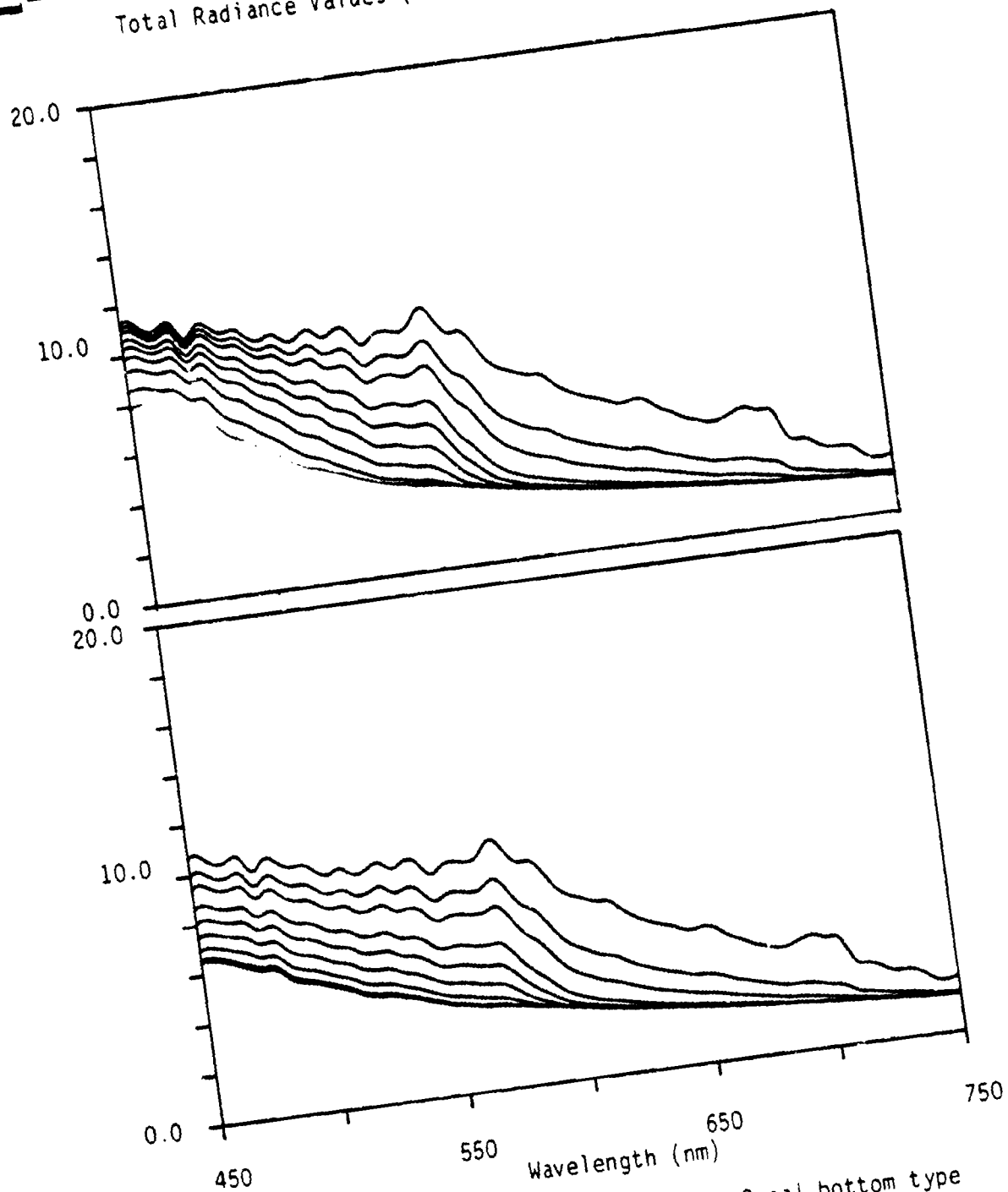


Figure A-94. Total radiance spectra for a Fire Coral bottom type at selected water depths (1, 2, 3, 5, 7, 10, 15, 25, and 40 m). Curves in the upper panel were generated for a visibility of 10 km and with water type 1 and in the lower panel for water type 2.

ERIM

Total Radiance Values (mw/(micron*cm*cm*sr))

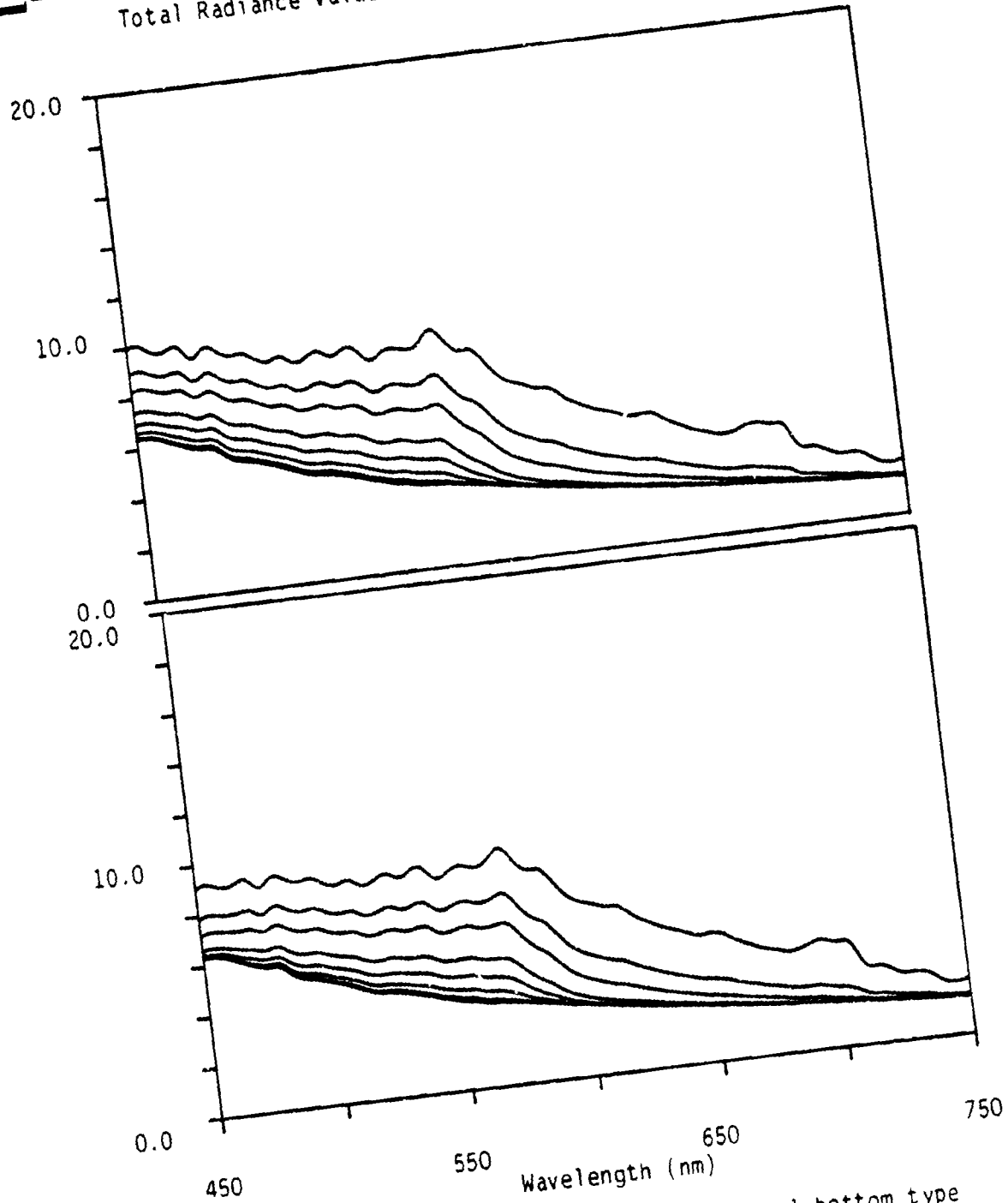


Figure A-95. Total radiance spectra for a Fire Coral bottom type at selected water depths (1,2,3,5,7,10,15,25, and 40 m). Curves in the upper panel were generated for a visibility of 10 km and with water type 3 and in the lower panel for water type 4.

A-99

Total Radiance Values (mw/(micron*cm*cm*sr))

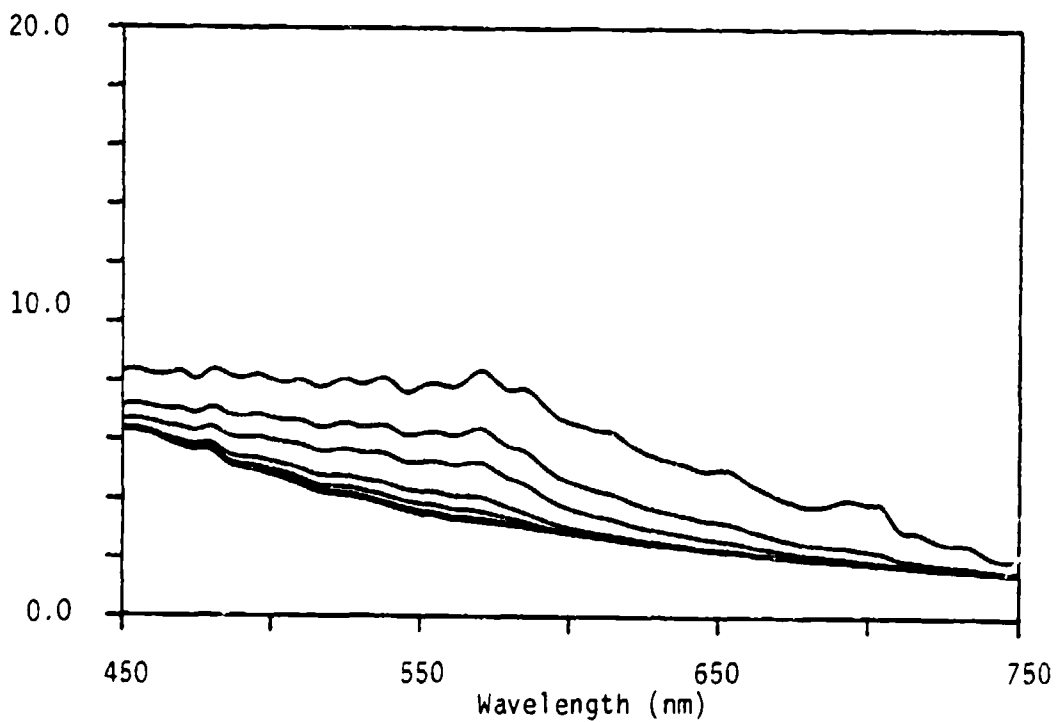


Figure A-96. Total radiance spectra for a Fire Coral bottom type at selected water depths (1,2,3,5,7,10, 15,25, and 40 m). Curves in the above panel were generated for a visibility of 10 km and with water type 5.

Total Radiance Values (mw/(micron*cm*cm*sr))

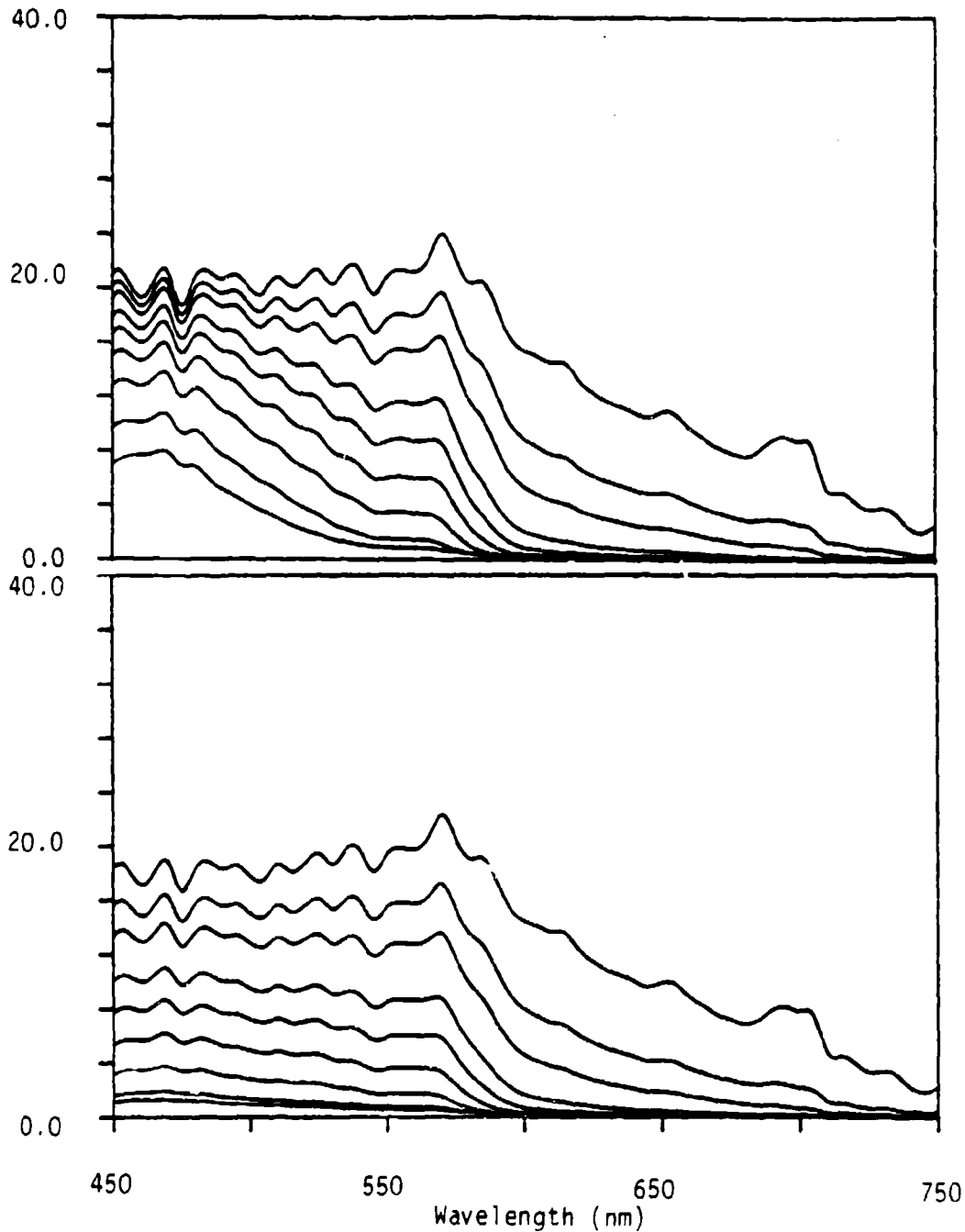


Figure A-97. Total radiance spectra for a Fire Coral bottom type at selected water depths (1,2,3,5,7,10, 15,25, and 40 m). Curves in the upper panel were generated with water type 1 and in the lower panel for water type 2. Spectra were calculated for a sensor position just below the sea surface.

Total Radiance Values (mw/(micron*cm*cm*sr))

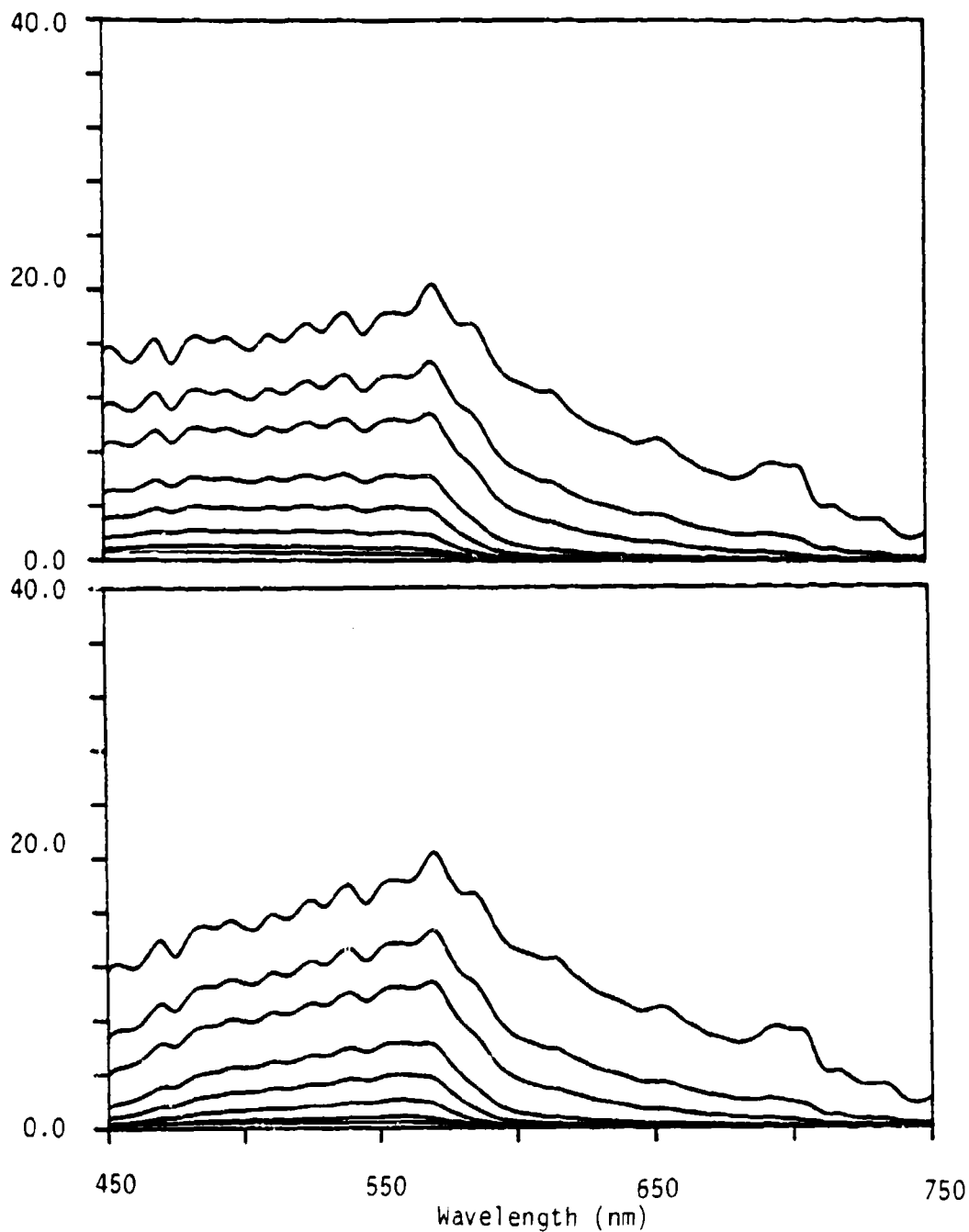


Figure A-98. Total radiance spectra for a Fire Coral bottom type at selected water depths (1,2,3,5,7,10, 15,25, and 40 m). Curves in the upper panel were generated with water type 3 and in the lower panel for water type 4. Spectra were calculated for a sensor position just below the sea surface.

Total Radiance Values (mw/(micron*cm*cm*sr))

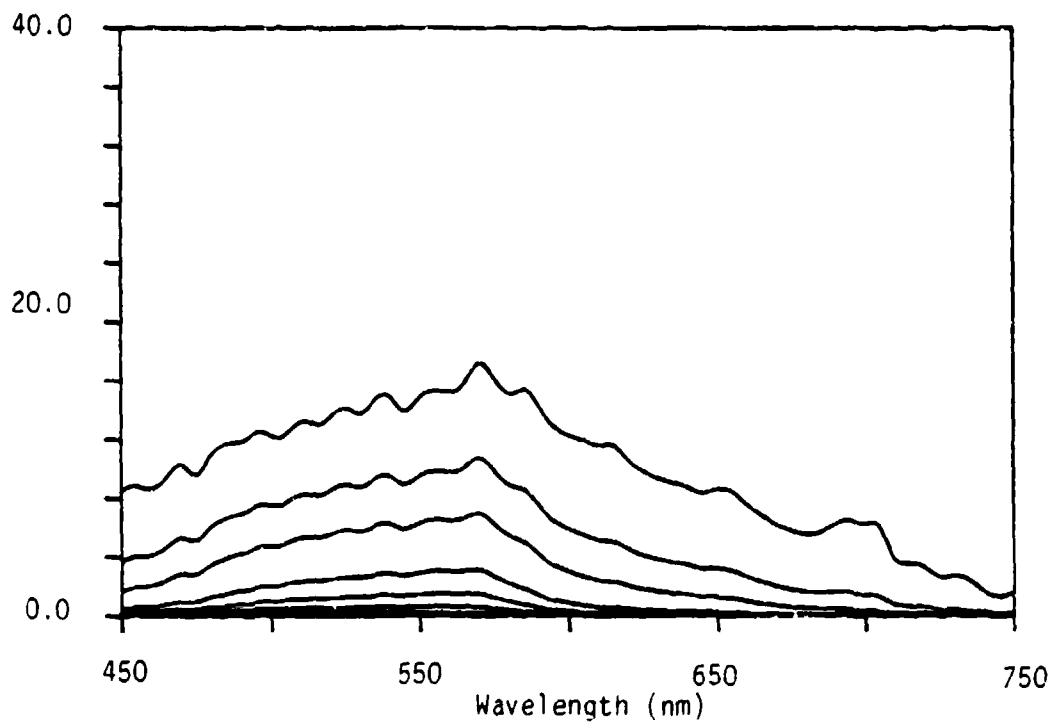


Figure A-99. Total radiance spectra for a Fire Coral bottom type at selected water depths (1,2,3,5,7,10, 15,25, and 40 m). Curves in the above panel were generated with water type 5. Spectra were calculated for a sensor position just below the sea surface.

Total Radiance Values (mw/(micron*cm*cm*sr))

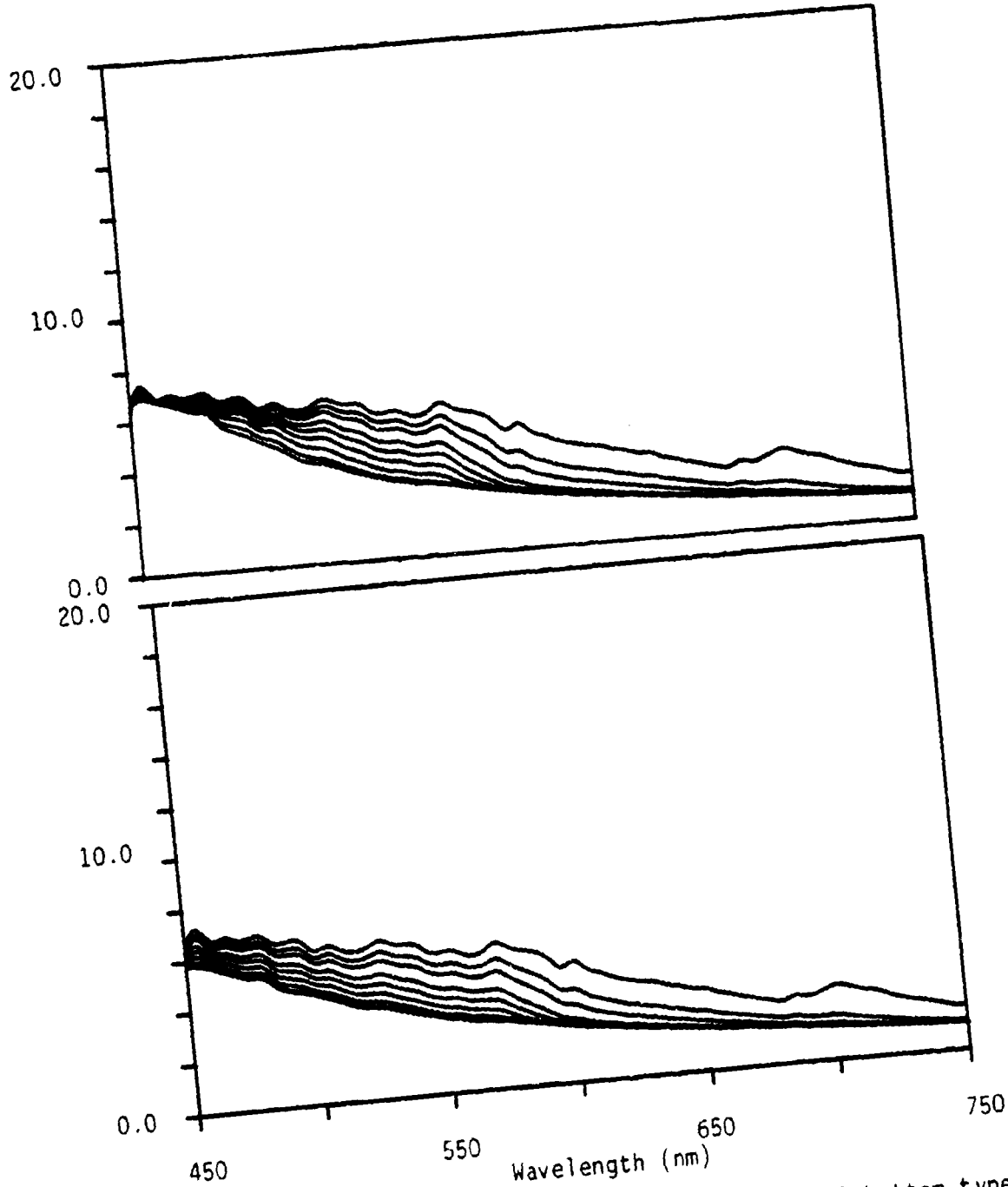


Figure A-100. Total radiance spectra for an Encrusting Coral bottom type at selected water depths (1, 2, 3, 5, 7, 10, 15, 25, and 40 m). Curves in the upper panel were generated for a visibility of 23 km and with water type 1 and in the lower panel for water type 2.

ERIM

Total Radiance Values (mw/(micron*cm*cm*sr))

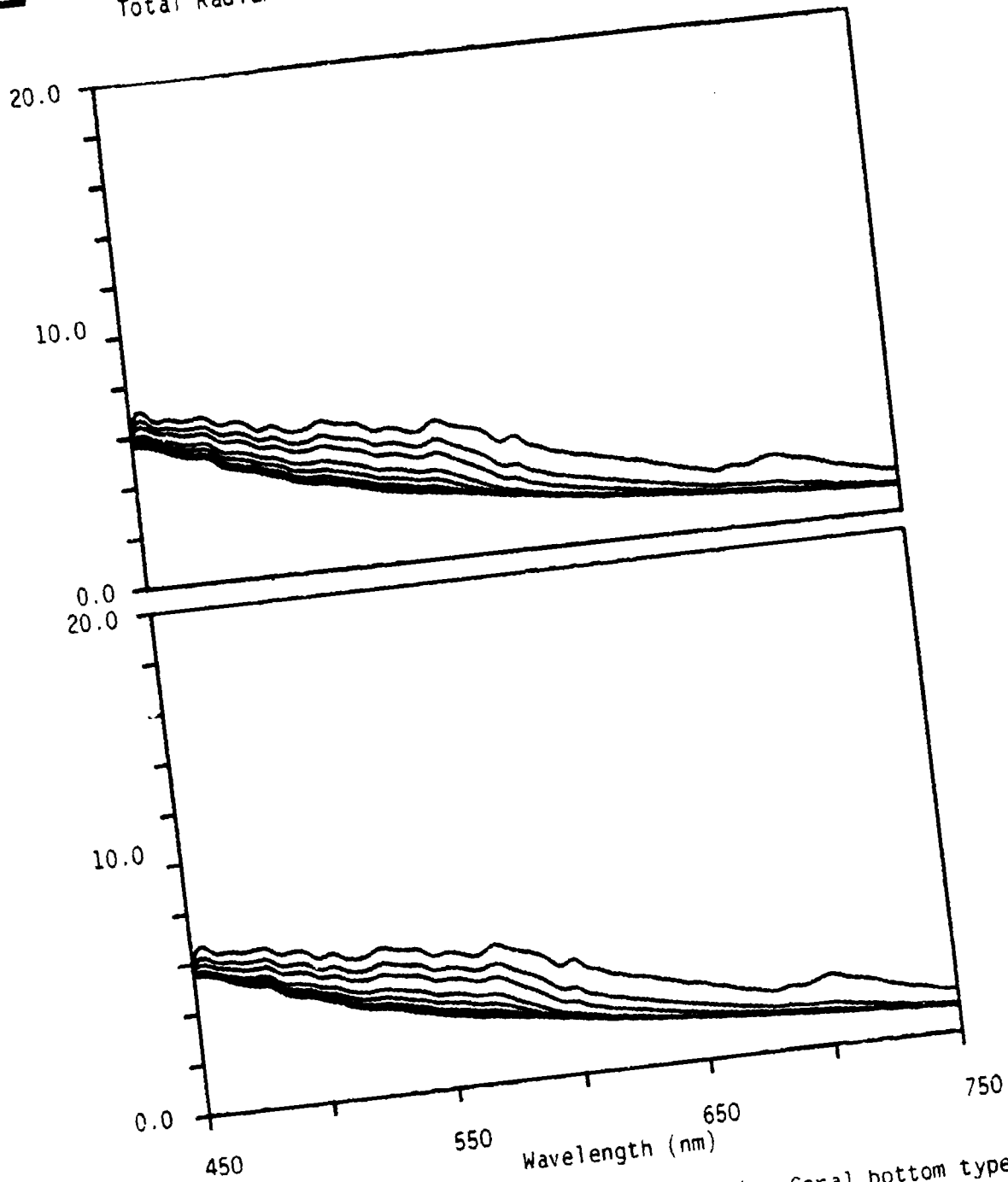


Figure A-101. Total radiance spectra for an Encrusting Coral bottom type at selected water depths (1, 2, 3, 5, 7, 10, 15, 25, and 40 m). Curves in the upper panel were generated for a visibility of 23 km and with water type 3 and in the lower panel for water type 4.

A-105

Total Radiance Values (mw/(micron*cm*cm*sr))

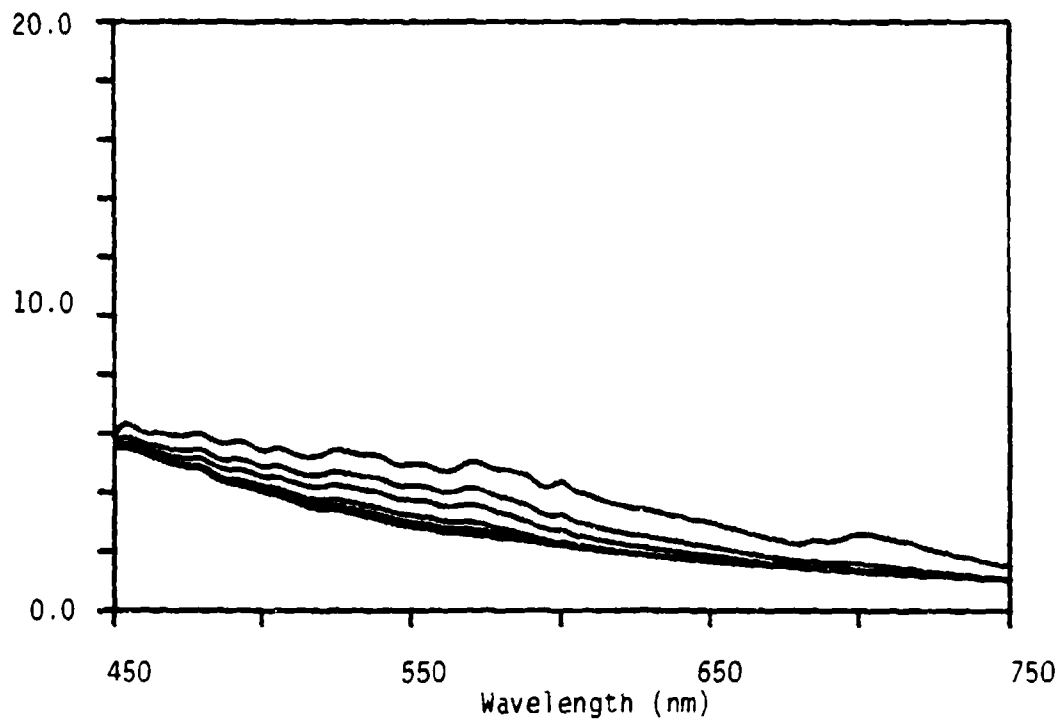


Figure A-102. Total radiance spectra for an Encrusting Coral bottom type at selected water depths (1,2,3,5,7,10, 15,25, and 40 m). Curves in the above panel were generated for a visibility of 23 km and with water type 5.

Σ ERIM

Total Radiance Values (mw/(micron*cm*cm*sr))

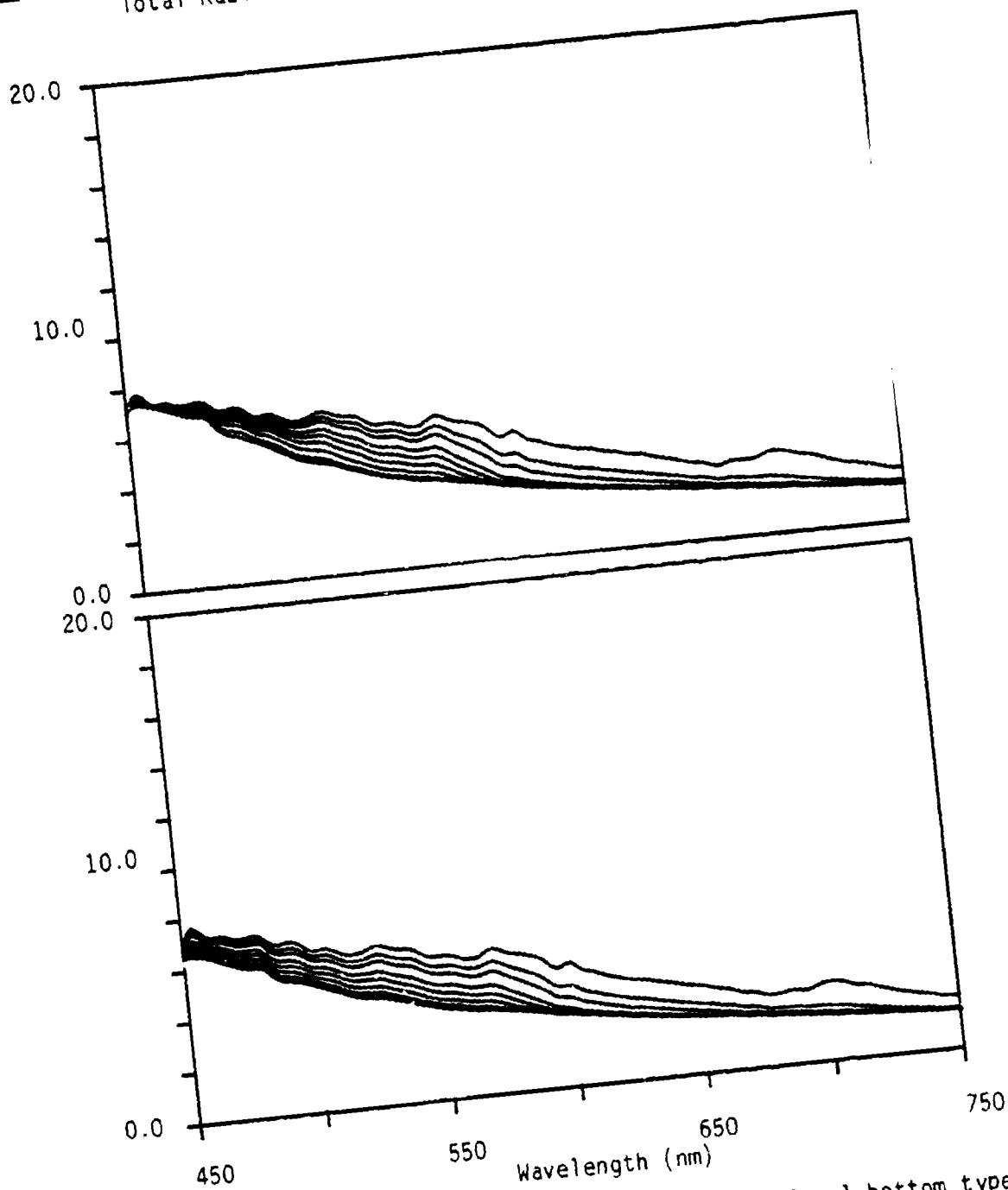


Figure A-103. Total radiance spectra for an Encrusting Coral bottom type at selected water depths (1, 2, 3, 5, 7, 10, 15, 25, and 40 m). Curves in the upper panel were generated for a visibility of 10 km and with water type 1 and in the lower panel for water type 2.

Total Radiance Values (mw/(micron*cm*cm*sr))

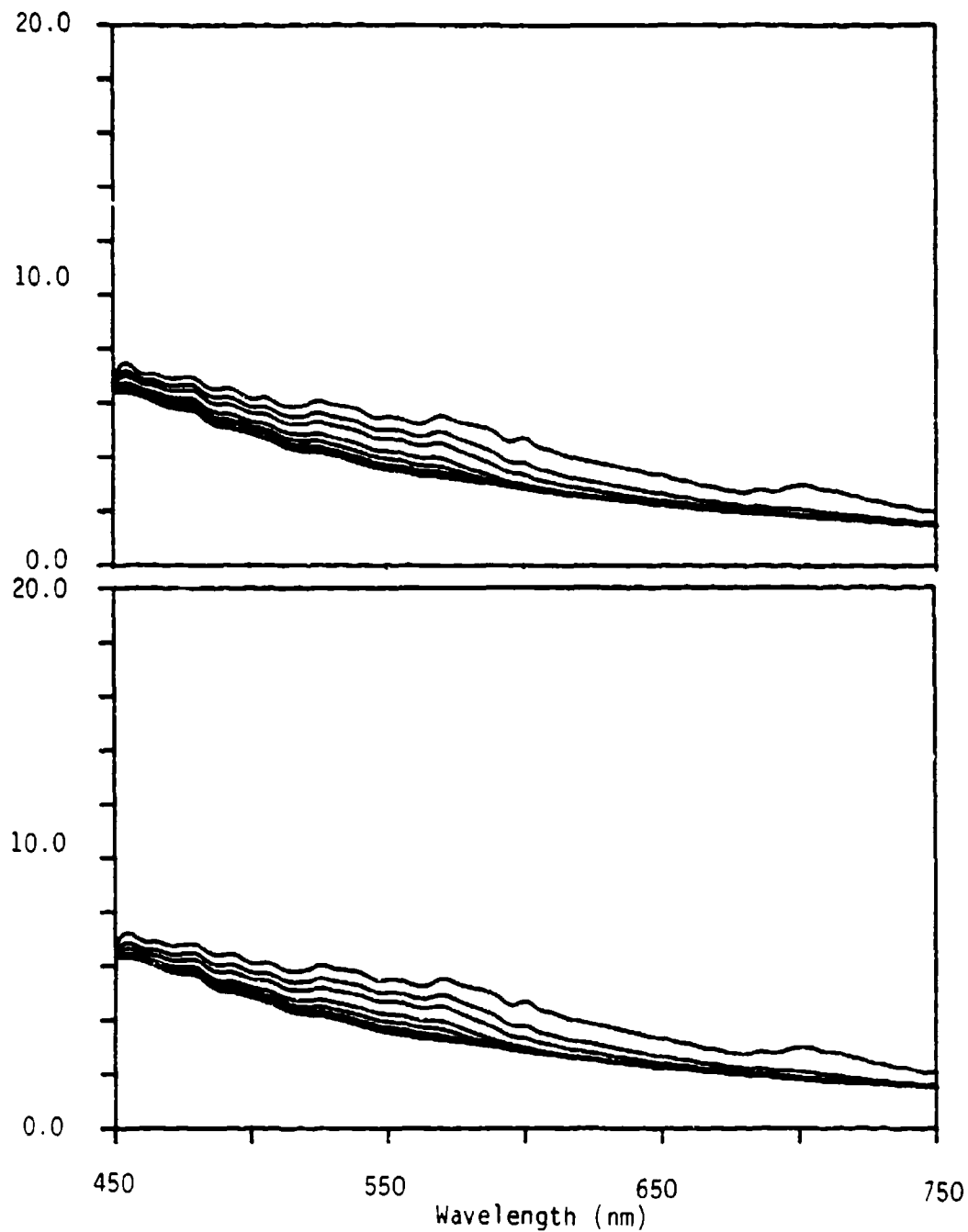


Figure A-104. Total radiance spectra for a Encrusting Coral bottom type at selected water depths (1,2,3,5,7,10, 15,25, and 40 m). Curves in the upper panel were generated for a visibility of 10 km and with water type 3 and in the lower panel for water type 4.

Total Radiance Values (mw/(micron*cm*cm*sr))

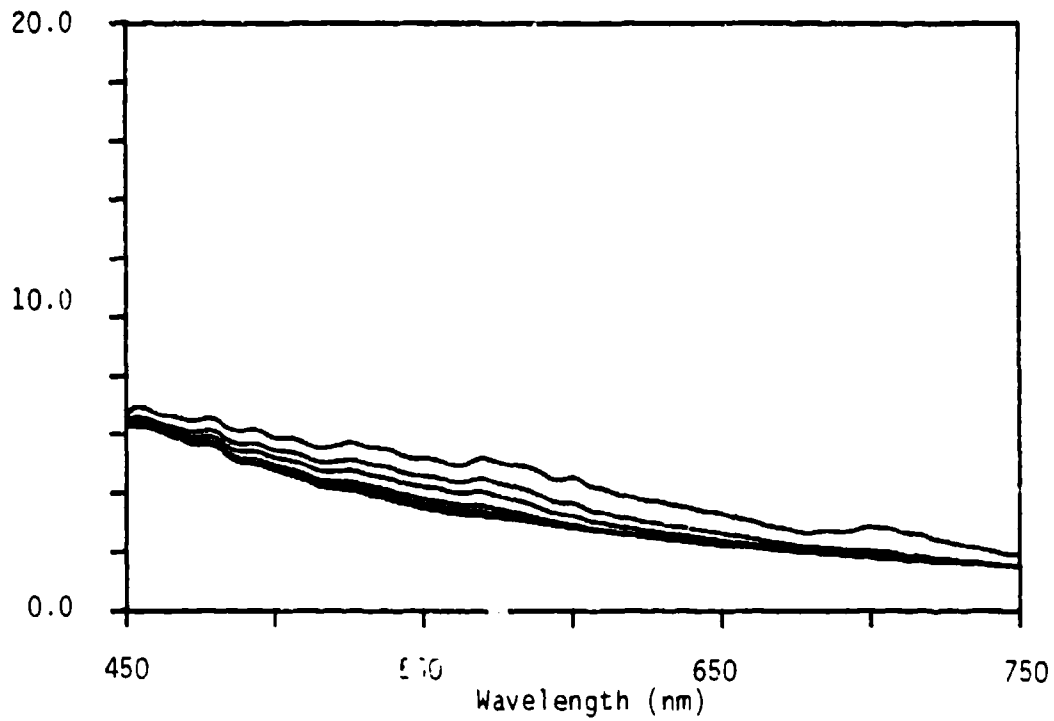


Figure A-105. Total radiance spectra for an Encrusting Coral bottom type at selected water depths (1,2,3,5,7,10, 15,25, and 40 m). Curves in the above panel were generated for a visibility of 10 km and with water type 5.

Total Radiance Values (mw/(micron*cm*cm*sr))

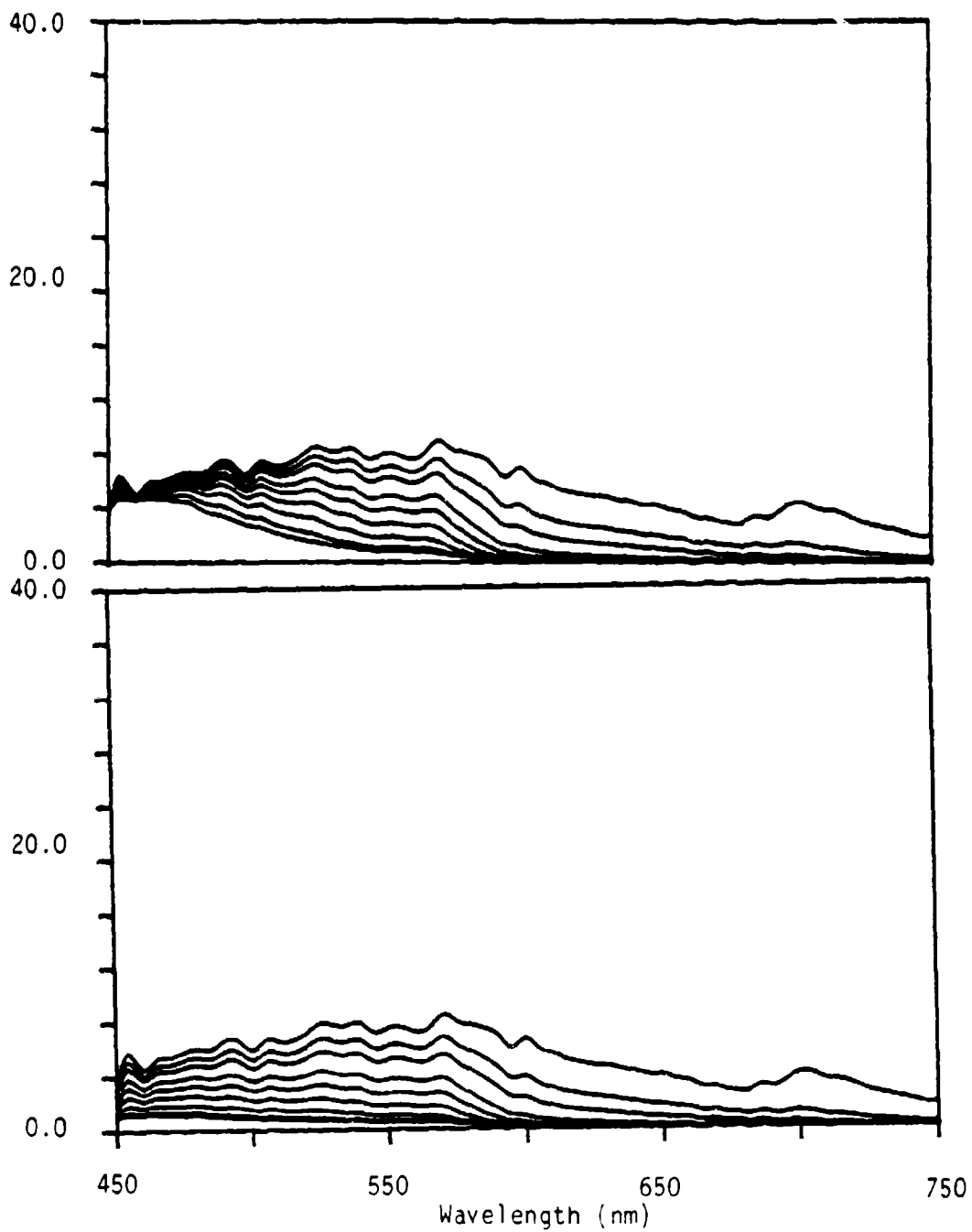


Figure A-106. Total radiance spectra for a Encrusting Coral bottom type at selected water depths (1,2,3,5,7,10, 15,25, and 40 m). Curves in the upper panel were generated with water type 1 and in the lower panel for water type 2. Spectra were calculated for a sensor position just below the sea surface.

Total Radiance Values (mw/(micron*cm*cm*sr))

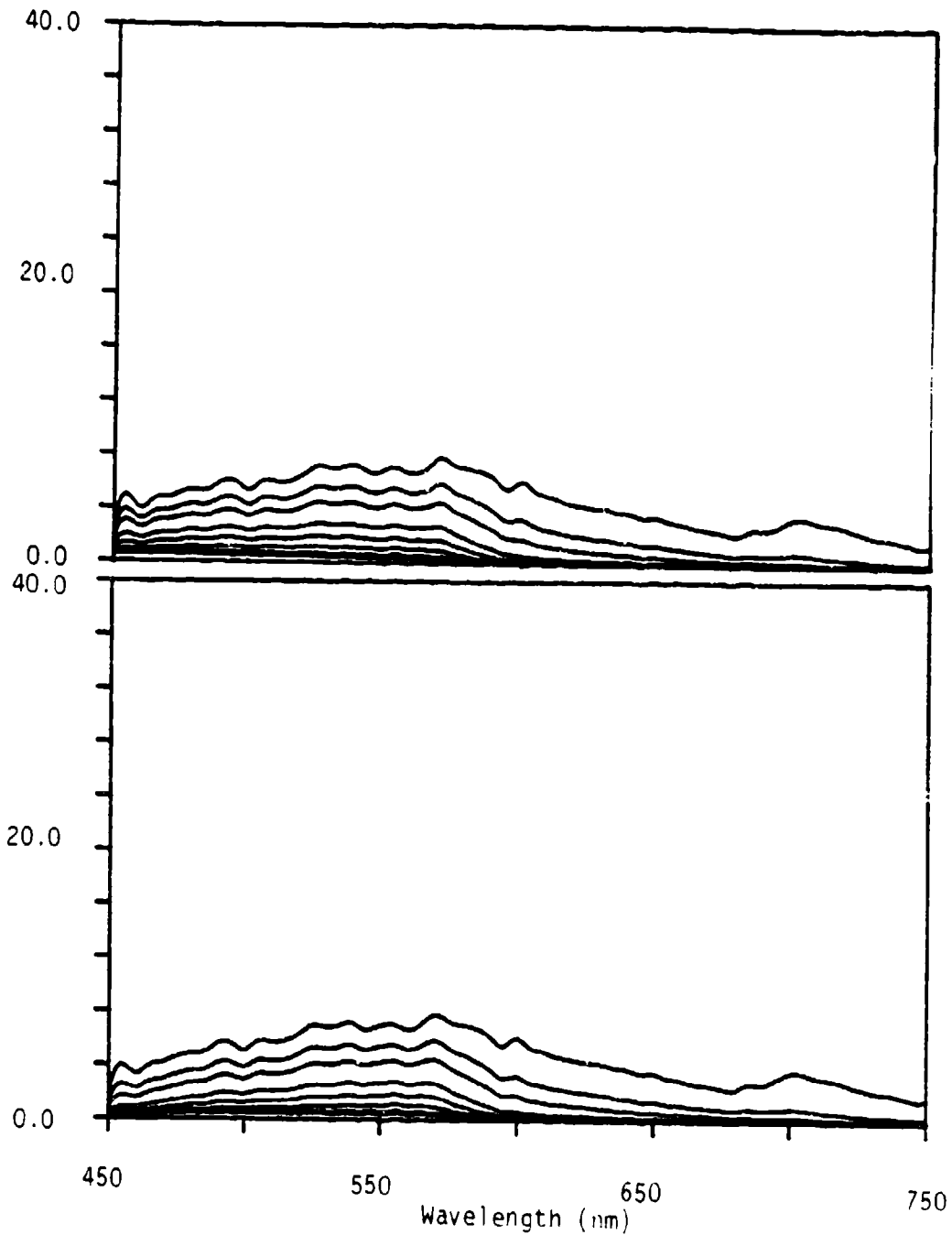


Figure A-107. Total radiance spectra for an Encrusting Coral bottom type at selected water depths (1,2,3,5,7,10, 15,25, and 40 m). Curves in the upper panel were generated with water type 3 and in the lower panel for water type 4. Spectra were calculated for a sensor position just below the sea surface.

Total Radiance Values (mw/(micron*cm*cm*sr))

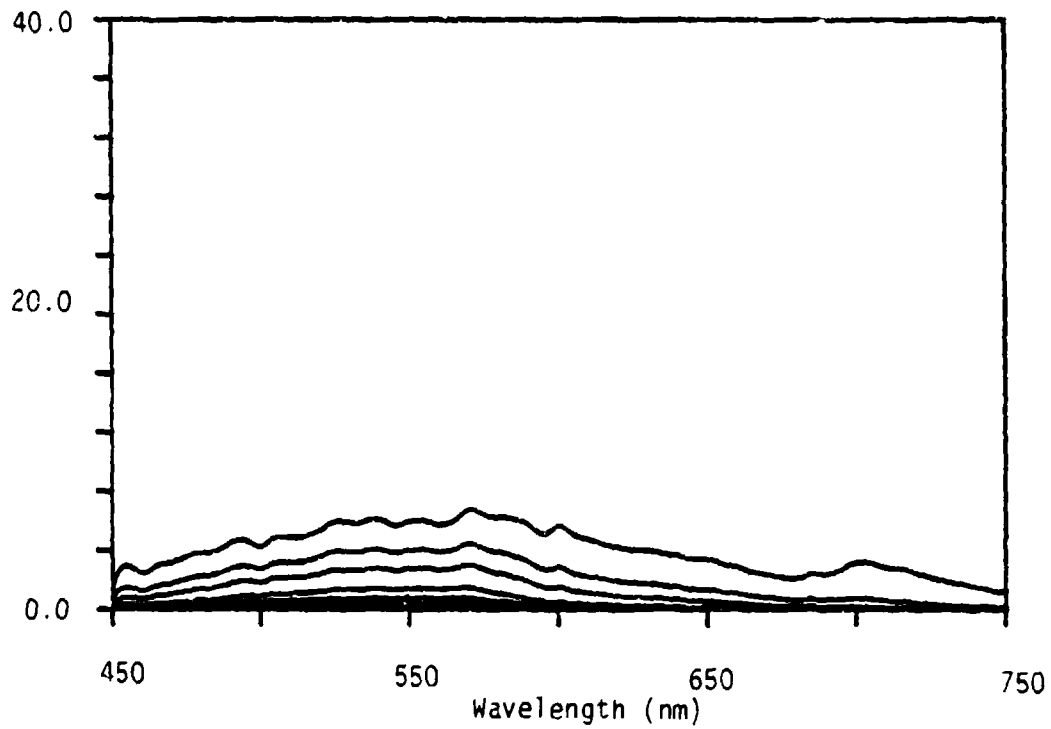


Figure A-108. Total radiance spectra for a Encrusting Coral bottom type at selected water depths (1,2,3,5,7,10, 15,25, and 40 m). Curves in the above panel were generated with water type 5. Spectra were calculated for a sensor position just below the sea surface.